EVIDENCE FOR THE ONION TISSUE SPECIFIC CONTRIBUTIONS OF THIOSULFINATE TOLERANCE GENE CLUSTERS TO *BURKHOLDERIA GLADIOLI* PV. *ALLIICOLA* VIRULENCE

by

SUJAN PAUDEL

(Under the Direction of Brian Kvitko)

ABSTRACT

Burkholderia onion pathogens are a routine threat to onion production in the United States causing diseases such as slippery skin and sour skin. Onion in response to pathogen attack produces toxic organosulfur defense compounds called thiosulfinates which induce thiol stress and inactivates essential bacterial enzymes. The thiosulfinate tolerance gene (TTG) cluster has been shown to confer resistance to these compounds in *Pantoea ananatis*, another bacterial onion pathogen. However, its presence and function in *Burkholderia* onion pathogens remain unexplored. Using comparative genomics and allicin zone of inhibition assays, we identified the widespread distribution of TTG cluster in onion and non-onion isolated *Burkholderia* onion pathogens and demonstrated their role in allicin tolerance *in vitro*. Phenotypic assays revealed that in *Burkholderia gladioli* pv. *alliicola* (Bga), the TTG cluster performs variable virulence role depending on the tissue type. Given the limited understanding of the genetic basis of virulence in Bga, we further characterized the putative genetic determinants of virulence in strain 20GA0385. Candidate virulence factors/regulators were identified using *in silico* analysis and deletion mutants were generated using allelic exchange. Infection assays demonstrated that, like TTG

cluster, the phytotoxin toxoflavin and the type II secretion system perform onion tissue specific virulence role in Bga. We also observed decoupling of Bga symptoms production and corresponding *in planta* population particularly in the scale tissue. The tissue specific virulence role of the TTG cluster is surprising, given the higher thiosulfinate content in onion bulbs compared to leaves. Using an *altR* promoter reporter construct, we found that its de-repression is transient during early infection but disappears with the onset of Bga induced scale necrosis. However, in the presence of a cell death-inducing factor, de-repression persists, and TTG mutant recovery from scale tissue is significantly reduced compared to the WT strain. The ability of Bga WT and *P. ananatis* WT strains to partially rescue the TTG mutant phenotype in the ZOI assay suggests that Bga may secrete factors that inactivate or suppress thiosulfinates. Future studies should focus on identifying the primary necrosis-inducing factor and potential Bga secreted factors conferring thiosulfinate resistance.

INDEX WORDS: onion, thiosulfinates, pathogen, slippery skin of onion, *Burkholderia gladioli pv. alliicola,* virulence, decoupling, necrosis, genetic determinants of virulence.

EVIDENCE FOR THE ONION TISSUE SPECIFIC CONTRIBUTIONS OF THIOSULFINATE TOLERANCE GENE CLUSTERS TO *BURKHOLDERIA GLADIOLI* PV. *ALLIICOLA* VIRULENCE

by

SUJAN PAUDEL

B.S., Agriculture and Forestry University, Nepal, 2017

M.S., University of Hawaii at Manoa, 2020

A Dissertation Submitted to the Graduate Faculty of The University of Georgia in Partial Fulfillment of the Requirements of the Degree

DOCTOR OF PHILOSOPHY

ATHENS, GEORGIA

2025

EVIDENCE FOR THE ONION TISSUE SPECIFIC CONTRIBUTIONS OF THIOSULFINATE TOLERANCE GENE CLUSTERS TO *BURKHOLDERIA GLADIOLI* PV. *ALLIICOLA* VIRULENCE

by

SUJAN PAUDEL

Major Professor:	Brian Kvitko
Committee:	Bhabesh Dutta Anthony E. Glenn Eric Lafontaine George Sundin

Electronic Version Approved:

Ron Walcott
Vice Provost for Graduate Education and Dean of the Graduate School
The University of Georgia
August 2025

DEDICATION

To my wife Shiwani Sapkota

and

my parents Khum lal Paudel and Nindra Acharya Paudel.

ACKNOWLEDGEMENTS

I am beyond grateful to my advisor, Dr. Brian Kvitko, for his unwavering support and guidance throughout my program. Your mentorship has been invaluable not only in shaping my research but also in helping me grow personally and professionally. Thank you for pushing me to be a better version of myself every day.

A heartfelt thanks to my committee members for your insightful feedback and constant support. Your contributions have been instrumental in enhancing the quality of our research. Special mention to our frequent collaborator and committee member, Dr. Bhabesh Dutta, whose insightful research suggestions and constant words of support and encouragement have made a lasting impact.

I am deeply thankful to my supervisor, Dr. Nagesh Sardesai, and the entire Pinkadelic Pop team for welcoming me during my three unforgettable months as a Crop Genome Engineering Intern at Corteva Agriscience. Your mentorship and camaraderie made the experience truly special.

A big shoutout to Dr. Rebecca Dunning, FFAR Fellows program director, and my incredible 2021-2024 FFAR Fellows cohort. These past three years have been a remarkable journey of self-reflection and professional growth. The FFAR Fellows program has been a cornerstone of my Ph.D. experience, and I am grateful for every moment. Special thanks to my Professional Development Plan mentors, Dr. Brian Kvitko, Chris Rhodes and Dr. Peter Rogers, for helping me hone my soft skills and build confidence. A heartfelt acknowledgment to Chris for

his relentless efforts in securing financial support and providing mentorship, without him, the FFAR program would not have become a reality.

To all past and present members of the Kvitko Lab - your support, advice, and camaraderie made this journey so much richer. I extend my gratitude to the UGA Plant Pathology department for fostering such a supportive environment and for being an academic home that I am proud to be a part of. Special thanks to Matt Seader for facilitating growth chamber space and for always being there to help care for my plants.

Finally, my deepest gratitude goes to my parents whose unwavering love and values of honesty and kindness have shaped the person I am today. To my sister and my beautiful niece Zea, your positive outlook on life and your courage inspires me every day. To my wife, Shiwani - you are my rock, my inspiration, and my greatest source of strength. The sacrifices you have made for us mean the world to me, and I am endlessly grateful to have you by my side. Thank you for everything.

TABLE OF CONTENTS

Page

CHAPTER 1

ONION PATHOGENIC *BURKHOLDERIA* SPECIES: ROLE AND REGULATION OF CHARACTERIZED VIRULENCE DETERMINANTS[1*]

---

[1]Paudel, S., Dutta, B. and Kvitko, BH. 2024. Onion-pathogenic *Burkholderia* species: Role and regulation of characterized virulence determinants. *Plant Pathology*, 73, 2281–2297

*Literature Review chapter

SP did literature search, investigation, writing – original draft, review, editing and visualization.

Abstract

Members of the bacterial genus *Burkholderia* are a routine threat to onion production worldwide. In addition to the common onion-pathogenic species, *Burkholderia cepacia*, *Burkholderia orbicola* and *Burkholderia gladioli*, other *Burkholderia* species have the potential to cause onion disease. Despite their impacts and long-known association with onion disease, the virulence mechanisms of onion-pathogenic *Burkholderia* are far less well understood than *Burkholderia* in human and murine infection models. In this review, we will focus on genetically characterized virulence factors in species that contribute to symptom production in onion and other plant hosts. Specifically, we will focus on the variable roles of specialized protein secretion systems (T2SS, T3SS and T4SS) and secreted proteins, thiosulfinate tolerance gene (TTG) clusters and the well-characterized phytotoxin toxoflavin in virulence. The regulation and roles of LuxI/LuxS quorum-sensing system and IclR-type transcriptional regulator, *qsmR*, as master regulators of secondary metabolite production and virulence factors will also be discussed.

Introduction

Burkholderia species have characteristically large genome sizes with the presence of multiple replicons. Another notable feature of the genus is the distribution of a wide array of insertion sequences (ISs), which is believed to have contributed to genomic plasticity and to acquisition of novel secondary metabolites and catabolic pathways (Lessie et al., 1996). Members of the genus can be pathogens or symbionts with animals, plants and fungi (Eberl & Vandamme, 2016; Partida-Martinez & Hertweck, 2005). The plant-pathogenic *Burkholderia* species have received less research attention compared to human/animal pathogens in the *Burkholderia cepacia* complex (Bcc) and the select agent *Burkholderia pseudomallei* complex. Important plant-pathogenic *Burkholderia* species are *Burkholderia glumae*, *Burkholderia gladioli*, Bcc and

Burkholderia plantarii. Species in Bcc are reported as pathogens of onion, banana and apricot (Burkholder, 1950; Fang et al., 2009; Lee et al., 2003). *B. gladioli* strains are known to infect a wide range of hosts including rice, onion, gladiolus, *Cymbidium*, mushroom, sweet potato and garlic and have been shown to produce symptoms in cactus, leek stalk, broccoli inflorescence, bean leaves and stalks, saffron, potato, cucumber, carrot and radish in laboratory assays (Abachi et al., 2024; Azegami et al., 1987; Burkholder, 1942; Moon et al., 2017; Serret-López et al., 2021; Zhang et al., 2020). *B. glumae* and *B. plantarii* are important rice pathogens (Azegami et al., 1987).

B. gladioli pv. *alliicola* (Bga) and some species in Bcc are more commonly associated with onion disease. Along with *Burkholderia cepacia*, other members in the Bcc have been isolated from soil and are efficient colonizers of the onion rhizosphere (Compant et al., 2008; Hall et al., 2015; Stopnisek et al., 2014). Jacobs et al. (2008) found that onion rhizosphere and field isolated *B. cepacia*, *Burkholderia cenocepacia*, *Burkholderia ambifaria* and *Burkholderia pyrrocinia* were able to cause tissue necrosis in laboratory onion scale assays. In a study involving cystic fibrosis (CF) and environmental strains of Bcc, 12 out of 14 environmental isolates were capable of onion tissue maceration at varying degrees relative to the *B. cepacia* type strain ATCC 25416 (Springman et al., 2009).

In a different study, a substantial proportion of strains obtained from organic soil and decayed onion exhibited onion virulence. This subgroup of strains consisted of *B. cepacia* type strain ATCC 25416 and *Burkholderia multivorans* type strain ATCC 17759 (Yohalem & Lorbeer, 1994). It is possible many other *Burkholderia* species isolated from soil will be discovered as potential onion pathogens in the future (Compant et al., 2008). The three onion-pathogenic species *Burkholderia orbicola*, *Burkholderia semiarida*, and *Burkholderia sola* are the latest

additions as new species to the complex (Velez et al., 2023). A genomic species group within *B. cenocepacia* was recently split into a new species, *B. orbicola*, using polyphasic approaches such as digital DNA–DNA hybridization, average nucleotide identity (ANI), core genes-based phylogenomic analysis, biochemical and phenotypic tests and chemotaxonomic analysis (Morales-Ruíz et al., 2022). We confirmed the three strains HI2424, MCO-3 and AU1054 as *B. orbicola* and strains J2315 and K56-2 as *B. cenocepacia* using type strain genome server (TYGS) analysis (Agnoli et al., 2014; Meier-Kolthoff & Göker, 2019; Paudel et al., 2024). As genomic approaches-based species identification has been more popular and convenient, the taxonomic status of strains previously identified as *B. cenocepacia* species should be revisited. Not only environmental species, *Burkholderia* CF isolates J2315 and K56-2 are also virulent on onion (Butler et al., 1995; Engledow et al., 2004). Significant knowledge gaps still exist in the understanding of virulence mechanisms of onion-pathogenic *Burkholderia* species. In this review, we summarize research on regulation and role of virulence determinants in the onion-pathogenic *Burkholderia* species. Most of the findings concerning *B. gladioli* reported in this review are based on comparison and inferences from the research done on *B. glumae* as it is one of the well-characterized plant pathogens of rice, is a close relative of *B. gladioli* and is capable of causing onion tissue necrosis (Karki, Shrestha et al., 2012; Vandamme et al., 2017). The alfalfa plant infection model has also been used to study virulence determinants in Bcc strains (Bernier et al., 2003). The findings from this infection model will also be briefly discussed.

Distribution, symptomatology and differentiation of onion-associated *Burkholderia* members

B. gladioli and other plant pathogens (*B. glumae* and *B. plantarii*) and opportunistic human pathogens (*B. pseudomallei*, *B. mallei* and Bcc) are kept together in the group *Burkholderia* sensu stricto (Bss) (Bach, 2022; Sawana et al., 2014). Within the Bss group, the Bcc members

form a distinct clade, the *B. pseudomallei*/*mallei* complex members form a separate clade, whereas the common plant-pathogenic members *B. gladioli*, *B. glumae* and *B. plantarii* form another distinct grouping (Sawana et al., 2014). Common onion-pathogenic members are isolated from the group Bcc and *B. gladioli* pv. *alliicola* (Bga).

Bga was first described as *Phytomonas alliicola* by W. H. Burkholder from a harvested rotten onion in 1942, New York State (Burkholder, 1942). The pathogen was later found as the causal agent of onion foliar and younger outer scales death in Iowa in 1942. The bacterium was subsequently reported and characterized from other onion-producing regions in Bulgaria (Stoyanova et al., 2011), New Zealand (Wright et al., 1993), South Korea (Lee et al., 2005), Poland (Kowalska et al., 2015), Slovenia (Lamovšek et al., 2016) and Mexico (Félix-Gastélum et al., 2017; Serret-López et al., 2021). Another important onion pathogen, *B. cepacia*, was first described in the 1950s by its distinct vinegar-like odour from the onion bulb (Burkholder, 1950). The symptoms caused by the two onion pathogens Bga and Bcc are hard to distinguish from each other because of their close phenotypic and phylogenetic relatedness (Baxter et al., 1997; Palleroni et al., 1972). Both pathogens are capable of infecting onion leaves and bulbs and are commonly isolated from soil and onion debris (Irwin & Vaughan, 1972; Kawamoto & Lorbeer, 1972a, 1972b, 1974). Burkholder described Bcc infection in Yellow Globe variety as restricted to outer fleshy scales, and shrinkage of the bulb was observed in the later stage of infection. Lesions from Bcc-inoculated onion leaves under greenhouse conditions expanded very slowly in the absence of water whereas the leaves infected with Bga produced sunken, elongated necrotic spots followed by eventual wilting and drying (Kawamoto & Lorbeer, 1974; Lee et al., 2005). Burkholder described the rotten bulbs caused by Bcc as slimy and yellow in appearance as opposed to the watery, glassy appearance in rots caused by Bga (Burkholder, 1950). Water-

soaked natural and artificial wounding may contribute to the spread of these pathogens in the field and storage conditions. No evidence of bacterial entry through the natural opening was found (Kawamoto & Lorbeer, 1974). Irrigation and rain splash may serve as a medium of Bcc inoculum dissemination from soil into the necks of plants (Jacobs et al., 2008; Teviotdale et al., 1989). Despite the similarity in the symptoms caused by these pathogens, ‘sour skin’ is commonly attributed to Bcc and 'slippery skin' is commonly used for disease description caused by Bga.

It was proposed that a group of five phenotypically similar, but genetically distinct species should be referred to as the *B. cepacia* complex at the International *Burkholderia* cepacia Working Group meeting 1997 (Vandamme et al., 1997). These phenotypically similar groups initially referred to as genomovar were labelled as species with the pending identification of differential tests for them. The *recA* gene for the identification of different genomovars within Bcc was first introduced in 2000 and has been extensively used as a diagnostic strategy for Bcc (Mahenthiralingam et al., 2000). This scheme was then frequently used in the next decade to differentiate and study the relationships between the members in Bcc. With the availability and convenience of whole genome sequencing, the ANI and digital DNA–DNA hybridization (ddH) methods were incorporated in other existing approaches including the *recA* gene PCR, *recA* RFLP, MLSA, phenotypic tests and chemotaxonomic characterization in the polyphasic study of phylogeny and new species description in the Bcc complex (Martina et al., 2018; Morales-Ruíz et al., 2022; Velez et al., 2023). Using different polyphasic and genomic approaches, as of 2023, at least 26 validly named, closely related species members are described in Bcc. The species *B. semiarida* and *B. sola*, isolated from onion, along with the recently characterized *B. orbicola* species, are recent additions to the list. With the transition into the whole genome-based species

characterization, the use of genomovar labels in the *Burkholderia* research community has been declining over the years.

Phylogenetic analysis and ANI assessment using core genes across 206 genomes of *B. gladioli* revealed the presence of three separate clades. Clade 1 exhibited three separate subclades, namely 1A, 1B and 1C, and comprised strains of *B. gladioli* pv. *cocovenenans*. *B. gladioli* pv. *alliicola* strains formed a distinct evolutionary Clade 2. *B. gladioli* pv. *agaricicola* and *B. gladioli* pv. *gladioli* strains were phylogenetically indistinguishable and grouped in Clade 3. Despite their designation as pathovars, strains in all pathovar and clade groups were able to cause both mushroom and onion tissue rot (Jones et al., 2021).

The *recA* gene-based primers BCR1 and BCR2 are useful for the identification of members within the Bcc complex (Mahenthiralingam et al., 2000). However, the primers are specific to Bcc only and are not able to discriminate the *Burkholderia* members outside the Bcc complex. The 385 bp long PCR product from BUR3 and BUR4 *recA* primers differentiated the *B. pseudomallei*/*B. mallei* members and plant-pathogenic species group from the Bcc complex (Payne et al., 2005). Both primers BCR1/BCR2 and BUR3/BUR4 cannot differentiate the clinical and environmental isolates in the Bcc complex. In the absence of whole genome sequencing, the BUR3/BUR4 primers can be used in differentiation and characterization of the onion-pathogenic species group in the *Burkholderia* genus (Figure 1.1). For the differentiation of Bga from Bcc, a 1644 bp partial *gyrB* gene-based phylogeny was developed (Zhang et al., 2019). A PCR-based diagnostic tool has been developed to detect *P. ananatis*, *Burkholderia* sp. and Enterobacter sp. from onion (Asselin et al., 2016). A signature region in the 16S and 23S rRNA has also been used to design primers to discriminate *B. gladioli* from other related *Burkholderia*

spp. (Bauernfeind et al., 1999). Readers are directed to Jin et al. (2020) for further information on the use of MLSA and specific loci for species resolution within the Bcc.

Characterized virulence factors and regulators in *Burkholderia cepacia* complex members

Protein secretion systems

The type II, type III, and type IV secretion systems are protein machineries used by many gram-negative bacteria to export proteins outside of the cell. The type II secretion system (T2SS) secretes folded protein in a two-step process: first proteins are translocated through the Sec or Tat pathway into the periplasm where protein folds into its tertiary confirmation (Costa et al., 2015). This is followed by the delivery of the protein across the outer membrane by the T2SS protein complex (Cianciotto, 2005, Johnson et al., 2006). The T2SS has been known to secrete a variety of enzymes like lipases, proteases, chitinases, and other enzymes to help bacteria cause disease in different hosts. Ulrich et al. 1970 in showed polygalacturonase (PGase) was produced during the infection of onion by *B. cepacia* (Ulrich, 1975). *B. cepacia* strain DSM 3959 also produces a lipase, which is trafficked through inner membrane following signal peptide cleavage (Hobson et al., 1993). In another study, *B. cepacia* strain KF1 has been shown to produce an extracellular metalloprotease and a transposon insertion mutant in the *B. cepacia dsbB* homolog was impaired in motility and protease production (Abe & Nakazawa, 1996). The authors speculated a pre-protease when secreted to the periplasm could be folded by the *dsb* (disulfide bond forming) system and the processed product could be excreted through the outer membrane, a feature typical of T2SS (Abe & Nakazawa, 1996). Gonzalez *et al.*, 1997 found the gene *pehA* for endopolygalacturonase production in *B. cepacia* strain ATCC25416 is plasmid encoded. Mutant derivatives of ATCC25416 that had an inactive *pehA* gene or were plasmid cured were unable to cause maceration of onion scale tissue but caused necrosis around the surrounding tissue of

inoculation (Gonzalez et al., 1997). This implies that the *pehA*-encoded PGase enzyme contributes to the increased aggressiveness of *B. cepacia* in onion tissue. Although no direct experimental evidence was provided, inferences of *pehA* secretion through T2SS in *B. cepacia* ATCC 25416 have been made based on observations from multiple studies (Somvanshi et al., 2010) (Figure 1.2a). The Bga strain CH1 secretes PGase (EC 3.2.1.15) but not pectate lyase (EC 4.2.2.2) or pectin lyase (EC 4.2.2.10). The PGase in Bga strain CH1, *B. cepacia* plasmid pPEC320 and *B. glumae pg-A* gene all shared high homology with conserved active sites of enzymes. The *E. coli* transformants with cloned Bga *pehA* gene caused dramatic onion tissue collapse (Lee et al., 2021).

In *B. cenocepacia*, the onion tissue necrosis is also correlated with the presence of *pehA* encoding PGase. Of the 56 surveyed agricultural and clinical isolates, 13 closely related *B. cenocepacia* strains (isolated mostly from onion), encoded a *pehA* gene and were pathogenic to onion. On the other hand, the strains that lacked the *pehA* gene (isolated mostly from CF patients) were unable to cause onion tissue necrosis. In addition, the maize rhizosphere isolated *B. orbicola* strain MCO-3, originally identified as *B cenocepacia,* also lacked the *pehA* gene and was also non-pathogenic to onion. This study suggests the polygalacturonase encoded by *pehA* could be an important virulence factor in *B. cenocepacia* and *B. orbicola* (Springman et al., 2009). Besides PGase, the T2SS secreted extracellular zinc metalloprotease in the *B. cenocepacia* strain K56-2 was also tested for its role as a virulence factor in alfalfa model. Neither *htrA* protease nor *zmpA* and *zmpB* extracellular zinc metalloprotease mutants resulted in reduced disease symptoms in alfalfa implying a lack of contribution to disease phenotype (Bernier et al., 2003, Uehlinger et al., 2009). The T2SS found in *B. cenocepacia* strain H111 shares high homology to the machinery in *B. pseudomallei* (Köthe et al., 2003). T2SS encoded

gsp insertional mutants lost *in vitro* protease or lipolytic activity. The mutants, however, were not altered in their ability to kill *Caenorhabditis elegans* suggesting no role of T2SS in nematode virulence (Köthe et al., 2003). In alfalfa seedling symptoms and *C. elegans* killing, there were no differences observed between the H-111 T2SS mutant *gspE* and the wild type, implying its lack of clear contribution in the disease phenotypes of both model systems (Uehlinger et al., 2009). Mutation in *B. orbicola* strain AU1054 T2SS pseudopilin *gspJ* gene led to reduced maceration area in onion and reduced growth in minimal media. The mutant was also impaired in its ability to hydrolyse casein and was defective in the degradation of polygalacturonic acid (Somvanshi et al., 2010). These studies in *B. cepacia, B. cenocepacia,* and *B. orbicola* suggest the T2SS secreted *pehA* endopolygalacturonases as a major virulence factor in onion infection models. However, in infection models involving alfalfa and nematodes, the T2SS appears to be non-essential for virulence.

T4SS: Mutational analysis of *B. cenocepacia* strain K56-2 revealed the presence of plant tissue water soaking (PTW) cluster with high homology to VirB-VirD4 translocation system of the type IV secretion system. Mutation in the VirD4 like protein encoding *ptwD4, ptwB4,* or *ptwB10* resulted in the complete loss of PTW phenotype in *B. cenocepacia* strain K56-2. The findings suggest the type IV secretion system induced PTW phenotype as a critical pathogenicity factor in this onion pathogenic *B. cenocepacia* strain (Figure 1.2b). Functionally, the plasmid-encoded cluster was proposed to export T4SS effectors responsible for the PTW phenotype. A second chromosomal cluster with high homology to VirB-VirD translocation system was also detected in the same strain although with no role in the PTW phenotype on onion (Engledow et al., 2004).

The PTW phenotype was also observed in surveyed strains in *B. cepacia*, *B. cenocepacia,* and *B. vietnamiensis* group. The *B. cepacia* ATCC 25416 *pehA* mutant impaired in onion tissue

maceration still showed plant tissue water-soaking phenotype (PTW) (Gonzalez et al., 1997). Although the presence of plasmid borne PTW T4SS gene cluster have been identified in *B. cenocepacia* ET12 lineage, studies related to *B. cepacia* T4SS clusters were not found. Predicting a putative effector translocating T4SS through in silico methods could pose challenges, given that T4SS can serve various functions, such as DNA uptake or release, conjugation, and effector translocation (Ding et al., 2003).

T3SS: The type III secretion system (T3SS) is a complex protein machine used by gram-negative bacteria to translocate effector proteins into eukaryotic cells. The T3SS is encoded by *hrp* genes (Hypersensitive Response and Pathogenicity) and contributes to the pathogenicity of multiple plant pathogens like *Xanthomonas euvesicatoria, Ralstonia solanacearum*, and *Pseudomonas syringae* (Alfano et al., 2000, Angot et al., 2006, Boucher et al., 1987, Lindgren et al., 1986, Rossier et al., 2000). The role of T3SS in host-range influence and symbiotic associations between bacteria and the legume host has also been studied (Okazaki et al., 2016, Teulet et al., 2019). The T3SS first came into attention in the *Burkholderia* genus from the select agent human pathogen *B. pseudomallei* where three different T3SS clusters were found. The Inv/Mxi-Spa (SP-1) family T3SS has high homology with T3SS of other human pathogens such as *Salmonella typhimurium* and *Shigella flexneri* as well as two *hrp2* T3SS family typically associated with plant interactions (Lee et al., 2010, Stevens et al., 2002).

The T3SS in *Burkholderia cepacia* complex is peculiar with no evidence for the presence of needle component *sctF* and an insertion of >10 kb region between *sctR* and *sctQ* genes. This system is widely distributed among the genomovars in Bcc and has been named *Burkholderia cepacia* complex injectisome (BCI) (Wallner et al., 2021). Glendinning and colleagues proposed the presence of putative T3SS clusters in genomovar II to VII. The cluster, however, is absent in

the *B. cepacia* genomovar I that also includes the onion isolated type strain ATCC 25416 (Glendinning et al., 2004, Parsons et al., 2001). The role of *B. cepacia* BCI T3SS in pathogenesis of murine infection model has been documented with low bacterial count recovered for BCI T3SS null mutant from lungs and spleens compared to the WT (Tomich et al., 2003). However, in the alfalfa seedling model, the *B. cenocepacia* H111 BCI T3SS mutant *bscN* was not altered in symptoms production compared to the Wild Type (Uehlinger et al., 2009). The BCI T3SS system may not be capable of functioning in the plant infection model as the potential absence of the needle component would impair the system's ability to penetrate the plant cell wall structure.

Siderophores

Siderophores are iron acquisition systems that help bacteria to thrive in the iron limited environment in hosts (Mietzner & Morse, 1994). Four different siderophores – ornibactin, pyochelin, salicylic acid (SA), and cepabactin are produced by members in Bcc (Meyer et al., 1995, Meyer et al., 1989, Sokol, 1986, Sokol et al., 1992, Stephan et al., 1993). The siderophore ornibactin contributes to virulence of *B. cenocepacia* in rodents, *C. elegans*, and *Galleria mellonella* animal models (Mathew et al., 2014, Sokol et al., 1999, Uehlinger et al., 2009). The ornibactin outer membrane receptor mutant *pvdA* was slightly reduced in alfalfa seedlings symptoms compared to the WT (Uehlinger et al., 2009). The *B. cenocepacia* K56-2 ornibactin outer membrane receptor mutant *orbA* (Sokol et al., 2000), however, was not altered in alfalfa virulence compared to WT (Bernier et al., 2003). The authors predicted the difference in phenotype of two ornibactin mutans *pvdA* and *orbA* could be due to differential level of siderophore utilization by the two mutants. The mutants *orbA* is still able to uptake ferric-SA whereas *pvdA* is impaired in uptake of both ferric-SA and ornibactin (Bernier et al., 2003, Sokol et al., 2000, Sokol et al., 1999).

Exopolysaccharides

The *B. cenocepacia* strain K56-2 can exhibit shiny colony variants (shv) as opposed to its normal rough matte colony morphology phenotype. These shiny variants had increased EPS production, piliation, and were more persistent in mouse model of infection compared to the WT (Chung et al., 2003). The shv strain K56-2 S76 with spontaneous mutation in the putative LysR family transcriptional regulator produced no symptoms in alfalfa seedlings (Uehlinger et al., 2009). Bacterial lipopolysaccharides (LPS), a cell surface component, is known to trigger immune response in vertebrates and invertebrates. The LPS in endophytic *B. cepacia* strain ASP B 2D elicits multiple plant defense responses such as intracellular Ca^{2+} influx, induces oxidative burst and extracellular alkalinization in tobacco (Gerber et al., 2004). Moreover, *B. cepacia* LPS triggered a swift burst of NO and prompted the expression of various defense, stress, and PR-associated genes in *Arabidopsis thaliana* (Zeidler et al., 2004). The LPS biosynthesis and expression mutants *hldA* and *salI* in *B. cenocepacia* strain K56-2 produced comparable alfalfa symptoms compared to the WT (Uehlinger et al., 2009).

Cepacian is a common exopolysaccharide (EPS) produced by different clinical and environmental isolates of *Burkholderia* genus (Cunha et al., 2004, Ferreira et al., 2010, Herasimenka et al., 2007). The sugar polymer is encoded in *bce-I* and *bce-II* gene clusters that are present in all sequenced *Burkholderia* genomes except *B. mallei* (Ferreira et al., 2011). Different strains of *Burkholderia cenocepacia, B. vietnamiensis*, *B. ambifaria*, *B. pyrrocinia*, *B. cepacia* Type strain ATCC 25416 were able to produce EPS when grown on agar supplemented with lyophilized onion extracts (Bartholdson et al., 2008). Insertional inactivation of *bceB* gene in the cepacian biosynthesis cluster resulted in the loss of EPS production in the onion extract supplemented media by *B. ambifaria,* which suggested the EPS produced is cepacian. The

production of cepacian, however, was not correlated with tissue maceration of onion bulbs (Bartholdson et al., 2008).

Other factors

The *Burkholderia cenocepacia* island (cci) is a horizontally acquired genomic island encoding gene regions phenotypically linked to bacterial virulence and metabolism (Baldwin et al., 2004). The porin gene mutant *opcI* in the cci island was not altered in alfalfa seedling symptoms compared to the WT (Uehlinger et al., 2009). In *B. cenocepacia* strain H111 and J2315, a protein homolog of unknown function was found that shared 53% identity with AidA (Autoinducer dependent A) of bacterial wilt pathogen *Ralstonia solanacearum* (Flavier et al., 1997, Huber et al., 2004). Western Blot analysis showed the presence of AidA signal in multiple species in Bcc including *B. cepacia* ATCC 25416, *B, ambifaria,* and *B. pyrrocinia*. *B. cenocepacia* strain H111 AidA was essential for slow killing of *C. elegans* (Huber et al., 2004). The *aidA* mutant did show a reduced alfalfa symptoms compared to WT, albeit with no statistical difference (Uehlinger et al., 2009).

Transposon mutagenesis analysis in *B. orbicola* strain AU1054 identified two mutants *aroA* and *purF,* in addition to T2SS Δ*gspJ* that were reduced in onion maceration area compared to the WT. The *aroA* product is predicted to be required for biosynthesis of chorismate precusor for aromatic amino acid synthesis and *purF* is predicted to encode a protein amidophosphoribosyltransferase, which is important in purine synthesis. Additional insertion mutants, *bnvR* (Unknown function containing helix-turn-helix motif) and *nhaX* (contains putative-proton exchanger domain) were important for virulence in *C. elegans* model but were dispensable for onion tissue maceration. Another mutant *argG* (predicted to encode

argininosuccinate synthase) was reduced in onion tissue maceration area and was required for *C. elegans* infection (Somvanshi et al., 2010).

Characterized virulence factors and regulators in *Burkholderia gladioli* and *B. glumae*

Besides onion, *B. gladioli* strains are also important pathogens of rice causing bacterial grain rot and leaf-sheath browning (Ura et al., 2006). Another important rice pathogen, *B. glumae* is a close relative of *B. gladioli* and causes bacterial grain rot and panicle blight. Rice yield loss of as high as 40% has been reported in the rice growing regions of Southern United States by this pathogen (Nandakumar et al., 2009). As the pathogen favors relatively high temperature for growth, climate change and global warming make this pathogen an increasing threat to rice production worldwide (Ham et al., 2011). Among the rice pathogenic bacterial species, *B. glumae* is established as a model pathogen for studying virulence and disease mechanisms. The characterized virulence factors and regulators in *B. glumae* include toxoflavin, the type II secretion system, the type III secretion system, and the quorum sensing system, are highly conserved in *B. gladioli* (Fory et al., 2014, Seo et al., 2015). In this section, we will discuss research findings from onion pathogenic *Burkholderia gladioli* studies and summarize work on relatively well characterized *B. glumae* pathosystem.

Toxoflavin

The phytotoxin toxoflavin is a well-characterized virulence factor in both *B. glumae* and *B. gladioli.* It was described as an effective electron carrier that produced H_2O_2 in the presence of oxygen bypassing the cytochrome system. The production of H_2O_2 was attributed to the toxicity of the compound based on observations in animals (Latuasan & Berends, 1961). The *tox* operon consists of polycistronic genes responsible for biosynthesis (*toxA – toxE*) and transport (*toxF –*

toxI) (Kim et al., 2004, Suzuki et al., 2004). A LysR-type regulator *toxR* along with an activator ToxJ are required to induce the expression of *toxABCDE* operon (Suzuki et al., 2004). The DNA binding motif along with genetic and biochemical evidence suggests ToxJ and ToxR along with co-inducer toxoflavin function together to regulate the expression of the toxoflavin synthesis pathway (Kim et al., 2009).

The role of toxoflavin in the virulence of *B. glumae* through the induction of tissue necrosis and chlorosis symptoms has been extensively studied. Sato *et al.*, 1989 found a reduction in rice seedlings growth when treated with toxoflavin (Figure 1.2c) (Sato et al., 1989). In another independent study, *B. glumae* strain was confirmed to produce a yellow phytotoxin that caused chlorotic spots on rice seedling leaves with concentration of 10 μg/ml or above (Figure 1.2c). The purified toxin inhibited the growth of rice seedling and caused the browning of lemma and palea of rice. While the phytotoxin was purified from then *P. glumae*-infected seedlings, rotting symptoms were not observed from the phytotoxin alone (Ilyama et al., 1995). *B. gladioli* strain MAFF302424 was also confirmed to produce toxoflavin (Furuya et al., 1997a). In a separate study, a correlation was observed between the production of toxoflavin and the pathogenicity of the bacterium in rice seedlings, dendrobium, gladiolus leaves, and onion bulbs (Iiyama et al., 1998) (Figure 1.2c). Toxoflavin producing strains of *B. glumae* and *B. gladioli* with 10^9 colony forming unit (cfu)/ml bacterial suspensions induced tobacco necrosis within 24 hr. However, two toxoflavin non-producing strains of *B. gladioli* also induced tobacco leaf necrosis suggesting the role of unidentified factors in elicitation of programmed cell death-like response. High concentrations of toxoflavin-producing strains induced brownish necrosis within 24 hours, while non-producing strains did not cause leaf necrosis. Purified toxoflavin at concentrations over 100 μg/ml also induced necrotic symptoms in tobacco, similar to live

bacterial cells, indicating a correlation between toxoflavin concentration and host symptoms. (Furuya et al., 1997b). In two other independent studies, toxoflavin mutants in *B. glumae* strains PG3 and B446 were unable to cause seedling rot in rice plants suggesting the potential role of toxin in pathogenicity on rice (Suzuki et al., 1998, Yoneyama et al., 1998). Based on independent studies with two different *B. glumae* strains BGR1 and PG9501, a correlation was observed between toxoflavin production amount and chlorosis symptoms on rice panicles but no relation between toxoflavin amount production with rice seedling rot symptoms was found (Suzuki et al., 2004). The ability of toxoflavin to induce wilting symptoms in various field crops has also been demonstrated in *B. glumae* (Jeong et al., 2003). The shikimate pathway genes *aroA* and *aroB* mutant in *B. glumae* strain 411gr-6 was significantly reduced in rice panicle blight and dramatically reduced in onion maceration area but still was able to produce toxoflavin like the WT strains. The study suggests that the toxoflavin production is not always correlated with bacterial virulence. The authors however didn't rule out the possibility of reduced toxoflavin production by *aroA* and *aroB* mutants in the host that could have caused reduced symptoms (Karki & Ham, 2014). Thus, the results from multiple studies suggest toxoflavin alone may induce chlorotic or wilting symptoms but may be dispensable for tissue necrosis. However, results on the role of toxin in symptom production vary with study.

Although toxoflavin production is widely distributed among all three clades of *B. gladioli* (Jones et al., 2021), the role of toxin in the virulence of the bacterium has been relatively less studied. The synteny and organization of toxoflavin biosynthesis and transport-related genes in *B. gladioli* strain BSR3 and *B. glumae* strain BGR1 are mostly conserved. (Lee et al., 2016). QS negative *B. gladioli* natural variant strain KACC11889 when complemented with the quorum sensing *tofIMR* genes restored toxoflavin production that caused severely reduced growth in rice

seedlings and maceration area in onion. This suggests toxoflavin may play a role in virulence of *B. gladioli* (Figure 1.2d) (Lee et al., 2016).

Protein secretion systems

T2SS: The T2SS is reported in both *B. gladioli* and *B. glumae* members. A comparative genomics study found the presence of one conserved T2SS located on chromosome 1 of *B. glumae* strains while two studied *B. gladioli* strains had two additional partial T2SS (Seo et al., 2015). The role of T2SS as a virulence factor has been studied in both *B. gladioli* and *B. glumae* (Figure 1.2c, 1.2d). Mutations in T2SS related *gspD*, *gspE*, *gspF*, and *gspK* genes in *Burkholderia gladioli* pv. *agaricicola* were impaired in the ability to cause mushroom cavity disease (Figure 1.2d). The study revealed the *gsp* operon in Bg pv. *agariciola* was similar to that in relatively well-characterized *B. pseudomallei* strain 1026b (Chowdhury & Heinemann, 2006). The 12 *gsp* genes in *B. glumae* strain BGR1 are arranged identically to the *gspD-N* locus present in *B. pseudomallei* strain MSHR668 (Burtnick et al., 2014, Goo et al., 2010). Mutations in T2SS genes *gspE*, *gspC*, *gspJ* caused reduced virulence in rice panicles suggesting the role of T2SS in the full virulence of the bacterium (Figure 1.2c) (Goo et al., 2010). Similarly, a *B. glumae* clinical isolate AU6208 defective in *lipA* gene, which encodes the lipase LipA, was much less pathogenic to rice compared with the WT strain. A mutation in the T2SS caused reduced lipase activity in the medium suggesting lipase can potentially be secreted through the T2SS (Figure 1.2c) (Devescovi et al., 2007). The LipA gene homolog is also found in *B. gladioli* strain BSR3 and shares 87% amino acid identity to *B. glumae* BGR1 LipA (Fory et al., 2014). The *pehA* gene, encoding polygalacturonases in *B. cepacia* strain ATCC 25416 has a homolog in *B. glumae.* The enzyme is an important virulence factor in *B. cepacia* whereas in *B. glumae,* the *pehA* and *pehB* single mutants were not impaired in rice panicle symptoms compared to the WT

(Figure 1.2c) (Degrassi et al., 2008, Gonzalez et al., 1997). In rice infection model, *B*. *glumae* BGR1 *gspD* mutant had 50-100 times lower cfu/panicle compared to WT. Along with the T3SS mutant, the T2SS mutant *gspD* had reduced growth *in planta* that may have contributed to reduced colonization and reduced virulence compared to the WT (Kang et al., 2008).

T3SS: Both *B. glumae* and *B. gladioli* have a single *hrp2* type T3SS (Wallner et al., 2021). The T3SS genes in *B. glumae* strain BGR1 and *B. gladioli* BSR3 were nearly identical (Seo et al., 2015). Both genomes encode for the putative type III secreted proteins: HrpK1 a putative T3SS translocator, an Hrp kinase domain-encoding effector, and an Awr-family protein. An additional YgbK domain containing putative effector protein was found in *B. gladioli* strain BSR3 but not in *B. glumae* strains. Putative effectors XopAL1 and HrpW harpin were present in *B. glumae* strain BGR1 but absent in *B. gladioli* strain BSR3 (Fory et al., 2014, Nguyen et al., 2017). The candidate harpin-like effector HrpW in *B. glumae* carries a different enzymatic domain compared to the typical pectate lyase domain found in HrpW harpin of *P. syringae* pv. tomato DC3000 (Charkowski et al., 1998). The prediction and annotation of these candidate effectors are based solely on homology and none of these candidates have been confirmed as T3SS secreted. The T3SS mutant *hrcC* had highly reduced diseased severity and cfu/panicle count in rice compared to the WT (Figure 1.2c). The *hrp* regulatory system in *B. glumae* is mediated by an AraC-type transcriptional activator HrpB. Mutation in most of the *hrp*T3SS genes caused the elimination of Tobacco HR response by *B. glumae* except for *hrpK* and *hpaP*. The *hrpK*-based HR response was cell density-dependent as the concentration above 10^7 CFU/ml elicited HR response while below 10^6 CFU/ml failed to induce HR (Kang et al., 2008).

While the studies in *B. glumae* suggest the positive role of T3SS in rice panicle symptoms, the role of *B. gladioli* T3SS in plant pathogenesis has not been established. Its role in

mycophagy through the injection of a prophage-tail-like effector has been reported (Swain et al., 2017). *B. gladioli* strain NGJ1 inhibited sclerotia growth and *Rhizoctonia solani* when treated with NGJ1 was unable to cause disease in rice and tomato. NGJ1 strain defective in T3SS *hrcC* was defective in its mycophagous ability. In the *in silico* analysis of NGJ1 secreted 35 candidate proteins, one protein Bg_9562 shared similarity with a phage tail protein and had a T3SS secretion signal. The T3SS mutants synthesized Bg_9562 protein but were not able to deliver the protein into the fungi and were unable to forage on the fungus. The protein, when expressed heterologously in *Ralstonia solanacearum* was able to gain mycophagous activity over *R. solani.* Low calcium level was later found to promote mycophagous ability of NGJ1. (Swain et al., 2017). The Bg_9562 mutant with deleted type III secretion signal in *Ralstonia solanacearum* was unable to cause wilting in tomato. The Bg_9562 effector when expressed in *R. solanacearum* T3SS- strain was unable to cause wilting in tomato suggesting the Bg_9562 delivery is dependent upon the T3SS in *R. solanacearum* (Chandan et al., 2023). A plethora of hydrolyzing enzymes were also secreted by NGJ1 extracellularly during low calcium condition. Of them, a potential T3SS effector β-1, 3- glucanase mutant was impaired in its mycophagous ability. The orthologs of Bg_9562 was found in other *B. gladioli* strains but not in other related *Burkholderia* species (Yadav et al., 2020). The role of *B. gladioli* T3SS in pathogenesis needs to be explored.

B. gladioli strain BSR3 and *B. plantarii* strain ATCC 43733 are reported to have a T4SS while it is absent in *B. glumae* strain BGR1. Whether it functions as an effector translocation system or conjugation system is not clear. The Type VI Secretion system (T6SS) is widely distributed in members of *B. glumae*, *B. gladioli,* and *B. plantarii.* Six different groups of T6SS were described based on their distribution in seven studied strains from plant pathogenic

Burkholderia group. *B. gladioli* strain BSR3 had group 1, 3, and 6 type T6SS and *B. glumae* strain BGR1 had group 1, 2, 4, and 5 type T6SS (Seo et al., 2015). *B. gladioli* strain NGJ1 utilizes two T6SS to secrete TseTbg effectors to mediate contact dependent killing of coinhabiting bacteria. The bacteria utilize the cognate immunity protein TsiTBg to protect itself from the killing (Yadav et al., 2021).

Other factors

In the Two-Component System (TCSs) based regulation of T3SS in early-stage bacterial invasion, the Lon protease acts as a negative regulator by degrading HrpG and HrpR in *X. citri* and *P. syringae* respectively (Zhou et al., 2016, Zhou et al., 2018). In *B. glumae*, the *lon* mutant had increased expression of T3SS genes but was impaired in the Hypersensitive Response (HR) and displayed reduced symptoms in rice stems. The lon protease also activates the expression of the response regulator GluR, part of the GluS/GluR two component system. The *gluR* regulator which controls cell division in *B. glumae* regulates T3SS gene expression and contributes to disease symptoms in rice and elicits tobacco HR response (Marunga et al., 2021). The *gluS* mutant had comparable symptoms to that of WT. Neither of the *gluS* and *gluR* mutants had role in bacterial colonization ability of *B. glumae.* The study highlighted the essential role of lon protease in virulence but negative role in T3SS gene regulation of *B. glumae* BGR1 (Marunga et al., 2022).

The sensor histidine kinase and response regulator mutants *pidS* and *pidR* gene of *B. glumae* were significantly less virulent on rice panicles compared to the WT strain. The *pidS/pidR* mutants were also reduced in onion tissue maceration compared to the WT (Karki et al., 2012a).

Insertional mutation in the serine and purine biosynthesis pathway caused significant reduction in the gladiolus lesion length caused by *B. gladioli* pv. *gladioli*. Mutation in the purine biosynthesis pathway related *purM* gene also caused significant reduction in growth of bacterial cells *in planta*. The *purM* mutant was also significantly reduced in toxoflavin production. The authors speculated that the growth defect of *purM* mutant *in planta* may be due to unavailability of nutrients to plants. Complementation of *purM* mutant restored the bacterial growth but only partially restored the lesion size on leaf (Endo et al., 2022). The *purM* gene encodes for aminoimadizole ribotide, a precursor of GTP. As GTP is a precursor of Toxoflavin biosynthetic pathway (Suzuki *et al.*, 2004), the inability of *purM* mutant to produce GTP precursor might have resulted in loss of toxoflavin production. Mutation in *serC* gene that encodes phosphoserine aminotransferase, did not impair bacterial growth *in planta* and mutant was not impaired in toxoflavin production (Endo et al., 2022).

Thiosulfinate tolerance gene (TTG) cluster

Onion, garlic and other *Allium* species, upon cell death, produce potent organosulfur phytoanticipins called thiosulfinates. In onion, thiosulfinates are produced when the enzyme alliinase, which is stored in vacuoles, mixes with the predominant cysteine sulfoxide precursor isoalliin in the cytoplasm after cellular decompartmentalization (Hughes et al., 2005; Lancaster & Collin, 1981). Thiosulfinates are highly reactive with cellular thiols and deplete the reduced glutathione pool, interfering with functioning of critical enzymes and cellular homeostasis (Müller et al., 2016; Reiter et al., 2020).

TTG clusters comprise a set of 7–11 clustered genes identified in bacterial onion pathogens *B. gladioli*, *B. cepacia*, *B. orbicola*, *Pantoea ananatis* and the garlic saprophyte *Pseudomonas fluorescens* PfAR-1. The cluster consists of thiol/redox-associated genes that

contribute to allicin tolerance in vitro (Borlinghaus et al., 2020; Stice et al., 2020). Additionally, the seven-gene *Burkholderia* TTG cluster contributed to improved growth of *B. cepacia*, Bga and *B. orbicola* in clarified onion juice and to Bga onion foliar necrosis and bacterial population. However, the cluster was inconsequential for Bga, *B. cepacia* and *B. orbicola* both for production of onion scale necrosis symptoms and bacterial population in scales (Paudel et al., 2024). This is counter to what has been observed in the necrotrophic onion pathogen *P. ananatis* where its TTG mutant was reduced in both onion scale necrosis and bacterial population in scales (Stice et al., 2020). *Burkholderia* onion pathogens might evade or suppress the production of thiosulfinates in necrotized onion scale tissue using unknown mechanisms.

The quorum sensing system as a regulatory switch for multiple virulence factors in *Burkholderia*

Quorum sensing (QS) is a bacterial cell density-dependent mechanism by which bacteria regulate different physiological, biochemical, enzymatic, conjugative, and virulence activities (Aguilar et al., 2003b, Fuqua et al., 1996, Lewenza & Sokol, 2001, Miller & Bassler, 2001). The QS system requires the synthesis of small signaling molecules which when detected by its receptor at a critical level regulate QS target genes. The signaling molecules often are N-acyl-L-homoserine lactones (AHLs) that are produced by LuxI family proteins. Members in the genus *Burkholderia* respond to six types of AHLs (C6, C8, C10, OHC8-HSL, OHC10-HSL, OC14-HSL) (Choudhary et al., 2013). In *B. glumae*, two types of AHL molecules N-octanoyl homoserine lactone (C8-HSL) and N-hexanyl homoserine lactone (C6-HSL) are produced (Kim et al., 2004). The AHL independent transcriptional factor LuxR binds to AHL which in general functions as a transcriptional activator with some exceptions.

The QS protein orthologs of *cepI* and *cepR* first reported in *B. cepacia* are distributed in all known species of *Burkholderia* (Lewenza et al., 1999). In *B. glumae* and *B. gladioli*, the CepI and CepR homologs are named *tofI* and *tofR* respectively. Besides *cepR*, *B. cenocepacia* also encodes a genomic island CciIR (cenocepacia island IR) system in which LuxI homolog CciI produces N-hexanoyl-L-homoserine lactose as a major AHL and CciR acts as a repressor as opposed to CepR (Malott et al., 2005). *B. cenocepacia* strain H111 lacks the CciIR QS system. In addition to the CepIR system, an orphan independent CepR2 system is also reported in *B. cenocepacia* strains (Malott et al., 2009). Non-AHL signaling molecules are also produced by some species of Bcc like *B. cenocepacia* (HHQ) and *B. ambifaria* (HMAQ) (Diggle et al., 2006, Vial et al., 2008). Fatty acid signaling molecule called *Burkholderia* Diffusible Signalling Factor (BDSF) is also reported in members of Bcc. The BDSF has been shown to negatively regulate intracellular cyclic diGMP levels (Deng et al., 2012).

The *rsaM* like gene was first reported in *P. fuscovaginae* QS system in between the LuxIR homologs *pfsI* and *pfsR* genes (Mattiuzzo et al., 2011). The protein encoded by *rsaM* did not show homology with any functionally characterized proteins. The presence of *rsaM*-like genes is shown to be distributed in β and δ proteobacteria genus like *Burkholderia, Actinetobacter*, *Acidithiobacillus*, and *Halothiobacillus* (Michalska et al., 2014). The RsaM protein has been found to downregulate AHL production in both *P. fuscovaginae* and *B. cepacia* (Mattiuzzo et al., 2011, Michalska et al., 2014). Deletion of *rsaM* homologs caused enhanced production of *N*-acyl-L-homoserine lactones in both *B. cenocepacia* strain H111 and *P. fuscovaginae* (Mattiuzzo et al., 2011, Michalska et al., 2014). The *B. cenocepacia* strain J2315 RsaM has a novel protein fold, but no known DNA-binding motifs in the monomer state were found. No interaction of Bc RsaM was observed with OHL for CepIR system and no evidence of

conformational or oligomerization state change of the protein triggered by the ligand molecule was observed. No solid evidence consistent with the regulation mechanism of the QS system by Bc RsaM has been observed. Studies however suggest the possible post transcriptional and/or post translational level regulation of QS system by RsaM protein (Michalska et al., 2014).

The first discovered QS-regulated trait in BCC was production of the siderophore ornibactin in clinical *B. cenocepacia* strain K56-2 (Sokol et al., 1999). Similarly, biofilm formation on abiotic surfaces, swarming motility, swimming motility, and production of different extracellular enzymes are quorum regulated traits in *Burkholderia*. The *cepIR* system in *B. cepacia* strain ATCC 25416 regulates polygalacturonase, proteases production and the stationary sigma factor RpoS, which helps in bacterial adaptation to heat, and oxidative stress. The sigma factor RpoS is negatively regulated by CepIR QS system. The *B. cepacia* Type strain ATCC 25416 *cepI* and *cepR* mutants were reduced in onion maceration compared to the WT strain (Figure 1.2a) (Aguilar et al., 2003a).

B. cenocepacia strain H111 and *B. cenocepacia* K56-2 QS mutants were abolished in protease production (Huber et al., 2001, Lewenza et al., 1999). Lipase production was unchanged in the *B. cenocepacia* H111 *cepI* or *cepR* mutant strains whereas in the *B. cenocepacia* K56-2 QS *cepR* mutant was reduced in lipase activity compared to the WT strain (Huber et al., 2001, Lewenza et al., 1999). Similarly, the discrepancies in the siderophore production by the QS mutants between *B. cenocepacia* strains K56-2, H111 and *B. cepacia* strain ATCC 25416 is observed (Aguilar et al., 2003a, Huber et al., 2001, Lewenza et al., 1999). The bacterial secretion system is also quorum regulated in *B. cenocepacia.* The T2SS genes were found to be negatively regulated by *cepIR* system whereas the expression of T3SS gene cluster was positively regulated by *cepI* in *B. cenocepacia* strain K56-2 (Figure 1.2b) (Subsin et al., 2007). Similarly, the T6SS in

B. cenocepacia is also quorum regulated. The LysR transcriptional regulator that exhibits shiny colony phenotype in strain K56-2 is also quorum regulated (O'Grady et al., 2009). The AidA protein, that contributes to slow killing of *C. elegans* by *B. cenocepacia* strain H111 is CepIR QS system regulated (Huber et al., 2004). Reciprocal and hierarchical regulation is observed between the three QS systems *cepI*/*cepR*, *cciI*/*cciR*, *cepR2* and a considerable overlap is found in the QS target genes in multiple strain background (Subramoni & Sokol, 2012). Readers are directed to review elsewhere on the detailed QS architecture and *cepI*/*cepR, cciI*/*cciIR*, *cepR, rpfF*/*rpfR* regulated traits in Bcc (Ganesh et al., 2020, Subramoni & Sokol, 2012, Suppiger et al., 2013).

The QS regulated traits in *B. cenocepacia* seem to have varying roles depending on the infection model, genomovar and strains under test. Gotschlich and team didn't find the correlation between AHL production and pathogenic potential in some clinical isolates of Bcc. However, the author didn't rule out the possibility of AHL negative strains in *in vitro* model could produce AHL during infection (Gotschlich et al., 2001). In the alfalfa infection model, *B. cenocepacia* strain H111 *cepI* and *cepR* mutants produced less severe symptoms compared to WT whereas in *B. cenocepacia* strain K56-2 *cepI* mutant had no effect on virulence (Figure 1.2b). The *cciI* single mutant and *cepIcciI* double mutants produced similar alfalfa seedling symptoms compared to the WT strain (Uehlinger et al., 2009).

The QS system also regulates multiple virulence trait in *B. glumae* and *B. gladioli.* T2SS delivered proteases and lipases in *B. glumae* are also known to be QS regulated (Figure 1.2c) (Goo et al., 2010). The QS system was also shown to regulate the production of toxoflavin and lipase in the *B. glumae* Type strain ATCC 33617 and clinical isolate AU6208 (Figure 1.2c) (Devescovi et al., 2007). The extracellular protease activity, encoded by metalloprotease *prtA* in

B. glumae 336gr-1 is mediated in a T2SS dependent manner (Figure 1.2c). The *tofIMR* mutant had abolished extracellular protease activity. However, the *tofI*, *tofM,* and *tofR* single mutant still retained the enzymatic activity (Lelis et al., 2019). *B. glumae* QS mutants were reduced in growth in both solid and liquid media compared to the WT strain at 37^0C (Chen et al., 2012). The production of toxoflavin by *tofI* and *tofR* single mutant on *B. glumae* strain 336gr-1 on solid medium was dependent on the method of inoculation (Chen et al., 2012). The strain specific differences in *tofI* dependent toxoflavin production on solid medium was evident for *B. glumae* strains BGR1 and 336gr-1 on multiple independent studies (Kim et al., 2004)0; (Kim et al., 2007); (Kato et al., 2014). The QS *tofI-tofR* mutant derivative in hypervirulent *B. glumae* strain 411gr-6 produced toxoflavin comparable to the less virulent strain 336gr-1. The *tofI-tofR* mutant in strain 336gr-1 was almost abolished in toxoflavin production (Lelis et al., 2023). This suggests the dependency of toxoflavin production by *B. glumae* on culture conditions, inoculation method and strain under study (Chen *et al.*, 2012; Kim et al., 2007). The deletion of *ΔtofM* mutant on *ΔtofI* or *ΔtofR* background completely abolished toxoflavin production suggesting the requirement of *tofM* for normal production of toxoflavin (Chen et al., 2012).

The SAM dependent methyltransferase which is required for biosynthesis of toxoflavin is also regulated by QS in *B. glumae* (Kang et al., 2019). The QS system also regulates the expression of toxoflavin biosynthesis *toxABCDE* and transport *toxFGHI* operon (Figure 1.2c). Besides toxoflavin production, the QS system also regulates arginine degradation, phosphate transport, flagellar motility, *katG* catalase activity, and fatty acid β oxidation in *B. glumae* (Chun et al., 2009, Kim et al., 2013). The *tofI* mutant of the clinical *B. glumae* isolate AU6208 was significantly reduced in rice panicle blight symptoms and seed germination compared to the WT strain (Figure 1.2c). The QS system was also shown to regulate the production of toxoflavin and

lipase in the *B. glumae* Type strain ATCC 33617 (Devescovi et al., 2007). The rice panicle symptoms caused by *B. glumae* WT strain 336gr-1, and the QS single mutants *tofI*, and *tofR* were indistinguishable whereas the *tofM* and *tofI-tofR* mutants in the same strain caused significantly reduced panicle symptoms and onion maceration area compared to the WT strain (Figure 1.2c). The *tofR* mutant caused significantly reduced onion maceration area whereas *tofI* mutant produced comparable symptoms to WT (Chen et al., 2012). In another independent study, the QS *tofI-tofR* mutants in both *B. glumae* strains 336gr-1 and 411gr-1 produced rice panicle symptoms, albeit substantially less than their WT counterparts (Lelis et al., 2023).

Motility is a critical component for the virulence of *B. glumae* strain BGR1. The *ΔtofI* mutant had normal flagella at 28^0C but lost swarming activity. At 37^0C, the QS deficient mutant lost flagella (Figure 1.2c). The quorum sensing master regulator (*qsmR*) gene, an IclR-type transcriptional regulator, is essential for the formation of flagella by *B. glumae* (Kim et al., 2007). The BGR1 *qsmR* mutant still showed slight swarming motility while *tofI* had completely defective motility suggesting the tighter regulation of motility by *tofI* compared to *qsmR* (Kim et al., 2013). The BGR1 *qsmR* regulator was found to be dependent upon *tofI/tofR* system for its expression but in strain 336gr-1, the *qsmR* was expressed independent of *tofIMR* QS system (Chen et al., 2015, Kim et al., 2007, Lelis et al., 2023). In *B. glumae* strains 336gr-1 and 411gr-1, Δ*qsmR* was abolished in LB agar toxoflavin production (Chen et al., 2015, Lelis et al., 2023). This was different to strain BGR1 Δ*qsmR*, where the toxoflavin production in solid media was comparable to WT (Kim et al., 2007). When the pathogenicity of the two strains was compared, the BGR1 strain *ΔqsmR* had a dramatic reduction in rice panicles disease score and the Bgr 336gr-1 *ΔqsmR* strain was also dramatically reduced in onion scale maceration area compared to the WT, Δ*tofI*, Δ*tofR*, and Δ*tofM* single mutants (Figure 1.2c) (Chen et al., 2015, Kim et al.,

2007). The *qsmR* mutant in strains 336gr-1 and 411gr-1 produced more pronounced reduction in rice panicle symptoms and bacterial population recovery compared to their *tofI-R* mutant derivatives. A *qsmR* clone from *B. glumae* strain 336 gr-1 when introduced into the avirulent *B. glumae* strain background 257 sh-1 restored toxoflavin production and virulence of strain 257 sh-1 in onion scales, rice kernels, and rice sheaths (Lelis et al., 2023). The variation in regulatory system by this master regulator among these closely related *B. glumae* strains BGR1 and 336gr-1 was noteworthy. The expression of *katG* gene, which encodes for a major catalase, is regulated by *qsmR*. Deletion of *katG* gene reduced the disease severity of rice panicles (Figure 1.2c) (Chun et al., 2009). Like the *tofIMR* mutant, the *qsmR* mutant in 336gr-1 was also abolished in extracellular protease activity and was almost abolished in toxoflavin production in both LB Broth and LB agar. This suggests a pivotal role of both *qsmR* and *tofIMR* systems in the regulation of multiple virulence factors in *B. glumae.* The findings suggest the shared regulatory pathway between QS *tofIMR* and *qsmR* system in the regulation of toxoflavin production and extracellular protease activity (Lelis et al., 2019).

There are other regulatory factors with some capacity to compensate for the absence of *tofI* and *tofR*. The *dgcB* gene which encodes for a component of the c-di-GMP signaling pathway, the *wzyB* gene encoding a putative O-antigen polymerase family protein, *flhD* gene encoding a transcriptional activator for flagellar biosynthesis, and *toxK* gene found upstream of *toxJ* contributed to quorum sensing independent production of toxoflavin. The *B. glumae* 336gr-1 *dgcB* mutant in *tofI* background produced the least onion scale maceration area compared to Δ*qsmR*, Δ*tofI*, Δ*tofM*, Δ*tofR*, and WT strain (Chen et al., 2015).

The *Burkholderia gladioli* pv. *agaricicola* strain ICMP11096 QS mutant *tofI* was abolished in production of cellulase, amylase, pectinase, and polygalacturonase (Figure 1.2d)

(Elshafie et al., 2019). The QS system is *B. gladioli* BSR3 strain also regulates key processes in the bacterium such as inositol phosphate metabolism pathway, glyoxylate cycle, oxalate synthesis, and swarming motility. The *qsmR* homolog and *flhDC* genes encoding a master flagella regulator, expression in *B. gladioli* strain BSR3 were QS independent. (Kim et al., 2014).

The *B. gladioli* natural variant strain KACC11889 encodes all toxoflavin biosynthesis and transport-related genes with high homology to genes from other *B. gladioli* strain BSR3 and KCTC12374. However, quorum sensing related genes were absent and the strain did not produce toxoflavin. The QS genes from *B. glumae* strain BGR1 and *B. gladioli* strain BSR3, when transformed and expressed in KACC11889 restored the production of toxoflavin in the strain (Figure 1.2d). The *tofIMR* complemented natural variant strain restored its virulence and caused similar damage to rice seedlings and onion scales as the *B. glumae* strain BGR1 and *B. gladioli* strain BSR3. Thus, QS system in *B. gladioli* BSR3 also regulates toxoflavin production and virulence factors (Figure 1.2d) (Lee et al., 2016). The *B. gladioli* pv. *agaricicola tofI* mutant was reduced in *Agaricus bisporus* (button mushroom) necrosis compared to the WT (Elshafie et al., 2019). Pineapple isolated avirulent *B. gladioli* strain UAPS0070 QS *tofI* and *tofR* mutants did induce onion bulb tissue maceration whereas in lettuce, the mutants exhibited reduced virulence (Figure 1.2d). The mutants were also impaired in swarming motility and antagonism against *Acinetobacter* sp. (Seynos-García et al., 2019).

Conclusion

Multiple members of the *Burkholderia* genus are routinely associated with plant diseases. Despite being first discovered as an onion pathogen, the virulence determinants and disease-causing mechanism of *B. cepacia* and other onion-pathogenic *Burkholderia* members are only partially understood. The virulence strategies employed by *Burkholderia* onion pathogens have

been shown to vary between species. The phytotoxin toxoflavin is described as an important virulence component of *B. glumae* and *B. gladioli* whereas members in the Bcc group producing this toxin have not been identified. Similarly, the PTW phenotype caused by T4SS is described in *B. cenocepacia* but whether the uncharacterized T4SS identified in *B*. *gladioli* performs similar functions is not clear. The well-characterized rice pathogen *B*. *glumae* serves as a valuable reference for the study of *B*. *gladioli* plant pathogenesis and virulence strategies. However, nuanced differences would be expected for virulence on rice and onion hosts. The strain-specific differences, genetic diversity, ecological adaptability and use of multiple infection models further adds to the complexity in understanding virulence determinants in *Burkholderia* species. For instance, the PGase-encoding *pehA* contributes to virulence in *B*. *cepacia* but its single mutant homologues *pehA* and *pehB* in *B*. *glumae* strains were not observed to contribute to rice panicle symptoms (Degrassi et al., 2008; Gonzalez et al., 1997). Similarly, the role of toxoflavin in the production of rice seedling symptoms is variable depending on the strain under study. The alfalfa infection model is commonly used to characterize the functional role of predicted virulence factors in *B*. *cenocepacia*. As multiple virulence factors have been shown to perform strain-specific roles in human/animal model infections, the possibility that the alfalfa-tested virulence factors perform a different role in alternate plant infection models like onion cannot be overlooked.

For many bacterial plant pathogens, virulence hinges on a key pathogenicity factor, for instance, the *hrp2* T3SS of *Xanthomonas* spp. or the T2SS-mediated secretion of plant cell wall-degrading enzymes by *Dickeya* spp. *Burkholderia* plant pathogens seem to deviate from conventional patterns of bacterial plant pathogen virulence strategies. Findings from multiple *Burkholderia* studies indicate that T2SS, T3SS and toxoflavin all make partial

contributions to plant disease. Translocated T3SS effectors have not yet been functionally characterized in onion-pathogenic *Burkholderia* species. *B. gladioli* isolates are also known to produce a variety of secondary metabolites in addition to toxoflavin. The role of these compounds in plant virulence is far less explored. Numerous uncharacterized secondary metabolites in *Burkholderia* could play roles in plant disease. The QS system is conserved across the *Burkholderia* genus and has been shown to regulate critical virulence factors such as toxoflavin, catalase, lipase and T2SS. The QS system and IclR- family transcriptional regulator, *qsmR*, seems to be critical for the interaction of *Burkholderia* isolates with rice, onion and other plant hosts. The diversity of virulence strategies employed by onion-pathogenic *Burkholderia* species pose challenges for disease management and accurate identification in field settings. The variable virulence role of the Bga TTG clusters in onion leaves compared to scales suggests the bacteria employ onion tissue-specific virulence strategies to infect the host. This tissue-to-tissue variation should be considered when assessing genetic resistance or tolerance to these pathogens. Additional research will be essential to unravel the pivotal bacterial genetic factors influencing *Burkholderia* onion disease.

Addendum

Knowledge gap

Despite being first reported as an onion rot pathogen in the 1930s, the research focus on members of *Burkholderia* genus is mostly centered around the development of antibiotics and drug discoveries for the cure of immunocompromised patients. The plant pathogen interactions aspects and virulence determinants for members in this genus are still not well understood.

It appears that the virulence in *B. glumae* is enhanced through multiple genetic determinants regulated by a complicated interplay of different regulatory elements. Toxoflavin has been long studied as a primary virulence factor in *B. glumae* with a role in blade necrosis and panicle chlorosis in rice. However, the role of toxoflavin in onion scale necrosis is still unclear. The role of type III secretion system in rice panicle necrosis by *B. glumae* has been documented. The *in silico* analysis predicted the presence of type III clusters in *B. gladioli* and *B. cepacia* strains but its functional role in plant disease phenotype has not been shown. The quorum sensing related *tofIMR* system is well conserved in the *Burkholderia* genus and has been shown to regulate putative virulence factors such as toxoflavin production, T2SS, T3SS, glycoxylate cycle, and motility to name a few. Plasmid-based expression of quorum sensing *tofIMR* system in *tofIMR* negative *B. gladioli* variant strain restored toxoflavin production and virulence in rice seedlings. However, the major virulence factor regulated by the quorum sensing system is still not clear.

The onion tissue specific virulence role of the thiosulfinate tolerance gene (TTG) clusters in Bga was discussed in the section above. However, key questions remain regarding the interaction between Bga and thiosulfinates in onion scale tissue. It is unclear whether Bga actively avoids thiosulfinate exposure in the scales or if it inhibits thiosulfinates production in scale tissue, thereby creating a less hostile environment. Alternatively, Bga may employ different tolerance mechanisms in the scales that are independent of the TTG cluster. The factors driving this tissue-specific reliance on the TTG cluster and whether thiosulfinate tolerance is necessary at all during scale infection remain unknown. Addressing these gaps could elucidate the strategies employed by Bga to overcome onion defenses and establish infection across different onion tissue types.

Objectives

The overall goal of this study is to characterize the putative determinants of virulence in bacterial onion pathogen *Burkholderia gladioli* pv. *alliicola* (Bga) and study the distribution, functional role and tissue specific virulence role of Thiosulfinate tolerance gene (TTG) cluster in Bga. To accomplish this aim, three objectives have been set:

1. Study the distribution and functional role of putative Thiosulfinate tolerance gene (TTG) gene clusters in *Burkholderia* onion pathogens.
2. Characterize the putative determinants of virulence in bacterial onion pathogen Bga.
3. Investigate the interactions between thiosulfinates and *Burkholderia gladioli* pv. *alliicola* in onion tissues.

Significance of research

Onion is a globally important vegetable crop, yet the disease mechanisms and virulence factors of the bacterial pathogen *Burkholderia gladioli* pv. *alliicola* (Bga) remain poorly understood. Despite being closely related, the virulence strategies employed by the three onion pathogens—Bga, *B. cenocepacia*, and *B. cepacia*—appear to be distinct. For example, *B. cepacia* utilizes the pectic enzyme hydrolase (PehA) to degrade plant cell walls, while *B. cenocepacia* employs the type IV secretion system to induce necrosis. In contrast, toxoflavin has been proposed as a key virulence factor in *B. gladioli* (Gonzalez et al., 1997; Lee et al., 2016; Zhang et al., 2009). These diverse pathogenic strategies highlight the complexity of onion bacterial diseases and underscore the need for research on pathogen biology and host-pathogen interactions to inform effective disease management strategies.

Through our functional genetics study, we aim to unravel the Bga pathosystem and identify key genetic determinants responsible for its disease phenotype. A deeper understanding of bacterial virulence mechanisms will enable us to distinguish aggressive isolates from mild or non-pathogenic ones. Additionally, our findings could provide potential molecular targets for disease resistance screening, paving the way for the development of resistant onion varieties in the future.

The variable virulence role of Bga TTG clusters depending on the onion tissue type was discussed in the section above. The indifferent role of Bga TTG clusters in onion scale colonization and necrosis area was surprising as onion bulbs produce higher thiosulfinates than leaf tissue (Cho et al., 2024). This study seeks to explore the interactions between onion-derived thiosulfinates and Bga in scales to further understand the phenomenological basis of Bga virulence based on onion tissue type. Understanding if Bga induces the release of thiosulfinates in scale tissue will further open avenues to explore if Bga evades thiosulfinates exposure or inhibits its production in the scale tissue. Gaining insights into these interactions could provide valuable information on how Bga adapts to and potentially circumvents the antimicrobial properties of thiosulfinates in onion scales. By deepening our understanding of Bga's behavior in scale tissue, this research has the potential to uncover fundamental aspects of bacterial pathogenesis in onion. These findings may not only shed light on Bga's adaptive mechanisms but also broaden our knowledge of pathogen interactions with host plant tissues, ultimately informing strategies for managing bacterial diseases in crops.

Among plant-pathogenic *Burkholderia* species, *B. glumae* is relatively well characterized. Its close phylogenetic relative, *B. gladioli*, has also been found to infect rice, and a strong correlation has been observed between disease severity in rice and the maceration area in onion

for *B. glumae*. While onion serves as a suitable surrogate host for functional genetic studies on *B. gladioli*, findings from *B. glumae* cannot be directly applied to *B. gladioli* due to the remarkable metabolic diversity within the *Burkholderia* genus. Nevertheless, given their close evolutionary relationship, *B. glumae* remains an important reference for studying *B. gladioli*.

As the second most widely cultivated vegetable crop worldwide, onion is an essential component of culinary traditions across cultures. However, the ability of *Burkholderia* species to thrive in the onion rhizosphere and cause severe disease poses a significant challenge to onion production. Understanding pathogen behavior and disease mechanisms is a critical first step in developing effective control strategies against these bacterial threats.

References

Abachi, H., Moallem, M., Taghavi, S., Hamidizade, M., Soleimani, A., Fazliarab, A. et al. (2024) Garlic bulb decay and soft rot caused by the cross-kingdom pathogen *Burkholderia gladioli*. *Plant Disease*, **108**, 684–693.

Abe, M. & Nakazawa, T. (1996) The *dsbB* gene product is required for protease production by *Burkholderia cepacia*. *Infection and Immunity*, **64**, 4378–4380.

Agnoli, K., Frauenknecht, C., Freitag, R., Schwager, S., Jenul, C., Vergunst, A. et al. (2014) The third replicon of members of the *Burkholderia cepacia* complex, plasmid pC3, plays a role in stress tolerance. *Applied and Environmental Microbiology*, **80**, 1340–1348.

Aguilar, C., Bertani, I. & Venturi, V. (2003a) Quorum-sensing system and stationary-phase sigma factor (rpoS) of the onion pathogen *Burkholderia cepacia* genomovar I type strain, ATCC 25416. *Applied and Environmental Microbiology*, **69**, 1739–1747.

Aguilar, C., Friscina, A., Devescovi, G., Kojic, M. & Venturi, V. (2003b) Identification of quorum-sensing-regulated genes of *Burkholderia cepacia*. *Journal of Bacteriology*, **185**, 6456–6462.

Alfano, J., Charkowski, A., Deng, W., Badel, J.L., Petnicki-Ocwieja, T., van Dijk, K. et al. (2000) The *pseudomonas syringae* Hrp pathogenicity Island has a tripartite mosaic structure composed of a cluster of type III secretion genes bounded by exchangeable effector and conserved effector loci that contribute to parasitic fitness and pathogenicity in plants. *Proceedings of the National Academy of Sciences of the United States of America*, **97**, 4856–4861.

Angot, A., Peeters, N., Lechner, E., Vailleay, F., Baud, C., Gentzbittel, L. et al. (2006) *Ralstonia solanacearum* requires F-box-like domain-containing type III effectors to promote disease on several host plants. *Proceedings of the National Academy of Sciences of the United States of America*, **103**, 14620–14625.

Asselin, J., Bonasera, J.M. & Beer, S.V. (2016) PCR primers for detection of *Pantoea ananatis*, *Burkholderia* spp., and *Enterobacter* sp. from onion. *Plant Disease*, **100**, 836–846.

Azegami, K., Nishiyama, K., Watanabe, Y., Kadota, I., Ohuchi, A. & Fukazawa, C. (1987) *Pseudomonas plantarii* sp. nov., the causal agent of rice seedling blight. *International Journal of Systematic and Evolutionary Microbiology*, **37**, 144–152.

Bach, E., Santanna, F.H., Dos Santos Seger, G.D. & Lmp, P. (2022) Pangenome inventory of *Burkholderia sensu lato*, *Burkholderia sensu stricto*, and the *Burkholderia cepacia* complex reveals the uniqueness of *Burkholderia catarinensis*. *Genomics*, **114**, 398–408.

Baldwin, A., Sokol, P., Parkhill, J. & Mahenthiralingam, E. (2004) The *Burkholderia cepacia* epidemic strain marker is part of a novel genomic Island encoding both virulence and metabolism-associated genes in *Burkholderia cenocepacia*. *Infection and Immunity*, **72**, 1537–1547.

Bartholdson, S., Brown, A., Mewburn, B., Clarke, D.J., Fry, S.C., Campopiano, D.J. et al. (2008) Plant host and sugar alcohol induced exopolysaccharide biosynthesis in the *Burkholderia cepacia* complex. *Microbiology*, **154**, 2513–2521.

Baxter, I.A., Lambert, P.A., & Simpson, I.N., (1997). Isolation from clinical sources of *Burkholderia cepacia* possessing characteristics of *Burkholderia gladioli*. *Journal of Antimicrobial Chemotherapy*, **39**, 169–175.

Bauernfeind, A., Schneider, I., Jungwirth, R. & Roller, C. (1999) Discrimination of *Burkholderia multivorans* and *Burkholderia vietnamiensis* from *Burkholderia cepacia* genomovars I, III, and IV by PCR. *Journal of Clinical Microbiology*, **37**, 1335–1339.

Bernier, S.P., Silo-Suh, L., Woods, D.E., Ohman, D.E. & Sokol, P.A. (2003) Comparative analysis of plant and animal models for characterization of *Burkholderia cepacia* virulence. *Infection and Immunity*, **71**, 5306–5313.

Borlinghaus, J., Bolger, A., Schier, C., Vogel, A., Usadel, B., Gruhlke, M.C.H. et al. (2020) Genetic and molecular characterization of multicomponent resistance of *Pseudomonas* against allicin. *Life Science Alliance*, **3**, e202000670.

Boucher, C.A., Van Gijsegem, F., Barberis, P.A., Arlat, M. & Zischek, C. (1987) *Pseudomonas solanacearum* genes controlling both pathogenicity on tomato and hypersensitivity on tobacco are clustered. *Journal of Bacteriology*, **169**, 5626–5632.

Burkholder, W. (1942) Three bacterial plant pathogens: *Phytomonas earyophylli* sp. n., *Phytomonas alliicola* sp. n., and *Phytomonas manihotis* (Arthaud-Berthet et Sondar) Viégas. *Phytopathology*, **32**, 141–149.

Burkholder, W. (1950) Sour skin, a bacterial rot of onion bulbs. *Phytopathology*, **40**, 115–117.

Burtnick, M.N., Brett, P.J. & Deshazer, D. (2014) Proteomic analysis of the *Burkholderia pseudomallei* type II secretome reveals hydrolytic enzymes, novel proteins, and the deubiquitinase TssM. *Infection and Immunity*, **82**, 3214–3226.

Butler, S.L., Doherty, C.J., Hughes, J.E., Nelson, J.W. & Govan, J.R. (1995) *Burkholderia cepacia* and cystic fibrosis: do natural environments present a potential hazard? *Journal of Clinical Microbiology*, **33**, 1001–1004.

Chandan, R., Kumar, R., Kabyashree, K., Kabyashree, K., Yadav, S.K., Roy, M. et al. (2023) A prophage tail-like protein facilitates the endophytic growth of *Burkholderia gladioli* and mounting immunity in tomato. *New Phytologist*, **240**, 1202–1218.

Charkowski, A.O., Alfano, J.R., Preston, G., Yuan, J., He, S.Y. & Collmer, A. (1998) The *Pseudomonas syringae* pv. *tomato* HrpW protein has domains similar to harpins and pectate lyases and can elicit the plant hypersensitive response and bind to pectate. *Journal of Bacteriology*, **180**, 5211–5217.

Chen, R., Barphagha, I. & Ham, J. (2015) Identification of potential genetic components involved in the deviant quorum-sensing signaling pathways of *Burkholderia glumae* through a functional genomics approach. *Frontiers in Cellular and Infection Microbiology*, **5**, 22.

Chen, R., Barphagha, I., Karki, H. & Ham, J. (2012) Dissection of quorum-sensing genes in *Burkholderia glumae* reveals non-canonical regulation and the new regulatory gene tofM for toxoflavin production. *PLoS One*, **7**, e52150.

Cho, H., Park, J., Kim, D., Han, J., Natesan, K., Choi, M., Lee, S., Kim, J., Cho, K., and Ahn, B. 2024. Understanding the defense mechanism of *Allium* plants through the onion isoallicin-omics study. Frontiers in Plant Science 15:1488553.

Choudhary, S., Hudaiberdiev, S., Gelencsér, Z., Coutinho, B., Venturi, V. & Pongor, S. (2013) The organization of the quorum sensing luxI/R family genes in *Burkholderia*. *International Journal of Molecular Sciences*, **14**, 13727–13747.

Chowdhury, P. & Heinemann, J. (2006) The general secretory pathway of *Burkholderia gladioli* pv. *agaricicola* BG164R is necessary for cavity disease in white button mushrooms. *Applied and Environmental Microbiology*, **72**, 3558–3565.

Chun, H., Choi, O., Goo, E., Kim, N., Kim, H., Kang, Y. et al. (2009) The quorum sensing-dependent gene *katG* of *Burkholderia glumae* is important for protection from visible light. *Journal of Bacteriology*, **191**, 4152–4157.

Chung, J.W., Altman, E., Beveridge, T.J. & Speert, D.P. (2003) Colonial morphology of *Burkholderia cepacia* complex genomovar III: implications in exopolysaccharide production, pilus expression, and persistence in the mouse. *Infection and Immunity*, **71**, 904–909.

Cianciotto, N. (2005) Type II secretion: a protein secretion system for all seasons. *Trends in Microbiology*, **13**, 581–588.

Compant, S., Nowak, J., Coenye, T., Clément, C. & Ait Barka, E. (2008) Diversity and occurrence of *Burkholderia* spp. in the natural environment. *FEMS Microbiology Reviews*, **32**, 607–626.

Costa, T., Felisberto-Rodrigues, C., Meir, A., Prevost, M.S., Redzej, A., Trokter, M. et al. (2015) Secretion systems in gram-negative bacteria: structural and mechanistic insights. *Nature Reviews Microbiology*, **13**, 343–359.

Cunha, M., Sousa, S., Leitao, J., Moreira, L., Videira, P. & Sá-Correia, I. (2004) Studies on the involvement of the exopolysaccharide produced by cystic fibrosis-associated isolates of the *Burkholderia cepacia* complex in biofilm formation and in persistence of respiratory infections. *Journal of Clinical Microbiology*, **42**, 3052–3058.

Degrassi, G., Devescovi, G., Kim, J., Hwang, I. & Venturi, V. (2008) Identification, characterization and regulation of two secreted polygalacturonases of the emerging rice pathogen *Burkholderia glumae*. *FEMS Microbiology Ecology*, **65**, 251–262.

Deng, Y., Schmid, N., Wang, C., Wang, J., Pessi, G., Wu, D. et al. (2012) Cis-2-dodecenoic acid receptor RpfR links quorum-sensing signal perception with regulation of virulence through cyclic dimeric guanosine monophosphate turnover. *Proceedings of the National Academy of Sciences of the United States of America*, **109**, 15479–15484.

Devescovi, G., Bigirimana, J., Degrassi, G., Cabrio, L., LiPuma, J.J., Kim, J. et al. (2007) Involvement of a quorum-sensing-regulated lipase secreted by a clinical isolate of *Burkholderia glumae* in severe disease symptoms in rice. *Applied and Environmental Microbiology*, **73**, 4950–4958.

Diggle, S., Lumjiaktase, P., Dipilato, F., Winzer, K., Kunakorn, M., Barrett, D.A. et al. (2006) Functional genetic analysis reveals a 2-alkyl-4-quinolone signaling system in the human pathogen *Burkholderia pseudomallei* and related bacteria. *Chemistry & Biology*, **13**, 701–710.

Ding, Z., Atmakuri, K. & Christie, P.J. (2003) The outs and ins of bacterial type IV secretion substrates. *Trends in Microbiology*, **11**, 527–535.

Eberl L & Vandamme P, 2016. Members of the genus *Burkholderia*: good and bad guys. *F1000Res* 5, F1000 faculty Rev-1007.

Elshafie, H., Devescovi, G., Venturi, V., Camele, I. & Bufo, S. (2019) Study of the regulatory role of N-acyl homoserine lactones mediated quorum sensing in the biological activity of *Burkholderia gladioli* pv. *agaricicola* causing soft rot of *Agaricus* spp. *Frontiers in Microbiology*, **10**, 2695

Endo, A., Hamamoto, H. & Oshima, K. (2022) Serine and purine synthesis pathways are involved in the virulence of *Burkholderia gladioli*, the causative agent of gladiolus rot. *Journal of General Plant Pathology*, **88**, 55–62.

Engledow, A., Medrano, E., Mahenthiralingam, E., Lipuma, J. & Gonzalez, C. (2004) Involvement of a plasmid-encoded type IV secretion system in the plant tissue watersoaking phenotype of *Burkholderia cenocepacia*. *Journal of Bacteriology*, **186**, 6015–6024.

Fang, Y., Li, B., Wang, F., Liu, B.P., Wu, Z.Y., Su, T. et al. (2009) Bacterial fruit rot of apricot caused by *Burkholderia cepacia* in China. *The Plant Pathology Journal*, **25**, 429–432.

Félix-Gastélum, R., Maldonado-Mendoza, I., Olivas-Peraza, N., Brito-Vega, H., Peñuelas-Rubio, O. & Longoria-Espinoza, R. (2017) First report of slippery skin caused by *Burkholderia gladioli* in stored onion bulbs in Mexico. *Plant Disease*, **101**, 1030.

Ferreira, A., Leitao, J., Silva, I., Pinheiro, P.F., Sousa, S.A., Ramos, C.G. et al. (2010) Distribution of cepacian biosynthesis genes among environmental and clinical *Burkholderia* strains and role of cepacian exopolysaccharide in resistance to stress conditions. *Applied and Environmental Microbiology*, **76**, 441–450.

Ferreira, A.S., Silva, I.N., Oliveira, V.H., Cunha, R. & Moreira, L.M. (2011) Insights into the role of extracellular polysaccharides in *Burkholderia* adaptation to different environments. *Frontiers in Cellular and Infection Microbiology*, **1**, 16.

Flavier, A.B., Ganova-Raeva, L.M., Schell, M.A. & Denny, T.P. (1997) Hierarchical autoinduction in *Ralstonia solanacearum*: control of acyl-homoserine lactone production by a novel autoregulatory system responsive to 3-hydroxypalmitic acid methyl ester. *Journal of Bacteriology*, **179**, 7089–7097.

Fory, P., Triplett, L., Ballen, C., Abello, J.F., Duitama, J., Aricapa, M.G. et al. (2014) Comparative analysis of two emerging rice seed bacterial pathogens. *Phytopathology*, **104**, 436–444.

Fuqua, C., Winans, S. & Greenberg, E. (1996) Census and consensus in bacterial ecosystems: the LuxR-LuxI family of quorum-sensing transcriptional regulators. *Annual Review of Microbiology*, **50**, 727–752.

Furuya, N., Iiyama, K., Shiozaki, N. & Matsuyama, N. (1997) Phytotoxin produced by *Burkholderia gladioli*. *Journal of the Faculty of Agriculture, Kyushu University*, **42**, 33–37.

Furuya, N., Iiyama, K., Ueda, Y. & Matsuyama, N. (1997) Reaction of tobacco and rice leaf tissue infiltrated with *Burkholderia glumae* or *B. gladioli*. *Journal of the Faculty of Agriculture, Kyushu University*, **42**, 43–51.

Ganesh, P.S., Vishnupriya, S., Vadivelu, J., Mariappan, V., Vellasamy, K.M. & Shankar, E.M. (2020) Intracellular survival and innate immune evasion of *Burkholderia cepacia*: improved understanding of quorum sensing-controlled virulence factors, biofilm, and inhibitors. *Microbiology and Immunology*, **64**, 87–98.

Gerber, I., Zeidler, D., Durner, J. & Dubery, I. (2004) Early perception responses of *Nicotiana tabacum* cells in response to lipopolysaccharides from *Burkholderia cepacia*. *Planta*, **218**, 647–657.

Glendinning, K., Parsons, Y., Duangsonk, K., Hales, B.A., Humphreys, D., Hart, C.A. et al. (2004) Sequence divergence in type III secretion gene clusters of the *Burkholderia cepacia* complex. *FEMS Microbiology Letters*, **235**, 229–235.

Gonzalez, C., Pettit, E., Valadez, V. & Provin, E. (1997) Mobilization, cloning, and sequence determination of a plasmid-encoded polygalacturonase from a phytopathogenic *Burkholderia (Pseudomonas) cepacia*. *Molecular Plant–Microbe Interactions*, **10**, 840–851.

Goo, E., Kang, Y., Kim, H. & Hwang, I. (2010) Proteomic analysis of quorum sensing-dependent proteins in *Burkholderia glumae*. *Journal of Proteome Research*, **9**, 3184–3199.

Götschlich, A., Huber, B., Geisenberger, O., Tögl, A., Steidle, A., Riedel, K. et al. (2001) Synthesis of multiple *N*-acylhomoserine lactones is wide-spread among the members of the *Burkholderia cepacia* complex. *Systematic and Applied Microbiology*, **24**, 1–14.

Hall, C., Busch, J., Shippy, K., Allender, C.J., Kaestli, M., Mayo, M. et al. (2015) Diverse *Burkholderia* species isolated from soils in the southern United States with no evidence of *B. pseudomallei*. *PLoS One*, **10**, e0143254.

Ham, J.H., Melanson, R.A. & Rush, M.C. (2011) *Burkholderia glumae*: next major pathogen of rice? *Molecular Plant Pathology*, **12**, 329–339.

Herasimenka, Y., Cescutti, P., Impallomeni, G., Campana, S., Taccetti, G., Ravenni, N. et al. (2007) Exopolysaccharides produced by clinical strains belonging to the *Burkholderia cepacia* complex. *Journal of Cystic Fibrosis*, **6**, 145–152.

Hobson, A., Buckley, C., Aamand, J., Jorgensen, S., Diderichsen, B. & McConnell, D. (1993) Activation of a bacterial lipase by its chaperone. *Proceedings of the National Academy of Sciences of the United States of America*, **90**, 5682–5686.

Huber, B., Feldmann, F., Köthe, M., Vandamme, P., Wopperer, J., Riedel, K. et al. (2004) Identification of a novel virulence factor in *Burkholderia cenocepacia* H111 required for efficient slow killing of *Caenorhabditis elegans*. *Infection and Immunity*, **72**, 7220–7230.

Huber, B., Riedel, K., Hentzer, M., Haydorn, A., Gotschlich, A., Givskov, M. et al. (2001) The cep quorum-sensing system of *Burkholderia cepacia* H111 controls biofilm formation and swarming motility. *Microbiology*, **147**, 2517–2528.

Hughes, J., Tregova, A., Tomsett, A.B., Jones, M.G., Cosstick, R. & Collin, H.A. (2005) Synthesis of the flavour precursor, alliin, in garlic tissue cultures. *Phytochemistry*, **66**, 187–194.

Iiyama, K., Furuya, N., Takanami, Y. & Matsuyama, N. (1995) A role of phytotoxin in virulence of *Pseudomonas glumae*. *Japanese Journal of Phytopathology*, **61**, 470–476.

Iiyama, K., Furuya, N., Ura, H. & Matsuyama, N. (1998) Role of phytotoxins in the pathogenesis of *Burkholderia* species. *Journal of the Faculty of Agriculture, Kyushu University*, **42**, 289–294.

Irwin, R. & Vaughan, E. (1972) Bacterial rot of onion and the relation of irrigation water to disease incidence. *Phytopathology*, **62**, 1103.

Jacobs, J.L., Fasi, A.C., Ramette, A., Smith, J.J., Hammerschmidt, R. & Sundin, G.W. (2008) Identification and onion pathogenicity of *Burkholderia cepacia* complex isolates from the onion rhizosphere and onion field soil. *Applied and Environmental Microbiology*, **74**, 3121–3129.

Jeong, Y., Kim, J., Kim, S., Kang, Y., Nagamatsu, T. & Hwang, I. (2003) Toxoflavin produced by *Burkholderia glumae* causing rice grain rot is responsible for inducing bacterial wilt in many field crops. *Plant Disease*, **87**, 890–895.

Jin, Y., Zhou, J., Zhou, J., Hu, M., Zhang, Q., Kong, N. et al. (2020) Genome-based classification of *Burkholderia cepacia* complex provides new insight into its taxonomic status. *Biology Direct*, **15**, 6.

Johnson, T., Abendroth, J., Hol, W. & Sandkvist, M. (2006) Type II secretion: from structure to function. *FEMS Microbiology Letters*, **255**, 175–186.

Jones, C., Webster, G., Mullins, A.J., Jenner, M., Bull, M.J., Dashti, Y. et al. (2021) Kill and cure: genomic phylogeny and bioactivity of *Burkholderia gladioli* bacteria capable of pathogenic and beneficial lifestyles. *Microbial*. *Genomics*, **7**, mgen000515.

Kang, Y., Kim, H., Goo, E., Jeong, H., An, J.H. & Hwang, I. (2019) Unraveling the role of quorum sensing-dependent metabolic homeostasis of the activated methyl cycle in a cooperative population of *Burkholderia glumae*. *Scientific Reports*, **9**, 11038.

Kang, Y., Kim, J., Kim, S., Kim, H., Lim, J.Y., Kim, M. et al. (2008) Proteomic analysis of the proteins regulated by HrpB from the plant pathogenic bacterium *Burkholderia glumae*. *Proteomics*, **8**, 106–121.

Karki, H.S., Barphagha, I.K. & Ham, J.H. (2012b) A conserved two-component regulatory system, PidS/PidR, globally regulates pigmentation and virulence-related phenotypes of *Burkholderia glumae*. *Molecular Plant Pathology*, **13**, 785–794.

Karki, H.S. & Ham, J.H. (2014) The roles of the shikimate pathway genes, *aroA* and *aroB*, in virulence, growth and UV tolerance of *Burkholderia glumae* strain 411gr-6. *Molecular Plant Pathology*, **15**, 940–947.

Karki, H.S., Shrestha, B.K., Han, J.W., Groth, D.E., Barphagha, I.K., Rush, M.C. et al. (2012a) Diversities in virulence, antifungal activity, pigmentation and DNA fingerprint among strains of *Burkholderia glumae*. *PLoS One*, **7**, e45376.

Kato, T., Morohoshi, T., Tsushima, S. & Ikeda, T. (2014) Characterization of three types of quorum-sensing mutants in *Burkholderia glumae* strains isolated in Japan. *Journal of Agricultural Science*, **6**, 16–26.

Kawamoto, S. & Lorbeer, J. (1972a) Histology of onion leaves infected with *Pseudomonas cepacia*. *Phytopathology*, **62**, 1266–1271.

Kawamoto, S. & Lorbeer, J. (1972b) Multiplication of *Pseudomonas cepacia* in onion leaves. *Phytopathology*, **62**, 1263–1265.

Kawamoto, S. & Lorbeer, J. (1974) Infection of onion leaves by *Pseudomonas cepacia*. *Phytopathology*, **64**, 1440–1445.

Kim, J., Kang, Y., Choi, O., Jeong, Y., Jeong, J.E., Lim, J.Y. et al. (2007) Regulation of polar flagellum genes is mediated by quorum sensing and FlhDC in *Burkholderia glumae*. *Molecular Microbiology*, **64**, 165–179.

Kim, J., Kim, J., Kang, Y., Jang, J.Y., Jog, G.J., Lim, J.Y. et al. (2004) Quorum sensing and the LysR-type transcriptional activator ToxR regulate toxoflavin biosynthesis and transport in *Burkholderia glumae*. *Molecular Microbiology*, **54**, 921–934.

Kim, J., Oh, J., Choi, O., Kang, Y., Kim, H., Goo, E. et al. (2009) Biochemical evidence for ToxR and ToxJ binding to the tox operons of *Burkholderia glumae* and mutational analysis of ToxR. *Journal of Bacteriology*, **191**, 4870–4878.

Kim, S., Park, J., Choi, O., Kim, J. & Seo, Y. (2014) Investigation of quorum sensing-dependent gene expression in *Burkholderia gladioli* BSR3 through RNA-seq analyses. *Journal of Microbiology and Biotechnology*, **24**, 1609–1621.

Kim, S., Park, J., Kim, J.H., Lee, J., Bang, B., Hwang, I. et al. (2013) RNAseq-based transcriptome analysis of *Burkholderia glumae* quorum sensing. *The Plant Pathology Journal*, **29**, 249–259.

Köthe, M., Antl, M., Huber, B., Stoecker, K., Ebrecht, D., Steinmetz, I. et al. (2003) Killing of *Caenorhabditis elegans* by *Burkholderia cepacia* is controlled by the Cep quorum-sensing system. *Cellular Microbiology*, **5**, 343–351.

Kowalska, B., Smolińska, U. & Oskiera, M. (2015) *Burkholderia gladioli* associated with soft rot of onion bulbs in Poland. *Journal of Plant Pathology*, **97**, 37–43.

Kumar, S., Stecher, G., Li, M., Knyaz, C. & Tamura, K. (2018) MEGA X: molecular evolutionary genetics analysis across computing platforms. *Molecular Biology and Evolution*, **35**, 1547–1549.

Lamovšek, J., Stare, B.G., Žerjav, M. & Urek, G. (2016) Soft rot of onion bulbs caused by *Burkholderia gladioli* pv. *alliicola* in Slovenia. *Journal of Plant Pathology*, **98**, 369–377.

Lancaster, J.E. & Collin, H.A. (1981) Presence of alliinase in isolated vacuoles and of alkyl cysteine sulphoxides in the cytoplasm of bulbs of onion (*Allium cepa*). *Plant Science Letters*, **22**, 169–176.

Latuasan, H. & Berends, W. (1961) On the origin of the toxicity of toxoflavin. *Biochimica et Biophysica Acta*, **52**, 502–508.

Lee, C., Lee, J.T., Park, H., Lee, E. & Min, G. (2021) Molecular analysis of the pathogenicity-related polygalacturonase gene *pehA* of *Burkholderia gladioli* pv. *alliicola* isolated from onion (*Allium cepae*. L). *Physiological and Molecular Plant Pathology*, **115**, 101670.

Lee, C.J., Lee, J.T., Kwor, J., Kim, B. & Park, W. (2005) Occurrence of bacterial soft rot of onion plants caused by *Burkholderia gladioli* pv. *alliicola* in Korea. *Australasian Plant Pathology*, **34**, 287–292.

Lee, J., Park, J., Kim, S., Park, I. & Seo, Y. (2016) Differential regulation of toxoflavin production and its role in the enhanced virulence of *Burkholderia gladioli*. *Molecular Plant Pathology*, **17**, 65–76.

Lee, Y., Chen, Y., Ouyang, X. & Gan, Y. (2010) Identification of tomato plant as a novel host model for *Burkholderia pseudomallei*. *BMC Microbiology*, **10**, 28.

Lee, Y.A., Shiao, Y.Y. & Chao, C.P. (2003) First report of *Burkholderia cepacia* as a pathogen of banana finger-tip rot in Taiwan. *Plant Disease*, **87**, 601.

Lelis, T., Bruno, J., Padilla, J., Barphagha, I. & Ham, J.H. (2023) *qsmR* encoding an IclR-family transcriptional factor is a core pathogenic determinant of *Burkholderia glumae* beyond the acyl-homoserine lactone-mediated quorum-sensing system. *bioRxiv* 2023.12.05.570247 [preprint].

Lelis, T., Peng, J., Barphagha, I., Chen, R. & Ham, J. (2019) The virulence function and regulation of the metalloprotease gene prtA in the plant-pathogenic bacterium *Burkholderia glumae*. *Molecular Plant–Microbe Interactions*, **32**, 841–852.

Lessie, T.G., Hendrickson, W., Manning, B.D. & Devereux, R. (1996) Genomic complexity and plasticity of *Burkholderia cepacia*. *FEMS Microbiology Letters*, **144**, 117–128.

Letunic, I. & Bork, P. (2021) Interactive tree of life (iTOL) v5: an online tool for phylogenetic tree display and annotation. *Nucleic Acids Research*, **49**, W293–W296.

Lewenza, S., Conway, B., Greenberg, E. & Sokol, P. (1999) Quorum sensing in *Burkholderia cepacia*: identification of the LuxRI homologs CepRI. *Journal of Bacteriology*, **181**, 748–756.

Lewenza, S. & Sokol, P. (2001) Regulation of ornibactin biosynthesis and N-acyl-L-homoserine lactone production by CepR in *Burkholderia cepacia*. *Journal of Bacteriology*, **183**, 2212–2218.

Lindgren, P., Peet, R. & Panopoulos, N. (1986) Gene cluster of *Pseudomonas syringae* pv. "*phaseolicola*" controls pathogenicity of bean plants and hypersensitivity of nonhost plants. *Journal of Bacteriology*, **168**, 512–522.

Mahenthiralingam, E., Bischof, J., Byrne, S.K., Radomski, C., Davies, J.E., Av-Gay, Y. et al. (2000) DNA-based diagnostic approaches for identification of *Burkholderia cepacia* complex, *Burkholderia vietnamiensis*, *Burkholderia multivorans*, *Burkholderia stabilis*, and *Burkholderia cepacia* genomovars I and III. *Journal of Clinical Microbiology*, **38**, 3165–3173.

Malott, R., Baldwin, A., Mahenthiralingam, E. & Sokol, P. (2005) Characterization of the cciIR quorum-sensing system in *Burkholderia cenocepacia*. *Infection and Immunity*, **73**, 4982–4992.

Malott, R.J., O'Grady, E.P., Toller, J., Inhülsen, S., Eberl, L. & Sokol, P.A. (2009) A *Burkholderia cenocepacia* orphan LuxR homolog is involved in quorum-sensing regulation. *Journal of Bacteriology*, **191**, 2447–2460.

Martina, P., Leguizamon, M., Prieto, C.I., Sousa, S.A., Montanaro, P., Draghi, W.O. et al. (2018) *Burkholderia puraquae* sp. nov., a novel species of the *Burkholderia*

cepacia complex isolated from hospital settings and agricultural soils. *International Journal of Systematic and Evolutionary Microbiology*, **68**, 14–20.

Marunga, J., Goo, E., Kang, Y. & Hwang, I. (2021) Identification of a genetically linked but functionally independent two-component system important for cell division of the rice pathogen *Burkholderia glumae*. *Frontiers in Microbiology*, **12**, 700333.

Marunga, J., Kang, Y., Goo, E. & Hwang, I. (2022) Hierarchical regulation of *Burkholderia glumae* type III secretion system by GluR response regulator and Lon protease. *Molecular Plant Pathology*, **23**, 1461–1471.

Mathew, A., Eberl, L. & Carlier, A. (2014) A novel siderophore-independent strategy of iron uptake in the genus *Burkholderia*. *Molecular Microbiology*, **91**, 805–820.

Mattiuzzo, M., Bertani, I., Ferluga, S., Cabrio, L., Bigirmana, J., Guaraccia, C. et al. (2011) The plant pathogen *Pseudomonas fuscovagina*e contains two conserved quorum sensing systems involved in virulence and negatively regulated by RsaL and the novel regulator RsaM. *Environmental Microbiology*, **13**, 145–162.

Meier-Kolthoff, J. & Göker, M. (2019) TYGS is an automated high-throughput platform for state-of-the-art genome-based taxonomy. *Nature Communications*, **10**, 2182.

Meyer, J., Van Van, T., Stintzi, A., Berge, O. & Winkelmann, G. (1995) Ornibactin production and transport properties in strains of *Burkholderia vietnamiensis* and *Burkholderia cepacia* (formerly *Pseudomonas cepacia*). *Biometals*, **8**, 309–317.

Meyer, J.M., Hohnadel, D. & Hall, F. (1989) Cepabactin from *Pseudomonas cepacia*, a new type of siderophore. *Microbiology*, **135**, 1479–1487.

Michalska, K., Chhor, G., Clancy, S., Jedrzejczak, R., Babnigg, G., Winans, S.C. et al. (2014) RsaM: a transcriptional regulator of *Burkholderia spp*. with novel fold. *The FEBS Journal*, **281**, 4293–4306.

Mietzner, T.A. & Morse, S.A. (1994) The role of iron-binding proteins in the survival of pathogenic bacteria. *Annual Review of Nutrition*, **14**, 471–493.

Miller, M. & Bassler, B. (2001) Quorum sensing in bacteria. *Annual Review of Microbiology*, **55**, 165–199

Moon, H., Park, H., Jeong, A., Han, S. & Park, C. (2017) Isolation and identification of *Burkholderia gladioli* on *Cymbidium* orchids in Korea. *Biotechnology and Biotechnological Equipment*, **31**, 280–288.

Morales-Ruíz, L.M., Rodríguez-Cisneros, M., Kerber-Díaz, J.C., Rojas-Rojas, F.U., Ibarra, J.A. & Estrada-De Los Santos, P. (2022) *Burkholderia orbicola* sp. nov., a novel species within the *Burkholderia cepacia* complex. *Archives of Microbiology*, **204**, 178.

Müller, A., Eller, J., Albrecht, F., Prochnow, P., Kuhlmann, K., Bandow, J.E. et al. (2016) Allicin induces thiol stress in bacteria through S-allylmercapto modification of protein cysteines. *Journal of Biological Chemistry*, **291**, 11477–11490.

Mullins, A.J. & Mahenthiralingam, E. (2021) The hidden genomic diversity, specialized metabolite capacity, and revised taxonomy of *Burkholderia sensu lato*. *Frontiers in Microbiology*, **12**, 726847.

Nandakumar, R., Shahjahan, A., Yuan, X., Dickstein, E.R., Groth, D.E., Clark, C.A. et al. (2009) *Burkholderia glumae* and *B. gladioli* cause bacterial panicle blight in rice in the southern United States. *Plant Disease*, **93**, 896–905.

Nguyen, T.T., Lee, H., Park, J., Park, I. & Seo, Y. (2017) Computational identification and comparative analysis of secreted and transmembrane proteins in six *Burkholderia* species. *The Plant Pathology Journal*, **33**, 148–162.

O'Grady, E.P., Viteri, D.F., Malott, R.J. & Sokol, P.A. (2009) Reciprocal regulation by the CepIR and CciIR quorum sensing systems in *Burkholderia cenocepacia*. *BMC Genomics*, **10**, 441.

Okazaki, S., Tittabutr, P., Teulet, A., Thouin, J., Fardoux, J., Chaintreuil, C. et al. (2016) *Rhizobium*–legume symbiosis in the absence of nod factors: two possible scenarios with or without the T3SS. *The ISME Journal*, **10**, 64–74.

Palleroni, N.J., Ballard, R.W., Ralston, E. & Doudoroff, M. (1972) Deoxyribonucleic acid homologies among some *Pseudomonas* species. *Journal of Bacteriology*, **110**, 1–11.

Parsons, Y., Glendinning, K., Thornton, V., Hales, B., Hart, C. & Winstanley, C. (2001) A putative type III secretion gene cluster is widely distributed in the *Burkholderia cepacia* complex but absent from genomovar I. *FEMS Microbiology Letters*, **203**, 103–108.

Partida-Martinez, L.P. & Hertweck, C. (2005) Pathogenic fungus harbours endosymbiotic bacteria for toxin production. *Nature*, **437**, 884–888.

Paudel, S., Zhao, M., Stice, S., Dutta, B. & Kvitko, B.H. (2024) Thiosulfinate tolerance gene clusters are common features of *Burkholderia* onion pathogens. *Molecular Plant–Microbe Interactions*, **37**, 507–519.

Payne, G.W., Vandamme, P., Morgan, S.H., Lipuma, J.J., Coenye, T., Weightman, A.J. et al. (2005) Development of a *recA* gene-based identification approach for the entire *Burkholderia* genus. *Applied and Environmental Microbiology*, **71**, 3917–3927.

Reiter, J., Hübbers, A.M., Albrecht, F., Leichert, L. & Slusarenko, A. (2020) Allicin, a natural antimicrobial defence substance from garlic, inhibits DNA gyrase activity in bacteria. *International Journal of Medical Microbiology*, **310**, 151359.

Rose, P., Whiteman, M., Moore, P., and Zhu, Y. 2005. Bioactive S-alk (en) yl cysteine sulfoxide metabolites in the genus *Allium*: the chemistry of potential therapeutic agents. Natural product reports 22:351-368.

Rossier, O., Van Den Ackerveken, G. & Bonas, U. (2000) HrpB2 and HrpF from *Xanthomonas* are type III-secreted proteins and essential for pathogenicity and recognition by the host plant. *Molecular Microbiology*, **38**, 828–838.

Sato, Z., Koiso, Y., Iwasaki, S., Matsuda, I. & Shirata, A. (1989) Toxins produced by *pseudomonas glumae*. *Japanese Journal of Phytopathology*, **55**, 353–356.

Sawana, A., Adeolu, M. & Gupta, R.S. (2014) Molecular signatures and phylogenomic analysis of the genus *Burkholderia*: proposal for division of this genus into the emended genus *Burkholderia* containing pathogenic organisms and a new genus *Paraburkholderia* gen. nov. harboring environmental species. *Frontiers in Genetics*, **5**, 429.

Seo, Y.S., Lim, J.Y., Park, J., Kim, S., Lee, H.H., Cheong, H. et al. (2015) Comparative genome analysis of rice-pathogenic *Burkholderia* provides insight into capacity to adapt to different environments and hosts. *BMC Genomics*, **16**, 349.

Serret-López, M., Aranda-Ocampo, S., Espinosa-Victoria, D., Ortiz-Martínez, L. & Ramírez-Razo, K. (2021) Polyphasic characterization of *Burkholderia gladioli* isolated from onion and evaluation of its potential pathogenicity for other crops. *Revista Mexicana de Fitopatología*, **39**, 21–40.

Seynos-García, E., Castañeda-Lucio, M., Muñoz-Rojas, J., López-Pliego, L., Villalobos, M., Bustillos-Cristales, R. et al. (2019) *Loci* identification of a N-acyl homoserine lactone type quorum sensing system and a new LysR-type transcriptional regulator associated with antimicrobial activity and swarming in *Burkholderia gladioli* UAPS07070. *Open Life Sciences*, **14**, 165–178.

Sokol, P. (1986) Production and utilization of pyochelin by clinical isolates of *Pseudomonas cepacia*. *Journal of Clinical Microbiology*, **23**, 560–562.

Sokol, P., Darling, P., Lewenza, S., Corbett, C. & Kooi, C. (2000) Identification of a siderophore receptor required for ferric ornibactin uptake in *Burkholderia cepacia*. *Infection and Immunity*, **68**, 6554–6560.

Sokol, P., Darling, P., Woods, D., Mahenthiralingam, E. & Kooi, C. (1999) Role of ornibactin biosynthesis in the virulence of *Burkholderia cepacia*: characterization of *pvdA*, the gene encoding l-ornithine N^5-oxygenase. *Infection and Immunity*, **67**, 4443–4455.

Sokol, P., Lewis, C. & Dennis, J. (1992) Isolation of a novel siderophore from *Pseudomonas cepacia*. *Journal of Medical Microbiology*, **36**, 184–189.

Somvanshi, V., Viswanathan, P., Jacobs, J., Mulks, M., Sundin, G. & Ciche, T. (2010) The type 2 secretion pseudopilin, *gspJ*, is required for multihost pathogenicity of *Burkholderia cenocepacia* AU1054. *Infection and Immunity*, **78**, 4110–4121.

Springman, A.C., Jacobs, J.L., Somvanshi, V.S., Sundin, G.W., Mulks, M.H., Whittam, T.S. et al. (2009) Genetic diversity and multihost pathogenicity of clinical and environmental strains of *Burkholderia cenocepacia*. *Applied and Environmental Microbiology*, **75**, 5250–5260.

Stephan, H., Freund, S., Beck, W., Jung, G., Meyer, J. & Winkelmann, G. (1993) Ornibactins—a new family of siderophores from *Pseudomonas*. *Biometals*, **6**, 93–100.

Stevens, M., Wood, M., Taylor, L., Monaghan, P., Hawes, P., Jones, P.W. et al. (2002) An Inv/mxi-Spa-like type III protein secretion system in *Burkholderia pseudomallei* modulates intracellular behaviour of the pathogen. *Molecular Microbiology*, **46**, 649–659.

Stice, S.P., Thao, K.K., Khang, C., Baltrus, D.A., Dutta, B. & Kvitko, B.H. (2020) Thiosulfinate tolerance is a virulence strategy of an atypical bacterial pathogen of onion. *Current Biology*, **30**, 3130–3140.e6.

Stopnisek, N., Bodenhausen, N., Frey, B., Fierer, N., Eberl, L. & Weisskopf, L. (2014) Genus-wide acid tolerance accounts for the biogeographical distribution of soil *Burkholderia* populations. *Environmental Microbiology*, **16**, 1503–1512.

Stoyanova, M., Hristova, P., Petrov, N., Moncheva, P. & Bogatzevska, N. (2011) Method for differentiating *Burkholderia gladioli* pathovars. *Science and Technologies*, **6**, 15–19.

Subramoni, S. & Sokol, P. (2012) Quorum sensing systems influence *Burkholderia cenocepacia* virulence. *Future Microbiology*, **7**, 1373–1787.

Subsin, B., Chambers, C., Visser, M. & Sokol, P. (2007) Identification of genes regulated by the cepIR quorum-sensing system in *Burkholderia cenocepacia* by high-throughput screening of a random promoter library. *Journal of Bacteriology*, **189**, 968–979.

Suppiger, A., Schmid, N., Aguilar, C., Pessi, G. & Eberl, L. (2013) Two quorum sensing systems control biofilm formation and virulence in members of the *Burkholderia cepacia* complex. *Virulence*, **4**, 400–409.

Suzuki, F., Sawada, H., Azegami, K. & Tsuchiya, K. (2004) Molecular characterization of the *tox* operon involved in toxoflavin biosynthesis of *Burkholderia glumae*. *Journal of General Plant Pathology*, **70**, 97–107.

Suzuki, F., Zhu, Y., Sawada, H. & Matsuda, I. (1998) Identification of proteins involved in toxin production by *Pseudomonas glumae*. *Japanese Journal of Phytopathology*, **64**, 75–79.

Swain, D., Yadav, S., Tyagi, I., Kumar, R., Kumar, R., Ghosh, S. et al. (2017) A prophage tail-like protein is deployed by *Burkholderia* bacteria to feed on fungi. *Nature Communications*, **8**, 404.

Teulet, A., Busset, N., Fardoux, J., Gully, D., Chaintreuil, C., Cartieaux, F. et al. (2019) The rhizobial type III effector ErnA confers the ability to form nodules in legumes. *Proceedings of the National Academy of Sciences of the United States of America*, **116**, 21758–21768.

Teviotdale, B., Davis, R., Guerard, J. & Harper, D. (1989) Effect of irrigation management on sour skin of onion. *Plant Disease*, **73**, 819–822.

Tomich, M., Griffith, A., Herfst, C., Burns, J. & Mohr, C. (2003) Attenuated virulence of a *Burkholderia cepacia* type III secretion mutant in a murine model of infection. *Infection and Immunity*, **71**, 1405–1415.

Uehlinger, S., Schwager, S., Bernier, S., Riedel, K., Nguyen, D.T., Sokol, P.A. et al. (2009) Identification of specific and universal virulence factors in *Burkholderia*

cenocepacia strains by using multiple infection hosts. *Infection and Immunity*, **77**, 4102–4110.

Ulrich, J. (1975) Pectic enzymes of *Pseudomonas cepacia* and penetration of polygalacturonase into cells. *Physiological Plant Pathology*, **5**, 37–44.

Ura, H., Furuya, N., Iiyama, K., Hidaka, M., Tsuchiya, K. & Matsuyama, N. (2006) *Burkholderia gladioli* associated with symptoms of bacterial grain rot and leaf-sheath browning of rice plants. *Journal of General Plant Pathology*, **72**, 98–103.

Vandamme, P., Holmes, B., Vancanneyt, M., Coeyne, T., Hoste, B., Coopman, R. et al. (1997) Occurrence of multiple genomovars of *Burkholderia cepacia* in cystic fibrosis patients and proposal of *Burkholderia multivorans* sp. nov. *International Journal of Systematic and Evolutionary Microbiology*, **47**, 1188–1200.

Vandamme, P., Peeters, C., De Smet, B., Price, E.P., Sarovich, D.S., Henry, D.A. et al. (2017) Comparative genomics of *Burkholderia singularis* sp. nov., a low G+C content, free-living bacterium that defies taxonomic dissection of the genus *Burkholderia*. *Frontiers in Microbiology*, **8**, 1679.

Velez, L., Aburjaile, F., Farias, A.G., Baia, A.D.B., Oliveira, W.J., Silva, A.M.F. et al. (2023) *Burkholderia semiarida* sp. nov. and *Burkholderia sola* sp. nov., two novel *B. cepacia* complex species causing onion sour skin. *Systematic and Applied Microbiology*, **46**, 126415.

Vial, L., Lépine, F., Milot, S., Groleau, M.C., Dekimpe, V., Woods, D.E. et al. (2008) *Burkholderia pseudomallei*, *B. thailandensis*, and *B. ambifaria* produce 4-hydroxy-2-

alkylquinoline analogues with a methyl group at the 3 position that is required for quorum-sensing regulation. *Journal of Bacteriology*, **190**, 5339–5352.

Wallner, A., Moulin, L., Busset, N., Rimbault, I. & Béna, G. (2021) Genetic diversity of type 3 secretion system in *Burkholderia* s.l. and links with plant host adaptation. *Frontiers in Microbiology*, **12**, 761215.

Wright, P., Clark, R. & Hale, C. (1993) A storage soft rot of New Zealand onions caused by *Pseudomonas gladioli* pv. *alliicola*. *New Zealand Journal of Crop and Horticultural Science*, **21**, 225–227.

Yadav, S.K., Das, J., Kumar, R. & Jha, G. (2020) Calcium regulates the mycophagous ability of *Burkholderia gladioli* strain NGJ1 in a type III secretion system-dependent manner. *BMC Microbiology*, **20**, 216.

Yadav, S.K., Magotra, A., Ghosh, S., Krishnan, A., Pradhan, A., Kumar, R. et al. (2021) Immunity proteins of dual nuclease T6SS effectors function as transcriptional repressors. *EMBO Reports*, **22**, e51857.

Yohalem, D.S. & Lorbeer, J.W. (1994) Intraspecific metabolic diversity among strains of *Burkholderia cepacia* isolated from decayed onions, soils, and the clinical environment. *Antonie Van Leeuwenhoek*, **65**, 111–131.

Yoneyama, K., Kono, Y., Yamaguchi, I., Horikoshi, M. & Hirooka, T. (1998) Toxoflavin is an essential factor for virulence of *Burkholderia glumae* causing rice seedling rot disease. *Japanese Journal of Phytopathology*, **64**, 91–96.

Zeidler, D., Zähringer, U., Gerber, I., Dubery, I., Hartung, T., Bors, W. et al. (2004) Innate immunity in *Arabidopsis thaliana*: lipopolysaccharides activate nitric oxide synthase (NOS) and induce defense genes. *Proceedings of the National Academy of Sciences of the United States of America*, **101**, 15811–15816.

Zhang, L., Gao, W., Yin, Y. & Wang, Z. (2019) Discrimination of *Burkholderia gladioli* pv. *alliicola* and *B*. *cepacia* complex using the *gyrB* gene of *B*. *gladioli* pv. *alliicola*. *Experimental and Therapeutic Medicine*, **17**, 1870–1876.

Zhang, X.X., Chen, J.Y., Wang, Z.Y., Zou, H.D., Luo, Z.X., Yao, Z.F. et al. (2020) *Burkholderia gladioli* causes bacterial internal browning in sweetpotato of China. *Australasian Plant Pathology*, **49**, 191–199.

Zhou, T., Yin, C., Zhang, Y., Shi, H., Wang, J., Sun, L. et al. (2016) Lon protease is involved in RhpRS-mediated regulation of type III secretion in *Pseudomonas syringae*. *Molecular Plant–Microbe Interactions*, **29**, 807–814.

Zhou, X., Teper, D., Andrade, M., Zhang, T., Chen, S., Song, W.Y. et al. (2018) A phosphorylation switch on Lon protease regulates bacterial type III secretion system in host. *mBio*, **9**, 2146.

Figures

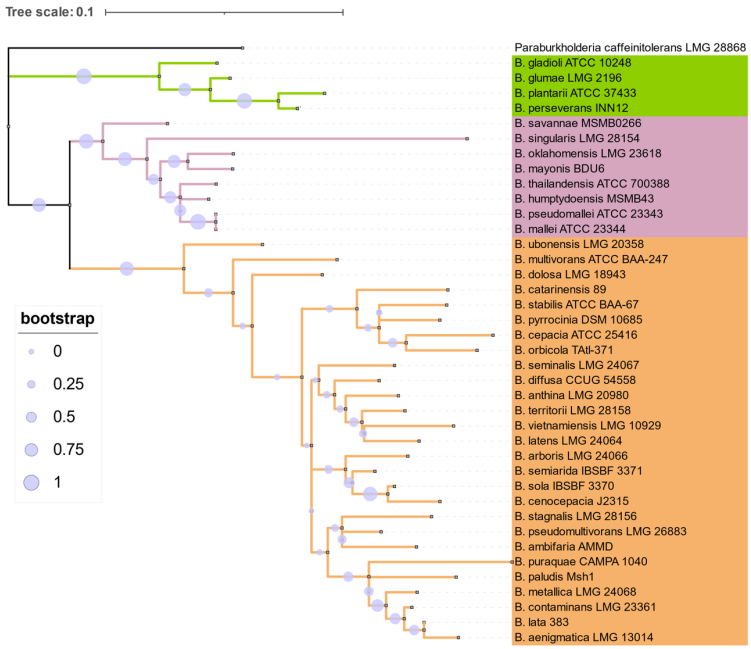

Figure 1.1 Maximum Likelihood method based phylogenetic tree based on 385 bp partial *recA* gene sequences on BUR3 and BUR4 primers described in Payne *et al.* 2005. Bootstrap method with 1000 replicate was used as a test of phylogeny. Gene sequences for the representative *Burkholderia* strains were extracted from NCBI GeneBank database. Strains information used for the phylogenetic analysis is derived from Mullins & Mahenthiralingam, 2021, Velez *et al.*, 2023 and Morales-Luiz *et al.*, 2022. The tree is rooted on the outgroup branch *Paraburkholderia caffeinitolerans* LMG 28868. Green shading on the stains represents plant pathogenic *Burkholderia* species, pink shading represents representative strains in the *Burkholderia pseudomallei – mallei* clade and orange shading represents the selected strains in *Burkholderia cepacia* complex. Phylogenetic tree generated using MEGA-X software (Kumar *et al.*, 2018) and formatted using Interactive Tree of Life (iTOL) web-based platform (Letunic and Bork, 2021).

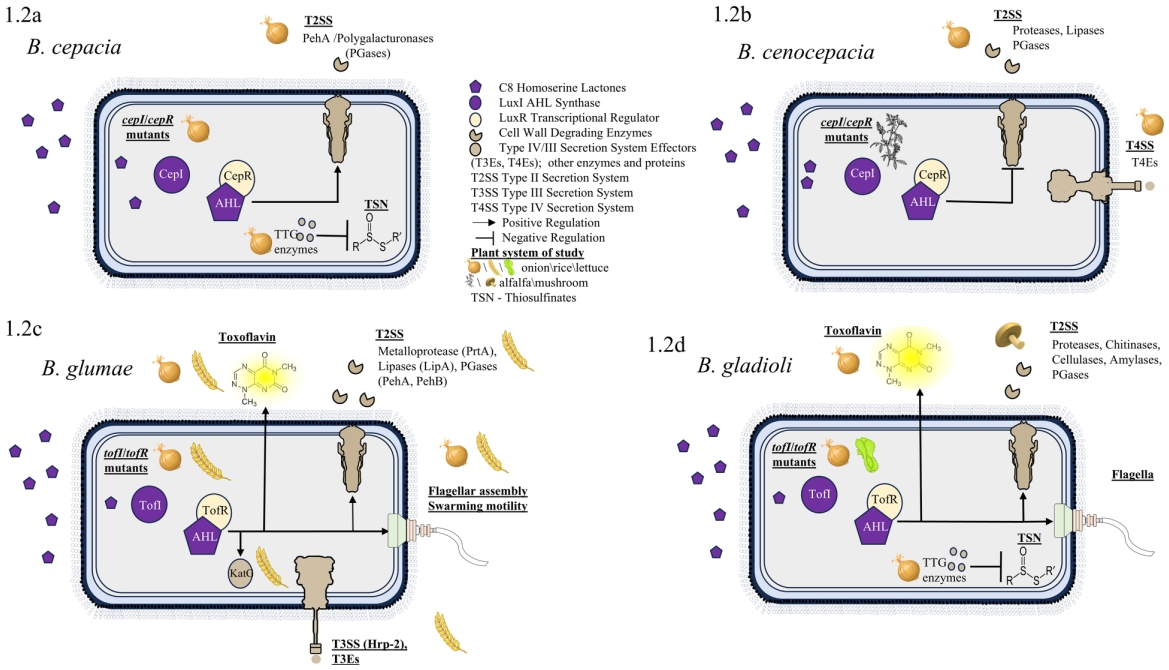

Figure 1.2 Characterized protein secretion system and other quorum sensing regulated virulence traits of onion pathogenic *Burkholderia* species tested in different plant infection models including onion. The LuxI, AHL and LuxR complex regulated traits are shown as described in 1.2a) *Burkholderia cepacia* genomovar I group (ATCC 25416), 1.2b) well characterized *B. cenocepacia* strains H111 and/or K56-2, 1.2c) *Burkholderia glumae*, and 1.2d) *Burkholderia gladioli*. The host infection model used is shown as a vector image (rice, onion, mushroom, alfalfa, lettuce) by the side of described virulence factor. Toxoflavin structure is retrieved from Bioaustralis fine chemicals website. References: Figure 1.2a: Sato et al., 1989; Ilyama et al., 1995; Ilyama et al., 1998; Suzuki et al., 1998; Suzuki et al., 2004; Gonzalez et al., 1997; Aguilar et al., 2003a; Paudel et al., 2024, Figure 1.2b: Huber et al., 2001; Lewenza et al., 1991; Uehlinger et al., 2009; Engledow et al., 2004, Figure 1.2c: Chun et al., 2009; Kang et al., 2008; Degrassi et al., 2008; Lelis et al., 2023; Devescovi et al., 2007; Chen et al., 2012; Lelis et al., 2019; Karki and Ham, 2014, Figure 1.2d: Jones et al., 2021; Lee et al., 2016; Chowdhury & Heinemann, 2006; Seynos-Garcia et al., 2019; Paudel et al., 2024.

CHAPTER 2

THIOSULFINATES TOLERANCE GENES ARE COMMON FEATURES OF *BURKHOLDERIA* ONION PATHOGENS[1]

[1] Paudel, S., Zhao, M., Stice, S., Dutta, B. & Kvitko, B.H. 2024. Thiosulfinate tolerance gene clusters are common features of *Burkholderia* onion pathogens. *Molecular Plant–Microbe Interactions*, **37**, 507–519. https://doi.org/10.1094/MPMI-01-24-0005-R

SP did investigation, formal analysis, resources, data curation, writing – original draft, review, editing, and visualization.

Abstract

Burkholderia gladioli pv. *alliicola*, *B. cepacia*, and *B. orbicola* are common bacterial pathogens of onion. Onions produce organosulfur thiosulfinate defensive compounds after cellular decompartmentalization. Using whole-genome sequencing and in silico analysis, we identified putative thiosulfinate tolerance gene (TTG) clusters in multiple onion-associated *Burkholderia* species similar to those characterized in other *Allium*-associated bacterial endophytes and pathogens. Sequence analysis revealed the presence of three *Burkholderia* TTG cluster types, with both Type A and Type B being broadly distributed in *B. gladioli*, *B. cepacia*, and *B. orbicola* in both the chromosome and plasmids. Based on isolate natural variation and generation of isogenic strains, we determined the in vitro and in vivo contribution of TTG clusters in *B. gladioli*, *B. cepacia*, and *B. orbicola*. The *Burkholderia* TTG clusters contributed to enhanced allicin tolerance and improved growth in filtered onion extracts by all three species. TTG clusters also made clear contributions to *B. gladioli* foliar necrosis symptoms and bacterial populations. Surprisingly, the TTG cluster did not contribute to bacterial populations in onion bulb scales by these three species. Based on our findings, we hypothesize onion-associated *Burkholderia* may evade or inhibit the production of thiosulfinates in onion bulb tissues.

Introduction

Onion (*Allium cepa* L.) production industry, valued at US $1 billion is a major contributor to the USA economy (Belo et al., 2023). Bacterial pathogens can infect onions at different stages of production from seedling to storage posing a serious challenge to growers (Mark et al., 2002; Zhao et al., 2022). Upon conducive environmental conditions, bacterial pathogens can cause more than 50% losses in production (Belo et al., 2023). Members in the *Burkholderia* genus are

historically associated with onion disease with its first report dating back to 1940s (Burkholder, 1942). *Burkholderia cepacia* complex (Bcc) group causes sour skin of onion whereas *Burkholderia gladioli* pv. *alliicola* (Bga) causes slippery skin (Burkholder, 1950). In addition to the common onion pathogenic members *B. cepacia, B. cenocepacia,* and *B. ambifaria*, three new onion pathogenic species *B. orbicola, B. semiarida,* and *B. sola* were recently described as members of the Bcc complex (Morales-Ruíz et al., 2022; Velez et al., 2023). While all described onion pathogenic members in *Burkholderia* infect bulbs and are storage pathogens, Bga is also associated with foliar necrosis (Kawamoto and Lorbeer, 1974; Lee et al., 2005).

Plants utilize different chemical compounds as a defense response against the attack of pathogens and pests. In many cases, the inactive form of these compounds is converted into the active form only after the pathogen/insect attack. Onion, garlic, and other *Allium* species produce rapid and potent organosulfur compounds as a consequence of tissue damage (Lancaster and Collin, 1981; Rose et al., 2005). In garlic, the thiosulfinate allicin produced by the reaction of alliinase on alliin is a primary volatile antimicrobial compound that inactivates enzymes and depletes the reduced glutathione pool. Allicin is the compound responsible for the odor of crushed garlic. Onion, on the other hand, when disrupted produces asymmetric 1- propenyl methyl thiosulfinates in onion extracts. The action of alliinase and another enzyme, lachrymatory factor synthase (LFS) converts isoalliin into syn-propanethial-S-oxide, which is an irritant that induces tears (Silvaroli et al., 2017).

A plasmid-borne cluster of eleven-genes named the allicin tolerance (*alt*) cluster was found to confer increased tolerance to allicin and enhance virulence in *Pantoea ananatis* on onion (Stice et al., 2020). Mutation in the *alt*/TTG (Thiosulfinate Tolerance Gene) region resulted in a smaller clearing zone in red onion scale necrosis assay and caused approximately

100-fold reduced bacterial population in onion tissue, and increased sensitivity to allicin and endogenous onion thiosulfinates. The PNA 97-1 mutant strain lacking the *alt*/TTG cluster was severely reduced in the bacterial colonization of onion bulbs and scales suggesting the role of *alt* cluster in the virulence of the bacterium. Multiple chromosomal TTG clusters conferring allicin tolerance were also characterized in the garlic saprophyte *Pseudomonas fluorescens* PfAR-1, with similar clusters identified in the garlic pathogen *Pseudomonas salomonii* (Borlinghaus et al., 2020; Stice et al., 2020). The *Pantoea* and *Pseudomonas* TTG clusters had similar gene content but dissimilar gene cluster syntenies.

TTG clusters have not been reported in onion pathogenic members of *Burkholderia* genus. The *Burkholderia* pathogens are likely exposed to thiosulfinates during the infection process. In this study, we sequenced representative onion-isolated *Burkholderia* strains from Georgia, USA, and explored the distribution and function of putative TTG-like clusters from *Burkholderia*. Using allicin Zone of Inhibition (ZOI) and onion juice growth assays, we demonstrated the contribution of the putative TTG-like cluster to allicin tolerance and filtered onion extract growth in multiple onion-associated *Burkholderia* species. Engineered TTG mutant and TTG encoding heterologous expression plasmid derivatives were generated to determine the contribution of TTG cluster to onion foliar/red scale necrosis and *in planta* bacterial populations. Our results suggest that the TTG cluster contributes to variable virulence roles in onion depending on onion tissue-type and *Burkholderia* species.

Results

Identification of putative TTG-like cluster in *Burkholderia* species.

Using *Pantoea ananatis* (Pan) PNA 97-1R TTG cluster gene sequences as a query, we performed a multigene blastX analysis to check the presence or absence of corresponding protein homologs in *Burkholderia*. Hits were obtained in the *Burkholderia* genus for multiple TTG gene sequences in the reference Pan PNA 97-1R *alt* TTG cluster. Further analysis of the hits in the whole genome sequence of *B. cepacia* 561 revealed the presence of putative TTG genes *altB*, *altC*, *altA*, *altE*, *altR*, *altI*, and *altJ*. The *altA, altB,* and *altC* genes are predicted to function as putative thiol/oxidoreductases, and *altJ* and *altE* encode for predicted peroxidase-like enzymes. The *altI* gene encodes for a putative carbon-sulfur lyase and *altR* encodes a putative repressor. Homolog of Pan TTG genes *altD, altG*, *altH,* and *gorB* were not found in the screened *B. cepacia* cluster. Similar TTG cluster genes were identified in the onion-isolated Bga strain 20GA0385. Clinker gene synteny analysis revealed the seven TTG genes were conserved in both Bga strain 20GA0385 and Pan strain PNA 97-1R, with 100% query coverage for all seven genes. Amino acid (aa) percent identity between the two strains for *altB, altA,* and *altC* genes was 81%, 67%, and 37%, respectively. The peroxidase-like *altE* and *altJ* shared 63% and 29% aa identities, respectively. The putative C-S lyase encoding *altI* and the putative repressor *altR* shared 48% and 39% identity, respectively. The gene synteny between the two clusters; however, was not conserved (Figure 2.1).

TTG clusters are widespread in *Burkholderia* species commonly isolated from onion.

To study the distribution of putative TTG clusters in onion-associated strains, we conducted whole genome sequencing and assembly of 66 *Burkholderia* strains isolated from symptomatic onion. The species of sequenced strain was confirmed using the Type Strain Genome Server platform (Meier-Kolthoff and Göker, 2019). Out of the 66 sequenced strains, 22 were identified as *B. orbicola*, 20 were *B. cepacia,* 20 were *B. gladioli,* and 4 were *B. ambifaria* (Supplementary

Table S3). Putative TTG-like clusters were found in 55 of the sequenced strains. All sequenced *B. orbicola* and *B. ambifaria* strains had TTG clusters. Among the 11 TTG negative strains, 2 were from *B. cepacia* species and 9 were from *B. gladioli* species. Interestingly, we discovered four strains that had two putative TTG clusters in a single strain, with three of these strains belonging to *B. orbicola* and one to *B. gladioli* (strain 20GA0350) (Figure 2.2A).

Three distinct TTG cluster types are found based on nucleotide homology.

To analyze the distribution and phylogeny of the TTG clusters, the identified putative TTG clusters were extracted from the respective genomes and aligned against each other. An additional 24 *Burkholderia* TTG sequences from closed genomes in the NCBI GenBank database were included in the alignment. The synteny of TTG cluster genes *altI* to *altB* was conserved for all the sequenced strains in our study. Among the NCBI GenBank extracted sequences, a slight difference in gene arrangement was observed in three *B. gladioli* strains and one *Paraburkholderia graminis* strain. The putative C-S lyase gene *altI* was present downstream of *altB* gene in the four strains. In the rest of the strains, the *altI* gene was present upstream of *altA* gene. The maximum-likelihood phylogenetic tree revealed the presence of three distinct TTG clades among the strains (Figure 2.2A). The first branch had 63 TTG sequences with relatively less diversity among them. The second cluster had 13 sequences and the third cluster had four TTG sequences from *B. gladioli* and *P. graminis* species. The three clusters were named Type A, Type B, and Type C TTG clusters based on nucleotide homology and branching in the phylogenetic tree. The *B. gladioli* strains in the Type A and Type B branches formed a distinct sub-clade and showed species-specific branching (Figure 2.2A). The three *B. gladioli* strains in the Type C branch also formed a distinct subgrouping (Figure 2.2A). No species-specific branching was observed for other *Burkholderia* species. Among strains with two putative TTG-

like clusters, three *B. orbicola* strains had one TTG cluster sequence each in Type A and Type B branches while *B. orbicola* strain HI2424 had both clusters in the Type A clade. Clinker gene arrow diagram between the representative strains in the Type A (ATCC 25416), Type B (BC93_12), and Type C (ATCC 10248) cluster revealed conserved gene synteny between the gene clusters with the exception of the predicted *altI* gene in the Type C cluster which was located downstream of *altB* gene. Cluster Type A (ATCC 25416) and Type B (BC93_12) shared ~89% nucleotide identity. Similarly, Type A and C cluster shared 77.48% nucleotide identity and Type B and C cluster were 77.35% identical (Figure 2.2B).

The TTG-like cluster in *Burkholderia* contributes to allicin tolerance *in vitro*.

To test the functional role of TTG-like clusters in sequenced strains, an allicin zone of inhibition (ZOI) assay was performed. Firstly, representative natural variant strains in *B. gladioli*, *B. cepacia*, and *B. orbicola* species with or without endogenous TTG clusters were tested for allicin tolerance. The TTG negative variant in all three species was highly sensitive to allicin based on the larger relative zones of inhibitions compared with the strains possessing the endogenous TTG cluster in the respective species group. (Figure 2.3A,2.3D, 2.3F). There was no significant difference in ZOI area between endogenous Type A and Type B cluster types in *B. gladioli* and *B. orbicola* representative strains (Figure 2.3A, 2.3F). The presence of two TTG clusters in a single strain was not observed to contribute to significantly higher allicin tolerance in *B. gladioli* and *B. orbicola* (Fig 2.3A, 2.3F). The functional role of the TTG cluster was further assessed by engineering a TTG deletion mutant in the Bga strain 20GA0385. The TTG mutant was more sensitive to allicin than the WT strain (Figure 2.3B). Although extensive attempts were made, we were unable to generate corresponding TTG mutants in *B. cepacia* and *B. orbicola* in part due to their high intrinsic resistance to aminoglycoside antibiotics creating challenges for clean

selection and recalcitrance to *sacB*-mediated counter-selection. Thus, we cloned the Type A TTG cluster (from Bga strain 20GA0385) and TTG Type B cluster (from *B. orbicola* strain BC93_12) into pBBR1MCS-2 for complementation and heterologous expression in strains lacking a native TTG cluster. Plasmid-based expression of either cluster type in the Bga 20GA0385 TTG mutant background restored the ZOI phenotype to WT level. The TTG Type B complementing plasmid conferred significantly higher allicin tolerance compared to the WT strain and the TTG Type A complementation clones (Figure 2.3B). To test if the functional role of TTG cluster is conserved across major onion pathogenic *Burkholderia* species, we transformed TTG Type A and Type B expression plasmids separately into TTG negative natural variant backgrounds: BC83_1 (*B. cepacia*), LMG 30279^{T} (*B. orbicola*), and BG92_3 (*B. gladioli*). The TTG expression isogenic lines were significantly more tolerant to allicin in all three species groups compared to their respective TTG negative WT (Figure 2.3C, 2.3E, 2.3G). In *B. cepacia* BC83_1, TTG Type B expression plasmid contributed significantly to enhanced allicin tolerance as compared to the TTG Type A (data not shown) and the WT strain (Figure 2.3E). No statistical difference in allicin tolerance was observed between Type A and TTG Type B expression plasmids in *B. orbicola* strain LMG 30279 and *B. gladioli* strain BG92_3 (data not shown).

TTG-negative strains have impaired growth in filtered onion juice.

Stice et al. 2020 demonstrated that endogenous onion thiosulfinates in onion juice restricted bacterial growth in a manner similar to synthesized allicin. To test if endogenous thiosulfinates affect the growth of TTG derivatives in different *Burkholderia species*, we conducted a filtered onion juice growth assay. In half-strength onion juice diluted with water, the Bga 20GA0385 TTG mutant had a dramatic growth slower than the WT strain over 48 h. The growth of the TTG mutant improved significantly when complemented with the plasmid harboring TTG gene cluster

(Figure 2.4A). The TTG Type A and Type B plasmid derivatives grew significantly better in onion juice than the TTG negative natural WT variant in *B. cepacia* and *B. orbicola* (Figure 2.4B, 2.4C). When analyzed across the three experimental repeats, the OD_{600} values recovered for *B. orbicola* LMG 30279 Type B strain were significantly higher compared to the TTG Type A strain derivative 16 to 48 hours post-inoculation (Table S2.4). The *B. cepacia* TTG Type B derivative growth was similar to the TTG Type A strain over 48 h across the three experimental repeats (Table S2.4).

TTG cluster in *B. gladioli* pv. *alliicola* contributes to foliar necrosis and bacterial populations.

The *B. gladioli* TTG mutant and the TTG plasmid derivatives in TTG-negative WT background were tested for their contribution to onion foliar necrosis and bacterial populations. The 20GA0385 ΔTTG was significantly reduced in onion seedling lesion length and bacterial population compared to the WT strain. The necrosis length and bacterial population were restored to the WT level when the TTG mutant was expressed with a TTG Type A complementing plasmid (Figure 2.5A, 2.5B). The TTG Type A plasmid also contributed to significantly higher necrosis length and bacterial populations when transformed in a TTG-negative natural variant strain BG92_3 (Figure 2.5A, 2.5B). In addition, a time course bacterial population growth assay for both Bga 20GA0385 and ΔTTG was performed. Bacterial populations at six hours post-inoculation were in the range of 10^4 CFU/mg of onion tissue. Bacterial populations for the WT strain increased gradually and reached the maximum plateau from Day 3 to Day 5 post-inoculation in the range of 10^6-10^8 CFU per mg of infected leaf tissue. The bacterial population recovered for ΔTTG Day 3 to Day 5 post-infection was significantly lower compared to the WT strain (Figure 2.6A).

TTG cluster in *Burkholderia* does not contribute to symptom production or bacterial populations in onion scale tissue.

The Red Scale Necrosis (RSN) assay was conducted with strains in three *Burkholderia* species to study the role of TTG cluster in lesion area and scale bacterial population. The *B. gladioli* 20GA0385 ΔTTG was not altered in the RSN area compared to the WT. The TTG Type A complementing plasmid clone had a significantly larger necrosis area compared to the TTG mutant. Bacterial populations for three *B. gladioli* 20GA0385 treatments (WT, ΔTTG, and ΔTTG p^{TTGA}) were not significantly different from each other 4 h and 3 days post-inoculation (Fig 5D). In the case of the *B. cepacia* strain BC83_1, the TTG Type B expression clone contributed to the RSN area, but the TTG Type A clone did not affect the RSN area (Figure 2.5E). Onion scale bacterial population for *B. cepacia* and *B. orbicola* TTG Type A expression clone was significantly reduced at 4 hours post-inoculation compared to the respective WT and TTG Type B expression clones (Figure 2.5F, 2.5H). No significant difference in bacterial population and the RSN area was observed for *B. cepacia* and *B. orbicola* WT and TTG plasmid derivatives at day 3 post-infection (Figure 2.5F, 2.5G, 2.5H). Onion scale bacterial population for *B. gladioli* 20GA0385 WT and ΔTTG strains from day 0 to day 5 were not significantly different from each other (Figure 2.6B).

Discussion

Using whole genome sequencing and phenotypic assays, we studied the distribution and functional role of TTG-like clusters in *Burkholderia* species commonly isolated from onion. RSN and foliar necrosis assays were conducted to investigate the role of TTG-like clusters in tissue-specific symptom production and bacterial population. A putative TTG-like cluster was identified in onion-isolated Bga strain 20GA0385. The genes present in the cluster had similar

predicted functions compared to TTG cluster genes in *P. ananatis* strain PNA 97-1 but the gene synteny and orientation were different (Figure 2.1). Whole genome sequencing revealed the widespread distribution of TTG-like clusters in onion-isolated *Burkholderia* species. Maximum likelihood-based phylogeny of whole genome sequenced and NCBI GenBank extracted representative TTG sequences highlighted the presence of three distinct clades (Figure 2.2A). These three clades were named Type A, Type B, and Type C TTG clusters based on nucleotide homology. The TTG Type A and Type B clusters both contributed to allicin tolerance in tested *B. gladioli*, *B. cepacia*, and *B. orbicola* strains (Figure 2.3A-G). The clusters also contributed to improved bacterial growth in half-strength onion-filtered extract (Figure 2.4). In the onion foliar assay, the Bga 20GA0385 TTG cluster contributed to necrosis length and bacterial *in planta* population count (Figure 2.5A, 2.5B, 2.6A). The TTG Type A cluster when expressed in the *B. gladioli* TTG negative strain BG92_3 background contributed significantly to onion foliar necrosis length and *in planta* bacterial population count (Figure 2.5A,2.5B). The TTG clusters Type A and Type B, however, were not required for red-scale necrosis area and scale bacterial load in *B. gladioli* and *B. orbicola* (Figure 2.5 C, D, G, H). The TTG Type B cluster in *B. cepacia* strain BC83_1 contributed significantly to the RSN area but was inconsequential for the red scale *in planta* population count. The *B. cepacia* BC83_1 TTG Type A cluster was not required for the RSN area or *in planta* bacterial load (Figure 2.6E,2.6F).

The role of the TTG cluster in conferring allicin tolerance in bacterial onion pathogen *P. ananatis* is well correlated with the bacterium's ability to colonize necrotized onion tissue. As members of the bacterial genus *Burkholderia* are routinely isolated from infected onion, we hypothesized they might utilize a similar strategy to combat and colonize the hostile onion environment. We sequenced and assembled the genomes for a panel of onion-isolated

Burkholderia strains collected over 40 years from Georgia, USA. A majority of the sequenced strains belonged to the three common onion-associated *Burkholderia* species: *B. gladioli*, *B. cepacia*, and *B. orbicola*. Putative TTG-like clusters were distributed in all three species. No congruence was observed between the core-gene-based species tree and the TTG cluster-based tree suggesting the TTG clusters might be horizontally acquired. Multiple genes in *P. ananatis* TTG cluster have also been predicted to be involved in horizontal gene transfer (Stice et al., 2018). Most of the *Burkholderia* strains used in the study have GC percentage of >66%. On the other hand, the TTG cluster for these strains had GC% ranging from 57-60%. The difference in GC percentage between the cluster and rest of the chromosome might be another indication of horizontal acquisition of these clusters by the bacterium (Juhas et al., 2009). Upon alignment of the TTG sequence region, three distinct groups were formed based on homology with the consensus. The grouping was also reflected in the phylogenetic tree. The Type A cluster was the most common while no Type C cluster was found in our sequenced panel of strains. Similarly, no Type B cluster was found in *B. cepacia* strains. Four strains harbored two putative TTG clusters simultaneously in their genome. The presence of multiple TTG clusters in the same strain is not exclusive to *Burkholderia* genus. The *Pseudomonas fluorescens* strain *Pf*AR-1 has three copies of TTG clusters that confer resistance to allicin when expressed heterologously in *E. coli* (Borlinghaus et al., 2020). The *B. orbicola* strain HI2424 harbors two Type A TTG clusters, one on the chromosome and the other in the plasmid. The Type C cluster was found in four strains deposited in the NCBI GenBank database but was not identified in our strain panel. The three strains harboring Type C cluster were from *B. gladioli* and they grouped closely to TTG cluster from *Paraburkholderia graminis* strain PHS1. The number of nucleotide substitutions in the Type C TTG strains suggests the TTG cluster might have existed before the differentiation of

Paraburkholderia genus from *Burkholderia.* The Type C cluster type was peculiar in the sense that the putative *altI* C-S lyase encoding gene was present downstream of *altJ* gene and transcribed in the same direction as *altJ*. Apart from this gene, the gene organization of other genes in the *Burkholderia* TTG cluster is conserved. One clinical *B. gladioli* strain BCC0507 had an insertion of a putative IS3 family transposase CDS in between the *altA* and *altC* gene (data not shown).

TTG cluster is a generic name to suggest the resistance to diversity of thiosulfinate compounds. The allicin tolerance cluster (*alt*) as the name implies is named based on the allicin tolerance phenotype following the convention of naming bacterial genes based on their associated phenotypes. The genes were named based on their *Pantoea ananatis* homologs. The gene synteny of the cluster among different bacterial genera, however, is not conserved. The *Burkholderia* TTG cluster is compact with seven genes as opposed to the bacterial onion pathogen *P. ananatis* which has eleven genes in its TTG cluster. The *gor* gene encoding glutathione reductase is associated with TTG clusters in some *Pantoea, Erwinia*, and *Pseudomonas* species but is absent in the *Burkholderia* TTG cluster (Couto et al., 2016; Borlinghaus et al., 2020). Similarly, three additional TTG genes *altD, altH*, and *altG* present in *P. ananatis* PNA 97-1 are absent in *Burkholderia.* The TTG cluster in *P. ananatis* shares some notable differences in gene synteny with the TTG cluster described in representative strains from *Pseudomonas* genus. Despite the differences between the two genera, the TTG cluster gene synteny is conserved among the *P. fluorescens* strain *Pf*AR-1, *P. salomonii* strain ICMP 14252, and *P. syringae* pv. *tomato* strain DC3000 within the *Pseudomonas* genus.

Although widely distributed in onion-isolated bacterial species, it is important to note that the TTG cluster is not exclusive to onion-pathogenic species. Members in the *P. fluorescens*

group are common saprophytes. Analysis of the TTG clusters in *Burkholderia* species deposited in NCBI GenBank database suggests the putative cluster is present in strains isolated from diverse ecosystems such as reactor sludge, clinical patient, soil, sputum, and plant hosts such as *Dendrobium* and *Gladiolus*. As the sequenced strains in our study are draft genomes, we were not able to definitively determine the chromosomal or plasmid origin of the TTG cluster. We used TTG clusters from NCBI closed genomes as a reference to analyze the genomic context of TTG clusters in our panel. In all *B. gladioli* and *B. cepacia* closed genomes in the database, the TTG cluster was harbored in a plasmid. *B. orbicola* strains harbored TTG clusters in both chromosomes or plasmids. We used BLAST analysis to compare 35 kb regions in the *B. cepacia* strain ATCC 25416 including the TTG Type A cluster, and its upstream and downstream gene region against the whole genome sequenced strains in our panel. The gene synteny of the 35 kb region was conserved and shared high nucleotide identity among the 24 strains harboring TTG clusters. Out of the 24 hits obtained from BLAST analysis, 6 were from *B. cepacia* strains and the remaining 18 were from *B. orbicola* species. The 35 kb plasmid region harbored in *B. cepacia* strain ATCC 25416 was 99.9% (3 Single Nucleotide Polymorphisms in ~35 kb region) % identical to the region harbored in chromosome 2 of *B. orbicola* strain HI2424. Although no conclusion can be drawn on the origin of TTG clusters in these strains, it can be predicted that the TTG clusters can be present in both chromosome or plasmids in *Burkholderia* strains.

The presence of two TTG cluster types in a single *Burkholderia* strain was found in four instances. When two of these strains were tested against the natural variant strains harboring a single or no TTG cluster using the allicin ZOI assay, enhanced resistance to allicin was not observed. This was in contrast to *P. fluorescens* strain *Pf*AR-1 and garlic pathogen *P. salomonii* strain ICMP14252, where the presence of two or more endogenous TTG clusters correlated with

enhanced tolerance compared to the single TTG cluster harboring *P. syringae* pv. *tomato* strain DC3000. The TTG Type B cluster conferred enhanced tolerance to allicin in *B. gladioli* strain 20GA0385 and *B. cepacia* strain BC83_1 compared to Type A TTG and WT strains. The enhanced phenotype by Type B cluster was not observed in *B. orbicola* strain LMG 30279 and *B. gladioli* strain BG92_3. Although variation was seen among the experimental repeats, we saw a qualitative growth difference between *B. cepacia* TTG Type A and Type B clusters in a couple of onion-filtered extract growth assay repeats (Figure 2.4B). The *B. orbicola* TTG Type B cluster grew significantly better in onion extract compared to the TTG Type A cluster (Table S2.4). It is not clear what might have contributed to enhanced tolerance by TTG Type B clusters as gene synteny is conserved in both cluster types.

The virulence role of the TTG cluster was analyzed using onion foliar and red scale necrosis and population assays. We observed contrasting virulence roles of *B. gladioli* TTG cluster depending on onion tissue type. The *in planta* foliar population count for Bga 20GA0385 WT strain increased consistently from Day 0 and reached the plateau on Day 3 (Figure 2.6A). The foliar necrosis symptoms by Bga WT strain started appearing on Day 2 and by Day 3, the necrosis extended across the tip with leaves appearing wilted and turned brittle in the subsequent days. The foliar population levels for the TTG mutant remained constant throughout the sampled period. The necrosis symptoms observed with the TTG mutant were restricted around the region of the point of inoculation. Although a 100-fold diluted suspension was used for scale time course assay, the population count for both WT and TTG mutant in red scale reached the peak at the same time as in the foliar tissue (Figure 2.6B). The necrosis area for the majority of both WT and TTG inoculated scales continued to increase even after the population count reached the plateau. Unlike in the foliar tissue, the TTG mutant population count from the red scale assay

was comparable to WT across all the sampling points (Figure 2.6B). These findings from the *in planta* population assay, contradict the results of the onion filtered extract growth assay, where the TTG mutant was severely impaired in the onion juice growth compared to the WT strain (Figure 2.4A). The differences in *in vitro* and *in planta* experiment results suggest that bacteria in onion scale tissue may utilize mechanisms to inhibit the onion-produced thiosulfinates in necrotized tissue. Alternatively, as thiosulfinates are produced by mixing of CSO precursors and alliinase following the disruption of the vacuole, bacteria may exhibit a hemibiotrophic lifestyle keeping the cells intact in the early stages of invasion. This is in line with what we observed in the red scale time course assay where the maximum necrosis area followed after the bacterial population reached the plateau. Based on these observations, we can speculate that the *Burkholderia* strain might be in a hemibiotrophic survival mode in onion scales.

The TTG clusters Type A and Type B were inconsequential for the population on red scale in both *B. orbicola* and *B. cepacia.* As we inoculated a relatively high number of bacteria (~10^8 CFU/ml) in the scales for all three tested species, we sampled a set of scales four hours post-inoculation to check if bacteria have enough threshold for growth inside the scale tissue. The bacterial count four hours post-inoculation was similar for all the treatments tested across the three species. Although not dramatic, we did see a significant population count reduction for TTG Type A plasmid derivative in both *B. cepacia* and *B. orbicola* compared to their respective WT strain. Surprisingly, this trend was not observed for the TTG Type B plasmid derivative that has the same plasmid backbone and was selected under the same conditions. The reduction in Day 0 bacterial population was not observed for *B. gladioli* treatments where a much lower kanamycin concentration (50 µg/ml) was used for selection. It is unclear why the Day 0 population reduction phenotype is specific only to TTG Type A plasmid derivative.

Through this study, we have shown the functional role of the TTG cluster is conserved in distantly related onion pathogenic members of the *Burkholderia* genus. Thiosulfinates are broad-acting antimicrobials (Hunter et al., 2005; Kim et al., 2006). Bacteria in the *Burkholderia* genus may have acquired tolerance mechanisms to evade or inhibit the produced thiosulfinates in a tissue-specific manner. Functional characterization of the TTG constituent genes and their interaction mechanisms with bacteria could open up details on how bacteria can survive and replicate in a challenging onion environment.

Materials and Methods

Bacterial growth conditions

Bacterial strains used for cloning, mutagenesis, and construction of the TTG expression plasmid in this study are listed in Table S2.1. Primers and synthesized dsDNA fragments used in the study are listed in Table S2.2. *Escherichia coli* strains DH5α and RHO5 and all *Burkholderia* strains used for the *in vitro* experiments were grown in LB (per liter, 10 g of tryptone, 5 g of yeast extract, 5 g of NaCl) broth or agar (15 g of agar) at 37°C and 28°C, respectively. Antibiotics and chemicals were supplemented with the growth media at the following final concentrations, per milliliter: 50 – 1000 µg of kanamycin, 10 µg of gentamicin, 100 – 200 µg of Diaminopimelic acid (DAP), 50 µg of X-Gal (5-bromo-4-chloro-3-indolyl-beta-D-galacto-pyranoside), 100 µg of Xgluc (5-bromo-4-chloro-3-indolyl-beta-D-glucuronic acid), and 40-60 µg of rifampicin, as appropriate.

Plant growth conditions

Onion sets (*Allium cepa L.* cv. Century) were planted in 10 cm x 8 cm (diameter x height) plastic pots filled with SunGrow 3B potting soil and maintained at greenhouse conditions with 25–28°C,

12L:12D photoperiod for 5 months from January to May until inoculation. To grow the onion seedlings, onion seeds (*Allium cepa* var. Texas Grano 1015Y) were sown in (5 cm x 5 cm) pots with SunGrow 3B potting soil and maintained at the same conditions as described above in the greenhouse for 8-12 weeks.

Identification of TTG-like cluster in *Burkholderia*

The nucleotide sequences of the individual genes in the TTG-like cluster in *P. ananatis* strain PNA 97-1R (NCBI Accession number: NZ_CP020945.2) were blasted against the *Burkholderia* genome database (taxid: 32008) in NCBI GenBank database using blastX web interface platform. The whole genome sequences of the hits obtained from the blastX search were screened for the presence of a putative TTG-like cluster. The locus tag numbers for the putative genes in the *Burkholderia* TTG-like alt cluster were determined using Geneious Prime v 2023.2.1.

The synteny analysis of the TTG cluster in Bga representative strain 20GA0385 was performed with Clinker web-based platform CAGECAT using *P. ananatis* PNA 97-1 (GenBank Accession: CP020945.2) TTG cluster as a reference (van den Belt et al., 2023). Bakta annotated TTG nucleotide clusters from PNA 97-1 and Bga strain 20GA0385 were used as input for CAGECAT synteny analysis (Schwengers et al., 2021). The identity threshold was set at 0.3 for the analysis.

Whole genome sequencing of select *Burkholderia* strains

A total of 66 *Burkholderia* strains isolated from onions in different regions of Georgia state, USA were sent for whole genome sequencing using Novogene Co., Ltd (Beijing, China) and MicrobesNG Illumina sequencing (Microbes NG, Birmingham, UK). Raw sequences were

filtered using fastp v 0.20.0 (Chen et al., 2018), and quality checks were conducted using fastqc v 0.11.9 (Andrews, 2010). The processed reads were assembled using SPAdes v 3.14 (--isolate --cov-cutoff auto mode) (Bankevich et al., 2012) and filtered for a minimum contig size of 500 bp. Assembled contigs were annotated using the Prokka annotation pipeline (Seemann, 2014). All whole genome sequences were uploaded to the NCBI GenBank database under BioProject ID PRJNA1048086. Strain metadata information is presented in Supplementary Table S3.

The species identity of the sequenced strains was confirmed using the Type Strain Genome Server (TYGS) (Meier-Kolthoff and Göker, 2019). Assemblies were uploaded to the server as inputs. A pairwise GGDC formula 2 (d_4) value of >70% was used as the cutoff for species identification. Bga strain 20GA0385 was also identity-confirmed using a 727 bp partial *recA* gene-based phylogeny (Supplementary Figure S1).

Phylogeny of TTG-like clusters based on whole genome and NCBI extracted sequences

The presence/absence of TTG cluster sequence in the assembled genome sequences was determined using Map to Reference (Bowtie) and/or custom BLAST plugin in Geneious Prime v 2023.2.1 (Langmead, 2010). The TTG cluster sequence from *B. gladioli* pv. *alliicola* strain FDAARGOS_389 (GenBank: CP023524.1) was used as a query sequence for both Map to Reference and custom BLAST analysis. All genome sequenced strains were used to create a custom BLAST database, and the query sequence was used as input against the custom database to perform the analysis. The matched regions obtained from the map to reference analysis and custom BLAST analysis were extracted and aligned using the MAFFT plugin in Geneious Prime. Putative *Burkholderia* TTG clusters from closed genomes in the NCBI GenBank database were also extracted and included in the alignment. Obtained hits smaller than 4952 bp corresponding to *altA – altR* gene region were excluded from further analysis. Metadata for the strains used in

the analysis is presented in Table S2.3. The aligned and trimmed sequence was used as input in MEGA X software for maximum likelihood method-based phylogenetic analysis (Kumar et al., 2018). Nucleotide substitution type with the Tajima-Nei substitution model was used and 1000 bootstrap replicates were used as a test of phylogeny. The obtained Newick (.nwk) tree was uploaded to the interactive Tree of Life (iTOL) database for further formatting (Letunic and Bork, 2021). The synteny analysis of the three TTG clusters A, B, and C from representative *Burkholderia* strains was performed using Clinker arrow diagram generated using CAGECAT webserver following the same parameters as described above (Schwengers et al., 2021). The percentage nucleotide identity among the three cluster was calculated using Geneious Prime.

Identity confirmation of *B. gladioli* strains FDAARGOS_389 and 20GA0385 was done using a 727 bp partial *recA*-based phylogenetic analysis. Genome assemblies from representative strains in *B. gladioli* Clade 1A, 1B, 1C, 2, and 3 as described in (Jones et al., 2021) were downloaded from the NCBI GenBank database. Assemblies from *B. cepacia* strain ATCC 25416 and *B. cenocepacia* J2315 were also downloaded from the NCBI GenBank database. The presence of partial *recA* gene sequence was determined in the downloaded assemblies using Bowtie Map to Reference plugin in Geneious Prime v 2023.9.0, with the FDAARGOS_389 partial *recA* gene sequence as a query. The mapped regions in the target assemblies were extracted and aligned using the MAFFT multiple align plugin in Geneious Prime. The aligned sequences were used as input to generate a maximum likelihood based phylogenetic tree using MEGA-X. For the test of phylogeny, 1000 replicates of the bootstrap method were used. The identity of strains FDAARGOS_389 and 20GA0385 was confirmed by analyzing their grouping in the phylogenetic tree relative to reference strains from different clades as described in (Jones et al., 2021)

Creation of *B. gladioli* TTG mutant strain

The unmarked deletion of the TTG cluster in Bga strain 20GA0385 was generated using an allelic exchange strategy. The 450 bp upstream (including 2 aa downstream of the stop codon in *altB* ORF) and 450 bp downstream flanking region (including 1 aa upstream of the stop codon in *altI* ORF) of TTG cluster from *B. gladioli* strain FDAARGOS_389 (GenBank: CP023522.1) along with attached attB1 and attB2 site was synthesized as a double-stranded DNA gblocks from Twist Biosciences. An AvrII restriction site was also included in between the deletion flank. The synthesized TTG fragment was BP cloned into suicide vector pR6KT2G using Gateway BP Clonase II enzyme mix (Thermo Fisher Scientific) (Stice et al., 2020). The cloned reaction following the treatment with Proteinase K was placed on the VMWP membrane (Millipore) and floated on top of sterile distilled water (dH_20) for 30 minutes. The de-salted mix was electroporated into *E. coli* MAH1 cells and transformants were selected on LB agar amended with gentamicin and Xgluc followed by incubation at 37^0C overnight (Kvitko et al., 2012). Selected transformants were grown overnight and the plasmid was prepped with GeneJet Plasmid Miniprep Kit (ThermoScientific, Watham, WA). The correct recombinant plasmid was confirmed with a HindIII restriction enzyme digest reaction and compared to a simulated pattern obtained using NEBcutter V2.0. One clone with the correct restriction digest size, was selected and sent for sequencing using pR6KT2GW-F and pR6KT2GW-R primer pair (Supplementary Table S2). The sequenced reads were aligned with the simulated vector created in Geneious Prime V 2021.1.6 to confirm the insert. The confirmed plasmid was then cloned into an LR-clonase compatible pK18mobsacB plasmid derivative pDEST1k18ms following the manufacturer's recommendations (Mijatović et al., 2021). Following the Proteinase K treatment, the cloned reaction product was transformed into chemically competent *E. coli* DH5α cells, and

the transformants were selected on LB amended with kanamycin and screened for the correct insert using BsrGI restriction digest. The clone with the correct digest pattern was sent for sequencing with M13R49 primer and the sequence was analyzed as described above using Geneious Prime to confirm the insert. The confirmed insert was then transformed into E. competent *E. coli* RHO5 pir+ mating strain and selected on LB plate amended with DAP and kanamycin plates. *E. coli* no DAP liquid culture control and parental controls were also included. The plasmid with the deletion construct in the RHO5 strain was mated with WT 20GA0385 strain and merodiploids were selected on LB plate amended with rifampicin and kanamycin. For the sucrose-based counter selection, 10 merodiploid colonies were selected and suspended in 5 ml of sterile LB media. 50 µl of the suspension was spread on an LB plate amended with rifampicin and 10% 1M sucrose followed by incubation at 30^0C for 48 hours. Isolated exconjugant colonies on the sucrose plate were patch-plated into both LB and LB amended with kanamycin plates to check the sensitivity of exconjugant clones to kanamycin. Kanamycin-sensitive exconjugants were screened for the mutant with colony PCR using altgenoF and altgenoR primers designed outside of the deletion flanks with the following PCR reaction mix: 10 µl of GoTaq Green master mix (Promega), 0.5 µl of each primer at 10 µM concentration, 3 µl of colony DNA template and 6 µl of sterile Milli-Q water to make a total of 20 µl single reaction. To prepare the colony DNA template for PCR, a sterile pipette tip was used to scrap kanamycin-sensitive exconjugants and suspended in 100 µl of sterile Milli-Q water. The suspension was denaturated at 95^0C for 10 minutes. The denatured mix was centrifuged for 2 minutes. The supernatant was then used as a DNA template for PCR reaction. The PCR conditions used were: 95^0C for 5 minutes followed by 35 cycles of 95^0C at 20 s, 60^0C at 30 s, 72^0C for 1 minute followed by a final extension at 72^0C for 5 minutes. Amplicon was expected only from the TTG

mutants. The PCR amplicon was visualized in 1.5% agarose gel stained with SYBR Safe DNA gel stain (Thermo Fisher Scientific). The PCR product of the selected deletion mutant was purified using Monarch PCR and DNA cleanup kit (NEB) and sent for sequencing at Eurofins Genomics LLC (Louisville, KY, USA). The sequenced reads were aligned with the extended TTG cluster region of strain 20GA0385 to confirm the deletion mutant. Summary diagram of the method used to generate the TTG deletion mutant is presented in Supplementary Figure S2.2.

Construction of TTG complementation plasmid

A broad host range pBBR1 derived plasmid pBBR1MCS-2 (GenBank: U23751.1) was used for building the TTG complementation plasmid. Primer pair altcomplngibF2 and altcomplngibR2 was designed to amplify the TTG gene cluster and 489 nucleotide region upstream of *altB* and 405 bp region downstream of *altI* gene region. A 35 bp Gibson overhang upstream and downstream of unique XbaI restriction site in the multiple cloning site (MCS) of the plasmid pBBR1MCS-2 was added to 5' region and 3' region of altcomplngibF2 and altcomplngibR2 primers respectively. The gene region was amplified from the *B. gladioli* strain FDAARGOS_389 strain using Q5 High-Fidelity DNA polymerase PCR (New England Biolabs) following 20 µl final volume and reaction components mentioned in the manufacturer's protocol (https://www.neb.com/en-us/protocols/2013/12/13/pcr-using-q5-high-fidelity-dna-polymerase-m0491). The PCR conditions used were: 98^0C for 30 s followed by 30 cycles of 98^0C for 10s, 59^0C for 30 s, 72^0C for 4 minutes, and final extension for 2 minutes. The PCR amplicon was visualized in 1.5% agarose gel and the band obtained in the expected region was excised and purified using a Monarch NEB Gel extraction kit. The PCR product from the repeated reaction was purified using Monarch NEB PCR cleanup kit and purified product was digested with AvrII and XbaI restriction enzyme. The visualized digest pattern in the gel was compared with the

simulated *in silico* pattern to confirm the TTG gene cluster-specific PCR product. The pBBR1MCS-2 plasmid was linearized with XbaI restriction enzyme and the gel product was excised and purified as described above. Gel-purified TTG PCR product and XbaI linearized plasmid were mixed in a reaction with NEB Hifi DNA assembly polymerase master mix following the manufacturer's protocol to perform the ligation reaction. The ligation mix was then transformed into chemically competent DH5α cells and selected on an LB plate amended with kanamycin and Xgal. The clone with insert was expected to be white on Xgal plates. White clones obtained on the plates were screened for the correct insert using genotyping primer pair altcomplnF designed upstream of the attB2 site and M13R49 primer binding region in the plasmid backbone. A product size of 544 bp was expected for the correct insert. The PCR conditions used were: 95^0C for 5 minutes followed by 35 cycles of 95^0C for 20 s, 55^0C for 30 s, 72^0C for 45 s, and a final extension for 5 minutes. Similarly, a second PCR primer set altgenocomplnR was designed downstream of the attB1 site and used with M13F43 primer in the plasmid backbone to genotype the TTG insert. The expected product size was 514 bp. PCR was performed in 20 µl reaction using GoTaq green master mix with reaction mix followed as described before. The PCR conditions used were: 95^0C for 5 minutes followed by 35 cycles of 95^0C for 20 s, 62^0C for 30 s, 72^0C for 45 s, and a final extension for 5 minutes. The insert was also confirmed using BsrGI restriction digest and whole plasmid sequencing at Plasmidsaurus (Plasmidsaurus, Eugene, OR).

For the construction of TTG Type B complementation plasmid, a primer pair with 35 bp overhang from upstream and downstream sequence region of unique XbaI restriction site was designed targeting 6842 bp of the TTG cluster gene region in the strain BC93_12. Colony PCR was performed in a 20 µl reaction using the Q5 polymerase protocol as described in the

manufacturer's protocol. The following PCR conditions were used: 98^0C for 30 s followed by 30 cycles of 98^0C for 10s, 61^0C for 30 s, 72^0C for 210 s, and final extension for 2 minutes. The gel purified PCR product was ligated to XbaI linearized pBBR1MCS-2 plasmid using NEB Hifi DNA assembly reaction and the reaction mixture was transformed to chemically competent DH5α cells and selected on LB plates amended with kanamycin and Xgal. Colonies appearing white on the Xgal kanamycin plates were screened for the insert using primer pair typeBgenocomplnR designed upstream of the attB2 sequence and standard primer M13F43 in the plasmid backbone. The expected product size was 627 bp. PCR conditions followed were the same as described above for primer pair altgenocomplnR and M13F43. A plasmid clone with the expected amplicon size was sent for sequencing at Plasmidsaurus.

Construction of TTG expression clone in TTG negative natural variant strains background

The sequenced confirmed Type A and TTG Type B gene clusters in pBBR1MCS-2 plasmid were transformed to electrocompetent RHO5 cells and selected on LB plate amended with DAP and kanamycin following incubation at 37^0C overnight. No DNA control was also included. The pBBR1MCS-2 Empty Vector (EV) was also transformed into electrocompetent RHO5 cells and selected following the same procedure. Single transformant Type A, Type B, and EV colonies growing on LB DAP kanamycin plate were inoculated to start an overnight culture and conjugated with representative TTG negative *Burkholderia* natural variant strains using biparental mating. *B. cepacia* natural variant BC83_1 conjugants were selected on LB plate amended with 1000 µg of kanamycin per mililitre, *B. orbicola* natural variant LMG 30279 TTG conjugants were selected on LB plate amended with 200 µg of kanamycin per mililitre whereas *B. gladioli* natural variant BG92_3 TTG conjugants and engineered 20GA0385 TTG mutants were selected on LB amended with rifampicin and 50 µg of kanamycin. Each of the TTG

negative natural variant strains and engineered TTG mutants were conjugated with pBBR1MCS-2 plasmid harboring both Type A and TTG Type B clusters. The insert was confirmed using the genotyping primers described in the previous section following the same procedure.

Preparation of allicin stock solution

The allicin stock preparation procedure was followed as described by (Stice et al., 2020) with slight modifications. Briefly, 15 µl of diallyl disulfide 96% (Carbosynth), 25 µl of glacial acetic acid (Sigma Aldrich), and 15 µl of 30% H_20_2 were mixed in a 200 ul PCR tube. The tube was sealed with parafilm, attached to a 500 ml beaker, and agitated at a 28^0C shaker for 6 h. The reaction mix was then suspended in 1 ml of methanol. The methanol allicin mix was used as a synthesized allicin stock for the ZOI assay.

Zone of inhibition assay

The ZOI assay was performed to test the quantitative/qualitative differences in resistance between the strains harboring endogenous or plasmid-based TTG clusters relative to the TTG-negative engineered strains or natural variant strains. The LB overnight cultures (O/N) (~24 hr) amended with appropriate antibiotics were started from a single colony of the representative strains. Polystyrene petri plates (100 mm x 15 mm) with 20 mL of LB agar and appropriate antibiotics as needed were spread with 300 µl of bacterial suspension. All natural variant strains were plated on LB media. *B. gladioli* BG92_3 strain was plated on LB amended with rifampicin and its TTG plasmid derivatives were plated on LB amended with kanamycin and rifampicin. *B. cepacia* TTG negative variant was plated on LB and its TTG plasmid derivatives were plated on LB amended with 1000 µg/ml kanamycin. *B. orbicola* strain LMG 30279 TTG plasmid derivatives were plated on LB amended with 200 µg/ml kanamycin plate and its WT was plated

on LB. The WT *B. gladioli* strain 20GA0385 and its engineered TTG mutant derivative were plated on LB and the Type A and TTG Type B plasmid complement derivatives were plated on LB amended with rifampicin and kanamycin for the ZOI assay. Three plate replicates were used per treatment. A circular well was poked at the center of the plate using the back end of sterile 10 µl pipette tips and 50 µl of the synthesized allicin stock was added to the wells. Plates were incubated at 28^{o}C for 24 h. The ZOI area was measured using ImageJ software (Abràmoff et al., 2004). The experiment was repeated at least 3 times. The statistical difference in the ZOI area among different natural variants within a species was determined using one-way Analysis of Variance (ANOVA) and Tukey's Honestly Significant Difference (HSD) test using agricolae library and the box plot was generated using ggplot2 function in RStudio v 2023.9.0.

Preparation of onion juice

Yellow onions were purchased from the grocery store and the crude juice was extracted following the procedure described by Stice et al., 2020. Briefly, a consumer-grade juicer (Breville Juice Fountain Elite) was used to crush the onion bulb which yielded 200-300 ml of crude onion extract. The extract was centrifuged (Sorvall RC5B Plus, Marshall Scientific, Hampton, NH) in a 250 ml centrifuge bottle (14000 g, 2 h, 4^{o}C). The upper phase liquid was sterilized using a Nalgene disposable 0.2-micron vacuum filter sterilization unit. The prepared juice was aliquoted and stored at -20^{0}C for less than 1 week for experimental use.

Preparation of bacterial inoculum

Bacterial inocula for the ZOI assays, onion foliar assays, RSN assays, and foliar and scale time course experiments were prepared following the same procedure for all tested *Burkholderia* strains. The test strains were streaked on an LB plate amended with appropriate antibiotics and

incubated at 28°C for 24 h. A day after, colony growth from the lawn was suspended in 300 µl of sterile Milli-Q water and incubated for 24 h overnight. A day after, colony growth from the lawn was scooped and suspended in 1 ml of ddH_20 /$MgCl_2$ and standardized to OD_{600} = 0.7 (~2.4 x 10^8 CFU/ml, *B. gladioli* 20GA0385). The standardized suspension was used for inoculation.

Onion filtered extract growth assay

The growth assay experiment was performed in 100-well honeycomb plates using the Bioscreen C system (Lab Systems, Helsinki, Finland). The standardized suspension volume of 40 µl was added to 360 µl of half-strength filtered onion extract (180 µl of onion juice diluted with 180 µl of sterile ddH20). Each honeycomb well was loaded with 380 µl of the mix and each treatment had six well replicates. The bioscreen experiment was run for 48 h with shaking at 28°C and the absorbance values were recorded every 30 minutes. The experiment was repeated three times for each tested species. Statistical analysis of OD_{600} values at each time point for different treatments was performed using the pairwise t-test function in RStudio 2023.09.0. The average OD_{600} reading of water-onion extract negative control treatment for each time point was subtracted from the OD_{600} reading values obtained for each well for all the treatments at the corresponding time point.

Onion foliar/seedling necrosis assay

Onion seedlings (*Allium cepa* L. cv Texas grano 1015 Y supersweet onions) of 8-12 weeks were used for the foliar assay. Inoculum for strains 20GA0385 pBBR1MCS-2 EV, 20GA0385 ΔTTG pBBR1MCS-2 EV, 20GA0385 ΔTTG pBBRR1MCS-2 TTG Type A, BG92-3 and its Type A and TTG Type B plasmid derivatives were prepared as previously described. Onion seedlings were trimmed to keep the oldest blade intact and approximately the midpoint of the blade was poked

on one side with a sterile 20 µl pipette tip to create a wound. The normalized bacterial suspension of 10 µl prepared with 0.25 mM $MgCl_2$ was deposited into the wounded tissue. Negative controls were inoculated with sterile 0.25 mM $MgCl_2$. Maximum lesion length was measured 3 days post inoculation (dpi). Each treatment had six biological repeats and the experiment was repeated at least three times.

For quantification of bacterial population in the infected blade tissue, a section of the infected tissue measuring 0.5 cm above and below the point of inoculation was cut and resuspended in 200 µl of Milli-Q H_20 in a 2-ml SARSTEDT microtube (SARSTEDT AG & Co., Numbrecht, Germany). The tissue was manually crushed using a sterile blue pestle and then ground with a SpeedMill PlUS homogenizer (AnalytiK Jena) two times for 1 minute each. To facilitate the maceration, three 3-mm zirconia beads (Glen Mills grinding media) and one 4.5 mm bead (store-bought) were added to the tissue and water mix. Serial dilutions were performed using 10 µl of the ground tissue and diluents were plated on LB plates amended with rifampicin and kanamycin. The number of colony-forming units (CFUs) was back-calculated to determine the bacterial population levels in the infected tissue.

The time course foliar assay was performed using 4-6 months old onion plants (cv. Century) grown in the greenhouse. *B. gladioli* strain 20GA0385 and its TTG mutant derivative were used for the study. The onion blades were trimmed to keep the oldest two leaves intact that were used for inoculation. The midpoint of the blade (measured from the tip to the base of the blade) was marked with a sharpie and a sterile 20 µl pipette tip was used to poke a hole on one side of the leaf to create wounding. Bacterial inoculum concentration of OD_{600} = 0.7, ~2.4 x 10^8 colony forming units (CFU)/ml for *B. gladioli* 20GA0385 WT and the TTG mutant, was used. Normalized bacterial suspension (10 µl) was deposited to the wounding site. Three plants were

inoculated per treatment (six blades total). A total of 36 onion plants (72 blades in total) were inoculated and sampled daily from 0 to 5 dpi. Day 0 samples were processed for bacterial quantification 6 hours post-inoculation.

The bacterial population in the infected tissue was quantified by sampling the tissue samples 0.5 cm above and 0.5 cm below the point of inoculation. The tissue was weighed in 200 µl of sterile Milli-Q H_20 in a 2-ml SARSTEDT microtube. The tube was filled with 3-mm zirconia beads for maceration with a GenoGrinder and an additional 4.5 mm bead was added for grinding with the SpeedMill PlUS homogenizer. For grinding with GenoGrinder, 30 seconds was used and the SpeedMill homogenizer was used for maceration two runs of 1 minute each. The resulting macerate was serially diluted to 10^8 in 0.25 mM $MgCl_2$ in 96-well styrene plates (20 µl, 180 µl). The dilutions were plated on LB square plates amended with rifampicin and cfu per mg was backcalculated for each treatment. The cfu/mg value for two inoculated leaves from the same plant was averaged to get a single cfu/mg value per biological replicate per treatment. The log folded cfu/mg values of three biological replicates per treatment were plotted against days post-inoculation. The statistical difference in bacteria population levels each day between the two treatments was analyzed using a pairwise t-test function in RStudio. The experiment was repeated two times.

RSN assay

The RSN assay was set up following the procedure described in (Stice et al., 2018), and (Shin et al., 2023) with slight modifications. Red onion bulbs were purchased from a grocery store and sliced into 3-5 x 3-5 cm-sized scales. The scales were surface sterilized in a 3% sodium hypochlorite solution for 2 minutes and rinsed in deionized water six times. After drying on a sterile paper towel for a few minutes, the scales were placed on an ethanol wiped pipette tip rack.

Each scale was wounded using a sterile 20 µl pipette tip and then inoculated with 10 µl of a standardized bacterial suspension. Sterile 0.25 mM $MgCl_2$ was inoculated as a negative control. The scales were placed on a flat potting tray (27 x 52 cm) lined with two layers of paper towel that had been moistened with 50 ml of deionized water. Another flat was placed on top of the tray to maintain humidity and the entire setup was incubated at room temperature for 72 h. Six scales were inoculated per treatment and the experiment was repeated three times.

The scale necrosis area after 72 h was measured using ImageJ. For quantification of bacteria in the necrotic onion tissue, approximately 0.5 x 0.5 cm area around the point of inoculation was excised with a sterile scalpel, suspended, and weighed in a 1.5 ml microcentrifuge tube with 200 µl of sterile water after 4- and 72-hour post-inoculation. The tissue was crushed manually with the end of a sterile wooden cocktail stick. The resulting macerate was diluted ten-fold in a dilution series with sterile 0.25 mM $MgCl_2$ in 96-well styrene plates (20 µl, 180 µl). The diluents (10 µl) were plated on LB amended with rifampicin and kanamycin as appropriate and incubated at 28ºC for 36 h. Colonies were counted and cfu per milligram was back-calculated for each sampled scale. Three scales treated with the negative control were processed 4 h post-inoculation and three were processed 72 h post-inoculation. For the rest of the treatments, six inoculated scales were processed. Statistical analysis of the differences between species-specific treatments was performed using the pairwise t-test function in RStudio.

The inoculum preparation, assay setup, and quantification of bacteria in infected onion tissues for the RSN time course experiment were conducted as described in the previous section. The *B. gladioli* strain 20GA0385 pBBR1MCS-2 EV and its TTG mutant derivative were used for the experiment. The bacterial suspension was normalized to OD_{600} value of 0.7 followed by 100-

fold dilution. Each scale was inoculated with 10 µl of diluted suspension. A total of 72 individual scales were inoculated and six scales per treatment were sampled daily from day 0 to day 5 post-inoculation. Subsequently, a dilution series ranging from 10^{-1} to 10^{-3} of the TTG mutant treatment was plated on an LB square plate amended with rifampicin and kanamycin as negative control. The statistical analysis of the difference in $\log_{10}$ fold cfu per milligram bacterial recovery between the two treatments at each time point was performed using a pairwise t-test function in RStudio.

References

Abràmoff, M., Magalhães, P.J., and Ram, S.J. 2004. Image processing with ImageJ. Biophotonics international 11:36-42.

Andrews, S. (2010). FastQC: a quality control tool for high throughput sequence data (Babraham Bioinformatics, Babraham Institute, Cambridge, United Kingdom).

Bankevich, A., Nurk, S., Antipov, D., Gurevich, A.A., Dvorkin, M., Kulikov, A.S., Lesin, V.M., Nikolenko, S.I., Pham, S., and Prjibelski, A.D. 2012. SPAdes: a new genome assembly algorithm and its applications to single-cell sequencing. Journal of Computational Biology 19:455-477.

Belo, T., du Toit, L., Waters, T., Derie, M., Schacht, B., and LaHue, G.T. 2023. Reducing the risk of onion bacterial diseases through managing irrigation frequency and final irrigation timing. Agricultural Water Management 288:108476.

Borlinghaus, J., Bolger, A., Schier, C., Vogel, A., Usadel, B., Gruhlke, M.C., and Slusarenko, A.J. 2020. Genetic and molecular characterization of multicomponent resistance of *Pseudomonas* against allicin. Life Sci Alliance 3. e202000670

Burkholder, W. 1942. Three bacterial plant pathogens: *Phytomonas earyophylli* sp. n., *Phytomonas alliicola* sp. n., and *Phytomonas manihotis* (Arthaud-Berthet et Sondar) Viégas. Phytopathology 32:141-149.

Burkholder, W. 1950. Sour skin, a bacterial rot of Onion bulbs. Phytopathology 40.

Chen, S., Zhou, Y., Chen, Y., and Gu, J. 2018. fastp: an ultra-fast all-in-one FASTQ preprocessor. Bioinformatics 34:i884-i890.

Hunter, R., Caira, M., and Stellenboom, N. 2005. Thiolsulfinate allicin from garlic: Inspiration for a new antimicrobial agent. Annals of the New York Academy of Sciences 1056:234-241.

Jones, C., Webster, G., Mullins, A.J., Jenner, M., Bull, M.J., Dashti, Y., Spilker, T., Parkhill, J., Connor, T.R., and LiPuma, J.J. 2021. Kill and cure: genomic phylogeny and bioactivity of *Burkholderia gladioli* bacteria capable of pathogenic and beneficial lifestyles. Microbial genomics 7.

Juhas, M., van der Meer, J.R., Gaillard, M., Harding, R.M., Hood, D.W., and Crook, D.W. 2009. Genomic islands: tools of bacterial horizontal gene transfer and evolution. FEMS Microbiol Rev 33:376-393.

Katagiri, F., Thilmony, R., and He, S. 2002. The *Arabidopsis thaliana-Pseudomonas syringae* interaction. The Arabidopsis Book/American Society of Plant Biologists 1.

Kawamoto, S., and Lorbeer, J. 1974. Infection of onion leaves by *Pseudomonas cepacia*. Phytopathology 64:1440-1445.

Kim, S., Kubec, R., and Musah, R.A. 2006. Antibacterial and antifungal activity of sulfur-containing compounds from *Petiveria alliacea* L. Journal of Ethnopharmacology 104:188-192.

Kumar, S., Stecher, G., Li, M., Knyaz, C., and Tamura, K. 2018. MEGAX: molecular evolutionary genetics analysis across computing platforms; . Molecular Biology and Evolution 35:1547-1549.

Kvitko, B.H., Bruckbauer, S., Prucha, J., McMillan, I., Breland, E.J., Lehman, S., Mladinich, K., Choi, K., Karkhoff-Schweizer, R., and Schweizer, H. 2012. A simple method for construction of pir+ Enterobacterial hosts for maintenance of R6K replicon plasmids. BMC research notes 5:1-7.

Lancaster, J., and Collin, H. 1981. Presence of alliinase in isolated vacuoles and of alkyl cysteine sulphoxides in the cytoplasm of bulbs of onion (*Allium cepa*). Plant Science Letters 22:169-176.

Langmead, B. 2010. Aligning short sequencing reads with Bowtie. Current protocols in bioinformatics 32:11.17. 11-11.17. 14.

Lee, C.J., Lee, J.T., Kwor, J., Kim, B., and Park, W. 2005. Occurrence of bacterial soft rot of onion plants caused by *Burkholderia gladioli* pv. *alliicola* in Korea. Australasian Plant Pathology 34:287-292.

Letunic, I., and Bork, P. 2021. Interactive Tree Of Life (iTOL) v5: an online tool for phylogenetic tree display and annotation. Nucleic acids research 49:W293-W296.

Mark, G., Gitaitis, R., and Lorbeer, J. 2002. Bacterial diseases of onion. *Allium* crop science: recent advances:267-292.

Meier-Kolthoff, J., and Göker, M. 2019. TYGS is an automated high-throughput platform for state-of-the-art genome-based taxonomy. Nature Communications 10:2182.

Mijatović, J., Severns, P.M., Kemerait, R.C., Walcott, R.R., and Kvitko, B.H. 2021. Patterns of seed-to-seedling transmission of *Xanthomonas citri* pv. *malvacearum*, the causal agent of cotton bacterial blight. Phytopathology 111:2176-2184.

Morales-Ruíz, L.M., Rodríguez-Cisneros, M., Kerber-Díaz, J.C., Rojas-Rojas, F.U., Ibarra, J.A., and Estrada-de Los Santos, P. 2022. *Burkholderia orbicola* sp. nov., a novel species within the *Burkholderia cepacia* complex. Arch Microbiol 204:178.

Rose, P., Whiteman, M., Moore, P., and Zhu, Y. 2005. Bioactive S-alk (en) yl cysteine sulfoxide metabolites in the genus *Allium*: the chemistry of potential therapeutic agents. Natural product reports 22:351-368.

Schwengers, O., Jelonek, L., Dieckmann, M.A., Beyvers, S., Blom, J., and Goesmann, A. 2021. Bakta: rapid and standardized annotation of bacterial genomes via alignment-free sequence identification. Microbial genomics 7:000685.

Seemann, T. 2014. Prokka: rapid prokaryotic genome annotation. Bioinformatics 30:2068-2069.

Shin, G.Y., Dutta, B., and Kvitko, B. 2023. The genetic requirements for HiVir-mediated onion necrosis by *Pantoea ananatis*, a necrotrophic plant pathogen. Molecular Plant-Microbe Interactions 36:381-391.

Silvaroli, J., Pleshinger, M., Banerjee, S., Kiser, P., and Golczak, M. 2017. Enzyme that makes you cry–crystal structure of lachrymatory factor synthase from *Allium cepa*. ACS chemical biology 12:2296-2304.

Stice, S., Stumpf, S., Gitaitis, R., Kvitko, B., and Dutta, B. 2018. *Pantoea ananatis genetic* diversity analysis reveals limited genomic diversity as well as accessory genes correlated with onion pathogenicity. Frontiers in microbiology 9:184.

Stice, S., Thao, K., Khang, C., Baltrus, D., Dutta, B., and Kvitko, B. 2020. Thiosulfinate tolerance is a virulence strategy of an atypical bacterial pathogen of onion. Current Biology 30:3130-3140. e3136.

van den Belt, M., Gilchrist, C., Booth, T.J., Chooi, Y., Medema, M.H., and Alanjary, M. 2023. CAGECAT: The CompArative GEne Cluster Analysis Toolbox for rapid search and visualisation of homologous gene clusters. BMC bioinformatics 24:1-8.

Velez, L., Aburjaile, F., Farias, A.G., Baia, A.D.B., Oliveira, W., Silva, A.F., Benko-Iseppon, A., Azevedo, V., Brenig, B., Ham, J., Souza, E., and Gama, M.S. 2023. *Burkholderia semiarida* sp. nov. and *Burkholderia sola* sp. nov., two novel *B. cepacia* complex species causing onion sour skin. Systematic and Applied Microbiology 46:126415.

Zhao, M., Tyson, C., Gitaitis, R., Kvitko, B., and Dutta, B. 2022. *Rouxiella badensis*, a new bacterial pathogen of onion causing bulb rot. Frontiers in Microbiology 13.

Figures

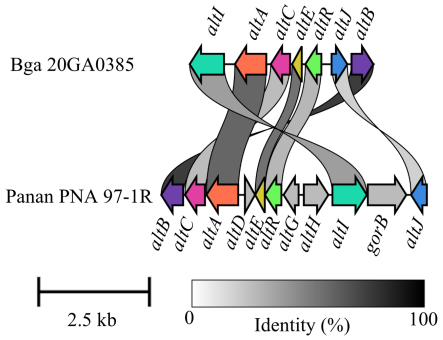

altB : D-glucose:NAD+ 1-oxidoreductase
altC : DsbA family oxidoreductase
altA : N-ethylmaleimide reductase
altE : CMD-like domain-containing protein
altR : HTH TetR family transcriptional regulator
altI : Aminotran-1-2 domain-containing protein
altJ : Osmotically inducible protein C
altD : Thioredoxin domain containing protein
altG : Thioredoxin-like protein
altH : DMT family transporter
gorB : glutathione disulfide reductase

Figure 2.1: Gene cluster organization representing seven genes in the putative Thiosulfinate Tolerance Gene (TTG) cluster in *Burkholderia gladioli* pv. *alliicola* strain 20GA0385. Gene synteny of the Bga cluster relative to *Pantoea ananatis* strain PNA 97-1 is shown using the Clinker arrow diagram. Genes are linked on color code based on amino acid homology between the two gene clusters, the percentage of which is shown in the gradient scale. The proposed function of the genes in the cluster based on Stice et al., 2020 is listed.

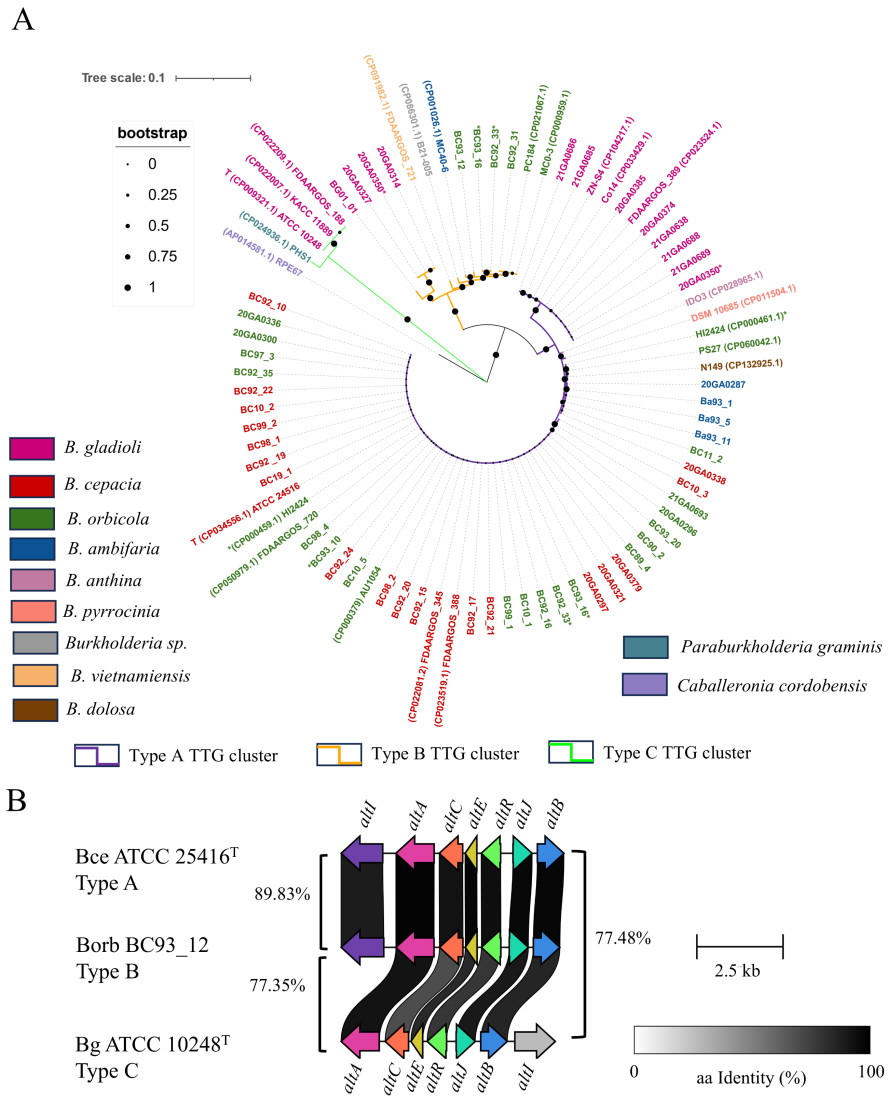

Figure. 2.2. The thiosulfinate tolerance gene (TTG) cluster is widely distributed in *Burkholderia* species. **A,** Maximum-likelihood method-based phylogenetic tree of n = 4,952-bp partial TTG cluster consensus nucleotide sequences corresponding to the *altA–altB* gene region derived from whole-genome sequenced *Burkholderia* isolates in the study and NCBI GenBank-extracted TTG cluster sequences; 1,000 bootstrap replicates were used as a test of phylogeny. Bootstrap support value on the scale of 0 to 1 is represented as a circle on the branch. Strain labels are color coded based on species, and branches are color coded based on TTG cluster type. The accession number of the GenBank-extracted sequences is provided in parentheses next to the strain name. Strains with two putative TTG clusters are noted with an asterisk next to the name. The letter T indicates a type strain. The tree is rooted in the *Caballeronia cordobensis* strain RPE67 branch. Strain 20GA0329, strain 20GA0341, and TTG cluster Type B sequence of *B. gladioli* strain BC93_10 are omitted from the alignment as the entire TTG sequence was not present in a single contig. Information about the strains used is presented in Supplementary Table S3. Identity confirmation of the strains extracted from the NCBI GenBank database was confirmed using the

Type Strain Genome Server (TYGS) webserver. **B,** Clinker arrow diagram showing the gene synteny and organization among the representative Type A, Type B, and Type C clusters in *Burkholderia* species. The links between the clusters are gradient coded based on amino acid identity, the percentage of which is shown in the gradient scale. Numbers accompanying square brackets between the clusters represent percentage nucleotide identity in between the *altA–altB* region, which is calculated using Geneious Prime. T = type strain, aa = amino acid, Bce = *B. cepacia*, Borb = *B. orbicola*, and Bg = *B. gladioli*.

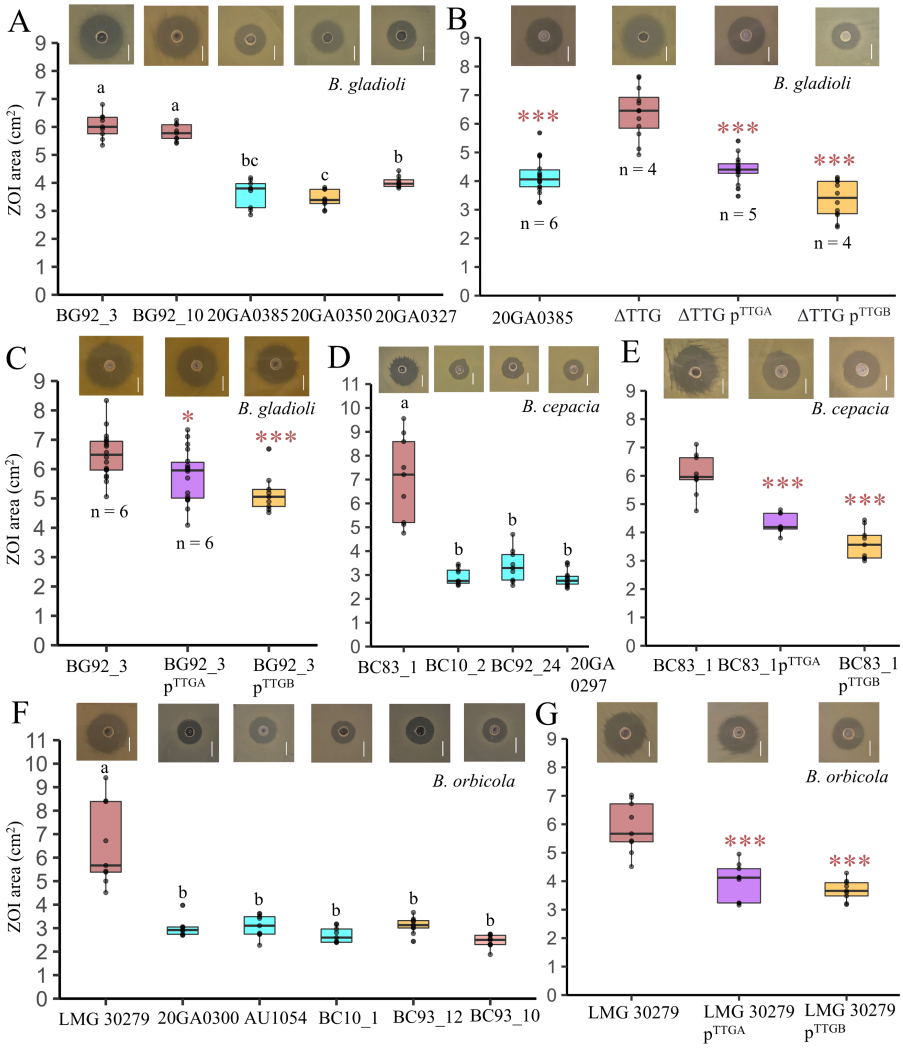

Figure 2.3. The thiosulfinate tolerance gene (TTG) cluster contributes to allicin thiosulfinate tolerance in *Burkholderia* species. **A,** Allicin zone of inhibition (ZOI) area of select natural variant isolates of *B. gladioli*. **B,** ZOI area of engineered TTG mutant and Type A and TTG Type B cluster-complementing strains of *B. gladioli* strain 20GA0385. **C,** ZOI area of TTG-negative *B. gladioli* strain BG92_3 relative to its TTG Type A and Type B plasmid derivatives. **D,** ZOI area of select natural variant isolates of *B. cepacia.* **E,** ZOI area of TTG-negative *B. cepacia* strain BC83_1 compared with its TTG Type A and Type B plasmid derivatives. **F,** ZOI area comparison of representative natural variants of *B. orbicola.* **G,** ZOI area of *B. orbicola* TTG-negative type strain LMG 30279 and its Type A and TTG Type B plasmid derivatives. The cyan-colored bar represents a strain with endogenous TTG Type A cluster; the brown bar represents a TTG-negative engineered or natural variant strain; the purple bar represents TTG-negative strains with TTG Type A expression plasmid; the orange bar represents a TTG-negative strain with TTG Type B expression plasmid or strains with endogenous TTG Type B cluster; and the salmon bar represents a strain with both Type A and TTG Type B cluster. Representative images of ZOI plates tested with corresponding treatments are presented above the box. The scale bar in the image represents a 1-cm length. Significance grouping based on analysis of variance (ANOVA) followed by Tukey's post-test is shown as letters above the boxes in natural variants experiments. A pairwise *t*-test was done to determine the significant differences in ZOI area between the isogenic TTG-lacking strains and plasmid-expressed TTG cluster strains. Level of significance: *** = 0.001; and * = 0.05. The experiment was repeated at least three times or as represented by *n* = number of independent experimental repeats. The depicted data point represents all biological replicates from independent experimental repeats. Each experiment was conducted with three biological replicates.

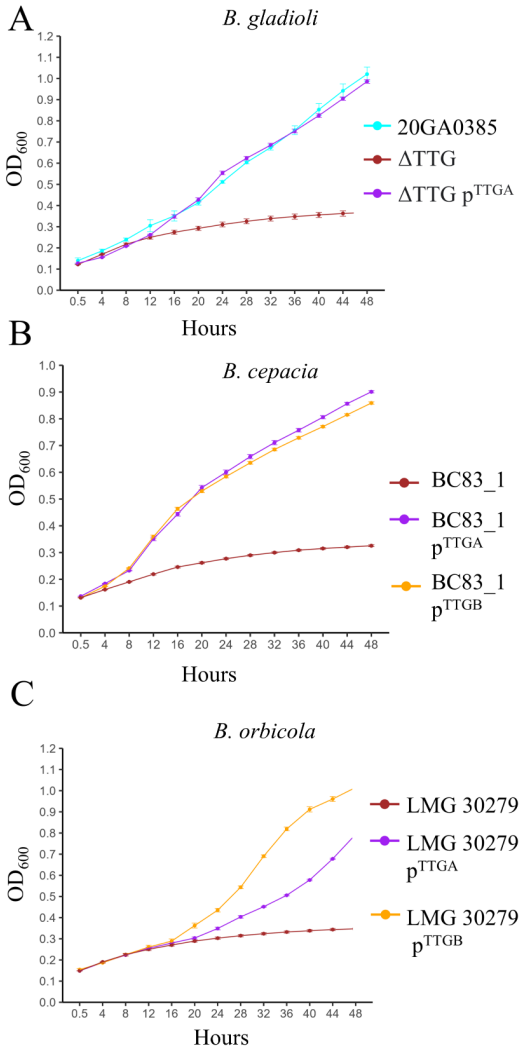

Figure. 2.4. The thiosulfinate tolerance gene (TTG)-negative strains are impaired in onion juice growth. Growth comparison of **A,** *Burkholderia gladioli* strain 20GA0385, TTG mutant derivative, and TTG Type A-complementing strain; **B,** *B. cepacia* TTG-negative natural variant BC83_1 and TTG Type A and Type B plasmid derivatives; and **C,** *B. orbicola* natural variant type strain LMG 30279 and TTG Type A and Type B plasmid derivatives in half-strength yellow onion juice for 48 h. Error bars represent ± standard error. Representative experimental data out of three performed independent experimental repeats are shown in the figure. Cyan represents a strain with endogenous TTG Type A cluster; brown represents a TTG-negative engineered or natural variant strain; purple represents TTG-negative strains with TTG Type A expression plasmid; and orange represents a TTG-negative strain with TTG Type B expression plasmid. An average of six technical replicates per treatment is shown per time point. The *y* axis crosses at 0.5 h postinoculation (hpi). The test of significance was done with recorded OD_{600} values at each time point in between the treatment strains and is presented in Table S2.4.

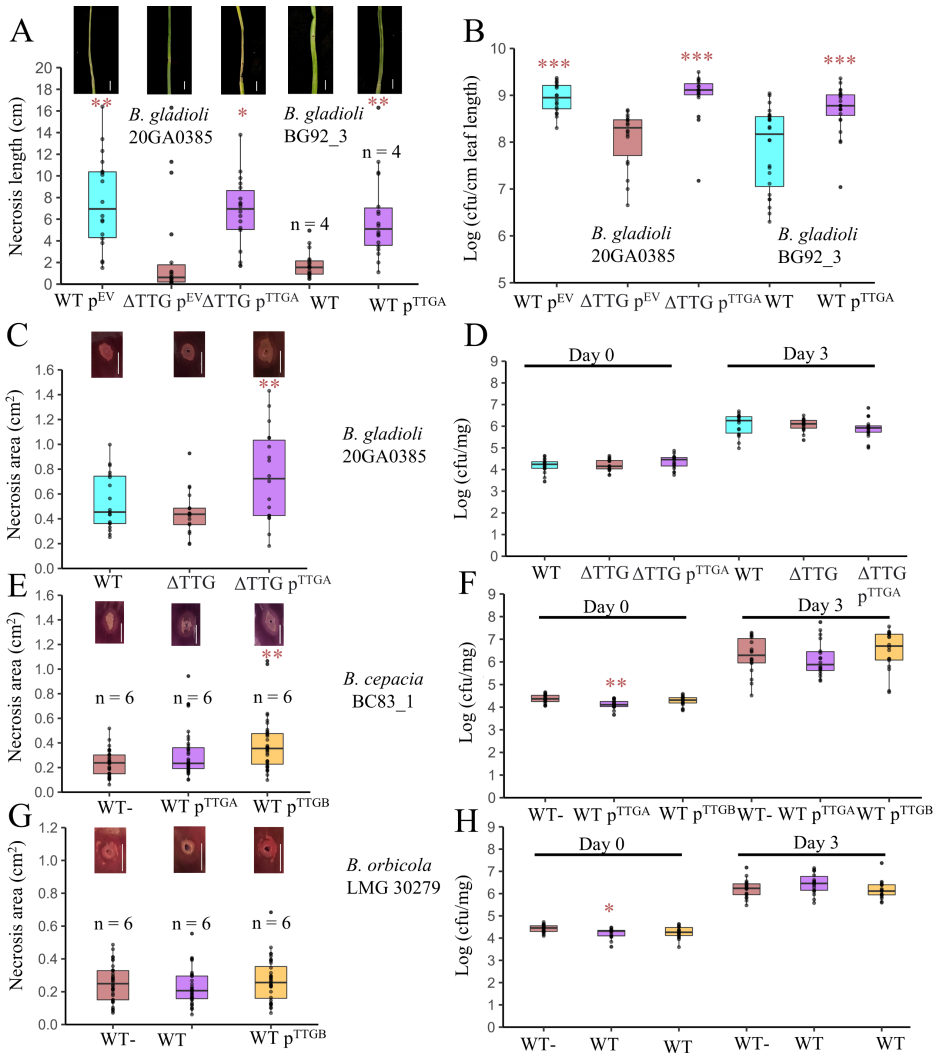

Figure 2.5. Onion foliar/red scale necrosis (RSN) assay and corresponding in planta population quantification of natural variants, engineered mutants, and thiosulfinate tolerance gene (TTG) plasmid-transformed strains of three *Burkholderia* species. **A and B,** Box plot showing onion foliar necrosis length and in planta *B. gladioli* bacterial population in onion leaf tissue at 3 days postinoculation (dpi). EV = Strain carrying empty vector pBBR1MCS-2. Box plot showing RSN area and in planta bacterial population count log (CFU/mg) of onion scale tissue at 4 h postinoculation (hpi) and 3 dpi for representative samples. **C and D,** *B. gladioli* strain 20GA0385 and its engineered TTG mutant derivative and TTG Type A complementation clone. **E and F,** *B. cepacia* TTG-negative natural variant BC83_1 and TTG Type A and Type B plasmid derivatives. **G and H,** *B. orbicola* TTG-negative natural variant type strain LMG 30279 and TTG Type A and Type B plasmid derivatives. Cyan represents a strain with endogenous TTG Type A cluster; brown represents a TTG-negative engineered or natural variant strain; purple represents TTG-negative strains with TTG Type A expression plasmid; and orange represents a TTG-negative strain with TTG Type B expression plasmid. The significant difference in necrosis length, RSN necrosis area, and in planta bacterial load of endogenous TTG cluster or plasmid-based TTG cluster-harboring strain was compared with its engineered TTG mutant or TTG-

negative wild type (WT) natural variant using pairwise *t*-test applying the Bonferroni coefficient. Each jitter point represents a biological replicate of all the experiments. The image above the box plot highlights tissue necrosis from representative samples for the corresponding inoculated treatment. The scale bar in the figure represents a 1-cm length. The experiment was repeated at least three times or as represented by *n* = number of independent experimental repeats. Each experiment had six technical replicates. Level of significance: *** = 0.001; ** = 0.01; and * = 0.05.

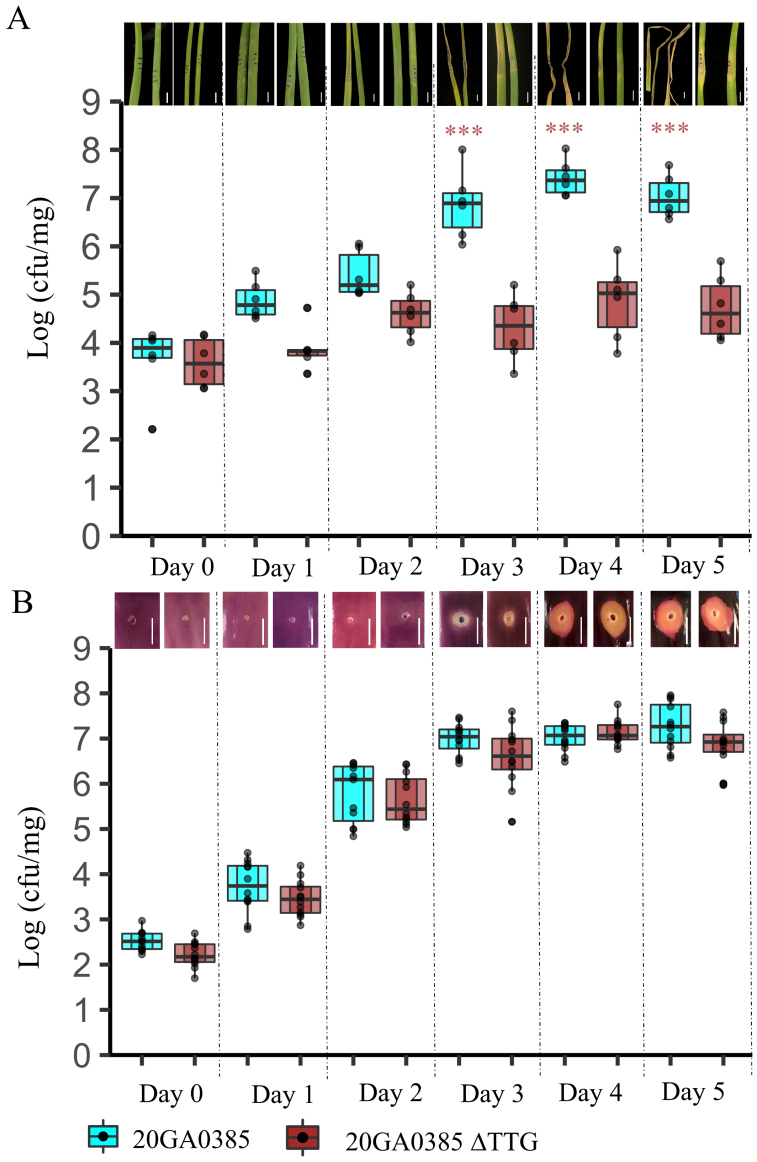

Figure. 2.6. *Burkholderia gladioli* thiosulfinate tolerance gene (TTG) cluster contributes to onion foliar bacterial load. In planta population quantification of TTG mutant and wild type

(WT) 20GA0385 strain from **A,** onion leaves and **B,** red scales from day 0 (6 h) to day 5 postinfection. A representative image of leaves or scales inoculated with approximately 2.4×10^6 CFU of WT and TTG mutant strain at each day postinoculation (dpi) is shown above the box plot. Significant differences in log (CFU/mg) of leaf or scale tissue between the two treatments for each day of sampling were calculated using a pairwise *t*-test applying the Bonferroni probability adjustment method. Level of significance: *** = 0.001. The scale bar represents a 1-cm length. The experiment was repeated two times.

Supplemental Tables

Table S2.1: Bacterial strains and plasmids used in cloning and mutagenesis

Name	Description	Reference
1. *Burkholderia* species		
20GA0385	TTG+, spontaneous rifampicin mutant (Rf^R) *B. gladioli* pv. *alliicola* (Bga) strain	This study
20GA0385 pBBR1MCS-2 EV	TTG+, spontaneous rifampicin mutant (Rf^R) of *B. gladioli* pv. *alliicola* 20GA0385 harboring empty vector pBBR1MCS2 (Km^R)	This study
20GA0385 ΔTTG	TTG-, TTG clusters deletion mutant of Bga strain 20GA0385	This study
20GA0385 ΔTTG pBBR1MCS-2 EV	TTG-, TTG clusters deletion mutant of Bga strain 20GA0385 harboring empty vector pBBR1MCS2 (Km^R)	This study
20GA0385 ΔTTG pBBR1MCS-2 TTG Type A	TTG+, TTG clusters deletion mutant of Bga strain 20GA0385 harboring Type A TTG cluster complementation construct, Km^R	This study
20GA0385 ΔTTG pBBR1MCS-2 TTG Type B	TTG+, TTG clusters deletion mutant of Bga strain 20GA0385 harboring TTG Type B cluster complementation construct from *B. orbicola* strain BC93_12, Km^R	This study
BG92_3 pBBR1MCS-2 TTG Type A	TTG negative spontaneous rifampicin mutant (Rf^R) of *B. gladioli* strain BG92_3 harboring Type A TTG cluster expression construct from Bga strain 20GA0385, Km^R	This study
BG92_3 pBBR1MCS-2 TTG Type B	TTG negative spontaneous rifampicin mutant (Rf^R) of *B. gladioli* strain BG92_3 harboring TTG Type B cluster expression construct from *B. orbicola* strain BC93_12, Km^R	This study
BC83_1 pBBR1MCS-2 TTG Type A	TTG negative *B. cepacia* strain BC83_1 harboring Type A TTG cluster expression construct from Bga strain 20GA0385, Km^R	This study
BG83_1 pBBR1MCS-2 TTG Type B	TTG negative *B. cepacia* strain BC83_1 harboring TTG Type B cluster expression construct from *B. orbicola* strain BC93_12, Km^R	This study

LMG 30279^T pBBR1MCS-2 TTG Type A	TTG negative *B. orbicola* Type strain LMG 30279 harboring Type A TTG cluster expression construct from Bga strain 20GA0385, Km^R	This study
LMG 30279^T pBBR1MCS-2 TTG Type B	TTG negative *B. orbicola* Type strain LMG 30279 harboring TTG Type B cluster expression construct from *B. orbicola* strain BC93_12, Km^R	This study
2. *E. coli* strains		
DH5α	General cloning strain	Liss, 1987
MaH1	DH5α derivative, attTn7 pir116 R6K replicon plasmids	Kvitko et al. 2012
RHO5	SM10 derivative, pir116, DAP-dependent conjugation strain	Kvitko et al. 2012
3. Plasmids		
pR6KT2G	Gateway-derivative of pR6KT2 with BP clonase compatible cassette, *sacB*, Gm^R, *gus*, Cm^R	Stice et al. 2020
pDONR1k18ms	Gateway-compatible sucrose counter-selection allelic exchange vector, Km^R, Cm^R	Mijatovic et al., 2022
pDEST1k18ms	LR clonase compatible derivative of pDONR1k18ms	Mijatovic et al., 2022
pBBR1MCS-2	pBBR1 origin-based mobilizable shuttle and expression vector with blue/white selection function. Km^R	Kovach et al., 1995
pBBR1MCS-2::EV	Empty expression vector, Km^R	Kovach et al., 1995

^{R}- Resistant, Km – Kanamycin, Gm – Gentamicin, Cm – Chloramphenicol, Rf – Rifampicin

Table S2.2: Primers and dsDNA gene blocks used in the study

Name	Sequence (5' – 3')	Description
recAgladF	GTG CCG GAA CTG CTG ATC T	To confirm the identity of *Burkholderia* strains and differentiate pv. *alliicola* within the *B. gladioli* genus
recAgladR	TTC GTC CAG GAT CTC GGC TT	
attB1	GGGGACAAGTTTGTACAAAAAAGCAGGCTT A	For Gateway recombination
attB2	GGGGACCACTTTGTACAAGAAAGCTGGGTA	
TTG deletion construct	attB1- CP023524.1, 37745 – 38144 bp – CCTAGG – CP023524.1, 44589 – 44988 bp – attB2	Deletion construct for TTG clusters synthesized from Twist

		Biosciences. Underlined is the AvrII restriction site
altgenoF	ACG CCG CCA TTG CTC AAT GA	Genotyping primers to confirm the TTG mutant
altgenoR	TGC TCA CTT TGG CAC AGC GCG	
altcomplngibF2	AGG GCG AAT TGG AGC TCC ACC GCG GTG GCG GCC GCT TTG AAC AGT ATT GCT GCT T	TTG complementation primers with 35 bp Gibson overhangs from plasmid pBBR1MCS-2
altcomplngibR2	ATA TCG AAT TCC TGC AGC CCG GGG GAT CCA CTA GTT AAT TCG GAG CAG TGA CCT	
altcomplngenoF	TTA TGC CGC TCA TTA ATG TA	Primers to genotype the TTG Type A insert in the plasmid pBBR1MCS-2
altgenocomplnR	TGCAAGCGCCAAGGAGTAA	
typeBgenocomplnR	TGA CCG AAG AGT GCG ACT	Primers to genotype TTG Type B insert in the plasmid pBBR1MCS-2

Table S2.3: Description of the whole genome sequenced and NCBI GenBank extracted strains used for the phylogenetic analysis

Strain	Species[a]	TTG cluster type	year of isolation	Host	location of isolation	replicon	Accession	Coordinates
20GA0385	*B. gladioli*	A	2020	*Allium cepa*	GA		JAXNZV010000022	103497-109958
Ba93_1	*B. ambifaria*	A	1993	*Allium cepa*	GA		JAYNCS010000019	51223-57688
Ba93_11	*B. ambifaria*	A	1993	*Allium cepa*	GA		JAYNCT010000019	51223-57685

Ba93_5	*B. ambifaria*	A	1993	*Allium cepa*	GA		JAYNCU010000020	51223-57688
BC10_1	*B. orbicola*	A	2010	*Allium cepa*	Tifton, GA		JAYNCV010000025	28243-34713
BC10_2	*B. cepacia*	A	2010	*Allium cepa*	Tifton, GA		JAYNCW010000043	5707-12172
BC10_3	*B. cepacia*	A	2010	*Allium cepa*	Tifton, GA		JAYNCX010000039	5722-12200
BC10_5	*B. orbicola*	A	2010	*Allium cepa*	Tifton, GA		JAYNCY010000025	28293-34764
BC11_2	*B. orbicola*	A	2011	*Allium cepa*	Toombs County, GA		JAYNCZ010000018	69730-76195
BC19_1	*B. cepacia*	A	2019	*Allium cepa*	GA		JAYNDA010000029	25457-31928
BC83_1	*B. cepacia*	0	1983	*Allium cepa*	Toombs County, GA			
BC89_4	*B. orbicola*	A	1989	*Allium cepa*	Toombs County, GA		JAYNDC010000037	28293-34764
BC89_5	*B. cepacia*	0	1989	*Allium cepa*	Toombs County, GA			
BC90_2	*B. orbicola*	A	1990	*Allium cepa*	GA		JAYNDE010000037	17260-23725
BC92_10	*B. cepacia*	A	1992	*Allium cepa*	GA		JAYNDF010000036	3140-- 9605
BC92_15	*B. cepacia*	A	1992	*Allium cepa*	GA		JAYNDG010000036	25457-31928
BC92_16	*B. orbicola*	A	1992	*Allium cepa*	GA		JAYNDH010000031	28294-34759
BC92_17	*B. cepacia*	A	1992	*Allium cepa*	GA		JAYNDI010000040	25507-31978
BC92_19	*B. cepacia*	A	1992	*Allium cepa*	GA		JAYNDJ010000042	25507-31972
BC92_20	*B. cepacia*	A	1992	*Allium cepa*	GA		JAYNDK010000042	25507-31972
BC92_21	*B. cepacia*	A	1992	*Allium cepa*	GA		JAYNDL010000045	2919-9384

BC92_22	*B. cepacia*	A	1992	*Allium cepa*	GA		JAYNDM010000053	25507-31972
BC92_24	*B. cepacia*	A	1992	*Allium cepa*	GA		JAYNDN010000046	3341-9806
BC92_31	*B. orbicola*	B	1992	*Allium cepa*	GA		JAYNDO010000042	5174-11613
BC92_33	*B. orbicola*	A+B	1992	*Allium cepa*	GA		JAYNDP010000032/ JAYNDP010000042	57945-64410; 19277-25706
BC92_35	*B. orbicola*	A	1992	*Allium cepa*	GA		JAYNDQ010000031	57944-64409
BC93_10	*B. orbicola*	A+B	1993	*Allium cepa*	GA		JAYNDR010000023/JAYNDR010000043	56795-63260;1-5119
BC93_12	*B. orbicola*	B	1993	*Allium cepa*	GA		JAYNDS010000044	11238-17668
BC93_16	*B. orbicola*	A+B	1993	*Allium cepa*	GA		JAYNDT010000032/ JAYNDT010000041	15837-22308;21358-27787
BC93_20	*B. orbicola*	A	1993	*Allium cepa*	GA		JAYNDU010000036	28293-34758
BC97_3	*B. orbicola*	A	1997	*Allium cepa*	GA		JAYNDV010000040	28293-34758
BC98_1	*B. cepacia*	A	1997	*Allium cepa*	GA		JAYNDW010000030	3341-9812
BC98_2	*B. cepacia*	A	1998	*Allium cepa*	GA		JAYNDX010000036	3341 – 9806
BC98_4	*B. orbicola*	A	1998	*Allium cepa*	Vidalia, GA		JAYNDY010000024	59569-66034
BC99_1	*B. orbicola*	A	1999	*Allium cepa*	Tatnall County, GA		JAYNDZ010000036.1	28291-34758
BC99_2	*B. cepacia*	A	1999	*Allium cepa*	Tattnall County, GA		JAYNEA010000028	3341 - 9808
BG01_01	*B. gladioli*	B	2001	*Allium cepa*	Toombs County, GA		JAYNEB010000019	21041-27483
BG88_4	*B. gladioli*	0	1988	*Allium cepa*	Toombs County, GA			

BG92_10	*B. gladioli*	0	1992	*Allium cepa*	GA			
BG92_12	*B. gladioli*	0	1992	*Allium cepa*	GA			
BG92_13	*B. gladioli*	0	1992	*Allium cepa*	GA			
BG92_14	*B. gladioli*	0	1992	*Allium cepa*	GA			
BG92_18	*B. gladioli*	0	1992	*Allium cepa*	GA			
BG92_3	*B. gladioli*	0	1992	*Allium cepa*	GA			
BG92_9	*B. gladioli*	0	1992	*Allium cepa*	GA			
BG93_9	*B. gladioli*	0	1993	*Allium cepa*	GA			
20GA0287	*B. ambifaria*	A	2020	*Allium cepa*	Tifton, GA		JAYNBY010000019	50714-57633
20GA0296	*B. orbicola*	A	2020	*Allium cepa*	Tattnall County, GA		JAYNBZ010000037	17260-23727
20GA0297	*B. cepacia*	A	2020	*Allium cepa*	Tattnall County, GA		JAYNCA010000032	3341 – 9812
20GA0300	*B. orbicola*	A	2020	*Allium cepa*	Tattnall County, GA		JAYNCB010000009	248185-254656
20GA0314	*B. gladioli*	B	2020	*Allium cepa*	Tattnall County, GA		JAYNCC010000017	14691 – 21168
20GA0321	*B. cepacia*	A	2020	*Allium cepa*	Tattnall County, GA		JAYNCD010000038	3432-9897
20GA0327	*B. gladioli*	B	2020	*Allium cepa*	Tattnall County, GA		JAYNCE010000039	6573-12999
20GA0329	*B. orbicola*	A	2020	*Allium cepa*	Tattnall County, GA		Multiple contigs	
20GA0336	*B. orbicola*	A	2020	*Allium cepa*	Tatnall County, GA		JAYNCG010000034	17260-23731
20GA0338	*B. cepacia*	A	2020	*Allium cepa*	Tattnall County, GA		JAYNCH010000029	51162-57624

20GA0341	*B. orbicola*	A	2020	*Allium cepa*	Tattnall County, GA		Multiple contigs	
20GA0350	*B. gladioli*	A+B	2020	*Allium cepa*	Toombs County, GA		JAYNCJ010000039/JAYNCJ010000055	52661-59087-59361;4454-10916
20GA0374	*B. gladioli*	A	2020	*Allium cepa*	Toombs County, GA		JAYNCK010000019	114626-121088
20GA0379	*B. cepacia*	A	2020	*Allium cepa*	Toombs County, GA		JAYNCL010000026	25507-31972
21GA0638	*B. gladioli*	A	2021	*Allium cepa*	Toombs County, GA		JAYNCM010000031	59250-65712
21GA0685	*B. gladioli*	A	2021	*Allium cepa*	GA		JAYNCN010000049	2072-8534
21GA0686	*B. gladioli*	A	2021	*Allium cepa*	Tattnall County, GA		JAYNCO010000047	1795-8534
21GA0688	*B. gladioli*	A	2021	*Allium cepa*	Tattnall County, GA		JAYNCP010000033	59250-65712
21GA0689	*B. gladioli*	A	2021	*Allium cepa*	Tattnall County, GA		JAYNCQ010000028	17046-23508
21GA0693	*B. orbicola*	A	2021	*Allium cepa*	Toombs County, GA		JAYNCR010000031	29481-35945
HI2424	*B. orbicola*	A		Soil	New York, USA	Chromosome 2	CP000459.1	103538-110002
HI2424	*B. orbicola*	A		Soil	New York, USA	Plasmid	CP000461.1	123493-129954
IDO3	*B. anthina*	A		Reactor Sludge	China	Plasmid	CP028965.1	370835-377296
KACC 11889	*B. gladioli*	C		*Gladiolus* sp.		Plasmid	CP022007.1	116721-122936
MC0-3	*B. orbicola*	B		Maize rhizosphere	Michigan, USA	Chromosome 2	CP000959.1	1404971-1411319
MC40-6	*B. ambifaria*	B	2004	Maize rhizosphere	Michigan, USA	Chromosome 2	CP001026.1	343413-349763
N149	*B. dolosa*	A	2021	Clinical	Vietnam	Plasmid	CP132925.1	120845-127306
PC184	*B. orbicola*	B		Sputum	USA	Chromosome 1	CP021067.1	2356645-2362993

PHS1	*Paraburkholderia graminis*	C		Soil	The Netherlands	Plasmid	CP024936.1	48150-54562
PS27	*B. orbicola*	A		Soil	India	Plasmid	CP060042.1	12901-19362
RPE67	*Caballeronia cordobensis*	Outgroup		Bacterial gut symbiont		Plasmid	AP014581.1	185771-192232
ZN-S4	*B. gladioli*	A	2019	*Dendrobium officinale*	China	Plasmid	CP104217.1	117601-124062
ATCC 10248	*B. gladioli*	C	1913	*Gladiolus sp.*	USA	Plasmid	CP009321.1	189356-195572
ATCC 25416	*B. cepacia*	A		*Allium cepa*	USA	Plasmid	CP034556.1	3110-9574
AU 1054	*B. orbicola*	A		Clinical	USA	Chromosome 2	CP000379	2166248-2159754
B21-005	*Burkholderia sp.*	B		Soil	Quebec, Canada	Chromosome 1	CP086301.1	3125534-3131884
Co14	*B. gladioli*	A		Fermented Corn Meal	China	Plasmid	CP033429.1	23994-30456
DSM 10685	*B. pyrrocinia*	A	1965	Soil	Japan	Chromosome 2	CP011504.1	1945836-1952294
FDAARGOS_188	*B. gladioli*	C				Plasmid	CP022209.1	141436-147652
FDAARGOS_345	*B. cepacia*	A		*Allium cepa*	USA	Plasmid	CP022081.2	157264-163728
FDAARGOS_388	*B. cepacia*	A		*Allium cepa*		Plasmid	CP023519.1	161482-167946
FDAARGOS_389	*B. gladioli*	A		*Allium cepa*		Plasmid	CP023524.1	38136-44611
FDAARGOS_720	*B. orbicola*	A		Clinical		Chromosome 2	CP050979.1	2101400-2107866
FDAARGOS_721	*B. vietnamiensis*	B		Clinical		Plasmid	CP091982.1	138220 – 142952

Table S2.4: Level of significance between OD_{600} values of different treatments at different time points across the three experimental repeats of onion juice assay. The average value of six data points of Onion Juice water negative control at each time point of each experimental repeat is subtracted from every single well of other treatments at the same corresponding time point. Total number of data points n = 18 per treatment. Analysis was done using a pairwise t-test function in Rstudio.

Hours	0.5	4	8	12	16	20	24	28	32	36	40	44	48
B. gladioli 20GA0385 ΔTTG Vs													
WT	ns	ns	ns	ns	ns	ns	**	** *	***	** *	** *	** *	** *
ΔTTG p^{TTGA}	ns	ns	ns	ns	ns	** *	***	** *	***	** *	** *	** *	** *
B. cepacia BC83_1 (TTG-) vs													
p^{TTGA}	ns	** *	** *	** *	** *	** *	***	** *	***	** *	** *	** *	** *
p^{TTGB}	ns	** *	** *	** *	** *	** *	***	** *	***	** *	** *	** *	** *
B. cepacia BC83_1 p^{TTGA} vs													
p^{TTGB}	ns	*	ns	ns	**	ns	ns	ns	ns	ns	ns	ns	ns
B. orbicola LMG 30279 (TTG-) vs													
p^{TTGA}	ns	ns	ns	ns	ns	** *	**	** *	***	** *	** *	** *	** *
p^{TTGB}	ns	ns	ns	** *	** *	** *	***	** *	***	** *	** *	** *	** *

B. orbicola LMG 30279 p^{TTGA} vs													
P^{TTGB}	ns	ns	ns	ns	**	** *	***	** *	***	** *	** *	** *	** *

Supplemental Figures

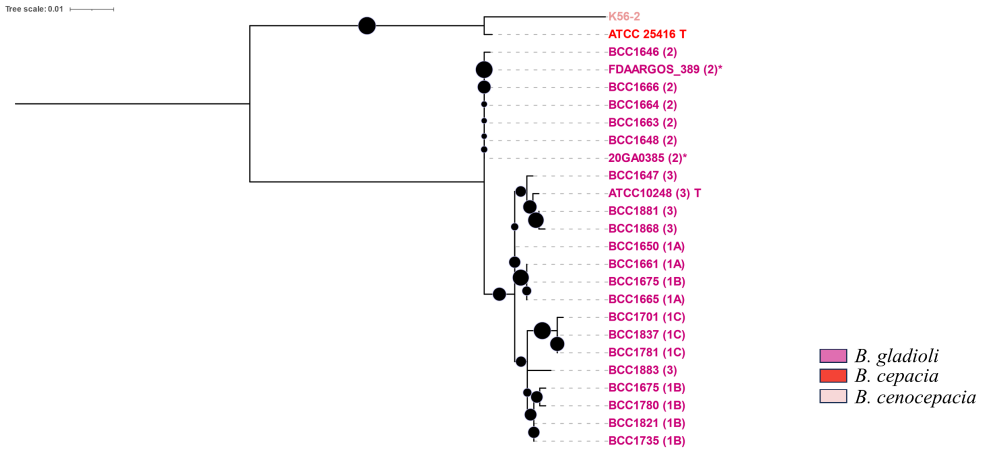

Supplementary Figure S2.1: Maximum likelihood phylogenetic tree of 727-bp partial *recA* gene differentiates *Burkholderia gladioli* pv. *alliicola* group from other pathovars in *B. gladioli. B. gladioli* 20GA0385 and NCBI GenBank extracted FDAARGOS_389 test strains for identity confirmation are represented by starburst symbol. Information about the strain and their pathovar designation is retrieved from Jones et al., 2021. The letter/number in parentheses represents the clade of the reference strain. The black circle represents bootstrap support of the branching on a scale of 0 to 1. T denotes a type strain. The tree is rooted in the branch of *B. cepacia* complex representative strains.

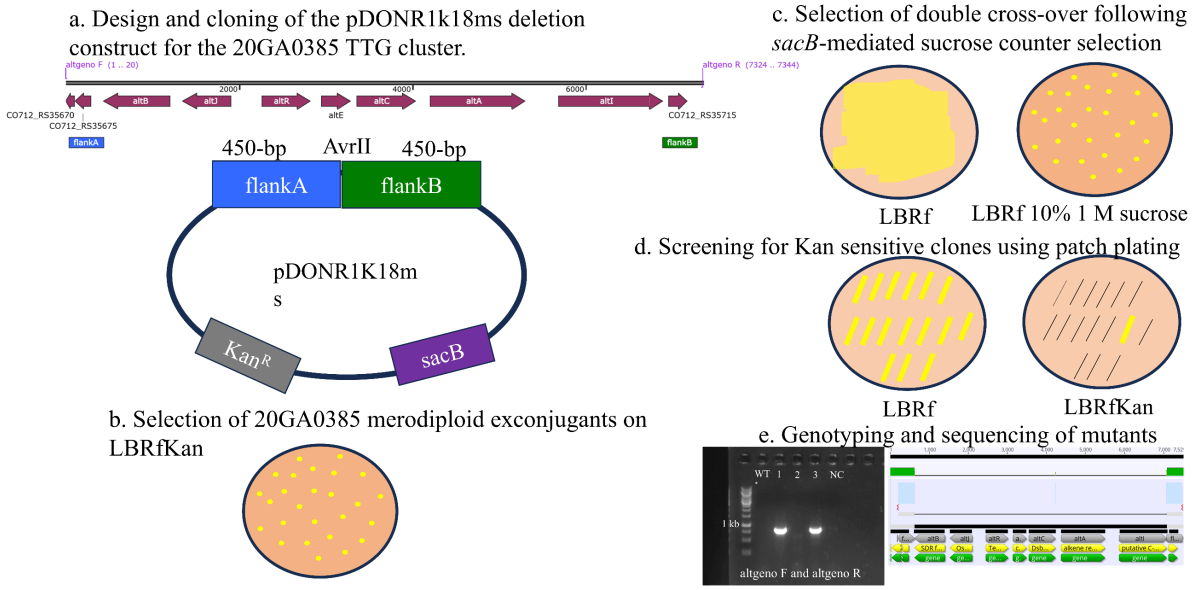

Supplementary Figure S2.2: Schematic diagram of the allelic exchange strategy used to generate in-frame deletion of TTG cluster in *Burkholderia gladioli* pv. *alliicola* strain 20GA0385. WT – Wild Type, R- Resistant, Rf- Rifampicin, Kan – Kanamycin, NC – Negative Control, * - No amplicon was observed because of large expected product size (~7.5 kb).

CHAPTER 3

DISTINCT VIRULENCE MECHANISMS OF *BURKHOLDERIA GLADIOLI* IN ONION FOLIAR AND BULB SCALE TISSUES[1]

[1]Paudel S, Franco Y, Zhao M, Dutta B, Kvitko BH. Distinct Virulence Mechanisms of *Burkholderia gladioli* in Onion Foliar and Bulb Scale Tissues. Mol Plant Microbe Interact. 2025. Jan 10. https://doi.org/10.1094/MPMI-10-24-0129-R. Epub ahead of print. PMID: 39792040.

SP did investigation, formal analysis, resources, data curation, writing – original draft, review, editing, and visualization.

Abstract

Slippery skin of onion caused by *Burkholderia gladioli* pv. *alliicola* (Bga) is a common bacterial disease reported from onion growing regions around the world. Despite the increasing attention in recent years, our understanding of the virulence mechanisms of this pathogen remains limited. In this study, we characterized the predicted genetic determinants of virulence in Bga strain 20GA0385 using reverse genetics approach. Using the closely related rice pathogen, *B. glumae* as a reference, comparative genomics analysis was performed to identify Bga candidate virulence factors and regulators. Marked and unmarked deletion mutants were generated using allelic exchange and the mutants were functionally validated using *in vitro* and *in vivo* assays. The role of mutants in pathogenic phenotypes was analyzed using onion foliar/seedling necrosis assays, the Red Scale Necrosis (RSN) assay and *in planta* bacterial population counts. The phytotoxin toxoflavin was a major contributor to foliar necrosis and bacterial populations whereas the type II and type III secretion system (T2SS/T3SS) were dispensable for foliar symptoms. In onion scale tissue, the T2SS single mutant *gspC* and its double and triple mutant derivatives all contributed to scale lesion area. Neither the lipocyclopeptide icosalide, toxoflavin, nor T3SS were required for scale symptoms. Our results suggest the quorum sensing *tofIMR* system in Bga regulates, toxoflavin, T2SS, and T3SS, contributing to onion symptom production. We show different virulence factors contribute to onion tissue-specific virulence patterns in Bga and that decreases in scale symptoms often do not result in decreased Bga populations in onion tissue.

Introduction

Onion is one of the world's most significant vegetable crops, cultivated on over 5 million hectares with an annual production of more than 100 million metric tons (Fayos et al., 2022). Bacterial diseases pose a substantial risk to the onion production as they can cause infection both in the field and during storage (Belo et al., 2023). Slippery skin of onion caused by *Burkholderia gladioli* pv. *allicola* (Bga) is one of the major diseases of onion in the United States (Schroeder et al., 2012). The pathogen is commonly isolated from onion fields and under storage conditions (Lee et al., 2005). Infected bulbs appear normal from the outside but are softer when pressed compared to the healthy ones. In the field, infection has been described to start from the neck of the onion and progress gradually to the basal plate before spreading to the neighboring bulbs (Wright et al., 1993). The rot caused by Bga is typically characterized by a watery, glassy appearance, whereas the rot associated with sour skin of onion, caused by the *Burkholderia cepacia* complex (Bcc), was described by Burkholder as slimy and yellow (Burkholder, 1950). Leaves infected by Bga developed water-soaked lesions with a bleached appearance, which often led to wilting and rot. Since its first discovery in the 1940s, the bacterium has been isolated and characterized from various onion growing regions in Asia, North and Central America, and Europe (Wright et al., 1993; Lee et al., 2005; Lamovšek et al., 2016; Félix-Gastélum et al., 2017). Despite its increasing economic significance to onion production, studies of the mechanisms of virulence in Bga are limited.

The comparatively well studied rice pathogen, *Burkholderia glumae* has been used as a useful reference model to infer virulence determinants in Bga because of their close phylogenetic relatedness (Vandamme et al., 2017). The ability of *B. glumae* to cause onion scale tissue

necrosis is often utilized for genetic characterization studies (Karki et al., 2012). The well characterized virulence factors such as the phytotoxin toxoflavin, type II and type III secretion systems (T2SS/T3SS) are conserved in both *B. gladioli* and *B. glumae* (Fory et al., 2014; Seo et al., 2015; Lee et al., 2016). *In silico* analysis have also shown the presence of putative T3SS and T6SS in both *B. gladioli* and *B. glumae* (Fory et al, 2014; Seo et al., 2015). In *B. glumae,* the contribution of toxoflavin to rice chlorotic symptoms and wilting symptoms in various field crops has been demonstrated (Jeong et al., 2003; Seo et al., 2015). Similarly, T2SS and T3SS also contribute to rice panicles symptoms and bacterial populations in *B. glumae* (Goo et al., 2010; Karki et al., 2012). Likewise, the T2SS has also been shown to be an important virulence factor in *B. gladioli* pv. *agaricicola* (Chowdhury and Heinemann, 2006). The *tofIMR* quorum sensing system has been extensively studied as an important virulence regulator in both *B. glumae* and *B. gladioli* (Chen et al., 2012; Lee et al., 2016; Elshafie et al., 2019; Paudel et al., 2024a). The thiosulfinate tolerance gene (TTG) clusters, that contribute to enhanced allicin tolerance *in vitro*, also contribute to onion foliar symptoms and bacterial populations in Bga. Comparative genomics of *Burkholderia* strains isolated from various ecological niches revealed the broad distribution of the icosalide *icoS* nonribosomal peptide synthetase (NRPS). The *icoS* gene is present in some plant pathogenic *Burkholderia* species, including *B. cepacia*, *B. gladioli* pv. *agaricicola*, and *B. gladioli* pv. *gladioli* (Dose et al., 2018). Notably, this gene is absent in rice-pathogenic *B. glumae* strains. In *B. gladioli* strain HKI0739, an endosymbiont, icosalide plays a protective role for its eukaryotic host against entomopathogens (Dose et al., 2018). Although the gene is present in Bga, its potential role in onion host interactions remains unexplored.

All four *B. gladioli* pathovars, pv. *cocovenenans*, pv. *agariciola*, pv. *gladioli*, and pv. *alliicola* are capable of onion scale necrosis and the utility of the pathovar concept for *B. gladioli* has been questioned (Abachi et al., 2024). The *alliicola* pathovar, originally isolated from onion, forms a distinct evolutionary clade in *B. gladioli* species (Jones et al., 2021). Despite some sporadic studies on separate host systems, the genetic basis of virulence in Bga is only partially understood. In this study, we characterized the putative genetic determinants of virulence in onion isolated Bga strain 20GA0385 and empirically demonstrated that different virulence factors contribute to different symptoms in specific tissues, foliage vs. scale. Our results suggest that the phytotoxin toxoflavin is a critical virulence factor for onion leaf tissue whereas the T2SS was a significant contributor to scale lesion development. However, the reduction in Bga symptom production in scale tissue was not associated with corresponding decrease in bacterial population. The decoupling was evident with T2SS mutant *gspC* in scale tissue and icosalide mutant in leaf tissue.

Results

Putative virulence factors are conserved in *B. gladioli* pv. *alliicola* and *B. glumae*

In effort to characterize the candidate virulence factors in onion pathogenic Bga strain 20GA0385, a comparative genomics analysis was performed between Bga and well characterized *B. glumae* strain BGR1. The toxoflavin biosynthesis operon, T2SS, T3SS, and quorum sensing *tofIMR* system were all conserved in synteny between *B. glumae* BGR1 and Bga strain 20GA0385 (Supplementary Figure S3.1A-D). The toxoflavin biosynthesis polycistronic operon genes shared more than 90% identity between the two strains. The T2SS constituent genes also shared a high percentage identity ranging from 76-97%. The T3SS machinery genes were also highly conserved sharing percentage identity ranging from 70-97%. The Quorum

Sensing (QS) genes also shared percentage identity from 80-97%. The antibiotic icosalide identified from a *B. gladioli* endosymbiont strain HKI0739 was absent from BGR1 but shared high percentage identity with a putative *icoS* gene found in 20GA0385 (Supplementary Table S1).

Functional validation of mutants

The production of toxoflavin by the Bga strain 20GA0385 and its *toxA* and *tofIMR* mutant derivatives was assessed by measuring the absorbance of a diffusible yellow pigment at 393 nm on various agar media (Figure 3.1A and B). The recorded absorbance values for toxoflavin biosynthesis mutant *toxA* were significantly lower than WT strain at both LB and LM agar media. The absorbance for *toxA* restoration clone was significantly higher compared to *toxA* mutant at both LB and LM agar media (Figure 3.1A; Supplementary Figure S3.2A). The *toxA* restoration clone had significantly higher absorbance compared to the WT strain (Figure 3.1A).

The *sctC* gene, which encodes the outer membrane secretin complex SctC within the T3SS machinery, was targeted for unmarked deletion in the Bga strain 20GA0385 (Kowal et al., 2013). The functional validation of T3SS was done using a tobacco cell death assay. The tobacco cell death area of T3SS Δ*sctC* mutant was visually compared to the WT strain. The cell death area of the *sctC* mutant was consistently reduced compared to the WT strain. The chromosomally restored *sctC* clone complemented the cell death phenotype of the *sctC* mutant (Figure 3.1C). The T2SS Δ*gspC* had comparable tobacco cell death phenotypes to the WT strain (Supplementary Figure S3.2E). The Δ*gspC*Δ*sctC* double and Δ*toxA*Δ*gspC*Δ*sctC* triple mutant strains were reduced in cell death area compared to the WT strain (Supplementary Figure S3.2E).

The *Chromobacterium* Acyl Homoserine Lactones (AHL) assay was performed to functionally validate the *tofIMR* mutant *in vivo* using CV026 reporter strain (McClean et al., 1997). The AHL molecules produced by the test treatment when recognized by the CV026 reporter strain produce violacein ring around the area of inoculation. The normalized suspension of the WT strain when inoculated in the CV026 lawn produced violet ring around the zone of inoculation whereas the *tofIMR mutant* did not (Figure 3.1D). Surprisingly, the plasmid based *tofIMR* complementation clone did not restore violacein production in the CV026 lawn background although other *tofIMR* phenotypes including *in planta* phenotypes were complemented as described below (Figure 3.1D).

The *gspC* gene, which encodes the inner membrane-anchored protein GspC was deleted in this study. The interaction between GspC and GspD protein is essential for the function of T2SS (Korotkov et al., 2011). The T2SS *gspC* mutant strain was validated using Casein hydrolysis protease plate assay. The WT strain produced a clearing area around the hole of inoculation on dry milk augmented agar plates whereas the T2SS Δ*gspC* lost the clearing phenotype (Figure 3.1E). The plasmid pBBR1MCS-2 with *gspC* ORF when expressed in *gspC* mutant background partially restored the clearing area suggesting the T2SS secreted proteases cause hydrolysis of casein in the agar plate (Figure 3.1E). The Δ*gspC*Δ*sctC*, Δ*gspC*Δ*icoS*::Gm^R*gus*, and Δ*toxA* Δ*gspC* Δ*sctC* double and triple mutant strains retained the *gspC* single mutant clearing zone phenotype (Supplementary Figure S3.2D). The clearing area for the T3SS *sctC* mutant was variable across the experimental repeats. Across a total of six observations, the clearing area for the *sctC* mutant strain was not significantly different from the WT strain (Figure 3.1F). Clearing area quantification was not performed for the *gspC* single

mutant or its double and triple mutant derivatives as a consistent visual phenotype was observed across all experimental repeats.

The swarming motility assay was done to visually compare the *in vitro* swarming behavior of icosalide single mutants to the WT strain. Both the triple stop codon interruption mutant Ψ*icoS* and the Δ*icoS*::Gm^R*gus* were reduced in swarming area compared to the WT strain (Supplementary Figure S3.2F). Surprisingly, the Δ*gspC*Δ*icoS*:: Gm^R*gus* double mutant was further reduced in swarming area compared to the icosalide single mutants. The T2SS *gspC* mutant produced a bigger swarming area compared to the two icosalide single mutants (Supplementary figure S3.2F).

We tested the growth of mutant strains in LB media. In LB medium, the *toxA* mutant, the *toxA* restoration clone, the T2SS mutant (*gspC*), *gspC* plasmid complementation clone, and the triple mutant (Δ*toxA*Δ*gspC*Δ*sctC*) all exhibited growth comparable to the WT strain over a 48-hour period (Supplementary Figure S3.5A-D). The quorum-sensing *tofIMR* mutant demonstrated similar growth to the WT strain during the stationary phase but reached the exponential phase slightly later. However, the *tofIM*R plasmid complementation clone displayed an unusual growth pattern compared to the WT (Supplementary Figure S5E). An atypical growth pattern was also observed with the icosalide single and double mutants and the Δ*gspC*Δ*sctC* double mutant (Supplementary Figure S3.5A, C). Notably, strains exhibiting this unusual growth pattern also showed increased adhesion to the agar media and were difficult to scrape from plates when preparing bacterial suspensions. This aligns with the irregular growth behavior observed in the Bioscreen assay. Despite these *in vitro* growth anomalies, the day 3 scale recovery of these strains were comparable to WT strain, as will be discussed later.

The toxoflavin production by *tofIMR* mutant was variable across different media conditions

We had observed variation in yellow pigmentation based on growth media. To test if the Bga 20GA0385 *tofIMR* system behaves similarly, the toxoflavin production by *tofIMR* mutant was quantified and compared to WT strain on LB, LM, and MGY media agar. The absorbance values were highest for MGY agar and lowest on LB agar (Figure 3.1A-B, Supplementary Figure S3.2A-C). On LM and LB media the *tofIMR* mutant produced significantly less toxoflavin compared to the WT strain. While the *tofIMR* plasmid complementation clone partially restored toxoflavin production on LM media, it did not restore production on LB media (Figure 3.1B; Supplementary Figure S3.2B). Interestingly, on MGY media, the *tofIMR* mutant exhibited significantly higher absorbance values than the WT strain (Supplementary Figure S3.2A-C). These findings highlight the noteworthy variation in toxoflavin production by the *tofIMR* mutant across different media conditions.

The QS *tofIMR* system regulates protease secretion, tobacco cell death and swarming motility in Bga strain 20GA0385

The QS *tofIMR* mutant was also tested in the casein protease plate assay and tobacco cell death assay to assess its role in regulation of T2SS- and T3SS-associated phenotypes, respectively. The mutant was significantly reduced in casein hydrolysis protease plate clearing area compared to the WT strain. The *tofIMR* complementation clone partially restored the *tofIMR* casein milk agar clearing area to the WT level (Figure 3.1G). The *tofIMR* inoculated tobacco leaves were reduced in cell death area compared to the WT strain (Figure 3.1C). The *tofIMR* complementation clone partially restored the cell death area of *tofIMR* mutant (Figure 3.1C).

In the swarming motility assay, the QS *tofIMR* mutant was restricted around the point of inoculation on the plate whereas the WT strain swarmed to the edge of the plate (Supplementary Figure S3.2F). The *tofIMR* complementation clone had a dramatically increased swarming area compared to the *tofIMR* mutant (Supplementary Figure S3.2F).

The phytotoxin toxoflavin is a key virulence factor in onion leaf tissue

The phytotoxin toxoflavin biosynthesis mutant *toxA* was significantly reduced in onion necrosis length and bacterial population compared to the WT (Figure 3.2A, B). In a previous study, we reported the positive contribution of the thiosulfinate tolerance gene clusters (TTG) to onion foliar necrosis and bacterial populations in Bga strain 20GA0385 (Paudel et al., 2024b). The *toxA* mutant in the TTG mutant background was also significantly reduced in both foliar lesion length and bacterial populations compared to the WT strain (Figure 3.2C, D). The reduction in necrosis length and bacterial population of *toxA* mutant was restored to WT levels with *toxA* chromosomal restoration clone (Supplementary Figure S3.4A, B). The icosalide *icoS* triple stop codon interruption mutant Ψ*icoS* and Gm^R*gus* marked deletion mutants were both unchanged in foliar necrosis length compared to the WT (Figure 3.2E, G). The two mutants, however, were significantly reduced in leaf bacterial populations *in planta* compared to the WT (Figure 3.2F, H). In the onion scale tissue, the Δ*toxA* and Δ*toxA*ΔTTG double mutants were not altered in necrosis area and bacterial populations compared to the WT strain (Figure 3.2I, J; Supplementary Figure 3.3A, D). Similarly, the icosalide single mutants, Ψ*icoS* and Δ*icoS::*Gm^R*gus* were both unchanged in RSN area and bacterial populations (Figure 3.2K, L; Supplementary Figure 3.3B, C).

The T2SS contributes to onion scale necrosis.

The T2SS mutant *gspC* and T3SS Δ*sctC* were tested for their virulence role using the foliar and RSN phenotypic assays. The *gspC* and *sctC* single mutants both produced comparable leaf lesion length and *in planta* populations compared to the WT strain (Figure 3.3A, B; Supplementary Figure S3.4C, D). In the RSN assay, the *gspC* mutant was reduced in necrosis area while the *sctC* mutant was unchanged relative to the WT strain (Figure 3.3D, E). The *gspC* sequence region when expressed in the *gspC* mutant background using the expression plasmid pBBR1MCS-2 partially restored the phenotype (Figure 3.3D). The Δ*gspC*Δ*sctC* and Δ*gspC*Δ*icoS*::Gm^R*gus* double mutants both resembled the *gspC* single mutant in RSN phenotypes and foliar necrosis symptoms (Figure 3.3F, G, C, H). The *gspC*/*sctC* double mutant was also not impaired in leaf bacterial populations compared to the WT (Supplementary Figure S3.4E). The Δ*gspC*Δ*icoS*::Gm^R*gus* population recovery from inoculated leaves was similar to the Δ*icoS*::Gm^R*gus* single mutant (Figure 3.2H; Figure 3.3I). The Δ*toxA*Δ*gspC*Δ*sctC* triple mutant when inoculated in onion seedling produced significantly shorter lesions length compared to the WT strain (Figure 3.4A). The mutant was also significantly reduced in seedling foliar population recovery compared to the WT (Figure 3.4B). Unexpectedly, the Δ*toxA*Δ*gspC*Δ*sctC* triple mutant did not recapitulate the red scale phenotype of the *gspC* single mutant (Figure 3.4C). To investigate whether this discrepancy was due to high initial bacterial inoculum concentration (OD_{600} = 0.7), we conducted the same test using 100-fold diluted inoculum. With the diluted bacterial suspension, the *gspC* mutant, and all *gspC* derivative strain were significantly reduced in RSN area compared to the WT strain (Figure 3.5). All the tested protein secretion system mutants and their double and triple mutant derivatives were unchanged in red onion scale bacterial populations relative to the WT strain at both high and low bacterial inoculum concentrations (Supplementary Figure 3.3E- I, 3.3K-N).

The QS *tofIMR* system regulates onion symptoms production

The QS *tofIMR* system that regulates many physiological and virulence traits in *Burkholderia* species was also tested for its contribution to virulence and bacterial population phenotype in RSN and foliar assays. The *tofIMR* mutant significantly contributed to RSN area (Figure 3.4D, Figure 3.5E). The *tofIMR* mutant when expressed with *tofIMR* plasmid complementation clone restored the RSN area to the WT levels (Figure 3.4D). The mutant, however, was not changed in scale population compared to the WT strain (Supplementary Figure S3.3J, O). Similarly, the *tofIMR* mutant was also significantly reduced in foliar necrosis length and bacterial populations compared to the WT. The *tofIMR* complementation clone in pBBR1MCS-2 plasmid restored the foliar necrosis length and bacterial populations phenotype to the WT level (Figure 3.4E, F).

Discussion

We characterized the contributions of putative virulence determinants to Bga onion leaf and scales symptoms production and in planta bacterial populations. Toxoflavin makes major contributions to foliar symptoms production and bacterial populations in leaves. While the T3SS had little effect on Bga virulence, the T2SS was necessary for symptom development in onion scales but did not contribute to foliar necrosis or bacterial population growth. Results from both foliar and RSN phenotypic assays suggest that the *tofIMR* quorum sensing system is a key virulence regulator in Bga strain 20GA0385 (Figure 3.4D-F). The *in vitro* and *in vivo* experimental results from protease and tobacco cell death assays are consistent with *tofIMR* regulation of T2SS and T3SS in Bga strain 20GA0385 (Figure 3.1C, G). In the phenotypic assays, we routinely observed decoupling of bacterial populations and onion tissue symptoms. This trend was more pronounced in onion scale tissue as compared to foliar tissue (Figure 3.3D-

G; Figure 3.5; Supplementary Figure S3.3). Our study suggests tissue specific virulence factors in Bga onion virulence.

The phytotoxin toxoflavin is an extensively studied virulence factor in *B. glumae.* The toxin contributes to foliar chlorosis and necrotic symptoms in rice leaf tissue (Ilyama et al., 1995; Suzuki et al., 1998; Yoneyama et al., 1998). The studies pertaining to the role of toxin in Bga onion scale and leaf symptoms production are limited. In our study, we found the toxin is a major contributor to Bga onion foliar symptoms (Figure 3.2A). In the Bga WT strain inoculated onion leaves, the symptoms appeared as a greyish lesion after 24-36 hours near the point of inoculation and gradually spread away from the point of inoculation. After 3-4 days, the lesion extended towards the tip of the blades and the leaf appeared wilted. The *toxA* mutant inoculated leaf samples in general produced lesions limited around the point of inoculation and rarely progressing towards the blade tip. The *toxA* mutant was also significantly reduced in leaf bacterial population *in planta* compared to WT (Figure 3.2B). However, the reduction in population was not dramatic. In scale tissue, the necrosis symptoms started appearing from the point of inoculation and developed radially away from the wounding site typically appearing as an oval shaped lesion 3-4 days post inoculation (dpi). Despite being reported as a major virulence factor in rice *Burkholderia* system by multiple independent studies, the lack of clear toxoflavin contribution to onion scale symptoms was surprising (Figure 3.2I).

TTG clusters have been characterized in several onion bacterial pathogens including *P. ananatis*, as well as *B. cepacia*, *B. orbicola*, and *B. gladioli* (Stice et al., 2020; Paudel et al., 2024b). The cluster in these species confers *in vitro* tolerance to allicin, a volatile antimicrobial defensive organosulfur compound produced by garlic. In a previous study, we demonstrated the contribution of TTG clusters in Bga strain 20GA0385 to onion foliar leaf symptoms and bacterial

populations (Paudel et al., 2024b). While the *toxA* single mutant was slightly reduced in *in planta* foliar population recovery, the Δ*toxA*ΔTTG double mutant population recovery from leaf tissue was further reduced compared to *toxA* single mutant (Figure 3.2B, D). The foliar population recovery of the Δ*toxA*ΔTTG double mutant was similar to that of the TTG single mutant reported previously (Paudel et al., 2024b). The *toxA* mutant was also severely reduced in leaves necrosis compared to the WT (Figure 3.2A). Despite the dramatic reduction, the *toxA* mutant still produced a necrotic lesion mostly centered around the point of inoculation. As the TTG cluster single mutant was also severely reduced in leaf bacterial population (Paudel et al., 2024b), toxoflavin independent necrosis factor could also be present in Bga. By contrast, both *toxA* and TTG cluster single mutants and the *toxA*/TTG double mutants did not contribute to RSN area nor scale bacterial populations.

The lipocyclopeptide antibiotic icosalide was described in the beetle endosymbiont *B. gladioli* strain HKI0739. The mutation in the non-ribosomal peptide synthetase (NRPS) encoding *icoS* gene increased the swarming motility of the strain HKI0739 (Dose et al., 2018). A putative icosalide homolog *icoS* was also found in the Bga strain 20GA0385 that shared a high identity percentage with the biosynthetic NRPS gene described previously (Supplementary Table S3.1). As the ORF encoding the putative icosalide biosynthetic gene is over 15 kb size, full gene complementation was not pragmatic. Thus, two independent mutations were generated to assess the virulence role of icosalide in 20GA0385. Both mutants were unchanged in their foliar and onion scale necrosis and onion scale populations (Figure 3.2E, G, K, L). The two mutants did contribute significantly to foliar populations (Figure 3.2F, H). As the T2SS *gspC* mutant contributed to RSN area, a double mutant was created by introducing *gspC* mutant into the Δ*icoS*::Gm^{R}*gus* background to check if it has further reduction in the RSN phenotype. The

double mutant was also significantly reduced in RSN symptoms as the *gspC* single mutant (Figure 3.3G). The role of Bga icosalide in swarming motility of the bacterium was analyzed by developing an *in vitro* swarming assay. In contrast to what was observed with the strain HKI0739 where mutants displayed increased swarming, both icosalide mutants were visually reduced in swarming area compared to the WT strain. A further reduced swarming area was observed for the *gspC/icoS*::Gm^R*gus* double mutant compared to both single mutants (Supplementary Figure S3.2F). While the icosalide mutants in HKI0739 demonstrate increased swarming behavior, our results indicate the opposite phenotype in Bga strain 20GA0385. Despite sharing high homology, the strain specific differences observed in the *in vitro* swarming phenotype between the two strains was noteworthy. The differences in ecological niche of the two strains harboring the icosalide cluster might have caused the differences in swarming behavior of the strains. Foliar assay results suggest the Bga icosalide cluster mutants recovery from infected leaf tissue was significantly lower compared to the WT strain (Figure 3.2F, H). As authors demonstrated the antibiotic activity of icosalide in HKI0739 strain suggesting its potential role in eukaryotic host protection, the Bga icosalide cluster could also help the bacteria interact with competitors promoting the colonization of bacteria in onion leaf tissue. Further experimental tests are needed to test this hypothesis.

The virulence-associated protein secretion systems, particularly T2SS, and T3SS have also been characterized as a virulence factor in *B. glumae* and *B. gladioli.* T2SS in *B. glumae* contributes to rice panicles symptoms and *in planta* populations and in *B. gladioli*, T2SS is required for mushroom tissue necrosis (Chowdhury and Heinemann, 2006; Devescovi et al., 2007; Kang et al., 2008; Goo et al., 2010). The role of *B. gladioli* T3SS in mycophagy has also been demonstrated (Swain et al., 2017). We found that neither T2SS nor T3SS contributed to

foliar necrosis nor *in planta* bacterial populations (Figure 3A, B; Supplementary Figure S3.4C, D). The T2SS mutant *gspC* and its double mutant derivatives all contributed positively to red scale necrosis symptoms production in both high (~6 x 10^6 CFU) and low (~6 x 10^4 CFU) inoculum (Figure 3.3D, F, G; Figure 3.5A-D). Surprisingly, the Δ*toxA*Δ*gspC*Δ*sctC* triple mutant showed a similar RSN area to the WT strain when higher initial bacterial concentration was used (Figure 3.4C). All the mutants that contributed to RSN area at higher inoculum concentration also showed similar results at lower inoculum concentration (Figure 3.5A-D). Consistent with the findings from *B. glumae* and *B. gladioli* pv. *agaricicola* studies, the T2SS in Bga also functions as an important virulence factor in onion scale tissues.

The observed decoupling between Bga *in planta* bacterial populations and tissue symptoms suggests that tissue-specific factors may influence the role of bacterial traits in disease development. In leaf tissue, icosalide may play a role in promoting bacterial growth rather than directly causing necrosis (Figure 3.2E-H). In contrast, in scale tissue, the absence of a clear link between reduced necrosis area and bacterial population levels was observed (Supplementary Figure S3.3). Even with a 100-fold lower starting concentration, mutants exhibiting reduced necrosis phenotypes still maintained similar bacterial population levels to the wild-type strain, suggesting that the bacterium's ability to colonize and replicate in onion scale tissue may be independent of its capacity to induce tissue necrosis (Supplementary Figure S3.3 K-O; Figure 3.5A-D). These findings highlight a complex relationship between bacterial virulence factors and tissue-specific disease outcomes.

The quorum sensing *tofIMR* system has been shown to regulate multiple virulence factors in *B. glumae* (Devescovi et al., 2007; Goo et al., 2010; Lelis et al., 2019). Across three different media conditions, variation in toxoflavin production between the WT and *tofIMR* mutant was

observed. The production was highest in MGY media compared to LM and LB media (Supplementary Figure S3.2B, C). The regulators that contribute to *tofIMR* independent production of toxoflavin have been described previously (Chen et al., 2015). While the *tofIMR* complementation clone partially restored toxoflavin production on LM media, it failed to do so on LB media. (Figure 3.1B; Supplementary Figure S3.2B-C).

Through the *in vitro* assays we also demonstrated that the *tofIMR* system regulates the function of T2SS, T3SS, and swarming motility in Bga (Figure 3.1 C, G; Supplementary. Figure S3.2D-F). The virulence phenotype of *tofIMR* mutant in both leaves and scale was complemented by *tofIMR* complementation clone (Figure 3.4D-F). Our results from multiple independent experiments suggest that quorum sensing *tofIMR* system regulates multiple virulence traits in Bga strain 20GA0385.

Among the tested virulence factors, only T2SS *gspC* contributed to red scale symptoms production. The *gspC* mutant still produced noticeable red scale necrosis symptoms relative to the *tofIMR* system suggesting other unknown factors could yet contribute to RSN phenotype. The *tofIMR* system may regulate additional unknown virulence factors.

In summary, we observed the phytotoxin toxoflavin and the T2SS play onion tissue-specific virulence roles in Bga strain 20GA0385. Despite the key role of toxoflavin in leaf tissue necrosis, its lack of a clear role in red scale necrosis was unexpected. Likewise, commonly studied protein secretion systems T2SS and T3SS were not required for foliar symptoms production or bacterial population growth. No combined effect or synergism of individual virulence factors on symptom production or bacterial population was observed with Bga in our study. Scale assay necrosis area results suggest additional unknown virulence factors/regulators could contribute to onion scale symptoms. Furthermore, the decoupling of bacterial populations

vs necrosis area particularly in the onion scale tissue suggests the bacterium is a well-adapted scale/bulb colonizer utilizing multiple virulence factors to infect the onion host. Future studies should focus on identification of additional virulence factors that contribute to onion symptom production and bacterial population in bulb tissues. Different management strategies would be required for the control of Bga foliar versus bulb symptoms.

Materials and Methods

Bacterial growth conditions

Escherichia coli strains and plasmids used for allelic exchange and construction of the complementing strains are listed in Supplementary Table S3.2. Primers and synthesized dsDNA fragments used in the study are listed in Supplementary Table S3.3. The mutants and the complementation clones generated in this study are listed in Supplementary Table S3.4. *Escherichia coli* strains DH5α, Mah1, RHO5, and Bga strain 20GA0385 used to generate mutants were grown in LB (per liter, 10 g of tryptone, 5 g of yeast extract, 5 g of NaCl) broth or LM (per liter, 10 g tryptone, 6 g yeast extract, 1.193 g KH_2PO_4, 0.6 g NaCl, 0.4 g $MgSO_4.7H_20$) at 37ºC and 28ºC, respectively. Liquid broth was supplemented with Difco Agar (per liter, 15 g for LB and 18 g for LM) to make solid media. Antibiotics and chemicals were supplemented with the growth media at the following final concentrations, per milliliter: 50 µg of kanamycin (Km), 10 µg of gentamicin (Gm), 100 – 200 µg of Diaminopimelic acid (DAP), 50 µg of X-Gal (5-bromo-4-chloro-3-indolyl-beta-D-galacto-pyranoside), 25 µg of chloramphenicol (Cam), 100 µg of Xgluc (5-bromo-4-chloro-3-indolyl-beta-D-glucuronic acid), and 40-60 µg of rifampicin, as appropriate.

Plant growth conditions

Onion sets (*Allium cepa L.* cv. Century) were planted in 10 cm x 8 cm (diameter x height) plastic pots filled with SunGrow 3B potting soil and maintained at greenhouse conditions with 25–28^{0}C, 12L:12D photoperiod for 5 months from January to May until inoculation. To grow the seedlings, onion seeds (*Allium cepa* var. Texas Grano 1015Y) were sown in 3-inch pots with Sungrow 3B potting soil and were maintained in growth chamber conditions at ~80^{0}F, 40-50% humidity and watered every 2-3 days.

Recombinant DNA techniques

PCR was conducted using GoTaq Green polymerase (Promega, Fitchburg, WI) or Q5 High-Fidelity DNA polymerase (New England Biolabs, Ipswich, MA) following manufacturer's protocols. Primers and double stranded DNA were ordered/synthesized from Eurofins Genomics LLC (Louisville,KY) and Twist Biosciences (South San Franscisco, CA) respectively. Plasmid DNA was purified using GeneJet Plasmid Miniprep Kit (Thermoscientific, Watham, WA). PCR product and Gel cleanup was performed using Monarch NEB PCR cleanup kit and Monarch NEB Gel extraction kit (New England Biolabs), respectively. Restriction digest was done with enzymes purchased from New England Biolabs following manufacturer's recommendations. Gateway recombination was done with Gateway BP or LR Clonase II enzyme mix from Thermo Fisher Scientific following manufacturer's recommendations. Gibson cloning was performed with Gibson Assembly Master Mix (2X) from New England Biolabs. Gateway reaction products were transformed into chemically competent DH5α cells unless noted otherwise. The purified plasmid with the deletion construct was then transformed into electro-competent RHO5 cells. Sanger sequencing of PCR product and plasmids was done with Eurofins Genomics LLC (Louisville, KY). Whole-plasmid sequencing was done at Plasmidsaurus (Plasmidsaurus, Eugene, OR). Sequences were analyzed using Geneious Prime v. 2023.2.1.

Identification of putative virulence factors in Bga strain 20GA0385

The rice pathogenic strain BGR1 (GenBank: GCA_000022645.2) was used as a reference to identify putative virulence factors and regulators in Bga strain 20GA0385 (Genebank: GCA_034365665.1). Another Bga strain FDAARGOS_389 was also included in the analysis as it had a closed genome available in the NCBI GeneBank database. The chromosome and plasmid sequences for each strain were downloaded from NCBI GenBank database and imported into the Geneious Prime v.2023.2.1 software. Sequences for *B. glumae* virulence factors were identified from the literature and map to reference plugin and/or custom BLAST feature was used in Geneious Prime v.2023.2.1 to locate corresponding sequence regions in FDAARGOS_389 and Bga strain 20GA0385. Obtained sequence information was utilized for designing the deletion construct and other downstream processes.

The gene synteny diagram and amino acid identity percentage was calculated using the Clinker CAGECAT bioinformatics web software (Gilchrist and Chooi, 2021). GeneBank format files of putative virulence factors/regulator were uploaded for Bga strain 20GA0385 and *B. glumae* strain BGR1 in the web server to generate the image. The minimum alignment sequence identity threshold was set to 0.3.

Construction of allelic exchange plasmids.

Deletions in strain 20GA0385 were made with pK18*mobsacB* or its Gateway compatible derivative pDONR1k-18ms (AddGene plasmid 72644) (Mijatović et al., 2021). For the unmarked deletion of toxoflavin biosynthesis gene *toxA* and type II secretion apparatus gene *gspC*, 450 bp region upstream and downstream of the respective genes (including start codon with 2 downstream amino acid encoding sequences and stop codon with 2 upstream amino acid

encoding sequences) were synthesized as double stranded DNA gblocks with *attB* sites from Twist Biosciences. A unique *Avr*II restriction site was also included in between the flanking region. The synthesized fragment was then BP cloned into pDONR1k18ms plasmid using Gateway BP recombination. The reaction mix was then transformed into chemically competent DH5α cells. The insert in the plasmid was confirmed by restriction digest and sequencing. To generate the T3SS outer membrane protein encoding *sctC* gene deletion mutant, upstream (907 bp) and downstream (790 bp) flanking regions of the ORF was amplified separately using Q5 polymerase PCR reactions. Forward primer amplifying upstream flank and reverse primer amplifying downstream flank were designed with *attB1* and *attB2* sites in the overhangs. Similarly, reverse primer amplifying upstream *sctC* flanking region and forward primer amplifying downstream *sctC* flanking region were designed with overlapping 5' Gibson overhangs. The Gel extracted purified PCR product was stitched together using Gibson Assembly master mix reaction. The Gibson reaction mix with an expected amplicon size of 1759 bp was excised from the gel, purified, and cloned into pDONR1k18ms using Gateway BP clonase II enzyme mix following manufacturer's recommendations. The quorum sensing *tofIMR* genes were deleted following a similar strategy as described for the *sctC* gene deletion. The upstream region of *tofI* ORF and downstream region of *tofR* was manually amplified using respective primer pairs tofIMRflankAF2/tofIMRflankAR1 and tofIMRflankBF1/tofIMRflankBR2 with Q5 polymerase-based PCR reaction following manufacturer's recommendations. Primers tofIMRflankAR1 and tofIMRflankBF1 were designed with 27 bp overlapping sequence region as 5' overhangs. The overlapping sequence region also included *Kpn*I, *Avr*II, and *Xho*I restriction sites. The two purified PCR products were ligated using overlap extension PCR following conditions and reaction mix as described in Stice et al.,

2020. The amplicon size corresponding to the 1636 bp obtained in the gel following overlap extension PCR was excised, purified and cloned into pDONR1k18ms plasmid using Gateway BP Clonase II enzyme reaction. The FRTGm^{R}*gus* marker was amplified from the plasmid pCPP5212 was added to the *Xho*I restriction site in between the deletion flanks to aid the selection of single and double crossovers in the downstream steps. The FRTGm^{R}*gus* cassette PCR product was excised from the gel, purified, and cloned into *Xho*I digested pDONR1k18ms Δ*tofIMR* deletion construct using NEB T4 ligase reaction following procedures described by Kvitko and Collmer 2012. The ligation reaction mix was transformed into DH5α and the correct insert was confirmed using restriction digest and sanger sequencing. The putative icosalide mutant was created by introducing a premature triple stop codons (TAA) 27 bp downstream of the start codon in the icosalide ORF. The triple stop codon along with a unique *Avr*II restriction site was synthesized along with 450 bp upstream and downstream region in pk18*mobsacB* vector from Twist Biosciences. An independent icosalide interruption mutant was also made mimicking the mutant made by Dose et al., 2018 with some modifications. The authors inserted a kanamycin resistance cassette at the icosalide ORF 7835 bp downstream of the start codon. The upstream (450 bp) and downstream (450 bp) sequence region corresponding to the kanamycin insertion site in Bga strain 20GA0385 along with a unique *Avr*II restriction site in between was synthesized in pk18*mobsacB* plasmid. Instead of kanamycin resistance cassette, the FRTGm^{R}*gus* region from the plasmid pCPP5212 was amplified using primer pair icogmgusF and icogmgusR, excised from the gel, and ligated into *Avr*II restriction site using Gibson assembly master mix. For the icosalide and *tofIMR* single crossovers selection, Xgluc and Gm was amended to the LBRfKm medium. The double crossovers were selected following *sacB*-mediated sucrose counter selection. The kanamycin sensitive clones following sucrose counter selection were screened

using patch plating. The *toxA* and *gspC* deletion mutants were genotyped using toxAgenoF/toxAgenoR and gspCgenoF/gspCgenoR primers respectively. The *sctC* deletion mutant was confirmed using primer pairs SctCgenoF2/SctCflankBR2 and SctCflankA-F/sctCgenoR. Primer pair SctCgenoF2 and SctCgenoR were designed outside of *sctC* deletion flanks. Similarly, *tofIMR* mutant was confirmed using primer pairs tofIMRgeno-F/GmGUSF and GmGUS-R/tofIMRgeno-R. The primer pair tofIMRgeno-F and tofIMRgeno-R were designed outside of tofIMR deletion flanks. The icosalide FRTGm^R*gus* interruption mutant was confirmed using primer pairs ico2genoF/GmGUSR2 and GmGUSF/ico2genoR. The ico2genoF and ico2genoR primer pair was designed outside of icosalide deletion flanks. The icosalide triple stop codon interruption mutant was confirmed using primer pair ico1genoF and ico1genoR followed by *Avr*II restriction digest using PCR product as DNA template. Each mutant was also confirmed by partial sangar sequencing of purified PCR product. The *gspC* deletion construct in RHO5 strain was introduced into *sctC* mutant background by biparental mating to generate *gspC sctC* double mutant. Similarly, *toxA* deletion construct was introduced into *gspCsctC* double mutant background by allelic exchange to generate *toxAgspCsctC* triple mutant. The *toxA* mutant was introduced into TTG background to generate *toxATTG* double mutant. Likewise, *gspC* single mutant was introduced into icosalide Gm^R*gus* mutant background to generate Δ*gspC* Δ*icoS* :: Gm^R*gus* double mutant.

Plasmid based complementation vectors.

The plasmid-based complementation of single mutants *gspC* and *tofIMR* was done using a broad-host-range expression vector pBBR1MCS-2 (GenBank ID: U02374) and its BP cloning compatible derivative pBBR1MCS2GW (Kovach et al., 1994). The gateway compatible derivative was constructed by first amplifying the gateway cassette from plasmid pR6KT2G

using primer pair pBBR1GW-F and pBBR1GW-R. The gel excised and purified PCR amplicon was ligated into *Xba*I digested linearized plasmid using Gibson Assembly master mix reaction. The desalted Gibson reaction was transformed into electrocompetent *ccdB* resistant DB3.1 cells and the transformants were selected on LBKmCam plates. The insert was confirmed using restriction digest and whole plasmid sequencing using PlasmidSaurus. To generate the *gspC* complementation construct, the *gspC* ORF along with 148 bp region was amplified using primer pair gspCcompnF and gspcompnR. The primer pair was designed with *attB* sites overhangs to facilitate Gateway recombination. The PCR gel extracted and purified product was cloned into pBBR1MCS2GW plasmid using Gateway BP clonase reaction. The correct insert was confirmed by genotyping using M13F43 and M13R49 primer pairs. The RHO5 strain with pBBR1MCS2GW plasmid harboring correct *gspC* construct was then conjugated into *gspC* mutant strain using biparental mating. The conjugants selected on LBRfKm plates were confirmed using M13F43 and M13R49 primer-based colony PCR. The PCR amplicon with correct size was excised from the gel, purified and sent for sequencing with M13F primer to confirm the *gspC* insert in the plasmid. The *tofIMR* complementation clone was constructed by PCR amplifying 2225 bp long *tofI-tofR* region using primer pair imrcomplnF and imrcomplnR. The purified *tofIMR* PCR product was then cloned into pBBR1MCS2GW plasmid using Gateway BP clonase II reaction. The *tofIMR* insert in the plasmid was confirmed using restriction digest and partial sanger sequencing using M13F primer. The pBBR1MCS2GW plasmid with *tofIMR* complementation construct was transformed to RHO5 cells and mated with *tofIMR* mutant using biparental mating. The conjugants were selected on LBRfKm plates and the correct insert was confirmed by genotyping using M13(-21) F and M13R primer pair.

Chromosomal restoration of mutants.

A chromosomal restoration strategy was then utilized to validate the role of *toxA* gene in yellow pigmentation. A 1691 bp region including the *toxA* ORF and upstream/downstream region was PCR amplified using toxAcomplnF2 and toxAcomplnR2 primer pair containing *attB* sites in the 5' overhang. The purified PCR product was BP cloned into plasmid pDONR1k18ms and the insert was confirmed using *BsrG*I restriction digest. The RHO5 strain containing the *toxA* restoration construct was then conjugated with *toxA* mutant strain using biparental mating. The sucrose counterselection and patch plating were followed as described above. The *toxA* restoration clone was genotyped by visualizing the yellow pigmentation of the Kan sensitive clones and by colony PCR using primer pair toxAgenocomplnF and toxAgenocomplnR designed outside of the restoration flanks. The *toxA* mutant strain was used as a positive control. The restored clone yielded a bigger amplicon size (1752 bp) in the agarose gel compared to the *toxA* mutant strain (1032 bp). The clone was also confirmed using Sanger sequencing. The *sctC* restoration clone for the *sctC* deletion mutant was obtained using a similar strategy. The *sctC* ORF including 454 bp upstream region and 390 bp downstream region was amplified using primer pair sctCresF and sctCresR containing *attB* sites. The expected amplicon size of 2638 bp was excised from the gel, purified, and cloned into pDONR1k18ms plasmid using BP clonase enzyme mix. The *sctC* insert in the plasmid was confirmed by genotyping using primer pair sctCflankBR and M13R49 and by *BsrG*I restriction digest. The sequence confirmed insert was transformed to RHO5 and conjugated with *sctC* mutant background using biparental mating. Further downstream steps to generate Km sensitive clones were followed as described previously. The kanamycin sensitive clones were screened for mutants using primer pair sctCseqF and sctComplnR using Q5 Polymerase based PCR. The restored clone gave the product size of 2410 bp whereas the *sctC* mutant gave amplicon size of 540 bp.

Preparation of bacterial inoculum

Bacterial inocula for the casein hydrolysis protease plate assay, *Chromobacterium* AHL assay, tobacco cell death assay, and *in planta* assays were prepared following similar procedure described by (Paudel et al., 2024b). Briefly, the test strains were streaked on LB or LM plates amended with appropriate antibiotics and incubated at 30^0C for 24 hours. After 24 hours, the plates were spread with 300 µl of sterile 0.25 mM $MgCl_2$/sterile milliQ H_20 and incubated overnight at 30^0C to produce even bacterial lawns. A day after, colony growth from the lawn was scraped and suspended in 1 ml of ddH_20 /$MgCl_2$ and standardized to OD_{600} = 0.68 - 0.7. The bacterial suspension was serially diluted and plated on LB or LM Rf agar to ensure starting CFU/ml concentration was similar for all the inoculated strains. As the *tofIMR* mutant was gradually reduced in CFU/ml plate recovery, the OD_{600} values for *tofIMR* mutant was variable across the repeats. The standardized suspension was used for inoculation.

Quantification of toxoflavin production

The quantification of toxoflavin production by *Burkholderia gladioli pv. alliicola* strain 20GA0385, along with its *toxA* and *tofIMR* mutants, was conducted following a modified version of the protocol described by Chen et al. (2012). Solid culture media plates were prepared by pouring 10 ml of LB, LM, or MGY media into VWR 60 mm × 15 mm petri dishes (VWR International, Radnor, PA). Strains were streaked onto the respective media from glycerol stocks to create a lawn, followed by incubation at 30°C for 24 hours. After incubation, the bacterial lawns were removed, and the agar containing diffused toxoflavin pigment was sampled using a metal borer (radius = 2.5 mm). Five punches were taken from each plate. The weighted agar in a microcentrifuge tube was then mixed with 1:2 (w/v) of chloroform under the fume hood, incubated for 15 minutes and centrifuged at 5000 g for 5 minutes. The chloroform layer was

carefully transferred to a new microcentrifuge tube, which was left open in the fume hood to air-dry. The dried residue was then resuspended in 1 ml of 80% methanol and vortexed. Absorbance values for the samples were measured at 393 nm wavelength. Non-inoculated agar plates underwent the same sampling process to serve as blanks. At least four OD_{393} values were recorded for each strain. Absorbance values were normalized based on the weight of the sampled agar, and statistical differences between strains were assessed using pairwise *t*-test function in RStudio.

Casein hydrolysis protease plate assay

The casein hydrolysis protease assay was performed for the type II secretion mutant *gspC*, its double and triple mutant derivatives, and the regulatory mutant *tofIMR* following the protocol described by (Brumfield et al., 2018). For the preparation of milk agar plates, 8g of instant skimmed dry milk powder (Kroger store brand) was mixed with sterile milliQ water and autoclaved at 121^0C for 60 minutes. The second component was prepared by weighing 4.58 g of brain-heart infusion (Becton, Dickinson and Company, Sparks, MD) and 6 g agar in 200 ml of sterile milliQ water and autoclaved separately. The milk agar plate was prepared by mixing 15 ml each of the two autoclaved components. The agar was punched by using the back end of a sterile 20 µl pipette tip. The hole was inoculated with 50 µl of normalized bacterial suspension standardized to OD_{600} value of 0.7. The plate was incubated at 30^0C for 24 hours. Clearing zone on the edge of the inoculated hole indicated the strains were able to hydrolyze casein in the milk powder. The experiment was repeated at least three times.

Tobacco cell death assay

The tobacco cell death assay was performed with 6–8-week-old tobacco plants (cv. Xanthi SX) grown 26^0C 12-h day, 22^0C 12-h night in a Coviron Adaptis growth chamber. At least 3 leaf panels of the third-to eight-oldest leaves were infiltrated with a normalized bacterial suspension of OD_{600} of 0.7 using a blunt syringe. Negative controls were inoculated with 0.25 mM $MgCl_2$. The cell death was allowed to develop for at least 3 days before taking the images. Cell death area of the mutants was compared visually to the WT strain. The experiment was repeated at least three times.

***Chromobacterium* AHL assay**

The AHL reporter *Chromobacterium violaceum* strain CV026 was streaked on a LM agar plate to make a lawn and incubated at 30^0C for 48 hours. A dense suspension of CV026 was prepared by scraping the bacterium from the lawn into sterile milliQ H_20. A bacterial lawn of CV026 was prepared on LM agar plate by using 300 µl of dense CV026 suspension. After letting it dry, the agar was punched with back end of a sterile 20 µl pipette tip to make holes. Normalized Bga suspension of 50 µl with OD_{600} = 0.7 was inoculated into the holes and incubated at 30^0C for 48 hours. The inoculated holes were monitored for the appearance of violet ring around the edges produced by the reporter strain. The CV026 bacterial suspension was used as negative control. The experiment was repeated three times on its entirety.

Swarming motility assay

Swarming motility plate assay was performed following the protocol as described by (Dose et al., 2018) with slight modifications. Briefly, MGY media was prepared by mixing 1.5 g glycerol, 0.188 g yeast extract and 1.5% agar in 144 ml milliQ water and autoclaved at 121^0C for 60 minutes. M9A salt was prepared by mixing 2.50 g K_2HPO_4 and 1 g KH_2PO_4 in 100 ml of milliQ

water and sterilized by autoclaving. Similarly, M9B was prepared by mixing 2.58 g of sodium citrate dihydrate, 5 g of $(NH_4)_2SO_4$ and 0.5 g of $MgSO_4.7H_2O$ in 100 ml of milliQ water. MGY agar media was prepared the same day of inoculation. After autoclaving, 6 ml each of warm M9A and M9B salt was mixed to MGY agar media and diluted in half with MGY broth and a 20 ml mix was poured into the plate. To prepare the bacterial suspension, WT and mutants were streaked to isolation on LB Rf or LBRfKm plates and a single colony was used to start overnight cultures (~24 h). A normalized bacterial suspension of 0.7 OD_{600} was prepared using sterile 0.25 mM $MgCl_2$ and 50 µl was inoculated into the center of the plate. Suspension was allowed to dry and incubated at 28^0C for 21 hours. At least one plate was plated for each strain and the experiment was repeated three times in its entirety.

Enriched media growth assay

To assess the growth of mutants contributing to the necrosis phenotype or bacterial population *in planta*, a growth assay was conducted in enriched LB medium using 100-well honeycomb plates with the Bioscreen C system (Lab Systems, Helsinki, Finland). The assay protocol followed the methodology described in (Paudel et al., 2024b). Normalized bacterial suspension for each test strains were prepared as described in the section above. The standardized suspension of 40 µl was added to the 360 µl of sterile LB media. Each of at least six honeycomb wells were loaded with 400 µl of the mix for each treatment and the experiment was run for 48 h with shaking at 28^0C. Mean of OD_{600} values for each strain at specific time point across the two independent experimental repeat was presented in the line graph prepared using ggplot2 function in RStudio 2023. 09.0.

Onion foliar assay

Onion plants (*Allium cepa* L. cv Century) 1.5 to 4.5 months old grown under greenhouse conditions from February to May were used for inoculation. The procedure for inoculation, sampling and bacterial quantification was followed as described by (Paudel et al., 2024b). Inoculum for Bga WT strain 20GA0385 and its mutant derivatives were prepared as described above. Onion plants were trimmed to keep the two oldest and tallest leaves intact. Two leaves per plant and three biological replicates per strain were inoculated. The approximate midpoint and 0.5 cm length top and bottom was marked for processing and the midpoint was poked/wounded with a sterile pipette tip on one side to drop the inoculum. Each leaf was inoculated with 10 µl of a normalized bacterial suspension. Two leaves were inoculated with 0.25 mM $MgCl_2$ as negative controls. The maximum necrosis length was measured 3 days post inoculation. The experiment was repeated at least three times in its entirety.

For quantification of bacterial population in the infected blade tissue, a pre-marked 0.5 cm section above and below the inoculation site was excised with a sterile scissor and added to 200 µl of Milli-Q H_20 in a 2-ml SARSTEDT microtube (SARSTEDT AG & Co., Numbrecht, Germany) along with three 3-mm zirconia beads (Glen Mills grinding media). The tissue was crushed using a Bead Ruptor Elite Bead Mill Homogenizer (Omni International, Kennesaw, GA) for 30 seconds at 4 m/s speed settings. Serial dilutions were performed by mixing 20 µl of the ground tissue with 180 µl of sterile 0.25 mM $MgCl_2$ in 96-well styrene plates. Diluents were plated on LB or LM plates amended with rifampicin. The number of colony-forming units (CFUs) was back-calculated to determine the bacterial population per mg of the infected tissue. The recovered CFU/mg values for two leaves per plant was averaged making it a total of three data points for three biological replicates per treatment.

Onion seedling assay

Onion seedling assay was done to determine the contribution of Δ*toxA*Δ*gspC*Δ*sctC* triple mutant to seedling necrosis and bacterial populations. Onion seedlings grown for 6-8 months were used for inoculation. One leaf per plant per pot was selected for inoculation. A normalized bacterial suspension of 0.7 OD_{600}, 10 µl was used to inoculate the mid-point of the marked seedlings. Bacterial CFU/ml plate recovery of the WT and mutant strains were determined on day 0 to ensure starting concentration was similar. The seedling necrosis length and in planta population counts were assessed at 3 dpi, following the protocol detailed in the onion foliar assay section above.

Red Scale Necrosis (RSN) assay

The RSN assay was done following the procedure described in (Stice et al., 2018; Shin et al., 2023; Paudel et al., 2024b) with slight modifications. The store brought red onion bulbs were cut into 3-5 cm x 3-5 cm sized scales. The scales were sterilized in a 3 % Sodium hypochlorite/Clorox solution and washed several times with deionized H_20. Six scales per strain were kept on top of a sterile pipette tip rack in a flat floored with wetted paper towels. The scales were wounded on the center with a pipette tip. The wounded scale was deposited with 10 µl of normalized bacterial suspension (OD_{600} = 0.82 for *tofIMR* and 0.68 – 0.7 for all other treatments). To ensure all the tested strains had comparable CFU/ml plate recoveries, 2 to 3 replicates of normalized bacterial suspension were plated on LB or LM media amended with rifampicin following serial dilutions. Strains that had comparable CFU/ml reading were further utilized for the experiment. The scales were incubated at room temperature for 3 days. Necrosis area around the point of inoculation was measured using ImageJ software. The experiment was repeated at least three times for each strain. For the quantification of bacterial populations from the inoculated scales, onion tissues were sampled at 3 dpi at the point of inoculation using

ethanol sterilized metal borer (r = 2.5 mm). The sample was processed for crushing and serial dilutions to calculate the CFU/mg for each scale following the procedure as described in the above section.

For mutants that exhibited significantly smaller area of red scale necrosis area compared to the WT strain, additional rounds of RSN assay were performed with a 100-fold diluted bacterial suspension of 0.7 OD_{600} density. CFU/ml recovery of 0.7 OD_{600} was calculated for each treatment to ensure the starting bacterial concentration was comparable for all treatments. The red scale assay procedure for inoculation, sampling, and *in planta* bacterial quantification was followed as described before.

Data analysis and presentation

The statistical difference in scale/foliar/seedling necrosis area and bacterial populations in Log (CFU/mg) between the WT and mutants was performed using pairwise t-test function applying the Bonferroni coefficient in R studio 2023.09.0. For treatments that had an unequal number of observations, Welch's t-test was performed with t.test function in R studio 2023.09.0 using "var.equal = FALSE" option.

The box plot was generated using ggplot function in R studio. The color of the box was assigned based on function. The WT strain was represented in green, secretion system mutants in grey, and mutants for the metabolites toxoflavin and icosalide in yellow, while regulator mutant *tofIMR* was assigned red. Double and triple mutants were given distinct colors: the *toxA* TTG mutant was marked in white, Δ*gspC*Δ*sctC* in cyan, Δ*gspC*Δ*icoS*::Gm^R*gus* in orange, and the triple mutant *toxA*/*gspC*/*sctC* was represented in purple.

References

Abachi, H., Moallem, M., Taghavi, S., Hamidizade, M., Soleimani, A., Fazliarab, A., Portier, P., and Osdaghi, E. 2024. Garlic bulb decay and soft rot caused by the cross-kingdom pathogen *Burkholderia gladioli*. Plant Disease 108:684-693.

Belo, T., du Toit, L., Waters, T., Derie, M., Schacht, B., and LaHue, G. 2023. Reducing the risk of onion bacterial diseases through managing irrigation frequency and final irrigation timing. Agricultural Water Management 288:108476.

Brumfield, K., Carignan, B., and Son, M. 2018. Genotypic and phenotypic assays to distinguish *Vibrio cholerae* biotype: Methods and Protocols. Pages 11-28 in.

Burkholder, W. 1950. Sour skin, a bacterial rot of onion bulbs. Phytopathology 40.

Chen, R., Barphagha, I., and Ham, J. 2015. Identification of potential genetic components involved in the deviant quorum-sensing signaling pathways of *Burkholderia glumae* through a functional genomics approach. Frontiers in cellular and infection microbiology 5:22.

Chen, R., Barphagha, I., Karki, H., and Ham, J. 2012. Dissection of quorum-sensing genes in *Burkholderia glumae* reveals non-canonical regulation and the new regulatory gene *tofM* for toxoflavin production. PloS one 7:e52150.

Chowdhury, P., and Heinemann, J. 2006. The general secretory pathway of *Burkholderia gladioli* pv. agaricicola BG164R is necessary for cavity disease in white button mushrooms. Applied and environmental microbiology 72:3558-3565.

Devescovi, G., Bigirimana, J., Degrassi, G., Cabrio, L., LiPuma, J., Kim, J., Hwang, I., and Venturi, V. 2007. Involvement of a quorum-sensing-regulated lipase secreted by a clinical

isolate of *Burkholderia glumae* in severe disease symptoms in rice. Applied and environmental microbiology 73:4950-4958.

Dose, B., Niehs, S.P., Scherlach, K., Flórez, L.V., Kaltenpoth, M., and Hertweck, C. 2018. Unexpected bacterial origin of the antibiotic icosalide: two-tailed depsipeptide assembly in multifarious *Burkholderia* symbionts. ACS Chemical Biology 13:2414-2420.

Elshafie, H., Devescovi, G., Venturi, V., Camele, I., and Bufo, S. 2019. Study of the regulatory role of N-acyl homoserine lactones mediated quorum sensing in the biological activity of *Burkholderia gladioli* pv. *agaricicola* causing soft rot of Agaricus spp. Frontiers in Microbiology 10:2695.

Fayos, O., Echávarri, B., Vallés, M., Mallor, C., Garcés-Claver, A., and Castillo, A. 2022. A simple and efficient method for onion pollen preservation: Germination, dehydration, storage conditions, and seed production. Scientia Horticulturae 305:111358.

Félix-Gastélum, R., Maldonado-Mendoza, I., Olivas-Peraza, N., Brito-Vega, H., Peñuelas-Rubio, O., and Longoria-Espinoza, R. 2017. First report of slippery skin caused by *Burkholderia gladioli* in stored onion bulbs in Mexico. Plant Disease 101:1030-1030.

Fory, P.A., Triplett, L., Ballen, C., Abello, J.F., Duitama, J., Aricapa, M.G., Prado, G.A., Correa, F., Hamilton, J., Leach, J.E., Tohme, J., and Mosquera, G.M. 2014. Comparative analysis of two emerging rice seed bacterial pathogens. Phytopathology 104:436-444.

Gilchrist, C.L.M., and Chooi, Y.H. 2021. clinker & clustermap.js: automatic generation of gene cluster comparison figures. Bioinformatics 37:2473-2475.

Goo, E., Kang, Y., Kim, H., and Hwang, I. 2010. Proteomic analysis of quorum sensing-dependent proteins in *Burkholderia glumae*. Journal of proteome research 9:3184-3199.

Ilyama, K., Furuya, N., Takanami, Y., and Matsuyama, N. 1995. A role of phytotoxin in virulence of *Pseudomonas glumae*. Japanese Journal of Phytopathology 61:470-476.

Jeong, Y., Kim, J., Kim, S., Kang, Y., Nagamatsu, T., and Hwang, I. 2003. Toxoflavin produced by *Burkholderia glumae* causing rice grain rot is responsible for inducing bacterial wilt in many field crops. Plant disease 87:890-895.

Jones, C., Webster, G., Mullins, A.J., Jenner, M., Bull, M.J., Dashti, Y., Spilker, T., Parkhill, J., Connor, T.R., LiPuma, J.J., Challis, G.L., and Mahenthiralingam, E. 2021. Kill and cure: genomic phylogeny and bioactivity of *Burkholderia gladioli* bacteria capable of pathogenic and beneficial lifestyles. Microbial Genomics 7.

Kang, Y., Kim, J., Kim, S., Kim, H., Lim, J., Kim, M., Kwak, J., Moon, J., and Hwang, I. 2008. Proteomic analysis of the proteins regulated by HrpB from the plant pathogenic bacterium *Burkholderia glumae*. Proteomics 8:106-121.

Karki, H., Shrestha, B., Han, J., Groth, D., Barphagha, I., Rush, M., Melanson, R., Kim, B., and Ham, J. 2012. Diversities in virulence, antifungal activity, pigmentation and DNA fingerprint among strains of *Burkholderia glumae*. PloS one 7:e45376.

Korotkov, K., Johnson, T., Jobling, M., Pruneda, J., Pardon, E., Héroux, A., Turley, S., Steyaert, J., Holmes, R.K., and Sandkvist, M. 2011. Structural and functional studies on the interaction of GspC and GspD in the type II secretion system. PLoS pathogens 7:e1002228.

Kovach, M., Phillips, R., Elzer, P., Roop 2nd, R., and Peterson, K. 1994. pBBR1MCS: a broad-host-range cloning vector. Biotechniques 16:800-802.

Kowal, J., Chami, M., Ringler, P., Müller, S.A., Kudryashev, M., Castaño-Díez, D., Amstutz, M., Cornelis, G.R., Stahlberg, H., and Engel, A. 2013. Structure of the dodecameric *Yersinia enterocolitica* secretin YscC and its trypsin-resistant core. Structure 21:2152-2161.

Kvitko, B., Ramos, A., Morello, J., Oh, H., and Collmer, A. 2007. Identification of harpins in *Pseudomonas syringae* pv. tomato DC3000, which are functionally similar to HrpK1 in promoting translocation of type III secretion system effectors. Journal of Bacteriology 189:8059-8072.

Kvitko, B., Bruckbauer, S., Prucha, J., McMillan, I., Breland, E., Lehman, S., Mladinich, K., Choi, K., Karkhoff-Schweizer, R., and Schweizer, H. 2012. A simple method for construction of pir+ Enterobacterial hosts for maintenance of R6K replicon plasmids. BMC research notes 5:1-7.

Lamovšek, J., Stare, B.G., Žerjav, M., and Urek, G. 2016. Soft rot of onion bulbs caused by *Burkholderia gladioli* pv. *alliicola* in Slovenia Journal of Plant Pathology 98:375.

Lee, C.J., Lee, J.T., Kwor, J., Kim, B., and Park, W. 2005. Occurrence of bacterial soft rot of onion plants caused by *Burkholderia gladioli* pv. *alliicola* in Korea. Australasian Plant Pathology 34:287-292.

Lee, J., Park, J., Kim, S., Park, I., and Seo, Y. 2016. Differential regulation of toxoflavin production and its role in the enhanced virulence of *Burkholderia gladioli*. Molecular Plant Pathology 17:65-76.

Lelis, T., Peng, J., Barphagha, I., Chen, R., and Ham, J. 2019. The virulence function and regulation of the metalloprotease gene *prtA* in the plant-pathogenic bacterium *Burkholderia glumae*. Molecular Plant-Microbe Interactions 32:841-852.

Liss, L. 1987. New M13 host: DH5αF′ competent cells. Focus 9:13.

López, C., Rholl, D., Trunck, L., and Schweizer, H. 2009. Versatile dual-technology system for markerless allele replacement in *Burkholderia pseudomallei*. Applied and environmental microbiology 75:6496-6503.

McClean, K.H., Winson, M.K., Fish, L., Taylor, A., Chhabra, S.R., Camara, M., Daykin, M., Lamb, J.H., Swift, S., and Bycroft, B.W. 1997. Quorum sensing and *Chromobacterium violaceum*: exploitation of violacein production and inhibition for the detection of N-acylhomoserine lactones. Microbiology 143:3703-3711.

Mijatović, J., Severns, P., Kemerait, R., Walcott, R., and Kvitko, B. 2021. Patterns of seed-to-seedling transmission of *Xanthomonas citri* pv. *malvacearum*, the causal agent of cotton bacterial blight. Phytopathology® 111:2176-2184.

Paudel, S., Dutta, B., and Kvitko, B. 2024a. Onion-pathogenic *Burkholderia* species: Role and regulation of characterized virulence determinants. Plant Pathology 73:2281-2297.

Paudel, S., Zhao, M., Stice, S.P., Dutta, B., and Kvitko, B.H. 2024b. Thiosulfinate tolerance gene clusters are common features of *Burkholderia* onion pathogens. Molecular Plant Microbe Interactions 37:507-519.

Schroeder, B., Humann, J., and Du Toit, L. 2012. Effects of postharvest onion curing parameters on the development of sour skin and slippery skin in storage. Plant Disease 96:1548-1555.

Seo, Y., Lim, J., Park, J., Kim, S., Lee, H., Cheong, H., Kim, S., Moon, J., and Hwang, I. 2015. Comparative genome analysis of rice-pathogenic *Burkholderia* provides insight into capacity to adapt to different environments and hosts. BMC genomics 16:1-11.

Shin, G., Dutta, B., and Kvitko, B.H. 2023. The Genetic requirements for HiVir-Mediated Onion Necrosis by *Pantoea ananatis*, a Necrotrophic Plant Pathogen. Molecular Plant-Microbe Interactions® 36:381-391.

Stice, S., Stumpf, S., Gitaitis, R., Kvitko, B., and Dutta, B. 2018. *Pantoea ananatis genetic* diversity analysis reveals limited genomic diversity as well as accessory genes correlated with onion pathogenicity. Frontiers in microbiology 9:184.

Stice, S., Thao, K., Khang, C., Baltrus, D., Dutta, B., and Kvitko, B. 2020. Thiosulfinate tolerance is a virulence strategy of an atypical bacterial pathogen of onion. Current Biology 30:3130-3140. e3136.

Suzuki, F., Sawada, H., and Matsuda, I. 1998. Molecular characterization of toxoflavin biosynthesis-related gene in *Pseudomonas* (*Burkholderia) glumae*. Japanese Journal of Phytopathology 64:276-281.

Swain, D., Yadav, S., Tyagi, I., Kumar, R., Kumar, R., Ghosh, S., Das, J., and Jha, G. 2017. A prophage tail-like protein is deployed by *Burkholderia* bacteria to feed on fungi. Nature communications 8:1-9.

Vandamme, P., Peeters, C., De Smet, B., Price, E.P., Sarovich, D., Henry, D., Hird, T.J., Zlosnik, J.A., Mayo, M., Warner, J., Baker, A., Currie, B., and Carlier, A. 2017. Comparative genomics of *Burkholderia singularis* sp. nov., a low G+C content, free-living bacterium that defies taxonomic dissection of the genus *Burkholderia*. Frontiers in Microbiology 8.

Wright, P., Clark, R., and Hale, C. 1993. A storage soft rot of New Zealand onions caused by *Pseudomonas gladioli* pv. *alliicola*. New Zealand Journal of Crop and Horticultural Science 21:225-227.

Yoneyama, K., Kono, Y., Yamaguchi, I., Horikoshi, M., and Hirooka, T. 1998. Toxoflavin is an essential factor for virulence of *Burkholderia glumae* causing rice seedling rot disease. Japanese Journal of Phytopathology 64:91-96.

Figures

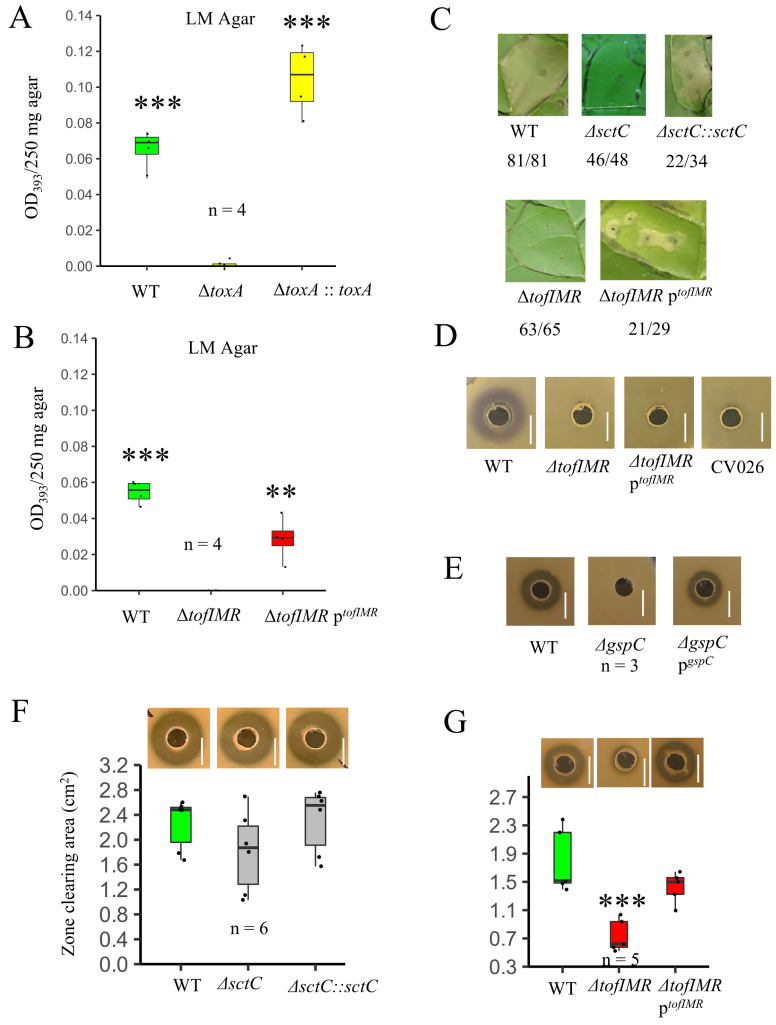

Figure 3.1: **Functional validation of select mutants generated in the study. A, B** Box plots illustrating the quantification of toxoflavin production by *toxA* mutant, *toxA* restoration clone in the top, quorum sensing *tofIMR* mutant and *tofIMR* plasmid complementation clone in the bottom all relative to the WT strain on LM agar media. n represents total number of observations. Statistical test performed using pairwise t-test and level of significance shown is in comparison to either *toxA* or *tofIMR* mutants. **C,** Tobacco cell death assay phenotype of different mutants compared to the WT strain. Representative image from one of the experimental repeats

is shown. The ratio of infiltrated spots displaying the representative image phenotype to the total number of infiltrated spots is shown at the bottom of each strain. **D,** *Chromobacterium* AHL reporter assay showing the purple violacein phenotype of (left to right) WT, Δ*tofIMR*, *tofIMR* complementation clone and CV026 negative control. **E,** Casein protease plate assay showing the clearing zone phenotype of tested (from left to right) WT, T2SS mutant *gspC* and the *gspC* plasmid complementation clone. n = total number of observations. Representative image from experimental repeats is shown for all the *in vitro*/*in vivo* assays. Box plot image with quantification of zone clearing area from the protease plate assay for **F,** WT, T3SS mutant *sctC* and *sctC* restoration clone and **G,** WT, QS mutant *tofIMR* and *tofIMR* complementation clone. n represents a total of observation. Representative image from experimental repeats presented at the top of corresponding box plot. The test of significance was performed using pairwise t-test function in RStudio. Level of significance: 0 '***' 0.001'**' 0.01.

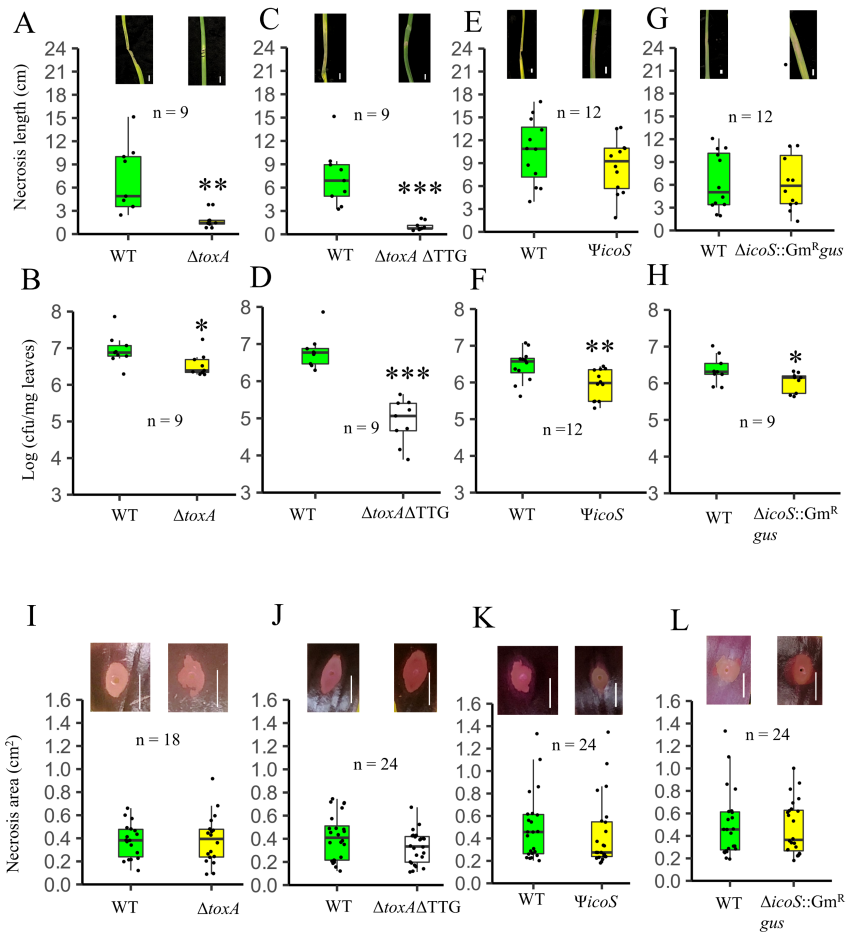

Figure 3.2: The phytotoxin toxoflavin in Bga strain 20GA0385 contributes to foliar necrosis and bacterial populations. Box plot showing onion foliar necrosis length and *in planta* bacterial populations of Bga WT 20GA0385 strain compared to **A**, **B,** *toxA*, **C**, **D,** Δ*toxA*ΔTTG **E**, **F,** Ψ*icoS* **G**, **H,** Δ*icoS*::Gm^R*gus* mutants. Box plot showing RSN area of Bga WT 20GA0385 strain compared to **I** Δ*toxA*, **J,** Δ*toxA*ΔTTG, **K,** Ψ*icoS*, **L,** Δ*icoS*::Gm^R*gus* mutants. A representative

image of infected leaves or scales inoculated with treatments at 3 dpi is presented above the box plot. n is the total number of observations across the experimental repeats. The test of significance between the necrosis length/area and bacterial populations was performed using pairwise t-test function in RStudio. Level of significance: 0 '***' 0.001 '**' 0.01 '*' 0.05. Scale: 1 cm.

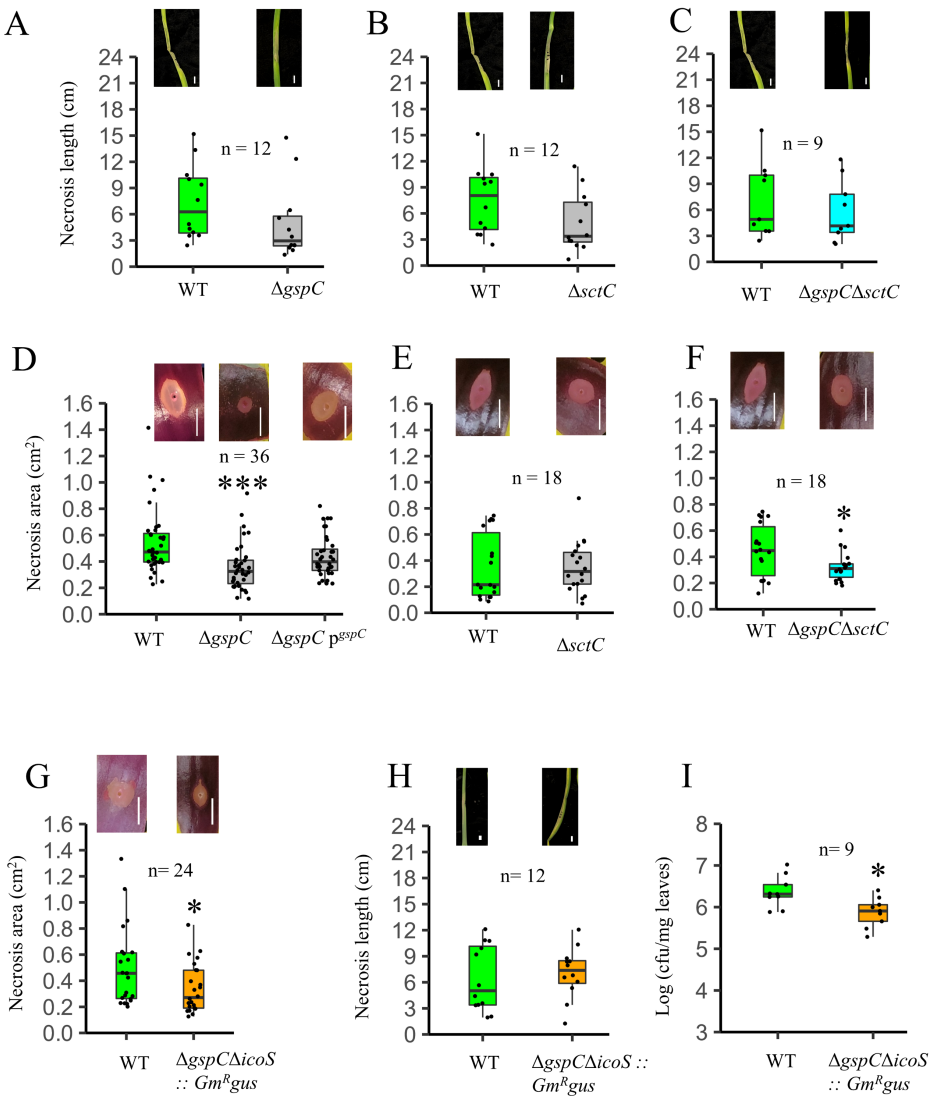

Figure 3.3: The T2SS contributes to RSN area but is not required for foliar symptoms. Box plot showing onion foliar necrosis length of Bga WT 20GA0385 strain compared to **A,** T2SS Δ*gspC*, **B,** T3SS Δ*sctC*, and **C,** Δ*gspC*Δ*sctC* mutants. Box plot showing RSN area of Bga WT 20GA0385 strain compared to **D,** T2SS Δ*gspC* and *gspC* plasmid complementation clone, **E,** T3SS Δ*sctC*, **F,** Δ*gspC* Δ*sctC* and **G,** Δ*gspC*Δ*icoS*::Gm^R*gus* mutants. Box plot showing the comparison of **H,** necrosis length and **I,** leaf bacterial populations between WT and Δ*gspC* Δ*icoS*::Gm^R*gus* mutant. A representative image of infected leaves or scales inoculated with

treatments at 3 dpi is presented above the box plot. n is the total number of observations across the experimental repeats. The test of significance between the necrosis length/area and bacterial populations was performed using pairwise t-test function in RStudio. Level of significance: 0 '***' 0.001 '**' 0.01 '*' 0.05. Scale: 1 cm.

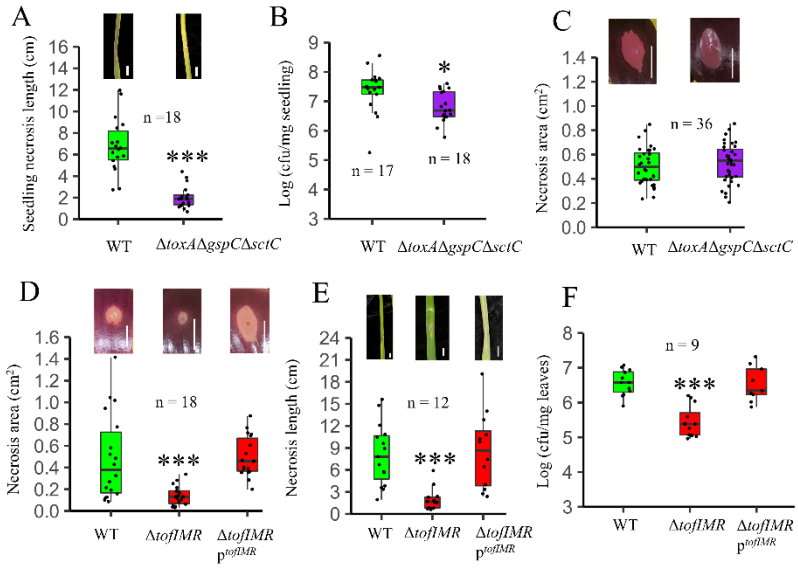

Figure 3.4: Box plot showing the comparison of **A,** seedling lesion length, **B,** seedling bacterial populations and **C,** RSN area between the WT and the Δ*toxA*Δ*gspC*Δ*sctC* triple mutant derivative. A representative image of inoculated seedling/scale at 3 dpi is shown above the box plot. **D-F**, **The *tofIMR* QS system regulates virulence phenotype of Bga strain 20GA0385**.Box plot showing the comparison of **D,** RSN area, **E,** foliar necrosis length, and **F,** foliar in planta populations between the WT, QS mutant *tofIMR* and the *tofIMR* plasmid complementation clone. n is the total number of inoculated samples across the experimental repeats. The test of significance between the necrosis length/area and bacterial populations was performed using pairwise t-test function in Rstudio. Level of significance: 0 '***' 0.001 '**' 0.01 '*' 0.05. Scale: 1 cm.

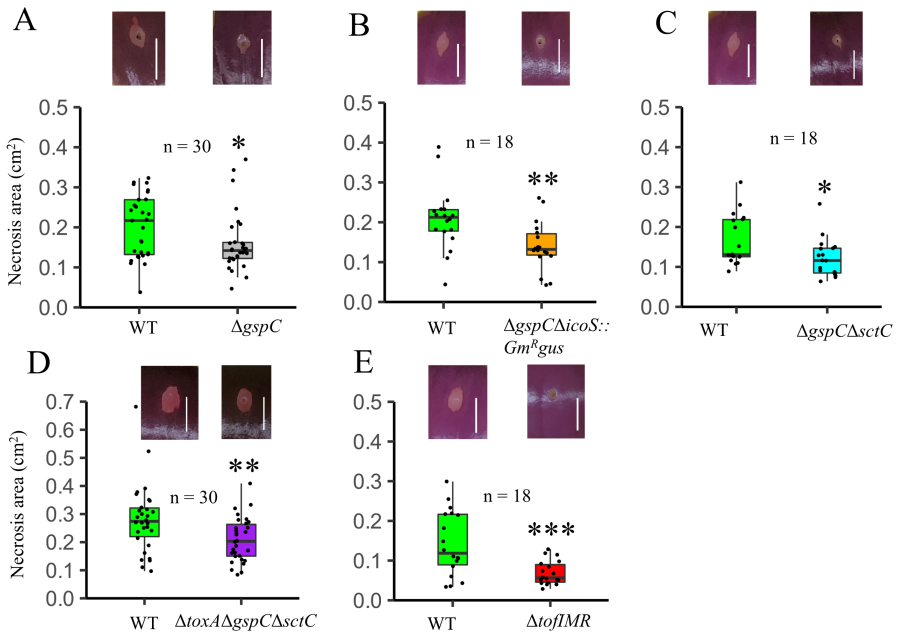

Figure 3.5: The virulence role of T2SS in onion scale is maintained in 100-fold diluted starting bacterial concentration. Box plot showing the RSN area of WT strain at 3 dpi compared to A, Δ*gspC*, B, Δ*gspC* ΔicoS::Gm^R*gus*, C, Δ*gspC*Δ*sctC*, D, Δ*toxA*Δ*gspC*Δ*sctC*, E, Δ*tofIMR* mutants. A representative image of infected leaves or scales inoculated with treatments at 3 dpi is presented above the box plot. n is the total number of observations across the experimental repeats. The test of significance between the necrosis length/area and bacterial populations was performed using pairwise t-test function in RStudio. Level of significance: 0 '***' 0.001 '**' 0.01 '*' 0.05. Scale: 1 cm.

Supplemental Tables

Supplementary Table S3.1: Amino acid identity % between the putative virulence factors/regulators in *B. glumae* strain BGR1 and Bga strain 20GA0385. Data generated using Clinker CAGECAT Web server.

Putative virulence factors	% aa identity
Toxoflavin (biosynthesis cluster) (*B. glumae* BGR1 vs Bga 20GA0385)	
ToxA	96
ToxB	98
ToxC	97
ToxD	96
ToxE	90
Type II secretion system (*B. glumae* BGR1 vs Bga 20GA0385)	
GspD	86

GspE	94
GspF	96
GspC	90
GspG	97
GspH	88
GspI	81
GspJ	76
GspK	78
GspL	84
GspM	83
GspN	81
Type III secretion system (*B. glumae* BGR1 vs Bga 20GA0385)	
SctS	94
SctR	97
SctQ	70
HpaP/SctP	75
SctV	91
SctU	90
SctG	88
HrpB2	91
SctJ	89
HrpB4	84
SctL	71
SctN	94
HrpB7	68
SctT	84
AraC	93
SctC	85
HrpW putative effector	59
Putative Response regulator	85
Icosalide (Bga 20GA0385 vs *B. gladioli* HKI0739)	
IcoS	97
Quorum sensing (*B. glumae* BGR1 vs Bga 20GA0385)	
TofI	87
TofM	80
TofR	92

Supplementary Table S3.2: *E. coli* genotype and plasmids used in the study.

E.coli strain	Purpose	Reference
DH5	General plasmid cloning strain	(Liss, 1987)
RHO5	*pir116*, DAP-dependent conjugation strain	(Kvitko et al., 2012a)

DB3.1	CcdB resistant gateway cassette maintenance strain	Invitrogen
RHO3pTNS3	DAP dependent conjugation strain SM10 derivative with Tn7 transposase helper plasmid (Amp^R)	(López et al., 2009a)
Mah1	DH5	(Kvitko et al., 2012a)
Plasmid vector		
pDONR1K18ms	Gateway compatible sucrose counter selection allelic exchange vector, Km^R, Cm^R	(Mijatović et al., 2021)
pR6KT2G	Gateway compatible R6K-based suicide vector for allelic exchange, *gus*, *sacB*, Gm^R, Cm^R	(Stice et al., 2020)
pDONR221	Gateway BP clonase compatible cloning vector	Invitrogen
pBBR1MCS-2	pBBR1 origin based mobilizable shuttle and expression vector with blue/white selection function. Km^R	(Kovach et al., 1994)
pBBR1MCS-2GW	Gateway BP compatible derivative of pBBR1MCS-2, Cm^R, Km^R	This study
pCPP5212	R6K- replicon based plasmid source for FRT-flanked Gm^R *gus* cassette for marked deletion, Gm^R, *gus*, Amp^R	(Kvitko et al., 2007)

Supplementary Table S3.3: Primers/Gene fragments used in this study for allelic exchange, sequencing, and PCR.

Name	Sequence (5' to 3')	Application
attB1	GGGGACAAGTTTGTACAAAAAAGC AGGCTTA	For Gateway recombination
attB2	GGGGACCACTTTGTACAAGAAAGC TGGGTA	
Soe.ar	TAACTCGAGTGCCTAGGTATGGTAC CT Underlined XhoI, AvrII, and KpnI sites	Overlapping sequence for the overlap extension PCR/ Gibson assembly
Soe.bf	AGGTACCATACCTAGGCACTCGAGT TA Underlined KpnI, AvrII, and XhoI sites	
pBBR1GW-F	**AGC GGC CGC CAC CGC GGT** TAA GCC GAA TTC TGC AGA	Primers to amplify the gateway cassette from the plasmid pR6KT2G. Underlined sequences are the Gibson overhangs upstream and downstream of XbaI restriction site in pBBR1MCS-2 plasmid.
pBBR1GW-R	**CTA GAA CTA GTG GAT CCC** TTC CTA TTC CGA AGT TCC	

Bglad-toxA-attB sites	attB1-CP023522.1,2488976 – 2489375bp-CCTAGG-CP023522.1, 2487856-2488255bp-attB2	Deletion construct for *toxA* synthesized from Twist Biosciences. Underlined is the AvrII restriction site
Bglad-gspC-attB sites	attB1- CP023522.1, 2924636-2925034bp-CCTAGG - CP023522.1, 2925429-2925828bp-attB2	Deletion construct for *gspC* gene synthesized from Twist Biosciences. Underlined is the AvrII restriction site
pCPP5242sacIF	TAATGAGCTCGCCAAGCTTGCATGCAGATT	Primers with SacI site (underlined) overhang to amplify FRTSp^R cassette from pCPP5242
pCPP5242sacIR	TAATGAGCTCACACAGGAACACTTAACGGCT	
tofIMRflankAF2	CG CGA TCC TGT GCC TGC CGG A	To amplify deletion flank upstream of *tofIMR* deletion construct for SOEing PCR
tofIMRflankAR1	AAG CCG CCT GAC CCG GCG AGT	
tofIMRflankBF1	AGA CGC CCT GAG GAC CTG AT	To amplify deletion flank downstream of *tofIMR* deletion construct for SOEing PCR
tofIMRflankBR2	CG GCG TGC TGA CCG GCA A	
tofIMRgenoF3	AAC TGA TCC CGC TCG TAT T	Amplification primers to detect the presence of *tofIMR* gene region in the allelic exchange plasmid pDONR1K18-ms
tofIMRgenoR3	ACG CAA TCT CGA AAT TGA ACC A	
imrcomplnF	GGG GAC AAG TTT GTA CAA AAA AGC AGG CTT AAA GGG TTG GTG CGG CGC GG	*tofIMR* mutant complementation primer
imrcomplnR	GGG GAC CAC TTT GTA CAA GAA AGC TGG GTA TCT GCC GGA TCA GGG CAT CA	
GmGUSF	AGA AAG GGA TCT TCA CTC GC	Primers to genotype and sequence the *tofIMR* mutant
GmGUSR	GTG TTC CGC TTC CTT TAG CA	
GmGUSR2	TTA CGA ACC GAA CAG GCT TA	
IMRgenoF	ATC GTA TTC ATC GAC GGC GA	
IMRgenoR	TTC AGT TGC GGC GTC GCG AT	
sctCflankAF	AG GAT CAC GTC TAC TGG CGC T	To amplify deletion flank upstream of *sctC* deletion construct
sctCflankAR	GGA TGT CGA TTC GGG AAG AT	
sctCflankBF	TTT CGA TCG GTG CAG CCC TT	To amplify deletion flank downstream of *sctC* deletion construct
sctCflankBR2	TCG AGG CCT TCC TTG CGC A	
sctCgenoF	GAA CTG GTG ATC GCG CTG	Genotyping primers to confirm the *sctC* mutant
sctCgenoR	TCC TTC ACT TCC TTG GCG AG	
sctCseq	CCA GCT CGA GTA TCT CTA CT	Primer to sequence the *sctC* mutant

toxAgenoF	TGG ATA TTT GCG TCG CAT GCT T	Primers to genotype the *toxA* mutant
toxAgenoR	CTT CCT GGC GCA GAT AGA G	
sctCresF	GGGGACCACT TTGTACAAGA AAGCTGGGTA ATCTTCAGGG CCTGGGTGA	Primers with *attB* sites to amplify the *sctC* restoration clone to generate the restoration construct.
sctCresR	GGGGACAAGT TTGTACAAAA AAGCAGGCTT AAGTGCCTGC GCGAGGATT	
toxAcomplnF2	GGG GAC AAG TTT GTA CAA AAA AGC AGG CTT ATC CGA ATT GAA TTG CCG A	Primers to amplify *toxA* upstream and downstream region for chromosomal restoration
toxAcomplnR2	GGG GAC CAC TTT GTA CAA GAA AGC TGG GTA CTT CCT GGC GCA GAT AGA G	
toxAgenocomplnF	TTC CGC CGC GTC CGC ATT	Genotyping primers to confirm the chromosomal restoration of *toxA* region in *toxA* mutant background
toxAgenocomplnR	ATA CGC GTC GAG CTT GTT GT	
gspCgenoF	TGG TGA ACG TGT TCG CCA GCA	Genotyping primers to confirm the *gspC* mutant
gspCgenoR	TTC CAG TTG TTC GGC ACC GGA T	
gspCcomplnF	GGG GAC AAG TTT GTA CAA AAA AGC AGG CTT AAG TGA AAC CTC TCT TTC AA	Primers to generate the *gspC* complementation construct with gateway overhangs.
gspCcomplnR	GGG GAC CAC TTT GTA CAA GAA AGC TGG GTA TTG CCG GAA TGA ACG TCA	
Bglad-ico1-attB sites	AATTGAAATTG AACGGCGATTATTTTCACCATTACTG AAATTAAAATCAAAGGTG CCATTTATTATTGATGGTGCATGATTT CAAATGTATCGGAATGC AAGGGGTAATTTCCTTGTCATCGTC GTGATACAGTATGTTTCAA ATCTTTCCGTAGACGGAATATTCAAT CCAGGTGAATCGAAAAA CCGAGCCGGGCTCTCATGCCCGGCT CGGTTGCTCCTGTCTGGG CAATCGGCTATATCCGCCGGCGAGT TGCCGTGAAATCGGCAGG AATCAGCCCGGTTTTTCGATTTATCA AACGCTCGATGATATTGC ATGGGCAACCGCCAATAATTCCCGC GCTGCCGTGGCGCACTGC CCGCGCTAAATAATGACGAGGATAA TTTTGAACGCCAAA<u>taacct aggtaataa</u>CATGAAATTCTGGAGCTCA	Icosalide triple stop codon interruption construct synthesized from Twist Biosciences. Underlined is the AvrII restriction site flanked by stop codons.

	CCGCGGCGCAATTGGAAA TGTGGTTTTCGCAGCAACGCGAGCC CGACAATCCCTTGTTCGACA GTCGTGCCTATGTGGATATCGGGGG GGCGATCCATTACCCGGCT TTCGAGGCGGCGGTGCGCCGTTTCA TCGAGGAAGCCCGGATCCT GCATTTCCGTTTCCTTGAAACATCGT CGGGGCCGGTTCAATTCGA AGCCGGCGGAGATGCCTTCGAGCC GACGTTCATCGACGTCTCGC GCGAGGACGATCCATTCGCGGCTTG CTGGAATGCGATGCAGGC CGAATCGAATCGTCCCTACGATGTC CTCTCCGGCAGGCTGTTCAG TCAAACGCTGTTCAAGCTGGGCGA CCAGCGGCATGTCTGGTACC AGCGCTAT	
icogenoF	ACT CCG TGA TGT TCA AAT T	Primers to amplify the icosalide stop codon interruption mutant
icogenoR	ACC GCG CAT CTG CCT GAT	
Bglad-ico2-attB sites	CGTTCGCCGACGTGGTGGCTGCCGT CAATCC GCCGCGCGCGTCTTCCCACGATCCG ATCTTC CAGGTGTTTTGCCAGTTCCAGCAAG GCCCTG GAAAGACTCGCGAGACGATCGCCG ACATGAC GATCGAAGCCATTCCGCGCACGCGC ATGGCG CGAGGTGCCGATCTCGCCGTCGTGT TCCTGGA CGCGGGCGAATATCTCAATGCTGAC GTTTCGTA CAGCGCCGATCTGTTCGACGCCGAG AGTATCG ATGCGCTGATCGAACTGTTCCTGCG CTTCCTGG CGGAAAGCGTGCAACGGCCCGATG CGGTGGT GGACGAGCTTTGGGATGCCGGTGTC GCCAGTG CGAGGGCCGCGGCTTCGGGCCCGG ATGTCTC GCGTCTGATCGACCGCCCGGGcctagg	Construct synthesized from Twist biosciences to generate FRTGm^{R}*gus* insertion mutant in the icosalide ORF. Underlined is the

	CAGCC CGGCGGGAACCTGGTACGCGCTCTC GCCGGC GCAGCAGGCGGTCTGGCTTCAGGA GCAGGCG GCCCGGCCGGGGACGTCGTTCTTCT CGGTTGC GGCCATGCGCTGCGCGCCGGAGGT CGATCGA ATGCGTCTGGTTGCTGCCTCGCGCG CTTTGATT GTTCAAAACCAGGCATTCTGGATTC AAGTGTCCG ACGCTGGCCTGCAATGCGAGGCGTC CACGCCG ACGACACGCTTCCAGCATTTCGTCG AACCAACGA CGATGACCGATGAAGCGATGCAACG GGCGGTGAT CGAGTGGCACGAGAAGCTCGACGA GGACCCGCG CGACAAGTCCGGTGCCGTCGCCGT GTTCGACTCT CCTGGTAGCGTGCTGGTGGCGTTGC GTTCGCCTCAT	
Ico2genoF	ATC GGC ACG GTG GCC GAA	Primers to genotype the icosalide FRT Gm^R*gus* insertion mutant
Ico2genoR	TGG CGA CAA CGA GAG CTT	

Supplementary Table S3.4: *Burkholderia* strains and mutants generated in the study.

Strain ID	Genotype	Description
20GA385	WT strain	Isolated from onion, Georgia Rf^R
BgdUGA1	20GA0385 Δ*toxA*	toxoflavin biosynthesis gene *toxA* deletion mutant
BgdUGA10	20GA0385 Δ*toxA* :: *toxA*	toxoflavin chromosomal restoration clone generated using allelic exchange on *toxA* mutant background
BgdUGA18	20GA0385 Δ*toxA*ΔTTG	toxoflavin deletion mutant generated in the thiosulfinate tolerance gene clusters mutant background
BgdUGA3	20GA0385 Δ*gspC*	Type II secretion system *gspC* unmarked deletion mutant

BgdUGA17	20GA0385 Δ*gspC* :: pBBR1MCS-2 *gspC*	plasmid based complementation clone of *gspC* mutant
BgdUGA6	20GA0385 Δ*sctC*	Type III secretion system *sctC* unmarked deletion mutant
BgdUGA14	20GA0385 Δ*sctC* :: *sctC*	*sctC* chromosomal restoration clone generated using allelic exchange on *sctC* mutant background
BgdUGA12	20GA0385 Δ*gspC* Δ *sctC*	T2SS *gspC* mutant generated on the T3SS *sctC* mutant background
BgdUGA29	20GA0385 Δ*toxA* Δ*gspC* Δ*sctC*	Toxoflavin *toxA* mutant generated on BgdUGA12 mutant background
BgdUGA25	20GA0385 Ψ*icoS*	Putative icosalide triple stop codon interruption mutant generated using allelic exchange
BgdUGA23	20GA0385 Δ*icoS*::Gm^R*gus*	Putative icosalide interruption mutant generated by introducing Gm^R*gus* cassette from plasmid pCPP5212 using allelic exchange
BgdUGA21	20GA0385 Δ*gspC* *icoS*::Gm^R*gus*	T2SS *gspC* mutant generated on BgdUGA23 mutant background
BgdUGA5	20GA0385 Δ*tofIMR*	Quorum sensing *tofIMR* marked deletion mutant generated by adding Gm^R*gus* cassette in between the deletion flanks
BgdUGA11	20GA0385 pBBR1MCS-2 *tofIMR*	Plasmid based complementation clone of *tofIMR* mutant

Supplemental Figures

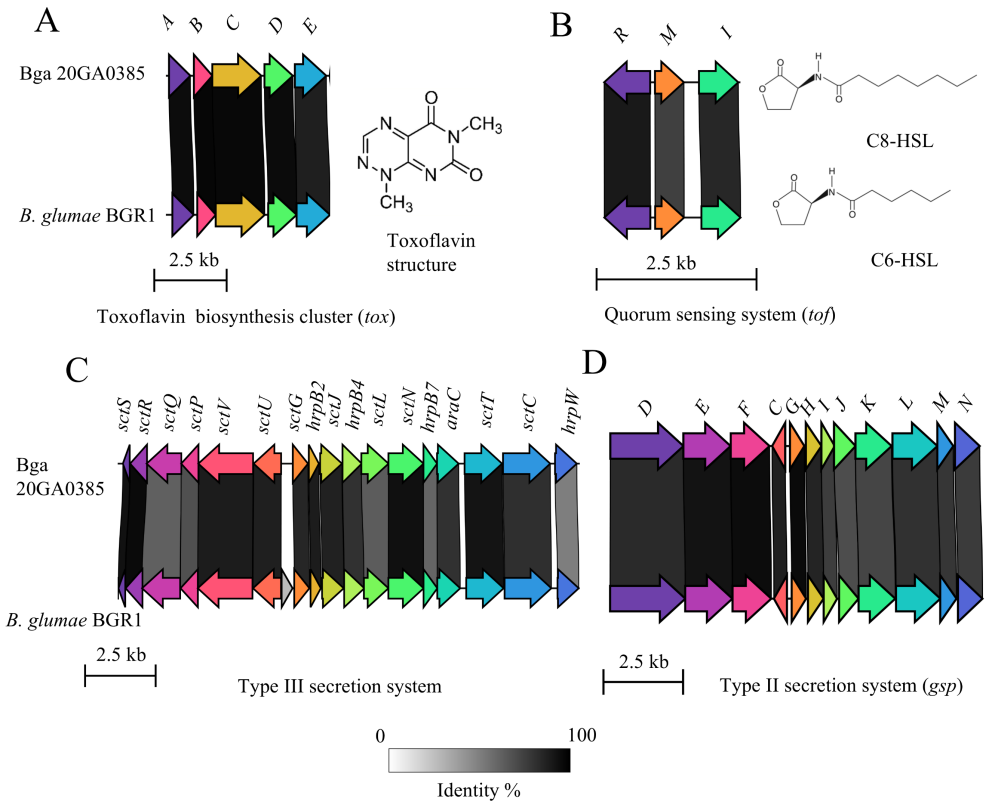

Supplementary Figure S3.1: Putative virulence factors and regulator are conserved in *B. gladioli* strain 20GA0385 and *B. glumae* strain BGR1. Clinker gene synteny arrow diagram showing the gene organization and synteny of putative virulence factors/regulator - **A,** toxoflavin biosynthesis gene cluster, **B,** quorum sensing *tofIMR* system**, C**, type II secretion system**,** and **D,** type III secretion system**.** Genes are color coded based on predicted function. The percentage of amino acid identity between the linked genes is shown in gradient scale. The annotation of genes in the cluster is used from CAGECAT web server platform. Image generated using Clinker CAGECAT web server. Toxoflavin and homo serine lactones structures used from the internet.

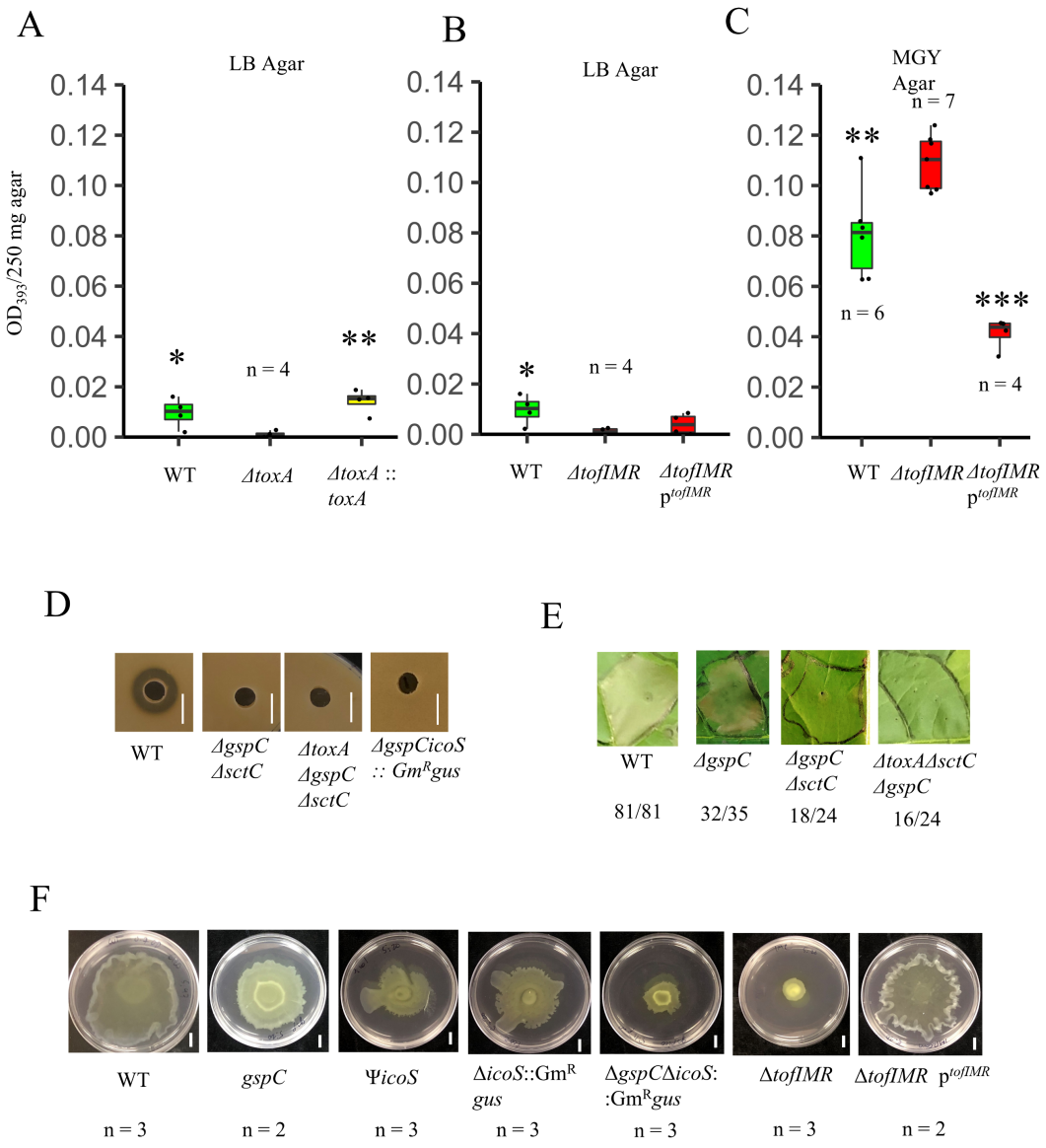

Supplementary Figure S3.2: Functional validation of select mutants utilized in the study. Box plot illustrating the quantification of toxoflavin production by **A**, WT, *toxA* mutant, *toxA* restoration clone in LB agar **B**, WT, quorum sensing *tofIMR* mutant and *tofIMR* plasmid complementation clone on LB agar media and **C**, WT, quorum sensing *tofIMR* mutant and *tofIMR* plasmid complementation clone on MGY agar media. n represents total number of observations. Statistical test performed using pairwise t-test and level of significance shown is in comparison to either *toxA* or *tofIMR* mutants. **D,** Casein protease plate assay showing the clearing zone phenotype of tested (from left to right) WT, Δ*gspC*Δ*sctC*, Δ*toxA*Δ*gspC*Δ*sctC* and Δ*gspC*Δ*icoS*::Gm^R*gus*. n = total number of observations. Representative image from experimental repeats is shown. **E**, Tobacco cell death assay phenotype of different mutants compared to the WT strain. Representative image from one of the experimental repeats is shown. The ratio of infiltrated spots displaying the representative image phenotype to the total number of infiltrated spots is shown at the bottom of each strain. **F,** swarming phenotype of the tested

mutants compared to the WT strain. Image taken after 21 hours. Representative image from one of the experimental repeats is shown. n is the number of independent experiments. Scale: 1 cm

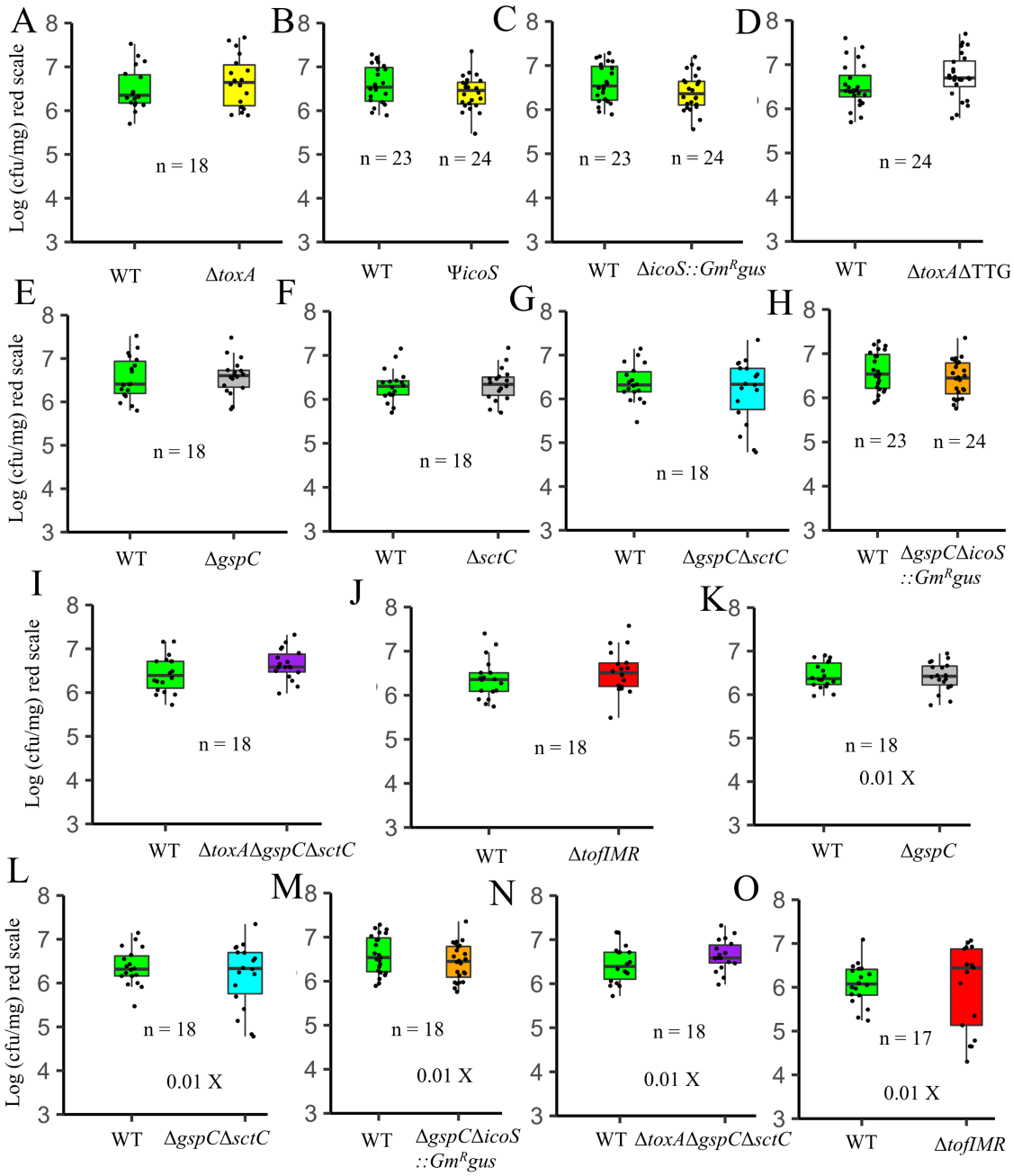

Supplementary Figure S3.3: Box plot showing the red scale in planta population count of WT strain compared to **A,** Δ*toxA* **B,** Ψ*icoS*, **C,** Δ*icoS*::Gm^R*gus*, **D,** Δ*toxA*ΔTTG, **E,** Δ*gspC* **F,** Δ*sctC* **G,** Δ*gspC*Δ*sctC*, **H,** Δ*gspC*Δ*icoS*::Gm^R*gus*, **I**, Δ*toxA*Δ*gspC*Δ*sctC*, **J,** Δ*tofIMR*, **K,** Δ*gspC*, **L,** Δ*gspC*Δ*sctC*, **M,** Δ*gspC*Δ*icoS*::Gm^R*gus* **N,** Δ*toxA*Δ*gspC*Δ*sctC*, and Δ*tofIMR* mutants. n is the total number of observations. 100-fold label in the **Figures K-O** represents that the treatments were compared at 100-fold diluted starting bacterial concentration. The test of significance

between the log fold bacterial populations was performed using pairwise t-test function in RStudio.

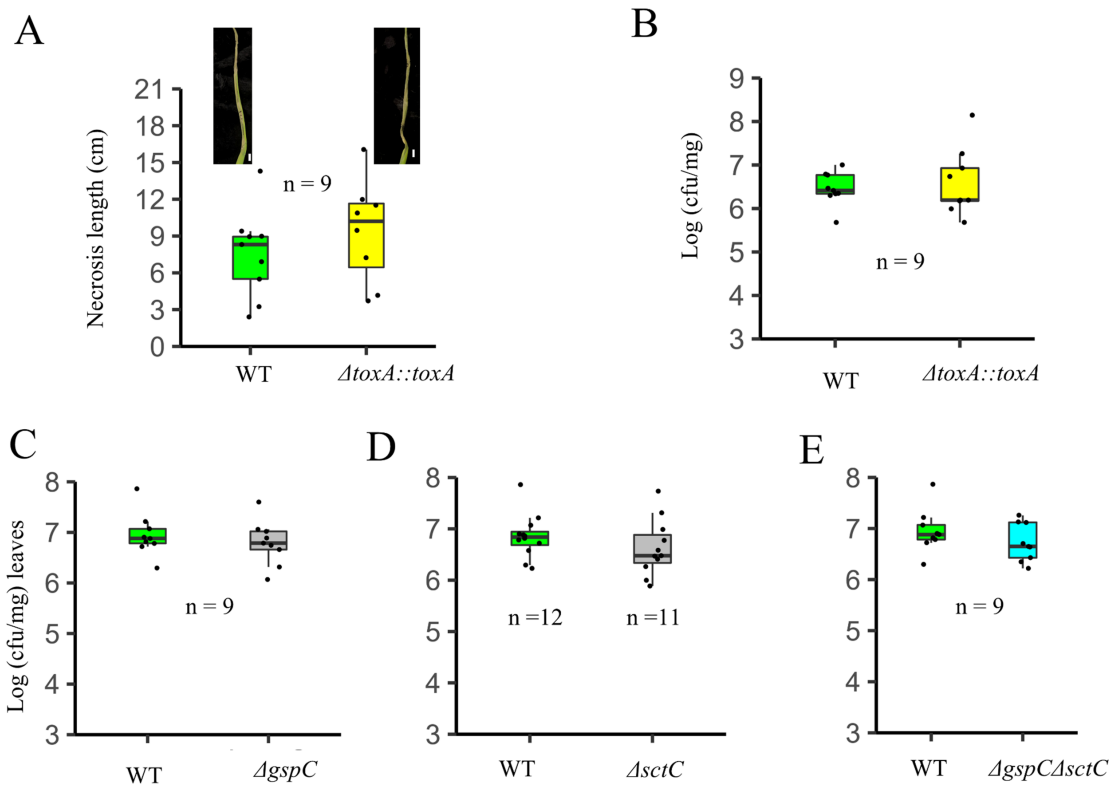

Supplementary Figure S3.4: Box plot showing the comparison of **A,** foliar necrosis length and **B,** in planta bacterial populations between the WT and *toxA* restoration clone. Box plot showing the comparison of in planta foliar bacterial populations of WT compared to **C,** Δ*gspC*, **D,** Δ*sctC*, and **E,** Δ*gspC*Δ*sctC***.** A representative image of infected leaves or scales inoculated with treatments at 3 dpi is presented above the box plot where applicable. n is the total number of observations across the experimental repeats.

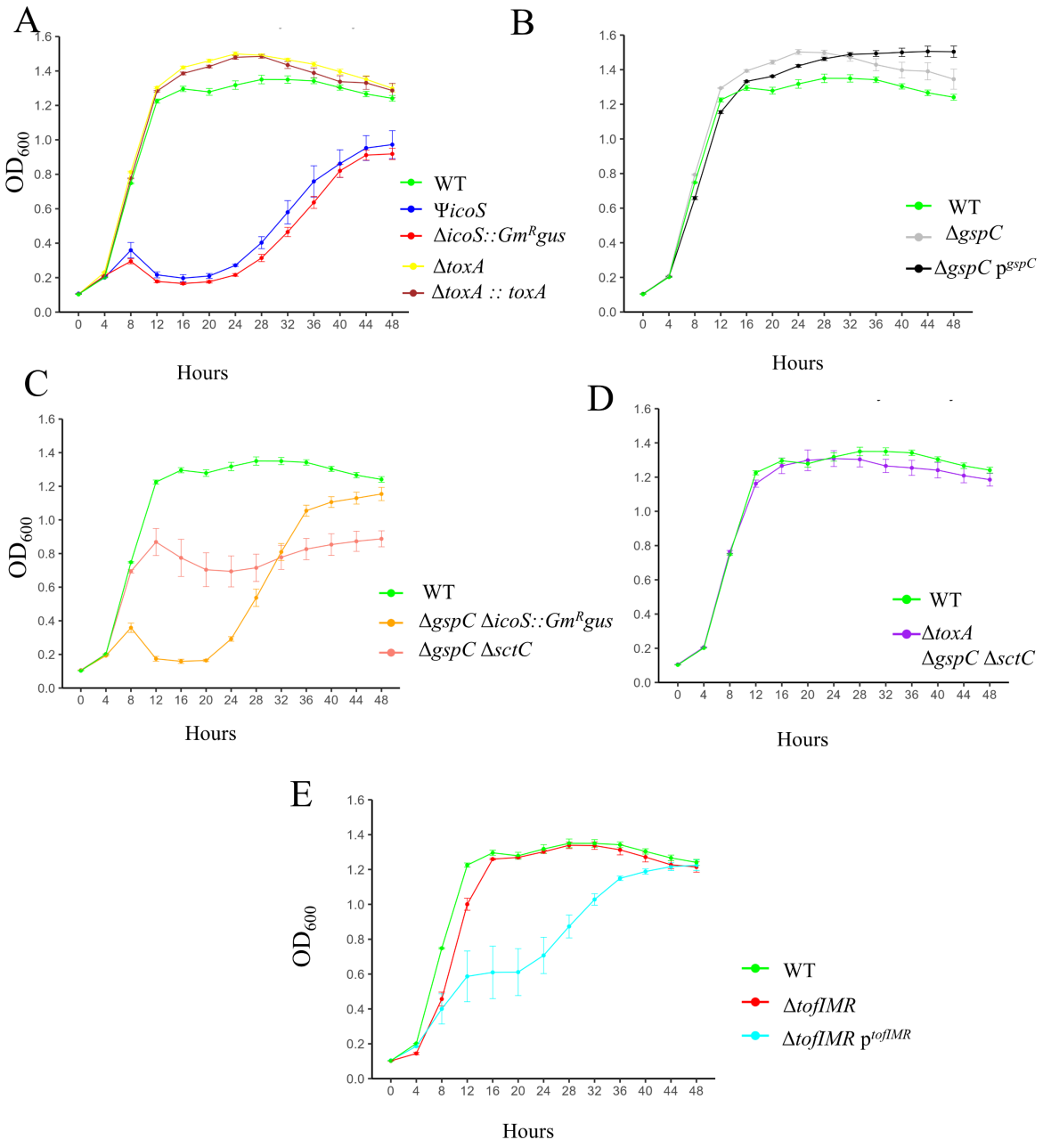

Supplementary Figure S3.5: Growth comparison of Bga 20GA0385 and its mutants in LB medium over 48 hours. Strains tested include **A**, secondary metabolite mutants, **B**, secretion system mutants, **C**, double mutants, **D**, triple mutants, and **E**, regulatory mutants generated in this study. Each data point represents the mean OD_{600} values from at least 12 observations across two independent experimental repeats. Error bars indicate the ± standard error. The color coding for the strains under comparison is detailed in the legend accompanying each figure.

CHAPTER 4

INVESTIGATING THE INTERACTIONS BETWEEN THIOSULFINATES AND *BURKHOLDERIA GLADIOLI* PV. *ALLIICOLA* IN ONION TISSUES[1]

[1]Paudel S, Franco Y, and Kvitko BH. To be submitted to *PLOS ONE*.

Abstract

Burkholderia gladioli pv. *alliicola* (Bga) is a common foliar, bulb, and storage pathogen of onion. Onion tissues produce bactericidal thiosulfinates upon cellular damage, which disrupt critical enzymatic functions and cellular homeostasis. The thiosulfinate tolerance gene (TTG) clusters in *Burkholderia* onion pathogens confer tolerance to the thiosulfinate allicin *in vitro* and promote growth in onion juice. The onion foliar necrosis and bacterial population was linked to the Bga TTG cluster, as demonstrated in a previous study, but unexpectedly, it had no impact on scale tissue populations. Using a thiosulfinate-inducible *altR* promoter reporter Tn*7* strain and exogenous necrosis-inducing pantaphos treatment, we further investigated the interactions of Bga with thiosulfinates. In onion leaves, the *altR* reporter de-repression corresponded with Bga induced necrosis progression consistent with necrosis-associated thiosulfinate release and with TTG contributing to Bga populations in leaves. In scales, as Bga induced necrosis advanced, *altR* promoter Lux reporter signal diminished, however the Lux signal coincided with the onset of pantaphos induced necrosis symptoms. The sensitivity of Bga TTG mutant during pantaphos-indcued necrosis in the scale tissue was demonstrated by its reduced recovery compared to the WT strain. Furthermore, preconditioning TTG mutants in scale tissue did not improve survival in onion juice, reinforcing that Bga resistance is not due to adaptive exclusion of thiosulfinates in the scale tissue. The partial rescue of TTG mutant phenotype by Bga WT strain in the zone of inhibition co-inoculation assay is consistent with the possible extracellular detoxification of thiosulfinates by Bga. These findings indicate that Bga most likely does not use exclusion-based methods to prevent thiosulfinates from entering bacterial cells but may instead actively externally detoxify thus effectively preventing exposure at concentrations of thiosulfinates produced via native disease-associated tissue necrosis.

Introduction

As a widely cultivated vegetable, onion (*Allium cepa* L.) is crucial to the agricultural economy of the state of Georgia and the United States as a whole. More than 12 bacterial diseases pose serious threats to the $1 billion (USD) onion industry in the US (Schwartz et al., 2015; Belo et al., 2023). Since onion bulbs can be stored for extended periods, bacterial diseases may occur under storage conditions, rendering the bulbs unmarketable (Belo et al., 2023). Among the bacterial diseases, slippery skin of onion, caused by bacterial pathogen *Burkholderia gladioli* pv. *alliicola* (Bga) is commonly observed in field and storage conditions. Bga has also been reported to produce onion foliar symptoms under field and greenhouse conditions (Lee et al., 2005; Paudel et al., 2024a).

Thiosulfinates are reactive organosulfur compounds commonly found in *Allium* species, produced in response to tissue damage that can be caused by wounding, herbivory, or disease-associated necrosis.These compounds are produced upon tissue damage through a series of chemical and enzymatic reactions leading to distinctive flavors and aromas of onions while also serving as volatile irritants and antimicrobial compounds (Rose et al., 2005; Eady et al., 2008; Leontiev et al., 2018). In onion, cellular damage enables the mixing and reaction of preformed predominant non-volatile precursor substrate isoalliin and the carbon-sulfur lyase enzyme alliinase, which are stored in separate sub-cellular compartments (Lancaster and Collin, 1981; Van Damme et al., 1992; Hughes et al., 2005). Thiosulfinates are volatile antimicrobial compounds that inactivate critical enzymes and deplete the reduced glutathione pool making cells susceptible to oxidative stress (Yamazaki et al., 2010; Müller et al., 2016; Reiter et al., 2020).

Thiosulfinate tolerance gene clusters are a set of redox-associated genes identified in multiple plant pathogenic bacterial genera. In onion pathogenic *P. ananatis* and multiple *Burkholderia* species, the cluster contributes to allicin tolerance *in vitro* and growth in onion juice (Stice et al., 2020; Paudel et al., 2024b). A chemical arms race model has been proposed between the necrotrophic pathogen *P. ananatis* and onion's thiosulfinate based defense response, wherein thiosulfinates are produced in response to *P. ananatis* induced necrosis. As a counter-defense strategy, *P. ananatis* utilizes the TTG cluster to withstand the toxic thiol stress induced by thiosulfinates (Stice et al., 2020).

Our previous study has shown that TTG clusters are also widely distributed among distantly related onion-pathogenic *Burkholderia* species. The TTG cluster in *B. cepacia, B. orbicola*, and *B. gladioli* confers tolerance to the thiosulfinate allicin in *in vitro* sensitivity assays. Surprisingly, and unlike what has been observed in *P. ananatis*, the TTG cluster in all three major onion pathogenic species *B. cepacia*, Bga, and *B. orbicola* didn't contribute to bacterial populations on the onion scale (Paudel et al., 2024b). This is unexpected given that the TTG mutants were impaired in their capacity to grow in onion juice and the Bga TTG genes made a clear contribution to bacterial populations in leaves with a lower reported thiosulfinate production capacity than scale and bulb tissue (Cho et al., 2024). This suggests the existence of other tissue-specific resistance mechanisms against thiosulfinates.

In this study, we hypothesize Bga might either suppress the production of thiosulfinates, inactivate/detoxify thiosulfinates in onion scale tissue or exclude uptake of these compounds (Figure 4.1). To assess thiosulfinate release during infection, we utilized the predicted transcriptional regulation of the *altR* gene within the TTG cluster by incorporating the *altR* promoter region into *lux* reporter construct. Additionally, Pantaphos-containing cell-free spent

medium was used as an external necrosis-inducing factor to examine Bga's response to cell death and thiosulfinates production during scale symptoms production (Shin et al., 2023). The *in vitro* Zone of Inhibition (ZOI) and *in planta* foliar coinfection assays were performed to test the potential involvement of Bga in extracellular detoxification of thiosulfinates.

Our findings indicate that during Bga-induced cell death, the bacterium is not natively exposed to thiosulfinates in scale tissue. However, when an external necrosis inducing factor is present, the *altR* promoter-reporter construct is de-repressed, and TTG mutant recovery is impaired in scale tissue. Furthermore, results from ZOI co-inoculation assays suggest that Bga secreted factors may play a role in detoxifying or inactivating thiosulfinates.

Methods

Bacterial growth conditions

Bacterial strains and plasmids utilized in the study are listed in Table 4.1. Primers and synthesized double stranded dsDNA fragments are listed in Table 4.2. *E. coli* strains Mah1, RHO5, all *Burkholderia* and *Pantoea* strains used in the study were grown in Luria-Bertani (LB; per liter, 10 g of tryptone, 5 g of yeast extract and 5 g of NaCl, 15 g agar) or LM (per liter, 10 g of tryptone, 6 g of yeast extract, 1.193 g of KH_2PO_4, 0.6 g of NaCl, 0.4 g of $MgSO_4.7H_20$, and 18 g of agar) media. *E. coli* strains were grown at 37^0C and *Burkholderia*/*Pantoea* strains were grown at 30^0C. Antibiotics and chemicals were supplemented with the media using the following final concentrations per milliliter: 50 µg of kanamycin, 10 µg of gentamicin, 100 µg of ampicillin, 25 µg of trimethoprim, and 100 to 200 µg of diaminopimelic acid (DAP) and 40 to 60 µg of rifampicin, as appropriate.

Plant growth conditions

Onion seedlings for leaf infection assay and coinoculation assay were grown and maintained following procedures described by Paudel et al., 2024a. Onion seeds (*Allium cepa* var. Texas Grano 1015Y) were sprinkled on top of Sungrow 3B potting soil kept on 3-inch pots. After covering the sprinkled seeds with a layer of potting soil, pots were maintained in growth chamber conditions at ~80^0F, 40-50% humidity and watered 1-2 times per week as needed.

Construction of *Burkholderia* and *Pantoea altR* promoter reporter construct

The promoter capture vector pTn5.7luxk6 (GenBank: KC332287.1) was utilized to design *altR* promoter reporter construct for *Burkholderia gladioli* pv. alliicola (Bga) strain 20GA0385 and *Pantoea ananatis* strain PNA97-1R. The 77 bp sequence region containing the predicted *altR* promoter of PNA97-1R along with an additional 30 bp upstream sequence of the StuI site and 30 bp downstream sequence of the DraIII site in the plasmid, was synthesized as double-stranded DNA (dsDNA) by Twist Biosciences. For the Bga *altR* reporter construct, 237 bp sequence region of the predicted 20GA0385 *altR* promoter region was amplified using primer pair pburkaltR-F and pburkaltR-R. The synthesized double-stranded DNA and PCR-amplified gel-extracted product were stitched to gel purified StuI and DraIII double digested vector using Gibson assembly following manufacturer's recommendations (https://www.neb.com/protocols/2012/09/25/gibson-assembly-master-mix-assembly). The Gibson reaction product was transformed into electrocompetent MahI cells and selected on LB agar plates amended with kanamycin. The bioluminescent clones containing the *P. ananatis altR* insert were plasmid purified using GeneJet Plasmid Miniprep kit (Thermoscientific, Watham, WA) and sequence confirmed using Sanger sequencing from Eurofins Genomics LLC (Louisville, KY). The plasmid containing Bga *altR* promoter construct was first confirmed by PCR using primer pair Tn7F and pBurkaltR-R. The representative clones that gave PCR

amplicon size of around 250 bp were purified using Monarch NEB PCR cleanup kit (New England Biolabs, Ipswich, MA) and confirmed using sanger sequencing from Eurofins and confirmed using whole plasmid sequencing from Plasmidsaurus (Plasmidsaurus, Eugene, OR). The sequence confirmed plasmid was transformed into electro competent RHO5 cells. RHO5 donors with *altR* reporter plasmid construct and RHO3/pTNS3 transposition helpers were conjugated with recipient Bga 20GA0385 and PNA 97-1R strains and selected on LBRfKan plates. *P. ananatis* transposition candidates were screened for the insert using zone of inhibition assays. Bga transposition candidates were screened for the insert by zone of inhibition assays and PCR using primer pairs glmSR/Tn7LF and glmSR/pburkaltR-R with expected product size of 356 bp and 657 bp respectively.

Construction of constitutive *lux* reporter construct

The promoter capture vector pTn7oLuxK4 (GenBank: KC332284.1) was used to build constitutively bioluminescent Bga 20GA0385 WT and ΔTTG strains. The plasmid harbored in Mah1 cells was purified and transformed to electro competent RHO5 cells. The RHO5 donor with the plasmid and RHO3/pTns3 transposition helper was conjugated into recipient WT or TTG strains and candidate clones were selected on LBRfKan plates. The candidate clones were screened for bioluminescence using Syngene Pxi imager (Discovery Scientific Solutions, AZ) under 2 minutes exposure.

Preparation of the pantaphos cell free spent medium

Pantaphos cell free spent medium prepared from the P_{SNARE} IPTG induced PNA97-1R overnight cultures were used as an external necrosis inducing factor in the onion red scale necrosis assays. The cell free spent medium was prepared following the procedures described by (Shin et al.,

2023). Briefly, overnight cultures of IPTG-inducible WT strain PNA97-1R::P_{SNARE}*hvr* and IPTG-inducible *hvrE* deletion mutant strain PNA97-1R Δ*hvrE* :: P_{SNARE} *hvr* were started in LM broth. Next day 50 µl of overnight culture was sub-cultured to a new 5 ml of LM media and grown until the OD_{600} value reached 0.6. This was followed by the addition of 50 µl of 1mM IPTG and cultures were left to grow overnight with shaking. Next day, the cultures were centrifuged at 4^0C for 10 min at 2,585 relative central force (Eppendorf 5810R). The supernatant was then filter-sterilized through a 0.2 µm filter. The filter sterilized medium was then stored at 4^0C for experimental use.

Onion leaf infection assay

The de-repression of *Burkholderia altR* promoter reporter construct *in planta* was monitored across three days post inoculation using onion seedling assay. Onion seedlings aged 8-12 weeks were inoculated with 20GA0385 Tn*7*$P_{altR}^{PNA\ 97\text{-}1}$LuxK6 and constitutively bioluminescent 20GA0385 P_{ompA}Tn*7*oLuxK4 construct 4, 3, 2, and 1 day before imaging. At least two leaves per seedling and a total of 3 seedlings were inoculated for each day before imaging. Three independent experimental repeats were performed. The bioluminescence in the inoculated seedling samples was visualized and analyzed using the Newton 7.0 In vivo optical imaging system (Scintica Instrumentation Inc, Webster, TX). Samples were cut and aligned in the imaging plane and incubated inside the machine in dark for 5 minutes to minimize autofluorescence signal from green tissue. The samples were imaged using the program recommended exposure settings. The images were exported from the machine software was then imported into Kuant v 4.5 software for further analysis. The photon count scale bar in the software was manually adjusted to ensure no background noise was observed in the seedlings. After adjusting the scale,

the samples that showed bioluminescence signal were counted as positive. Samples that showed bioluminescence signal over the total number of inoculated samples were reported for each day.

Preparation of bacterial inoculum

Normalized bacterial suspension for the scale necrosis assay, scale assay and foliar assay was prepared following the procedures described by Paudel et al., 2024a;2024b. Briefly, strains were streaked on LB plates amended with appropriate antibiotics and incubated at 30^0C for 24 hours. The streaked area was suspended with 300 µl of sterile H_20 and spread to produce bacterial lawns. The plate was further incubated for 24 h and the next day, the lawn was scraped and suspended in 1 ml of sterile H_20 and standardized to OD_{600} = 0.7 (~6 x 10^8 CFU/ml). The standardized suspension was used for inoculation.

Onion scale necrosis assay

Onion red scale necrosis (RSN) assay was performed following procedure described by (Paudel et al., 2024a; Paudel et al., 2024b). Grocery store bought red onions were cut into 3-5 cm x 3-5 cm pieces, soaked in 3 % sodium hypochlorite solution for 2 minutes and rinsed in dH_20 for 5-6 times. Washed scales were dried in a paper towel and kept on top of 200 µl pipette tip rack placed on top of ethanol sterilized flats. A 200 µl sterile pipette tip was used to wound the scales in the center and normalized bacterial suspension of OD_{600} = 0.7, 10 µl was deposited into the wound. The inoculated scales were then covered and incubated at room temperature for 3 days.

For the red scale necrosis assays, 10 µl of cell free spent medium of PNA97-1R::P_{SNARE} *hvr* / PNA97-1R Δ*hvrE* ::P_{SNARE} *hvr* was mixed with normalized suspension of Bga WT Tn7$P_{altR}^{PNA\ 97\text{-}1R}$LuxK6 and 20 µl of the mix was inoculated into scales. To monitor the colonization of Bga 20GA0385 strain in scale tissue in the presence of cell free spent medium,

constitutively bioluminescent version of WT strain was mixed with cell free spent medium of PNA97-1R:: P_{SNARE} *hvr* / PNA97-1R Δ*hvrE* :: P_{SNARE} *hvr* and inoculated into wounded scales. A total of six scales were inoculated per strain and bioluminescence/de-repression in the scale was monitored from day 1 to day 3 post inoculation in 24 hours interval using analytikJena UV chemstudio imager. Exposure time of 2 minutes was used for samples 24 h post inoculation whereas for the rest of the days, 5 minutes exposure setting was used. Scales that showed visible bioluminescence were counted as positive. The total number of scales that showed presence of bioluminescence over total number of inoculated scales were reported for each day. A total of three independent experimental repeats were performed.

Bioluminescent labeled Bga 20GA0385 WT and ΔTTG strains were mixed with cell free medium as described above and inoculated into red scale tissue to count the recovery of Bga strains 24 to 72 hours post inoculation. A total of six scales were inoculated per treatment and each day, four symptomatic scales were randomly processed for *in planta* population count. The samples were processed following the procedure as described by (Paudel et al., 2024a; Paudel et al., 2024b). Symptomatic area around the point of inoculation was sampled with an ethanol sterilized metal borer (r = 2.5 mm) and mixed with 200 µl sterile miiliQH_20 in a 2-ml SARSTEDT microtube (SARSTEDT AG & Co., Numbrecht, Germany) containing three 3-mm zirconia beads (Glen Mills grinding media). The sample was crushed in a Bead Ruptor Elite Bead Mill Homogenizer (Omni International, Kennesaw, GA) for 30 seconds at 4 m/s speed settings. The sample was serially diluted (20 µl, 180 µl) in a 96-well styrene plates and diluents were plated on LM media amended with rifampicin. The colony forming unit (CFUs) were back-calculated to determine CFUs per mg of infected sample. The experiment was repeated at least three times. The differences in the population recovery between the WT and TTG mutant from

the co-inoculation mix for each day was analyzed for significance using pairwise t-test function in RStudio v 2023.09.0.

Preparation of onion juice

Yellow onions were purchased from a grocery store, and crude juice was extracted following the method outlined by (Stice et al., 2020). In brief, an onion bulb was processed using a consumer-grade juicer (Breville Juice Fountain Elite), producing approximately 200 to 300 mL of crude onion extract. The extract was then centrifuged at 14,000 × g for 2 hours at 4°C using a Sorvall RC5B Plus centrifuge (Marshall Scientific, Hampton, NH) in a 250-mL centrifuge bottle. The supernatant was sterilized through a Nalgene disposable 0.2-micron vacuum filter unit. The filtered juice was then aliquoted and stored at –20°C for up to one week before use in experiments.

Onion scale preconditioning assay

Six yellow onion scales were inoculated with normalized suspension of WT and TTG strains and incubated in room temperature for 3 days. The necrotized onion tissue around the point of inoculation with conditioned WT or TTG strain was sampled using ethanol sterilized metal borer (r = 2.5 mm) and mixed with 200 µl sterile water in a 2-ml SARSTEDT and crushed with homogenizer as described above. 88 µl of crushed sample from each scale was mixed with half strength onion juice to make a total volume of 5280 µl for one strain. Each well in the 100-well honeycomb plates was inoculated with 400 µl of the mix. Each strain was inoculated into a total of 12 wells. Six wells were inoculated with 200 µg/ml kanamycin as a normalization control. The absorbance values recorded for kanamycin treated wells were averaged and subtracted from each of the remaining six wells for each time point. For the non-conditioned controls, normalized

bacterial suspension of WT and TTG mutant strain was mixed with half strength onion juice and 400 µl of the mix was loaded into each well for a total of six wells per strain. At least three wells were inoculated with half strength onion juice as the negative control. Average reading of negative control was subtracted from the individual reading of each well. The obtained absorbance readings across 48-hour time period were plotted in a line graph using ggplot function in Rstudio.

Preparation of allicin stock solution

The allicin solution for the zone of inhibition assay was prepared as described by (Stice et al., 2020; Paudel et al., 2024b). Briefly, 25 µl of glacial acetic acid (Sigma Aldrich), 15 µl of diallyl disulfide 96% (Carbosynth), and 15 µl of 30% H_2O_2 were all mixed together in a 200 µl PCR tube. The PCR tube was properly sealed, affixed to a 500 ml-beaker using tape and agitated in 30^0C shaker for 6 h. After 6 h, the tube was centrifuged for 10 seconds and suspended in 1 ml of methanol. The mix was used as a synthesized allicin stock for the zone of inhibition assay. A fresh stock was made for each experiment.

Zone of inhibition assays

The de-repression of Bga $P_{altR}^{PNA\ 97\text{-}1R}$Tn*7*LuxK6 and Bga $P_{altR}^{20GA0385}$Tn*7*LuxK6 strains was tested using allicin ZOI assay. Overnight cultures (5 ml, ~24h) were started from a single colony in LBKan broth. 300 µl of the culture was spread in LBKan plates and synthesized allicin was added in the hole punched at the center of the agar plate. The plates were incubated for 18 h and visualized for bioluminescence using analytikJena imager under 2- or 5-minute exposure. Experiment was repeated in its entirety two times.

To check whether the Bga 20GA0385 WT or PNA 97-1R WT strain can rescue the *in vitro* phenotype of their respective TTG mutant derivatives, a ZOI co-inoculation assay was done. Overnight cultures (5 ml, ~24 h) of WT or ΔTTG P_{ompA}Tn*7*oLuxK4 strain were started in LB media amended with rifampicin and equal volume of both strains was mixed. For WT only and ΔTTG only treatment, cultures were half diluted with sterile LB. The suspension of 400 µl volume was spread to make a lawn on LB agar and left to dry for 10 minutes. Agar hole was punched in the center of the plate with the back end of a sterile 20 µl Rainin pipette tips. The hole was then inoculated with 50 µl of synthesized allicin and the plates were incubated in 30^0C for 24 hours. Next day, brightfield and bioluminescence images of the plates were visualized using analytiKjena imager. Exposure settings of 2 min was used for bioluminescence. The inhibition area was measured using ImageJ 1.54g software. The difference in inhibition area between the treatments was analyzed for level of significance using pairwise t-test function in R studio. The ZOI area between different strains was presented in a box plot generated using ggplot function in R studio.

The ZOI co-inoculation assay was also done with TTG positive *P. ananatis* PNA 97-1R and TTG lacking natural variant *P. ananatis* strain PNA 02-18 Tn*7* Lux to see if the former is able to rescue the phenotype of the latter. The procedure followed was the same as described above. For the PNA 97-1R and PNA 02-18 Tn*7*Lux co-inoculation mix, an exposure setting of 5 min was used to visualize the ZOI area as needed. For rest of the treatments, 2 min exposure settings were sufficient to visualize the ZOI area. The experiment was repeated four times in its entirety.

Onion seedling and leaves co-inoculation assay

The co-inoculation assay was done with 8-12 weeks old seedling to test if the Bga 20GA0385 strain can rescue the population of ΔTTG strain *in planta*. Seedlings were marked approximately at the midpoint for inoculation and 0.5 cm up and down of the inoculation point for processing. Normalized bacterial suspension for the WT and ΔTTG Tn*7*oLuxK4 strain was prepared as described in the above section. For co-inoculation mix, equal volume of normalized bacterial suspension was mixed and 20 µl of the mix was inoculated into the seedling. For WT and TTG standalone treatments, normalized suspension was half diluted with sterile H_20 and 20 µl of the mix was inoculated. After 3 days post inoculation, necrosis length was measured, and samples were excised from the pre-marked area and processed for CFUs count following the procedure as described above for the onion scale necrosis assay. The CFU recovery was normalized per cm length of the sampled tissue. The cfu of TTG mutant from the coinoculation mix was determined by counting the bioluminescent clones from the serial diluted co-inoculated tissue macerate suspension plated on LM agar amended with rifampicin. One seedling leaf per plant per pot and a total of six pots were inoculated per treatment. The experiment was repeated three times in its entirety.

Mature onion plants were also inoculated to test if the Bga WT strain can rescue the TTG mutant population in the co-inoculation mix. Small onion sets (cv. Century) were transferred to 4-inch pots and allowed to grow for 9-11 weeks under greenhouse conditions before inoculation. Two oldest leaves per plant were inoculated and a total of 3 plants were inoculated per treatment. The leaf samples were marked and processed for CFU count as described above. The cfu/mg reading of two leaves per plant was averaged and used as a single data point for further analysis. The experiment was repeated six times in its entirety.

Results

Derepression of Bga $P_{altR}^{PNA\ 97\text{-}1R}$ or Bga $P_{altR}^{20GA0385}$ reporter construct is observed in zone of inhibition assay.

Promoter capture vector pTn*7altR*LuxK6 was utilized to build the Bga 20GA0385 promoter reporter construct containing the predicted *P. ananatis* PNA 97-1R and Bga 20GA0385 *altR* promoter sequence region. The construct was utilized to ascertain the release of thiosulfinates in red scale tissue. In the allicin zone of inhibition assay, a bright bioluminescent ring was observed at the border of ZOI area for both WT $P_{altR}^{PNA\ 97\text{-}1R}$ Lux and WT $P_{altR}^{20GA0385}$Lux strains which is consistent with allicin exposure-based derepression of *altR*. A relatively strong bioluminescence signal was observed for 20GA0385 $P_{altR}^{PNA\ 97\text{-}1R}$Lux construct as compared to 20GA0385 $P_{altR}^{20GA0385}$Lux construct. De-repression ring was observed for the 20GA0385 $P_{altR}^{PNA\ 97\text{-}1R}$Lux strain with a 2-minute exposure setting, but not for the 20GA0385 $P_{altR}^{20GA0385}$Lux strain under the same conditions. De-repression ring was observed with 20GA0385 $P_{altR}^{20GA0385}$Lux strain at 5- minute exposure (Supplementary Figure S4.1). The 20GA0385 $P_{altR}^{PNA\ 97\text{-}1R}$Lux construct was used for further experiments.

De-repression of Bga $P_{altR}^{PNA\ 97\text{-}1R}$ construct was observed with onset and progression of necrosis in onion seedling assays.

As the Bga TTG cluster contributed to onion foliar necrosis and *in planta* bacterial population, we hypothesize that upon onset and progression of foliar necrosis, the 20GA0385 $P_{altR}^{PNA\ 97\text{-}1R}$LuxK6 construct is de-repressed. Seedlings aged 8-12 weeks were either inoculated with 20GA0385 $P_{altR}^{PNA\ 97\text{-}1R}$Lux construct and constitutive 20GA0385 P_{ompA} Lux strains to monitor the bioluminescence signal from day 1 to day 3 post-inoculation. With the onset of necrosis 24 h

post inoculation, de-repression of the reporter construct was observed in 80% of the inoculated seedlings. Along with the progression of necrosis, de-repression was also consistently observed. By day 3, as the inoculated seedlings were severely necrotic and wilting, de-repression frequency was observed in 59% of the inoculated seedlings leaves (Figure 4.2A). Bioluminescence was also consistently observed in the seedlings inoculated with the P_{ompA} constitutive reporter construct across all three days post inoculation. The percentage of inoculated seedlings that showed bioluminescence signal was reduced to 80% three days post inoculation (Figure 4.2B).

De-repression of Bga $P_{altR}^{PNA\ 97\text{-}1R}$ displays different patterns during Bga native necrosis than during pantaphos cell free spent medium induced necrosis in scale tissue.

Pantaphos cell free spent medium was used as an external necrosis inducing factor in the red scale necrosis assay to monitor the de-repression of 20GA0385 $P_{altR}^{PNA\ 97\text{-}1R}$Lux promoter reporter in the necrotized onion scale tissue. In scales inoculated with mixture of pantaphos containing cell free spent medium and 20GA0385 $P_{altR}^{PNA\ 97\text{-}1R}$ strain, de-repression was observed in all the inoculated scales with the onset of pantaphos induced scale necrosis 48 h post inoculation. The number of inoculated scales that showed positive bioluminescence signal was reduced to 33% 72 h post inoculation (Figure 4.3A). The constitutive bioluminescent construct 20GA0385 P_{ompA} Lux showed bioluminescence signal in all the inoculated scales at all time points post inoculation suggesting the bacterium is not impaired in its ability to colonize the necrotized scale tissue in the presence of cell free spent medium (Figure 4.3B).

The *hvrE* gene in the Hivir biosynthetic gene cluster is an essential gene without which *P. ananatis* is not able to produce the pantaphos toxin (Shin et al., 2023). In the scale assay using a mixture of P_{SNARE} Δ*hvrE* cell free spent medium and 20GA0385 $P_{altR}^{PNA\ 97\text{-}1R}$ strain, de-repression was observed 24 h post inoculation in all the inoculated scales. After 24 h, the de-

repression signal gradually went away and by day 3, only three inoculated scales showed a de-repression signal (Figure 4.3C). The bacterium was able to successfully colonize onion scales in the presence of P_{SNARE} Δ*hvrE* cell free spent medium as evident from the bioluminescence signal observed in all the inoculated scales across all time point (Figure 4.3D).

The recovery of TTG mutant from scale tissue was reduced compared to WT strain during pantaphos induced necrosis.

Red scale assay with the cell free spent medium was also performed to test the recovery of WT and TTG mutant population from the necrotized onion scale tissue. The recovery of the Bga TTG mutant from pantaphos containing cell free spent medium mixture was significantly lower compared to the WT strain at day 2 and day 3 post inoculation (Figure 4.4A). When the cell free spent medium of P_{SNARE} Δ*hvrE* was used, the recovery of TTG mutant from inoculated scale tissue was similar to WT strain from day 1 to day 3 post inoculation (Figure 4.4B).

Preconditioning the Bga TTG mutant in scale tissue didn't impact its growth behavior in onion juice growth assays.

The TTG cluster in Bga strain contributes to improved growth in the onion juice assay. To check if preconditioning the TTG mutant in the scale tissue protects them from thiosulfinate exposure, the necrotic area in the TTG inoculated scale tissue was sampled and exposed to onion juice. Over the period of 48 h, the TTG strain preconditioned in the scale tissue for 3 days showed dramatically reduced growth compared to the WT strain similarly preconditioned for 3 days. The growth pattern of the nonconditioned WT and TTG mutant strains in the scale tissue resembled the previously observed pattern for WT and TTG strains (Figure 4.5) (Paudel et al., 2024b).

Bga WT strain was able to partially rescue the allicin sensitivity phenotype of the TTG mutant in *in vitro* zone of inhibition coinoculation assays.

The ZOI co-inoculation assay was done to test if the Bga WT strain secretes factors that could help in extracellular detoxification of thiosulfinates by the bacterium. In the ZOI co-inoculation assay, the ZOI area of TTG mutant from the WT/TTG co-inoculation mix was significantly lower than the ZOI area of TTG mutant only strain. The ZOI area of TTG strain in the co-inoculation mix was still significantly bigger than WT only strain suggesting the rescue phenotype is only partial (Figure 4.6).

The TTG cluster in *P. ananatis* contributes to bacterial population in scales (Stice et al., 2020). The ZOI co-inoculation assay was also done with *P. ananatis* WT and TTG strain to check if the WT strain can rescue the zone of inhibition phenotype of TTG mutant in the co-inoculation mix. The ZOI area of TTG mutant in the WT and TTG mix was significantly higher than the ZOI area of TTG alone treatment. The area, however, was still significantly bigger than the WT alone treatment (Supplementary Figure S4.2A). Stice et al., demonstrated that the ZOI phenotype of TTG-lacking natural variant strain PNA 02-18 was not rescued by PNA 97-1R WT strain. We repeated the experiment and further corroborated that the ZOI area of PNA 02-18 strain from the co-inoculation mix was comparable to ZOI area of PNA 02-18 alone treatment. (Supplementary Figure S4.2B). The ZOI area for PNA 02 -18 strain was significantly larger than ZOI area of PNA 97-1R strain.

Bga WT strain didn't rescue TTG mutant population in onion foliar rescue assays.

The co-inoculation assay was also performed with onion seedlings and mature onion plants to check if the Bga WT strain can rescue the TTG leaf population from the mix. The CFU/cm

recovery of TTG mutant from the WT and TTG co-inoculation mix was similar to the recovery of TTG alone treatment. As expected, the bacterial population of WT strain from the infected seedling sample was significantly higher than TTG mutant (Figure 4.7). The TTG mutant was also not rescued by WT strain in the mature onion leaves co-inoculation assay (Supplementary Figure S4.3)

Discussion

Using the *altR* promoter reporter construct, pantaphos cell free spent medium as external necrosis inducing factor, and ZOI co-inoculation assays, we elucidated the phenomenological basis for the tissue specific virulence role of TTG cluster in Bga strain 20GA0385. In the absence of external necrosis inducing factor, the de-repression of Bga *altR* promoter reporter construct in the scale tissue was transient during the early stages of infection and the signal gradually went away after the appearance of Bga induced necrosis symptoms. However, in the presence of pantaphos as onion scale necrosis inducing factor, the de-repression of Bga *altR* reporter was pronounced with the onset of pantaphos induced necrosis symptoms. In line with the thiosulfinate-based sensitization of the TTG strain in scale tissue with the presence of pantaphos cell-free spent medium, the recovery of the TTG mutant was significantly lower than that of the WT strain following the onset of Hivir-mediated necrosis. Incubating the TTG strains in onion scales before exposing them to onion juice did not impact their growth impairment in onion juice suggesting that Bga's thiosulfinate resistance mechanism in scale tissue may not be attributed to a thiosulfinate exclusion factor. In the ZOI co-inoculation assay, the Bga WT strain was able to partially rescue the ZOI phenotype of TTG mutant strain suggesting the potential extracellular detoxification of thiosulfinates by Bga WT strain.

The Bga TTG clusters contributed to foliar necrosis length and bacterial population in onion leaves but not in scales. This is surprising as the amount of thiosulfinates production in the bulb tissue is much higher compared to the leaf tissue (Cho et al., 2024). We proposed two hypotheses to further examine the mechanism of Bga thiosulfinate resistance in scale tissue. In the first hypothesis, the bacteria produce thiosulfinates exclusion factor to prevent thiosulfinate uptake into the bacterial cells, e.g. grow in a resistant biofilm, which prevents the exposure of the bacteria to thiosulfinates released in scale tissue (Figure 4.1A). If the bacterium can develop protective mechanisms against thiosulfinate exposure in the scale tissue, the growth of the scale pre-conditioned TTG mutant would be expected to remain unaffected in onion juice. Similarly, in the case of Bga thiosulfinate exclusion or evasion, the *altR* de-repression of the WT strain and scale population recovery of the TTG mutant is expected to be similar to the WT strain recovery in the presence of external necrosis inducing factor. The second hypothesis is based on thiosulfinate inhibition or suppression model where the bacterium inhibits the thiosulfinates precursor enzyme alliinase or inactivate/destroy thiosulfinate produced in scale tissue (Figure 4.1B). This study was designed to test these two proposed models of Bga thiosulfinate resistance in scale tissue.

The *altR* gene, a predicted TetR family transcriptional regulator is one of the conserved genes in the TTG cluster across different bacterial genera (Borlinghaus et al., 2020; Stice et al., 2020; Paudel et al., 2024b). The TetR crystal structure has been described as a homodimer containing two DNA-binding domains at the end of each monomer (Orth et al., 2000). They often function as autorepressors binding to incomplete palindromic regions upstream of their own coding region or regulated region (Orth et al., 2000; Pushparajan et al., 2020). The *altR* promoter reporter construct was designed to determine if the thiosulfinates are being released in

the onion scale tissue. In the presence of thiosulfinates, the *altR* promoter reporter construct was de-repressed as seen by the bright bioluminescent ring in the edge of ZOI area (Supplementary Figure S4.1). While the *altR* de-repression ring was observed with *altR* promoter region of both *P. ananatis* PNA 97-1R and Bga 20GA0385 in the reporter construct, the signal was stronger for the former. As the TTG cluster contributed to Bga virulence in leaf tissue, extensive de-repression of *altR* construct was observed in leaf tissue from day 1 to day 3 post inoculation (Figure 4.2A). As the population of WT strain in the inoculated leaf tissue gradually increases and reaches the highest threshold day 3 post inoculation (Paudel et al., 2024b), similar de-repression pattern was expected in the leaf tissue. However, the de-repression percentage decreased as the necrosis in the seedling progressed. Similar trend was also observed with seedlings inoculated with the constitutive reporter construct (Figure 4.2B). As previous bacterial recovery assay was performed with mature plants, the growth behavior of bacterium in younger seedlings might be different which could have caused the differences in observations. Alternatively, the *ompA* promoter might not have been expressed fully constitutively in planta.

In the scale tissue, the de-repression of the *altR* promoter reporter was observed as early as 6 h post inoculation (data not shown) and was visible 24-hour post inoculation. But as the Bga induced necrosis became visible, the de-repression signal was largely lost with the progression of symptoms (Figure 4.3C). It is possible the transient de-repression observed during the early stages of infection might be due to the bacterial exposure to wound induced thiosulfinate release in scale tissue. As the underlying mechanisms behind Bga induced cell death is not yet properly understood, we utilized pantaphos toxin as external necrosis inducing factor in the Bga scale co-inoculation assay. (Stice et al., 2020) showed the *pepM* gene in Hivir biosynthetic gene cluster is required for onion cell death in scale tissue. (Shin et al., 2023) demonstrated that the use of

bacterial cell free spent medium from IPTG induced P_{SNARE} driven *hvr* strain was sufficient to produce pantaphos like symptoms in red scales. As *P. ananatis* TTG cluster helps the bacterium colonize the necrotized onion tissue, the P_{SNARE} *hvr* cell free spent medium was utilized as necrosis factor to determine the fate of Bga TTG mutant in scale tissue upon exposure to thiosulfinates. In the presence of an external necrosis factor, we saw the Bga *altR* promoter reporter construct is de-repressed and the TTG mutant in the scale tissue is sensitized to thiosulfinate exposure as seen from its reduced population recovery compared to the WT strain (Figure 4.3A, Figure 4.4A). We also observed that preconditioning TTG mutants in scale and exposing them to thiosulfinates didn't change their growth behavior in onion juice (Figure 4.5). All these experimental results suggest that Bga exclusion of thiosulfinates in scale tissue is unlikely and Bga potentially suppresses or inhibits thiosulfinates or thiosulfinates precursors inside the scale tissue.

In the ZOI assay, (Stice et al., 2020) reported that the PNA 97-1R WT strain was not able to rescue the ZOI area phenotype of TTG lacking variant strain PNA 02-18 suggesting extracellular detoxification of thiosulfinates by *P. ananatis* is unlikely. When we utilized genetically engineered TTG mutant for the ZOI co-inoculation assay, we saw that Bga WT strain partially rescues the ZOI phenotype of TTG mutant strain (Figure 4.6). The rescue phenotype was also observed in the ZOI assay performed with the *P. ananatis* PNA 97-1R WT and TTG mutant strains (Supplementary Figure S4.2A). This observation suggests that the Bga WT strain and *P. ananatis* WT strain may contribute extracellularly to the detoxification of allicin present in the ZOI assay, potentially through secreted factors or enzymatic activity. It is also important to note that the ZOI *in vitro* assay does not contain the enzyme alliinase which suggest the rescue mechanism might be independent of suppression or inhibition of alliinase. Consistent to what

was seen before, the PNA 97-1R strain was not able to rescue the phenotype of TTG negative natural variant strain PNA 02-18 (Supplementary Figure S4.2B). As the rescue phenotype was not observed with the TTG lacking PNA 02-18 strain, it is possible that the TTG strain must be capable of receiving the secreted donor rescue factor. The recovery of the Bga TTG mutant from the WT and TTG co-inoculation mix in seedling tissue was similar to the recovery of TTG mutant alone. The rescue effect of the Bga WT strain was also not observed in the mature onion leaves co-inoculation assay. It is possible multiple biological, chemical, and physical barriers including the plant immune responses and bacterial behavior may have caused differences in observations *in vitro* vs *in planta*.

Our study delves deeper into the phenomenon behind Bga's tissue-specific virulence, shedding light on its interactions with onion thiosulfinates. Using *altR* promoter reporter and pantaphos cell free spent medium, we observed that Bga *altR* promoter de-repression was enhanced in pantaphos necrotized scale tissue, while the TTG mutant was more susceptible to thiosulfinate exposure, suggesting that Bga does not rely on exclusion but may actively suppress or inactivate released thiosulfinates within scale tissue. This hypothesis is further supported by the observation that preconditioning TTG mutants in scale tissue did not improve their survival upon exposure to thiosulfinate in onion juice, implying that Bga's resistance mechanism is not dependent on environmental adaptation. The sharp reduction in de-repression signal with the onset of Bga induced necrosis in scale tissue suggests Bga might avoid thiosulfinate exposure during native scale necrosis (Figure 4.8A). The consistent derepression of *altR* reporter construct in the early stages of inoculation, likely due to wound- induced thiosulfinate release, further supports this idea (Figure 4.3C). While the Bga WT strain and *P. ananatis* WT strain appear to contribute to extracellular detoxification in the ZOI assay, the rescue phenotype was absent with

the TTG-lacking PNA 02-18 strain, indicating that recipient strain compatibility may influence the detoxification effect. It is possible that Bga secretes enzymatic or chemical compounds capable of inactivating or detoxifying the produced thiosulfinates, or that it prevents their formation within onion scales (Figure 4.8B). Future experiments could focus on screening for the Bga secreted factors that could inactivate or detoxify thiosulfinates. Furthermore, investigating the bacterial transcriptional response using RNA-seq could provide insight into differences in onion tissue-specific gene regulation.

References

Belo, T., du Toit, L., Waters, T., Derie, M., Schacht, B., and LaHue, G. 2023. Reducing the risk of onion bacterial diseases through managing irrigation frequency and final irrigation timing. Agricultural Water Management 288:108476.

Borlinghaus, J., Bolger, A., Schier, C., Vogel, A., Usadel, B., Gruhlke, M., and Slusarenko, A. 2020. Genetic and molecular characterization of multicomponent resistance of *Pseudomonas* against allicin. Life science alliance 3.

Cho, H., Park, J., Kim, D., Han, J., Natesan, K., Choi, M., Lee, S., Kim, J., Cho, K., and Ahn, B. 2024. Understanding the defense mechanism of *Allium* plants through the onion isoallicin-omics study. Frontiers in Plant Science 15:1488553.

Eady, C.C., Kamoi, T., Kato, M., Porter, N.G., Davis, S., Shaw, M., Kamoi, A., and Imai, S. 2008. Silencing onion lachrymatory factor synthase causes a significant change in the sulfur secondary metabolite profile. Plant physiology 147:2096-2106.

Hughes, J., Tregova, A., Tomsett, A., Jones, M., Cosstick, R., and Collin, H. 2005. Synthesis of the flavour precursor, alliin, in garlic tissue cultures. Phytochemistry 66:187-194.

Kovach, M., Phillips, R., Elzer, P., Roop 2nd, R., and Peterson, K. 1994. pBBR1MCS: a broad-host-range cloning vector. Biotechniques 16:800-802.

Kvitko, B., Ramos, A., Morello, J., Oh, H., and Collmer, A. 2007. Identification of harpins in *Pseudomonas syringae* pv. tomato DC3000, which are functionally similar to HrpK1 in promoting translocation of type III secretion system effectors. Journal of Bacteriology 189:8059-8072.

Kvitko, B., Bruckbauer, S., Prucha, J., McMillan, I., Breland, E., Lehman, S., Mladinich, K., Choi, K., Karkhoff-Schweizer, R., and Schweizer, H. 2012a. A simple method for construction of pir+ Enterobacterial hosts for maintenance of R6K replicon plasmids. BMC research notes 5:1-7.

Kvitko, B.H., Bruckbauer, S., Prucha, J., McMillan, I., Breland, E.J., Lehman, S., Mladinich, K., Choi, K., Karkhoff-Schweizer, R., and Schweizer, H. 2012b. A simple method for construction of pir+ Enterobacterial hosts for maintenance of R6K replicon plasmids. BMC research notes 5:1-7.

Lancaster, J.E., and Collin, H.A. 1981. Presence of alliinase in isolated vacuoles and of alkyl cysteine sulphoxides in the cytoplasm of bulbs of onion (*Allium cepa*). Plant Science Letters 22:169-176.

Lee, C.J., Lee, J.T., Kwor, J., Kim, B., and Park, W. 2005. Occurrence of bacterial soft rot of onion plants caused by *Burkholderia gladioli* pv. *alliicola* in Korea. Australasian Plant Pathology 34:287-292.

Leontiev, R., Hohaus, N., Jacob, C., Gruhlke, M., and Slusarenko, A.J. 2018. A comparison of the antibacterial and antifungal activities of thiosulfinate analogues of allicin. Scientific reports 8:6763.

Liss, L. 1987. New M13 host: DH5αF′ competent cells. Focus 9:13.

López, C., Rholl, D., Trunck, L., and Schweizer, H. 2009a. Versatile dual-technology system for markerless allele replacement in *Burkholderia pseudomallei*. Applied and environmental microbiology 75:6496-6503.

López, C.M., Rholl, D.A., Trunck, L.A., and Schweizer, H.P. 2009b. Versatile dual-technology system for markerless allele replacement in *Burkholderia pseudomallei*. Applied and environmental microbiology 75:6496-6503.

Mijatović, J., Severns, P., Kemerait, R., Walcott, R., and Kvitko, B. 2021. Patterns of seed-to-seedling transmission of *Xanthomonas citri* pv. *malvacearum*, the causal agent of cotton bacterial blight. Phytopathology® 111:2176-2184.

Müller, A., Eller, J., Albrecht, F., Prochnow, P., Kuhlmann, K., Bandow, J.E.S.,

Alan, J., and Leichert, L. 2016. Allicin induces thiol stress in bacteria through S-allylmercapto modification of protein cysteines. Journal of Biological Chemistry 291:11477-11490.

Orth, P., Schnappinger, D., Hillen, W., Saenger, W., and Hinrichs, W. 2000. Structural basis of gene regulation by the tetracycline inducible Tet repressor–operator system. Nature structural biology 7:215-219.

Paudel, S., Franco, Y., Zhao, M., Dutta, B., and Kvitko, B.H. 2024a. Distinct Virulence Mechanisms of *Burkholderia gladioli* in Onion Foliar and Bulb Scale Tissues. Molecular Plant-Microbe Interactions.

Paudel, S., Zhao, M., Stice, S.P., Dutta, B., and Kvitko, B.H. 2024b. Thiosulfinate Tolerance Gene Clusters Are Common Features of *Burkholderia* Onion Pathogens. Mol Plant Microbe Interact 37:507-519.

Pushparajan, A., Ramachandran, R., Gopi Reji, J., and Ajay Kumar, R. 2020. *Mycobacterium tuberculosis* TetR family transcriptional regulator Rv1019 is a negative regulator of the mfd-mazG operon encoding DNA repair proteins. FEBS letters 594:2867-2880.

Reiter, J., Hübbers, A., Albrecht, F., Leichert, L., and Slusarenko, A. 2020. Allicin, a natural antimicrobial defence substance from garlic, inhibits DNA gyrase activity in bacteria. International Journal of Medical Microbiology 310:151359.

Rose, P., Whiteman, M., Moore, P.K., and Zhu, Y. 2005. Bioactive S-alk (en) yl cysteine sulfoxide metabolites in the genus *Allium*: the chemistry of potential therapeutic agents. Natural product reports 22:351-368.

Schwartz, H., du Toit, L., and Coutinho, T. 2015. Diseases of Onion and Garlic (*Allium cepa* L. and *A. sativum* L., Respectively). The American Phytopathological Society: St Paul, MN, USA.

Shin, G., Dutta, B., and Kvitko, B.H. 2023. The Genetic Requirements for HiVir-Mediated Onion Necrosis by *Pantoea ananatis*, a Necrotrophic Plant Pathogen. Molecular Plant-Microbe Interactions® 36:381-391.

Stice, S., Thao, K., Khang, C., Baltrus, D., Dutta, B., and Kvitko, B. 2020. Thiosulfinate tolerance is a virulence strategy of an atypical bacterial pathogen of onion. Current Biology 30:3130-3140. e3136.

Van Damme, E., Smeets, K., Torrekens, S., Van Leuven, F., and Peumans, W.J. 1992. Isolation and characterization of alliinase cDNA clones from garlic (*Allium sativum* L.) and related species. European Journal of Biochemistry 209:751-757.

Wright, P., Clark, R., and Hale, C. 1993. A storage soft rot of New Zealand onions caused by *Pseudomonas gladioli* pv. *alliicola*. New Zealand journal of crop and horticultural science 21:225-227.

Yamazaki, Y., Iwasaki, K., Mikami, M., and Yagihashi, A. 2010. Distribution of eleven flavor precursors, S-alk (en) yl-L-cysteine derivatives, in seven *Allium* vegetables. Food science and technology research 17:55-62.

Tables

Table 4.1: Strains and plasmid used in the study.

E.coli strain	Purpose	Reference
MahI	DH5	(Kvitko et al., 2012b)
RHO5	*pir116*, DAP-dependent conjugation strain	(Kvitko et al., 2012b)
RHO3pTNS3	DAP dependent conjugation strain SM10 derivative with Tn7 transposase helper plasmid (Amp^R)	(López et al., 2009b)
20GA0385	*Burkholderia gladioli* pv. *alliicola* (Bga) WT strain (Rf^R)	(Paudel et al., 2024b)
20GA0385 ΔTTG	TTG mutant derivative of Bga 20GA0385 (Rf^R)	(Paudel et al., 2024b)
PNA 97-1R	*Pantoea ananatis*, WT strain (Rf^R)	(Stice et al., 2020)
PNA 97-1R ΔTTG	TTG mutant derivative of PNA 97-1R (Rf^R)	(Stice et al., 2020)
PNA 02-18 P_{PA134}Tn*7* Lux	TTG lacking *P. ananatis* natural variant strain with PA134 promoter driven constitutive bioluminescence (Rf^R, Km^R)	(Stice et al., 2020)
20GA0385 P_{ompA}Tn*7*LuxK6	*ompA* promoter driven constitutive bioluminescent Bga 20GA0385 strain (Rf^R, Km^R)	This study
20GA0385 ΔTTG P_{ompA}Tn*7*LuxK6	*ompA* promoter driven constitutive bioluminescent Bga 20GA0385 ΔTTG strain (Rf^R, Km^R)	This study
20GA0385 $P_{altR}^{PNA\ 97\text{-}1R}$ Tn*7*LuxK6	*Burkholderia altR* promoter reporter construct with *P. ananatis* PNA 97-1R *altR* promoter region (Rf^R, Km^R)	This study

20GA0385 $P_{altR}^{20GA0385}$ Tn*7*LuxK6	*Burkholderia altR* promoter reporter construct with Bga 20GA0385 *altR* promoter region	This study
PNA 97-1R ::P_{SNARE} *hvr*	Hivir IPTG inducible *P. ananatis* strain with pSNARE inserted in front of *hvrA* gene of pantaphos biosynthesis gene cluster (Rf^R, Tmp^R). Used to generate cell free spent medium for co-infection assays in this study.	(Shin et al., 2023)
PNA 97-1R Δ*hvrE* :: P_{SNARE} *hvr*	Hivir IPTG inducible *P. ananatis* Δ*hvrE* mutant strain with P_{SNARE} inserted in front of *hvrA* gene of pantaphos biosynthesis gene cluster (Rf^R, Tmp^R). Used to generate cell free spent medium for co-infection assays in this study.	(Shin et al., 2023)
pTn5.7Lux K6	Promoter capture vector, R6K replicon (Km^R)	KC332287.1

Table 4.2 Primers and double stranded synthesized DNA used in the study.

Primer/dsDNA	Sequence (5' – 3')	Purpose
pBurkaltRF	**AGA TTT CAC TTA TCT GGT TGG CCT GCA AGG** AGA TTG ATC GGA GGA ATT TA	Primer to amplify the *altR* promoter region of Bga 20GA0385. Underlined is the gibson overhang upstream of stuI restriction site in the pTn5.7LuxK6
pBurkaltRR	**GCC TGC TTT TTT GTA CAA ACT TGT CAC CGC** TAT CCT CCG GCA CAC TGC CA	Primer to amplify the *altR* promoter region of Bga 20GA0385. Underlined is the gibson overhang dowstream of DraIII restriction site in the pTn5.7LuxK6
Tn7F	CACTTATCTGGTTGGCCTG	Primer in the Tn*7* border used to genotype the Bga *altR* reporter construct
glmsR	GAC GTC AAG CAC TTG CAG TTA	Primer downstream of *glmS* gene to genotype the Bga *altR* reporter construct

PNA 97-1R *altR* Tn7LuxK6	**AGATTTCACTTATCTGGTTGGCCTGCAAGG**GGAAAAAACGCCGATTGCTTGCCATAGAAGGGTGTGAAGGATACAATCTACCAACTAGTAGATTGAAGGATTTTAAA**GCGGTGACAAGTTTGTACAAAAAAGCAGGC**	Synthesized double stranded DNA sequence of *P. ananatis* PNA97-1R *altR* promoter region. The StuI upstream region and DraIII downstream sequence as Gibson overhang are presented in bold text.

Figures

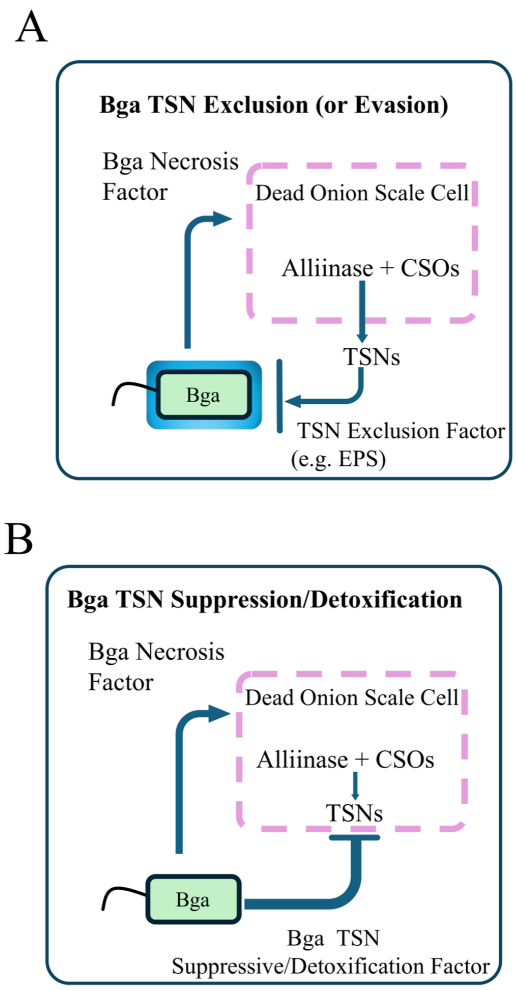

Figure 4.1: Proposed models for thiosulfinate resistance mechanisms of *Burkholderia gladioli* pv. *alliicola* (Bga) in necrotized onion scales tissue. **A**, In the Bga thiosulfinates (TSNs) exclusion model, the bacterium evades or excludes thiosulfinates exposure using the TSNs exclusion factor such as exopolysaccharides (EPS) and biofilm formation. **B**, In the Bga TSN suppression/detoxification model, the bacterium inhibits the TSN precursor CS lyase enzyme alliinase or detoxify/inactivate thiosulfinates in scale tissue.

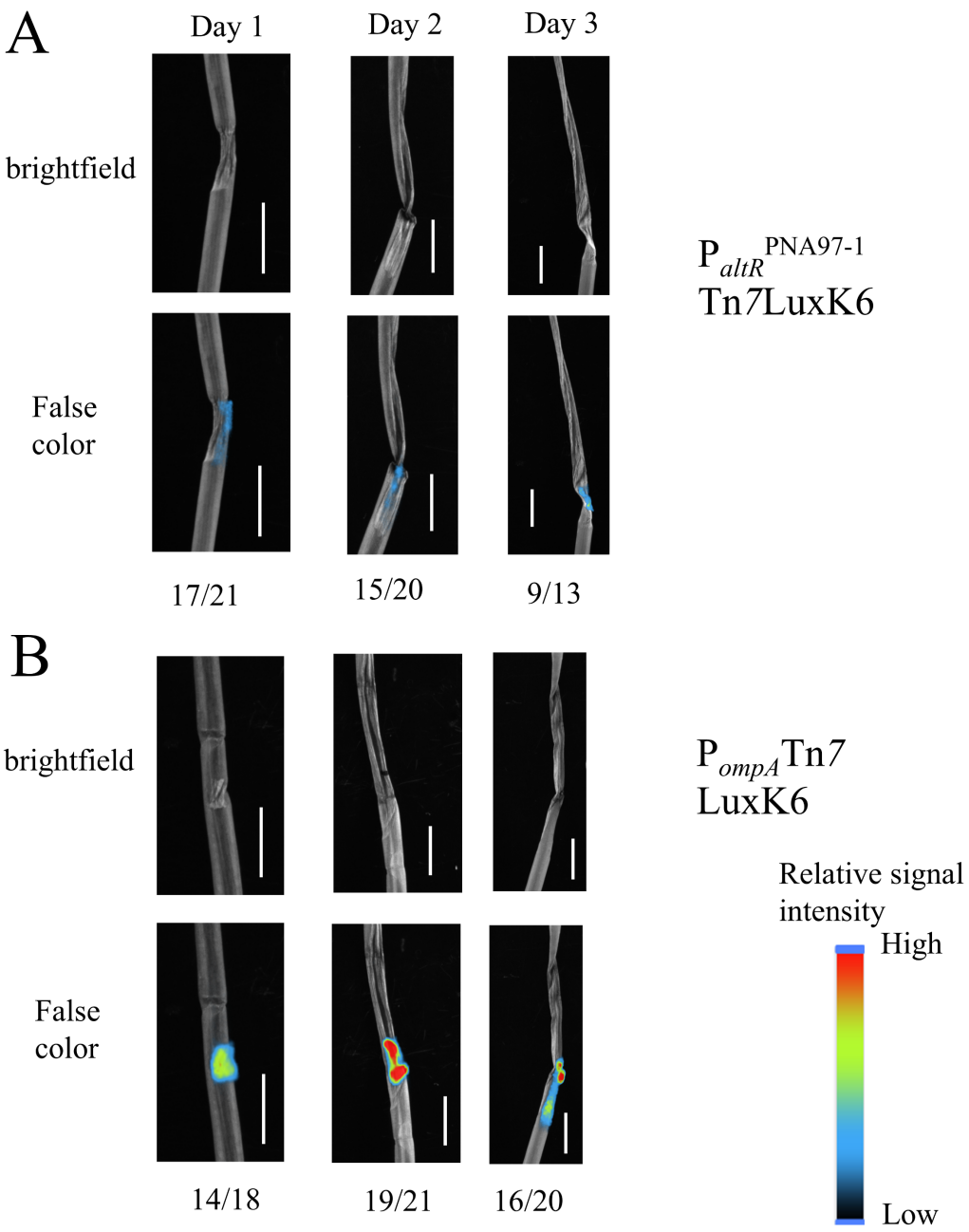

Figure 4.2: De-repression of Bga *altR* promoter reporter construct is consistent with the initiation and progression of foliar necrosis. Representative brightfield and corresponding false color image of seedlings inoculated with **A** 20GA0385 $P_{altR}^{PNA\ 97\text{-}1R}$Tn*7*LuxK6 strain and **B** 20GA0385 P_{ompA}Tn*7* LuxK4 strain from day 1 to day 3 post inoculation. The number in the numerator is the number of inoculated leaves that showed positive bioluminescence signal for samples visualized on corresponding day. The number in the denominator is the total number of inoculated leaves. Legend bar represents the relative intensity of visible signal from low to high. Scale: 1 cm. Bioluminescence signal visualized using Newton 7.0 camera and analyzed using Kuant v 2.5 software.

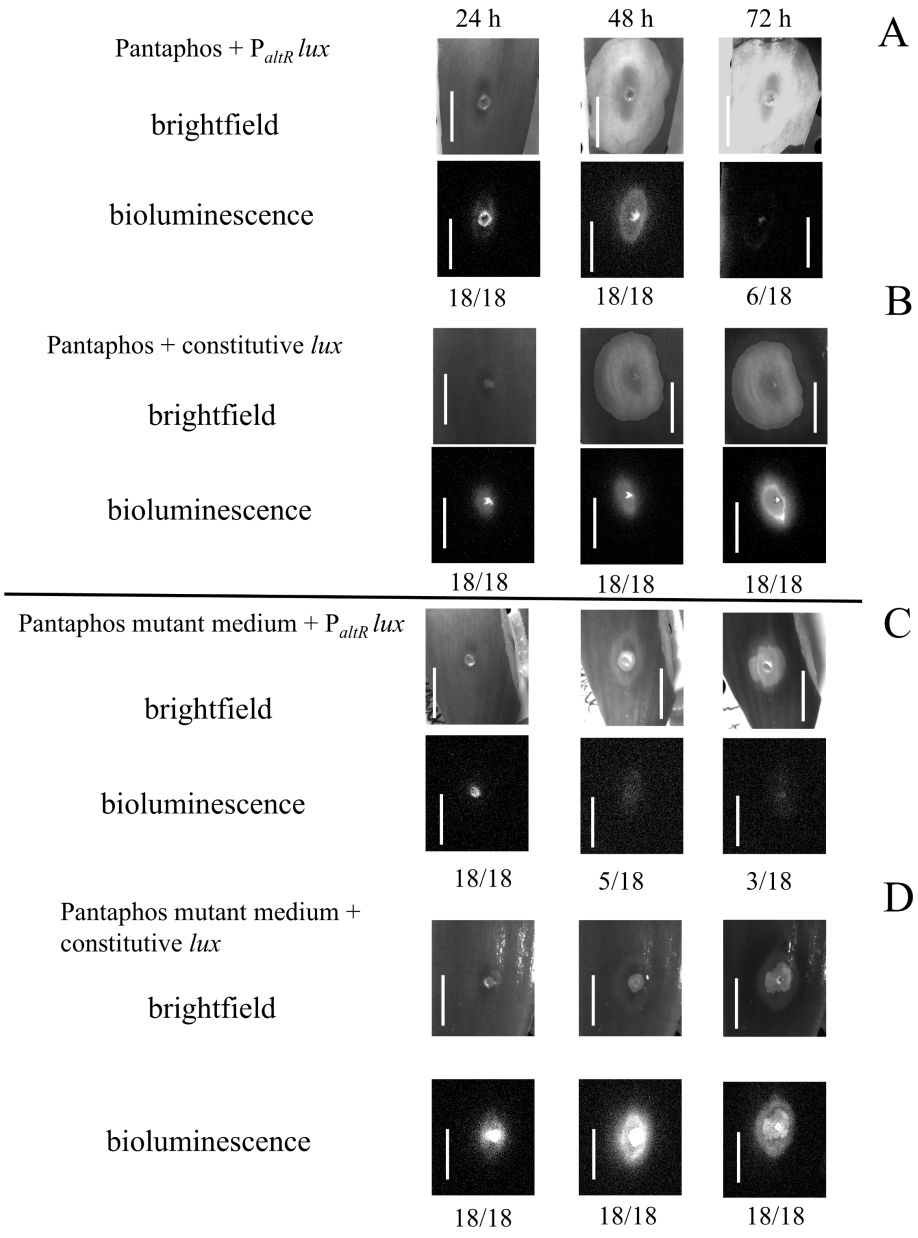

Figure 4.3: The Bga *altR* promoter reporter construct is de-repressed in the presence of pantaphos mediated scale necrosis symptoms. Representative brightfield and corresponding bioluminescence image of scales inoculated with **A,** Cell free spent medium of PNA 97-1R P_{SNARE} *hvr* strain and Bga $P_{altR}^{PNA\ 97\text{-}1R}$Tn*7*LuxK6 strain; **B,** Cell free spent medium of PNA 97-1R P_{SNARE} *hvr* strain and 20GA0385 P_{ompA}Tn*7* LuxK4; **C,** Cell free spent medium of PNA 97-1R Δ*hvrE* P_{SNARE} *hvr* and Bga $P_{altR}^{PNA\ 97\text{-}1R}$Tn*7*LuxK6 and **D,** Cell free spent medium of PNA 97-1R Δ*hvrE* P_{SNARE} Δ*hvrE* strain and 20GA0385 P_{ompA}Tn*7* LuxK4. The number in the numerator is the number of inoculated scales that showed positive bioluminescence signal for samples visualized on the corresponding day. Brightfield and bioluminescence image of a representative scale sample is presented from Day 1 to Day 3 post inoculation. Brightness and contrast of the

presented scales were adjusted to enhance the visibility for presentation. Number in the denominator is the total number of inoculated scales across three independent experimental repeats. Samples were imaged under 2 min exposure for 24 h time point and under 5 min exposure for rest of time point. Scale: 1 cm.

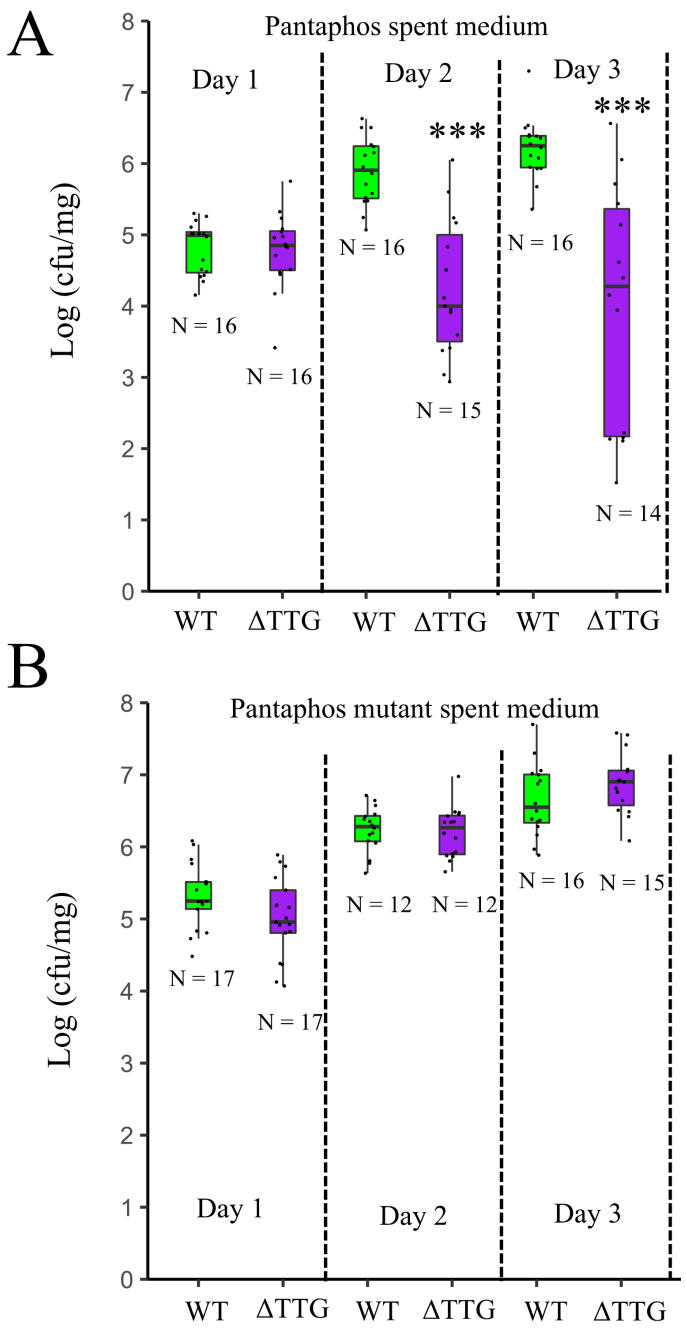

Figure 4.4: The TTG mutant exhibits impaired scale recovery in the presence of pantaphos cell-free spent medium, which serves as an external necrosis-inducing factor. Bacterial population recovery of Bga WT Tn7 LuxK4 and ΔTTG Tn7 LuxK4 strains from inoculated scales was monitored from day 1 to day 3 post-inoculation containing cell-free spent medium from **A**, PNA 97-1R P_{SNARE} *hvr* and **B**, PNA 97-1R Δ*hvrE* P_{SNARE} *hvr*. N is the total number of scales inoculated across four independent experimental repeats. Level of significance: 0 '***' 0.001 '**'0.01 '*' 0.05.

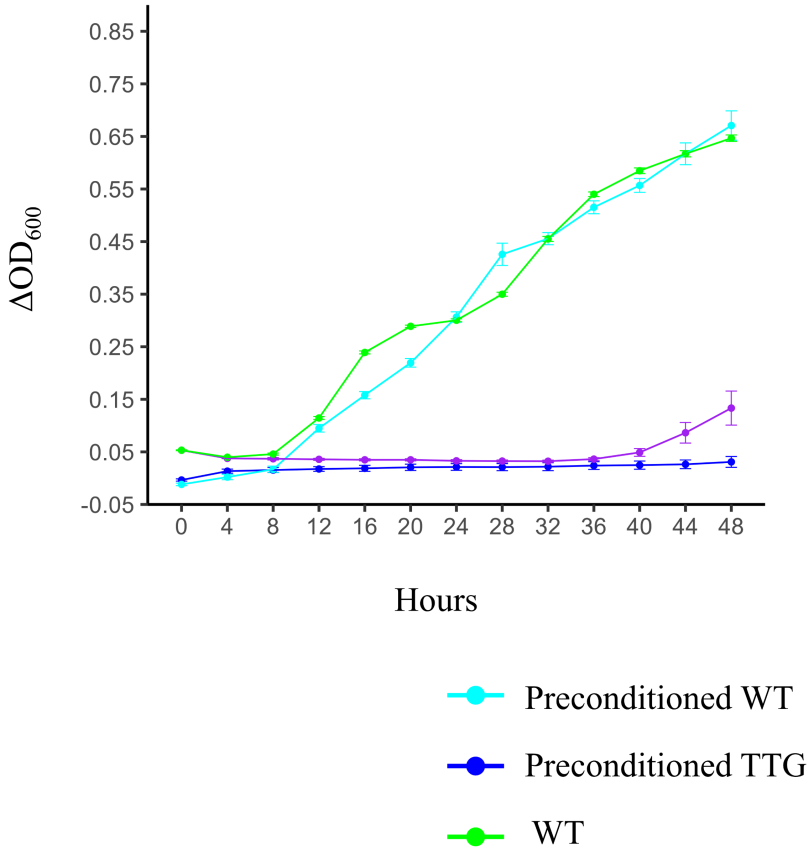

Figure 4.5: Preconditioning the TTG mutant in the scales didn't change its growth behavior in onion juice. Line graph showing the growth of preconditioned/non-conditioned Bga WT and TTG mutant strains in onion juice over the period of 48 hours. Absorbance values were normalized by subtracting the average absorbance of the kanamycin-treated normalization control or half-strength onion juice (negative control) from each well. The graph presents the average values from two independent experimental repeats at each time point. Error bars represent ± standard error. Cyan represents preconditioned WT strain, blue represents preconditioned TTG mutant strain, green represents non-conditioned WT strain and violet represent non conditioned TTG mutant strain.

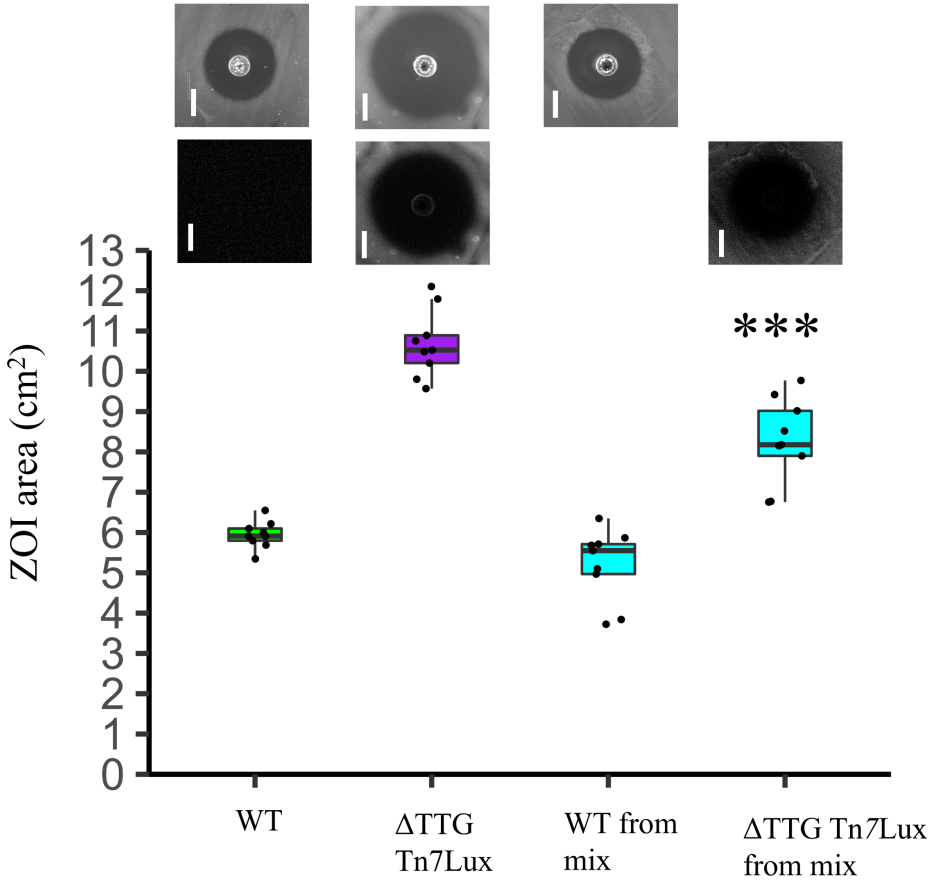

Figure 4.6: Bga WT strain is able to partially rescue the phenotype of TTG mutant strain in the zone of inhibition (ZOI) coinoculation assay. Box plot showing the allicin ZOI area of Bga 20GA0385 WT, TTG mutant, WT from co-inoculation mix and TTG from co-inoculation mix. Representative brightfield and/or bioluminescence images of ZOI plates treated with corresponding strains are presented above the box. Bioluminescence images were taken under 2 minutes exposure. Experimental data from three independent repeats (n = 9) is presented. Statistical difference in ZOI area between the TTG mutant and TTG mutant in co-inoculation mix was calculated using pairwise t-test function in Rstudio. Level of significance: *** < 0.001. Scale: 1 cm.

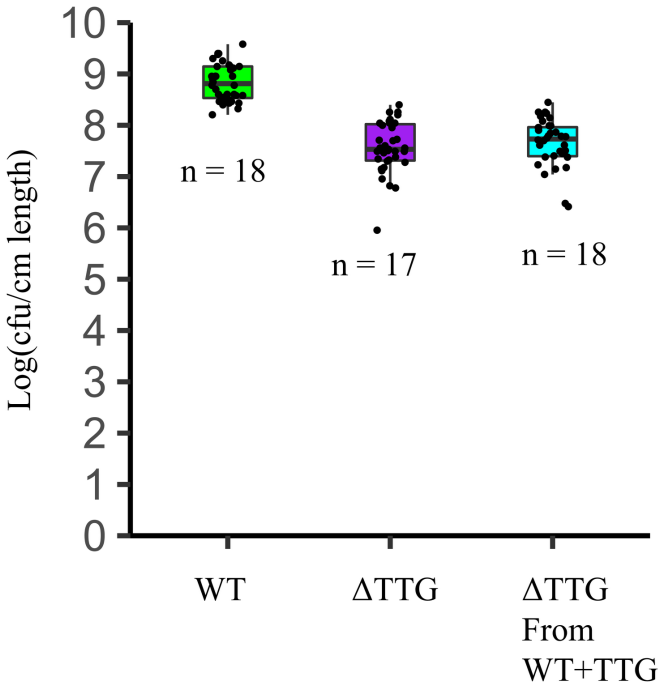

Figure 4.7: Bga WT strain didn't rescue the population of TTG mutant from the infected seedlings in the co-infection assay. Box plot showing the CFU/cm recovery of Bga WT, TTG mutant, and TTG mutant from co-infection mix after three days post inoculation. N is the total number of observations across three independent experimental repeats.

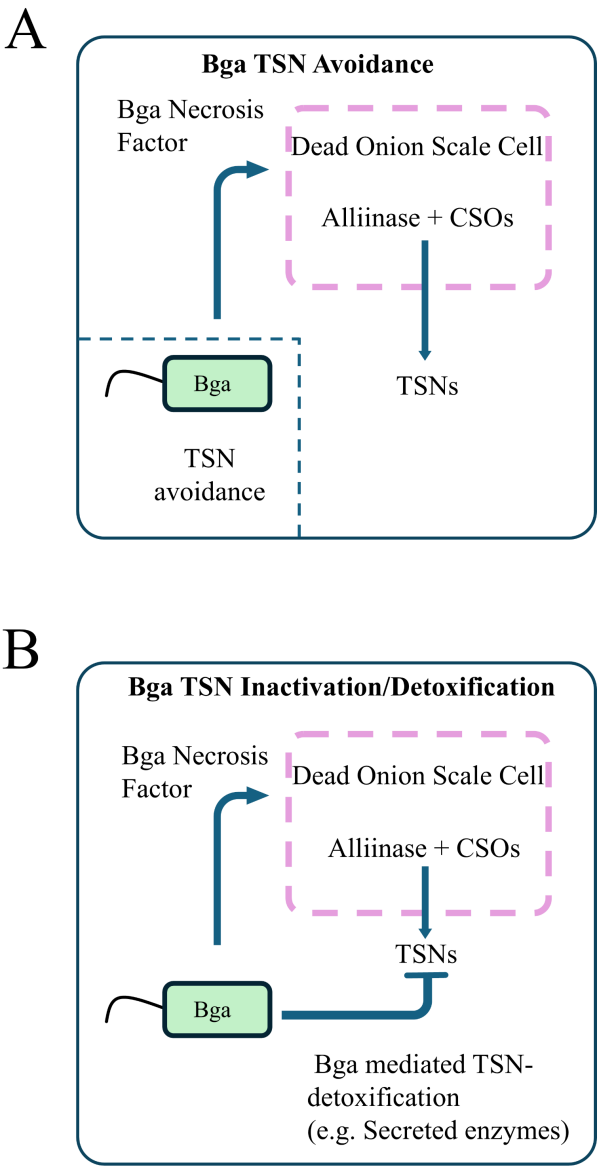

Figure 4.8: Revised model for the Bga thiosulfinate resistance mechanisms in onion scale tissue following experiments conducted in the study. **B,** In the Bga TSN inactivation/detoxification, the bacterium inactivates or detoxifies the TSNs produced during native necrosis using enzymes or chemical compounds.

Supplemental Figures

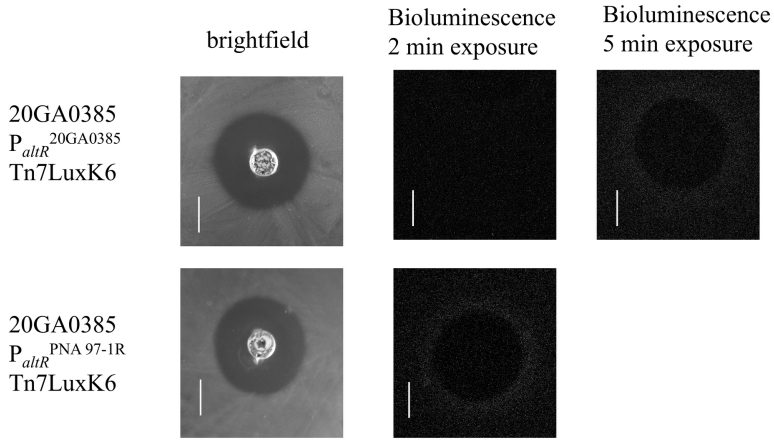

Supplementary Figure S4.1. The derepression of Bga *altR* reporter construct is seen as bright ring in the ZOI assay. Representative brightfield and bioluminescence images of **Top**, Bga $P_{altR}^{PNA\ 97\text{-}1R}$Tn*7*LuxK6 strain and **Bottom**, Bga $P_{altR}^{20GA0385}$Tn*7*LuxK6. Images taken 18 hours post inoculation. Scale: 1 cm.

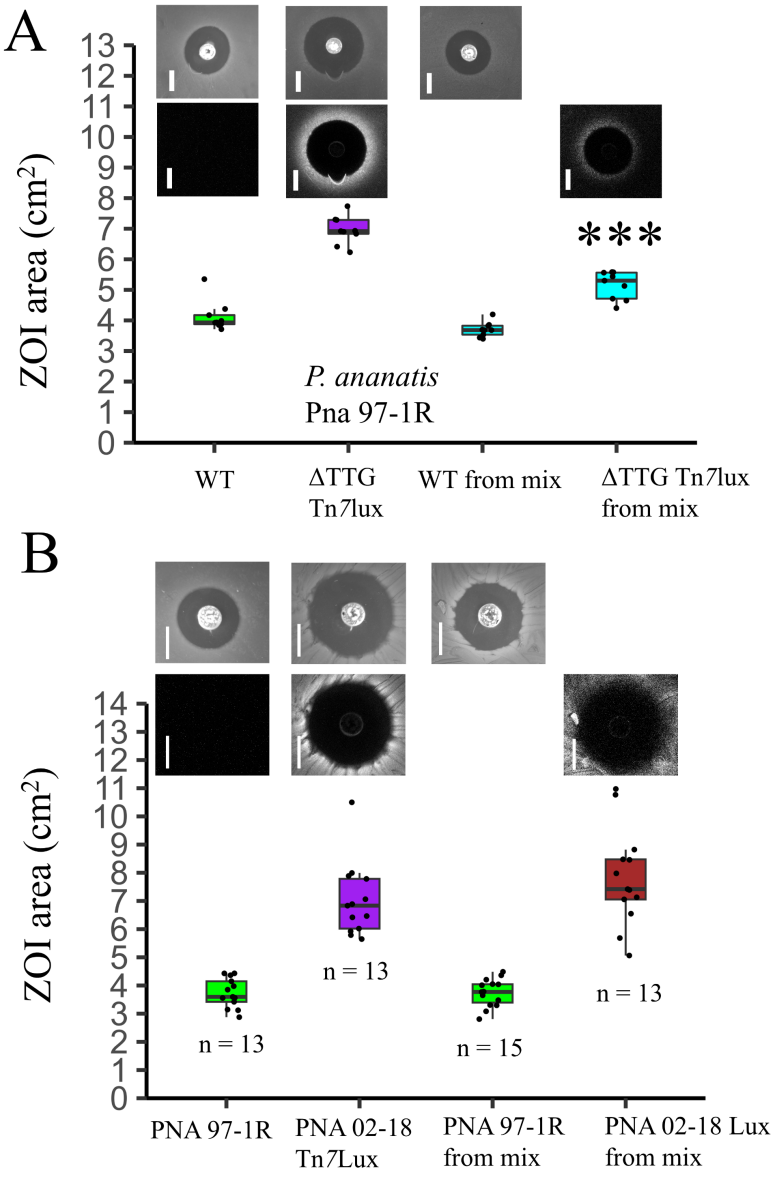

Supplementary Figure S4.2. *Pantoea ananatis* PNA 97-1R strain doesn't rescue the phenotype of **A**, engineered TTG mutant and **B**, TTG negative natural variant strain PNA 02-18 in zone of inhibition co-inoculation assay. Box plot showing the allicin ZOI area of Pna 97-1R, **A**, PNA 97-1R ΔTTG , **B**, PNA 02-18 Tn*7*Lux, PNA 97-1R from co-inoculation mix and PNA 02-18 Tn*7*Lux/ PNA 97-1R ΔTTG from co-inoculation mix. Representative brightfield and/or bioluminescence images of ZOI plates treated with corresponding strains are presented above the box. n is the total number of data points across four independent experimental repeats. Statistical difference in ZOI area between the PNA 02- 18 Tn*7*Lux/ PNA 97-1R ΔTTG standalone treatment and PNA 02- 18 Tn*7*Lux/ PNA 97-1R ΔTTG in co-inoculation mix was calculated using pairwise t-test function in Rstudio. Level of significance: 0.01>* < 0.05. Scale: 1 cm.

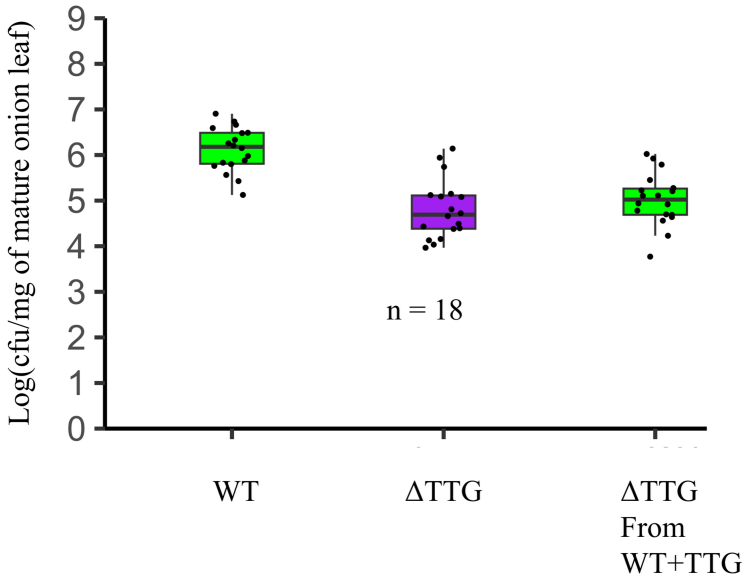

Supplementary Figure S4.3: Bga WT strain didn't rescue the population of TTG mutant from the infected mature onion plants in the co-infection assay. Box plot showing the CFU/mg recovery of Bga WT, TTG mutant, and TTG mutant from co-infection mix after three days post inoculation. n is the total number of observations across six independent experimental repeats.

CHAPTER 5

CONCLUSIONS

Our research focused on identifying the genetic determinants of virulence in the bacterial onion pathogen *Burkholderia gladioli* pv. *alliicola* (Bga). The thiosulfinate tolerance gene (TTG) clusters have been recognized as virulence factors that facilitate colonization in the bacterial onion pathogen *Pantoea ananatis* and help the bacterium resist thiol toxicity (Stice et al., 2020). Additionally, these clusters have been shown to enhance allicin resistance in the garlic saprophyte *Pseudomonas fluorescens* (Borlinghaus et al., 2020). Given that multiple *Burkholderia* species are known onion pathogens, we hypothesized that Bga encounters toxic thiosulfinates during disease progression. To investigate this, we utilized *in silico* analysis, zone of inhibition assays, and onion infection assays to examine the distribution and functional role of putative TTG clusters in *Burkholderia* onion pathogens isolated from Georgia. From this study, we determined the following:

1. Putative TTG-like clusters were widespread in multiple *Burkholderia* onion pathogenic species such as Bga, *B. cepacia*, *B. orbicola*, and *B. ambifaria. In silico* analyses also revealed the presence of putative TTG-like clusters in *Burkholderia* strains isolated from non-onion hosts.
2. Three distinct TTG cluster types – Type A, Type B, and Type C were described based on nucleotide homology. Four strains harbored both Type A and Type B cluster types.

3. TTG lacking natural variants of *B. cepacia*, *B. gladioli*, and *B. cepacia* were more sensitive to allicin as compared to TTG containing strains.
4. Using TTG complementation expression plasmids, we found that TTG clusters in *B. cepacia*, *B. orbicola*, and *B. gladioli* contributed to allicin tolerance and improved growth in onion juice.
5. Bga TTG clusters contribute to onion foliar necrosis and bacterial populations.
6. TTG clusters in *B. gladioli*, *B. cepacia*, and *B. orbicola* were inconsequential for onion scale necrosis and bacterial population.

Despite differences in gene synteny and organization compared to the necrotrophic onion pathogen *Pantoea ananatis*, we found that TTG clusters are functionally conserved in distantly related onion-pathogenic *Burkholderia* species. However, unlike *P. ananatis*, the TTG mutant in Bga was not impaired in scale tissue colonization compared to the wild type strain. This suggests that Bga onion pathogens may have additional mechanisms to counter the effects of thiosulfinates during scale tissue infection.

The variable role of TTG clusters in Bga virulence prompted us to further investigate the genetic basis of pathogenicity in this bacterium. Given the economic significance of Bga in onion production and its ability to cause both foliar and bulb symptoms, understanding the broader genetic determinants of its virulence is crucial. The occurrence of slippery skin disease in onions, caused by *Burkholderia gladioli* pv. *alliicola* (Bga), has been extensively documented in onion growing regions worldwide. Overhead irrigation condition during field curing is a risk factor to increase bacterial rot incidence caused by Bga (Wright et al., 1993). The threat of Bga to onion production is considerable, as another common onion pathogen group, *Burkholderia cepacia* complex, has been described as relatively less successful foliar pathogen. While several

studies have characterized the Bga strains isolated from onion growing regions, the understanding of underlying genetic basis of virulence in Bga is limited. Utilizing comparative genomics, allelic exchange and phenotypic assays, we did a comprehensive survey on the role of Bga genetic factors and regulators in onion virulence. The key findings from this study are as follows:

1. The well characterized putative virulence factors and regulators- the phytotoxin toxoflavin, T2SS, type III secretin system (T3SS), and the *tofIMR* QS system was well conserved in Bga and well- studied rice pathogenic close relative *B. glumae.*
2. Of the studied virulence factors, the phytotoxin toxoflavin and the TTG cluster contributed to onion foliar necrosis and bacterial populations.
3. In the onion scale tissue, the T2SS was the sole contributor to necrosis among the tested virulence factors.
4. The phytotoxin toxoflavin and the T2SS perform onion tissue specific virulence role in Bga.
5. The well studied virulence factor T3SS was inconsequential for Bga onion foliar/scale symptoms and in planta populations.
6. The *tofIMR* QS system regulates onion foliar/scale symptoms production as well as the function of multiple virulence factors in Bga.
7. The decoupling of Bga symptoms production and bacterial population was evident particularly in the onion scale tissue.

Like the TTG cluster, we observed a variable virulence role of toxoflavin and type II secretion system depending on the onion tissue type. This suggests that the Bga pathogen have evolved diverse strategies to colonize and infect different onion tissues. The contrasting role of

TTG cluster in onion foliar and scale tissue is surprising as thiosulfinate production in maturing bulb is considerably higher than the leaf tissue (Cho et al., 2024).

We utilized predicted genetic features of TTG cluster and co-inoculation assays to further study the onion tissue specific contributions of TTG cluster to Bga virulence. The main findings of this study are as follows:

1. The de-repression of Bga altR reporter construct was consistent with the onset and progression of foliar necrosis.
2. In the scale tissue, the de-repression was observed in the early stages of infection but gradually went away with the onset of Bga induced necrosis.
3. In the presence of pantaphos as external necrosis factor, the altR reporter construct was consistently de-repressed with the onset of pantaphos induced scale necrosis.
4. Preconditioning the TTG mutant in the scale tissue and exposing them to onion juice didn't improve the growth of the TTG mutant.
5. The Bga 20GA0385 WT strain was able to partially rescue the ZOI area phenotype of respective TTG mutants in co-inoculation mix.
6. Experimental results suggest Bga thiosulfinate exclusion in onion scale is unlikely.

In the absence of alliinase in ZOI assay, we still saw the partial rescue of TTG mutant by Bga WT strain in the co-inoculation assay suggests Bga might inactivate the produced thiosulfinates in the scale tissue. Our study provides further insights into onion tissue specific virulence strategies of Bga TTG cluster.

Using a combination of bacterial genetics and phenotypic assays, we comprehensively characterized the role of Bga virulence determinants in onion disease phenotype. Our findings

enhance the understanding of the diverse strategies this bacterium employs to infect onion. Notably, our study highlights the tissue-specific virulence features of Bga, a trait that is relatively uncommon among bacterial plant pathogens. The decoupling of scale symptoms and corresponding *in planta* bacterial population is also an unusual phenomenon in plant pathogenic bacteria. The variable virulence role of multiple virulence factors in Bga suggests different strategies would be necessary to effectively manage Bga foliar and bulb symptoms. The widespread distribution of TTG clusters in the onion isolated *Burkholderia* strains means that the cluster can be utilized as a diagnostic marker for early pathogen detection, enabling farmers to implement timely and effective management strategies.

Understanding the pathogen biology and virulence mechanisms is the initial and foremost step in developing long-term disease resistance strategies. We anticipate that our research findings will offer additional insights into host defense and microbial interactions, potentially leading to the development of new strategies for managing bacterial diseases in *Allium* species.

Among the tested virulence factors, the T2SS made minor contributions to onion scale necrosis. Future studies on primary scale necrosis mediating factor in Bga could provide further improve the understanding of Bga virulence mechanisms. Similarly, in the foliar tissue toxoflavin independent necrosis factor could also exist. Transposon mutagenesis can be utilized to screen for the potential Bga secreted factor that can inactivate or suppress thiosulfinates. Similarly, understanding the onion tissue specific Bga transcriptional profile could provide targets to elucidate the thiosulfinate resistance mechanism in scale tissue.

References

Borlinghaus, J., Bolger, A., Schier, C., Vogel, A., Usadel, B., Gruhlke, M., and Slusarenko, A. 2020. Genetic and molecular characterization of multicomponent resistance of *Pseudomonas* against allicin. Life science alliance 3.

Cho, H., Park, J., Kim, D., Han, J., Natesan, K., Choi, M., Lee, S., Kim, J., Cho, K., and Ahn, B. 2024. Understanding the defense mechanism of *Allium* plants through the onion isoallicin-omics study. Frontiers in Plant Science 15:1488553.

Stice, S., Thao, K., Khang, C., Baltrus, D., Dutta, B., and Kvitko, B. 2020. Thiosulfinate tolerance is a virulence strategy of an atypical bacterial pathogen of onion. Current Biology 30:3130-3140. e3136.